UNIVERSIDADE DA BEIRA INTERIOR
Ciências da Saúde

Coadministration of antiepileptic drugs and P-glycoprotein inhibitors of flavonoid-type: a strategy to overcome the drug resistance in epilepsy

Ana Filipa da Silva Ferreira

Tese para obtenção do Grau de Doutor em
Ciências Farmacêuticas
(3º ciclo de estudos)

Orientador: Professor Doutor Gilberto Lourenço Alves
Coorientador: Professor Doutor Amílcar Celta Falcão Ramos Ferreira

Covilhã, março 2018

The experimental work presented in this thesis was carried out at the Health Sciences Research Centre, Faculty of Health Sciences, University of Beira Interior (CICS-UBI) and at the Center for Neuroscience and Cell Biology (CNC), University of Coimbra, under the scientific supervision of Professor Gilberto Lourenço Alves and Professor Amílcar Celta Falcão Ramos Ferreira.

The work underlying the present thesis was supported by FCT - Foundation for Science and Technology, Lisbon, Portugal (SFRH/BD/84936/2012). This work was also supported by FEDER funds through the POCI - COMPETE 2020 - Operational Programme Competitiveness and Internationalisation in Axis I - Strengthening research, technological development and innovation (Project POCI-01-0145-FEDER-007491) and National Funds by FCT (Project UID/Multi /00709/2013).

Aos meus Pais

Ao Edgar

"Sabemos muito mais do que julgamos, podemos muito mais do que imaginamos."

José Saramago

Agradecimentos

Terminada esta longa e árdua etapa resta-me registar os meus sinceros agradecimentos a todos aqueles que foram parte integrante deste caminho e que contribuíram para a sua finalização.

Ao Professor Gilberto Alves, meu orientador,
agradeço em primeiro lugar o convite que me endereçou para a realização deste trabalho de investigação com vista ao grau de Doutor. Gostaria ainda de salientar a minha sincera gratidão pelo notável contributo e orientação científica, fundamentais para a execução deste trabalho, pela constante dedicação, disponibilidade e ensinamentos transmitidos.

Ao Professor Amílcar Falcão, meu coorientador,
agradeço pela orientação científica, profissionalismo, e todo o conhecimento e recomendações transmitidas durante estes anos.

Ao Professor Márcio Rodrigues,
companheiro e apoio essencial desde o início deste trabalho. Agradeço a pronta disponibilidade e auxílio sempre que o meu desespero imperava sobre o resto. O seu contributo científico, partilha do saber e valiosos conselhos foram fundamentais.

À Professora Ana Fortuna,
agradeço o contributo científico, os ensinamentos e esclarecimentos científicos transmitidos que se revelaram de grande importância no decorrer deste projeto.

À Professora Adriana Santos,
agradeço a amabilidade e disponibilidade que sempre teve para comigo, bem como todo o entusiasmo, incentivo e saberes transmitidos.

Ao Centro de Investigação em Ciências da Saúde da Universidade da Beira Interior,
aos Professores, Investigadores, Colegas e Funcionários que tiveram um papel fundamental no desenrolar deste trabalho e cujo auxílio nas mais diversas vertentes foi essencial na sua concretização.

Aos Colegas do grupo de doutoramento,
A partilha de alegrias e frustrações, vitórias e fracassos foi essencial para tornar mais fácil esta longa jornada.

***Aos Amigos*,**

aos de Sempre, e a todos Aqueles e Aquelas que se juntaram durante esta longa etapa. Fazem parte daquilo que sou e foram e serão sempre essenciais para tornar todos os caminhos menos sinuosos e todas as batalhas mais gratificantes.

***Ao Edgar*,**

um agradecimento muito especial. Por estar sempre ao meu lado e por todo o Amor, Apoio e Suporte, fundamentais para seguir sempre em frente. Pela Confiança, Orgulho, Compreensão e Motivação constantes e por nunca me deixar desistir.

***Aos meus Pais João Paulo e Lurdes*,**

pilares essenciais na minha vida. Obrigada pelo Amor, Confiança e Dedicação incondicional que sempre depositaram em mim, fulcrais para ultrapassar todas as adversidades e querer fazer sempre mais e melhor. Tudo o que sou a vocês vos devo. Obrigada por tudo!

TABLE OF CONTENTS

Table of contents

RESUMO ALARGADO

Resumo alargado

A epilepsia é uma das doenças neurológicas crónicas mais comuns e tem um grande impacto negativo na qualidade de vida dos doentes, sendo de extrema importância os esforços continuados para desenvolver novos fármacos antiepiléticos e novas abordagens terapêuticas. Contudo, apesar dos avanços significativos alcançados nos últimos anos, os fenómenos de farmacorresistência associados aos fármacos antiepiléticos são provavelmente um dos principais problemas no que diz respeito à terapêutica da epilepsia, afetando 30-40% dos doentes. De facto, esta situação tem proporcionado um ímpeto crescente para o desenvolvimento de abordagens terapêuticas inovadoras e mais eficazes. A sobreexpressão de transportadores de efluxo de fármacos, como a glicoproteína-P (P-gp), ao nível da barreira hematoencefálica, tem sido sugerida como um dos principais mecanismos subjacentes à epilepsia refratária. Desta forma, vários esforços têm sido realizados no sentido de descobrir e desenvolver inibidores da P-gp que sejam úteis de um ponto de vista terapêutico. No entanto, as múltiplas desvantagens apresentadas pelas primeiras gerações de inibidores da P-gp demonstraram a necessidade de encontrar agentes mais potentes e mais seguros, tendo sido dado um ênfase especial nos últimos anos a compostos flavonoides. Além do seu interesse potencial como inibidores da P-gp, uma panóplia de outras propriedades farmacológicas importantes têm sido atribuídas a estes compostos fitoquímicos, entre as quais, por exemplo, efeitos anti-inflamatórios, antioxidantes, antitumorais, antimicrobianos, antivirais, hormonais e, mesmo, anticonvulsivantes.

Tendo em consideração todos estes aspetos, a presente tese teve como principal objetivo realizar uma avaliação abrangente, *in vitro* e *in vivo,* do papel potencial dos flavonoides como inibidores da P-gp, e também explorar uma estratégia de terapia combinada de flavonoides/fármacos antiepiléticos como possível abordagem para superar a farmacorresistência verificada na epilepsia.

Este projeto envolveu o desenvolvimento e validação de técnicas bioanalíticas apropriadas e fiáveis para apoiar a execução dos estudos pretendidos. Neste contexto, métodos de cromatografia líquida de alta eficiência acoplados à deteção por fotodíodos (HPLC-DAD) foram devidamente desenvolvidos e validados para a quantificação dos fármacos antiepiléticos alvo de interesse e de alguns dos seus principais metabolitos em amostras de cultura celular e em matrizes de plasma e cérebro de rato. Uma técnica adicional de HPLC-DAD foi também desenvolvida para a quantificação de vários fármacos antiepiléticos e metabolitos em plasma humano, constituindo uma ferramenta útil para apoiar a monitorização terapêutica destes fármacos na prática clínica.

De acordo com os resultados obtidos num conjunto de ensaios *in vitro*, cinco dos onze flavonoides testados, nomeadamente, a baicaleína, a (-)-epigalocatequina galato [(-)-EPG], o kaempferol, a quercetina e a silimarina demonstraram ter um potencial interessante na inibição

da atividade da P-gp. Estes flavonoides promoveram também um aumento significativo da acumulação intracelular dos fármacos antiepiléticos carbamazepina (CBZ), oxcarbazepina (OXC) e fenitoína (PHT), e dos seus metabolitos ativos carbamazepina-10,11-epóxido (CBZ-E) e licarbazepina (LIC), na linha celular *Madin-Darby canine kidney*, transfetada com o gene de resistência a múltiplos fármacos 1 (*MDR1*) que codifica para a P-gp humana (MDCK-MRD1), evidenciando-se como candidatos promissores para reverter a resistência associada aos fármacos antiepiléticos. Além disso, com exceção da lamotrigina (LTG), todos os fármacos antiepiléticos testados (CBZ, PHT e OXC), assim como os seus respetivos metabolitos ativos (CBZ-E e LIC), demonstraram ser substratos da P-gp neste modelo celular. Adicionalmente, a CBZ, CBZ-E, LIC, LTG, OXC e PHT promoveram uma diminuição significativa nas concentrações intracelulares de rodamina 123 (um substrato "sonda" clássico da P-gp), o que sugere um efeito indutor, mediado pelos próprios fármacos e metabolitos, da atividade funcional da P-gp.

Reconhecendo-se as várias propriedades biológicas atribuídas aos flavonoides e tendo-se em consideração que misturas complexas de flavonoides são consumidas diariamente na nossa dieta, não se poderá ignorar o seu potencial farmacológico sinérgico. Neste sentido, foi concretizada uma avaliação dos potenciais efeitos sinérgicos da baicaleína, (-)-EPG, kaempferol, quercetina e silimarina relativamente à inibição da P-gp, primeiro *in vitro* e depois *in vivo*. Na verdade, comparativamente aos resultados individuais obtidos, algumas combinações duais de flavonoides apresentaram um potencial acrescido para inibição da P-gp *in vitro*. Além disso, algumas dessas combinações, nomeadamente (-)-EPG/silimarina e kaempferol/baicaleína, proporcionaram um aumento substancial da acumulação intracelular de CBZ, OXC e PHT, bem como dos seus metabolitos CBZ-E e LIC, na linha celular MDCK-MDR1, sendo estes efeitos comparáveis aos obtidos com o verapamilo, inibidor de referência da P-gp. Assim, enquanto os flavonoides baicaleína, (-)-EPG, kaempferol, quercetina e silimarina testados individualmente aumentaram em 1,2 a 31 vezes a acumulação intracelular dos fármacos antiepiléticos e metabolitos ativos considerados nas células MDCK-MDR1, as combinações duais desses flavonoides permitiram alcançar aumentos de cerca de 1,5 a 76 vezes. Adicionalmente, o efeito da combinação da (-)-EPG com a silimarina foi também avaliado em ensaios de transporte com a LIC (substrato da P-gp) através de uma monocamada de células MDCK-MDR1 montadas em câmaras de Ussing; como esperado, esta combinação aumentou o coeficiente de permeabilidade aparente da LIC.

Em geral, os resultados dos estudos *in vitro* foram suportados pelos resultados dos estudos *in vivo*. De facto, após pré-tratamento de ratos Wistar machos com silimarina observou-se um aumento nas concentrações plasmáticas dos fármacos antiepiléticos alvo (CBZ, OXC e PHT). No entanto, é de ressaltar que os principais efeitos induzidos pela silimarina foram notados na farmacocinética da OXC, para a qual foi observado um aumento estatisticamente significativo na sua concentração plasmática máxima (50%) e na sua extensão de exposição sistémica (41%), tendo tais efeitos um impacto direto nas concentrações farmacológicas alcançadas no cérebro. Por outro lado, o uso de combinações duais de (-)-EPG/silimarina na inibição da atividade da P-gp foi também avaliado *in vivo* em ratos Wistar, sendo evidente o potencial sinérgico destes

dois flavonoides no aumento do grau de exposição sistémica à OXC e LIC (metabolito farmacologicamente ativo da OXC), o que ocorreu numa extensão comparável à observada para o verapamilo (controlo positivo). De facto, o pré-tratamento de ratos Wistar com combinações de silimarina/(-)-EPG originou concentrações plasmáticas máximas de OXC semelhantes àquelas obtidas na presença do verapamilo. Além disso, os efeitos promovidos pelas combinações de silimarina/(-)-EPG no que diz respeito à magnitude da exposição sistémica ao fármaco foram também refletidos nos níveis de OXC e LIC alcançados no cérebro (biofase).

Assim, de acordo com os nossos resultados, a terapia combinada de flavonoides/fármacos antiepiléticos pode ser considerada como uma abordagem promissora que deve continuar a ser explorada no sentido de superar a farmacorresistência mediada pela P-gp. A disponibilidade desta informação resultante de ensaios *in vitro* e *in vivo* contribui também para apoiar a hipótese do envolvimento de transportadores de efluxo, em particular da P-gp, na condição de epilepsia farmacorresistente. Considerando todo o seu potencial intrínseco e propriedades biológicas indiscutíveis, os compostos de tipo flavonoide podem então emergir como uma alternativa aos inibidores da P-gp disponíveis para um tratamento prospetivo dos doentes com epilepsia refratária.

Palavras-Chave

Ensaios *in vitro,* Epilepsia, Fármacos antiepiléticos, Farmacocinética, Farmacorresistência, Flavonoides, Glicoproteína-P, Rato

ABSTRACT

Abstract

The resistance to antiepileptic drugs (AEDs) remains a major unsolved therapeutic problem, which affects 30-40% of patients with epilepsy. The overexpression of multidrug efflux transporters, as the P-glycoprotein (P-gp), at the level of the blood-brain barrier of epileptic patients has been suggested as a key mechanism underlying the refractory epilepsy. Bearing this in mind, efforts have been made to search for therapeutically useful P-gp inhibitors. In an attempt to find potent and safer P-gp inhibitor drugs, a particular emphasis has been given to flavonoid compounds. Actually, apart from their potential value as P-gp inhibitors, these phytochemical compounds have been recognised as having a panoply of important pharmacological properties like anti-inflammatory, antioxidant, antitumoral, antimicrobial, antiviral, hormonal and even anticonvulsant effects. Taking this into account, the purpose of the present thesis was to conduct a comprehensive *in vitro* and *in vivo* evaluation of the potential of flavonoids as P-gp inhibitors, but also to explore a strategy of flavonoid/AED combined therapy as a possible approach to overcome the P-gp–mediated pharmacoresistance in epilepsy.

This project involved the development and validation of appropriate and reliable bioanalytical techniques to support the accomplishment of the intended studies. Thus, high-performance liquid chromatography methods coupled with diode array detection (HPLC-DAD) were properly validated for the quantification of the target AEDs and some of their main metabolites in cell culture samples and in rat plasma and brain matrices. An additional HPLC-DAD technique was also developed to quantify several AEDs and metabolites in human plasma, which has shown to be a useful tool for the therapeutic drug monitoring in the clinical practice.

According to the results of a set of *in vitro* assays, five out of eleven flavonoids tested, namely baicalein, (-)-epigallocatechin gallate [(-)-EPG], kaempferol, quercetin and silymarin demonstrated to have an interesting potential in inhibiting the P-gp activity. These promising flavonoids also promoted a significant increase in the intracellular accumulation of the AEDs carbamazepine (CBZ), oxcarbazepine (OXC) and phenytoin (PHT) and their active metabolites carbamazepine-10,11-epoxide (CBZ-E) and licarbazepine (LIC) in the Madin-Darby canine kidney cell line transfected with the human multidrug resistance-1 gene which encodes the human P-gp (MDCK-MRD1), showing up as important drug candidates to overcome the AED-resistance. Actually, excluding LTG, all the AEDs tested (CBZ, OXC and PHT) as well as their active metabolites (CBZ-E and LIC) were found to be P-gp substrates in the MDCK-MDR1 cells. Additionally, CBZ, CBZ-E, LIC, LTG, OXC and PHT promoted a statistically significant decrease of the intracellular concentration of rhodamine 123 (a classic P-gp probe substrate), suggesting an inducer effect on the functional activity of P-gp.

An assessment of the potential synergic effects of baicalein, (-)-EPG, kaempferol, quercetin and silymarin on the P-gp inhibition was also performed, firstly in *in vitro* conditions and then

in *in vivo* experiments. Indeed, when compared to their individual activity, some dual flavonoid combinations exhibited an increased potential in inhibiting the P-gp in the *in vitro* assays. Moreover, the dual combinations of (-)-EPG/silymarin and kaempferol/baicalein demonstrated a great potential in enhancing the intracellular accumulation of CBZ, OXC and PHT and their metabolites CBZ-E and LIC in the MDCK-MDR1 cells and such effects were comparable to those promoted by verapamil (the standard P-gp inhibitor). The effect of the combination of (-)-EPG/silymarin was also tested in transport assays of LIC (P-gp substrate) through MDCK-MDR1 cells mounted in Ussing chambers; as expected, this combination of flavonoids increased the apparent permeability coefficient of LIC.

Overall, these *in vitro* findings were further supported by *in vivo* results. In fact, after the pretreatment of male Wistar rats with silymarin an increasing in the plasma concentrations of the studied AEDs (CBZ, OXC and PHT) was observed. Nevertheless, it should be highlighted that the main effects induced by silymarin were found on the OXC pharmacokinetics, for which was found a statistically significant increase in the peak plasma concentration (50%) and in the extent of systemic exposure (41%), having a direct impact on the drug concentrations reached in the brain. On the other hand, the use of dual combinations of (-)-EPG/silymarin on the inhibition of the activity of P-gp was also evaluated *in vivo* in Wistar rats, being noticeable the synergic potential of (-)-EPG/silymarin combinations in enhancing the degree of systemic exposure to OXC and LIC (a pharmacologically active metabolite of OXC), and it occurred in a comparable extent to that observed for verapamil (positive control). Indeed, the pretreatment of male Wistar rats with dual silymarin/(-)-EPG combinations originated peak plasma concentrations of OXC similar to those achieved in the presence of verapamil. Moreover, the effects promoted by silymarin/(-)-EPG combinations on the magnitude of systemic drug exposure were also reflected in the corresponding drug levels attained in the brain (biophase). Hence, according to our findings, it seems that the flavonoid/AED combined therapy can be thought as a promising approach that should continue to be exploited in order to overcome the P-gp–mediated pharmacoresistance. The availability of this *in vitro* and *in vivo* information also adds support to the efflux transporter hypothesis in explaining the pharmacoresistant epilepsy. Considering all its intrinsic potential and indisputable properties, the flavonoid-type compounds may emerge as an alternative to the available P-gp inhibitors for a prospective management of patients with drug-refractory epilepsy.

Keywords

Antiepileptic drugs, Epilepsy, Flavonoids, *In vitro* assays, P-glycoprotein, Pharmacokinetics, Pharmacoresistance, Rat

LIST OF FIGURES

List of figures

LIST OF TABLES

List of tables

LIST OF ABBREVIATIONS

List of abbreviations

A

ABC	Adenosine triphosphate-binding cassette
AED	Antiepileptic drug
ATP	Adenosine triphosphate
AUC	Area under the concentration-time curve
AUC_{0-t}	AUC from time zero to the last sampling time
$AUC_{0-\infty}$	AUC from zero to infinity

B

BCRP	Breast cancer resistance protein
Bias	Deviation from nominal concentration

C

CBZ	Carbamazepine
CBZ-E	Carbamazepine-10,11-epoxide
$CI_{95\%}$	95% confidence interval
C_{last}	Last quantifiable concentration
CL_t	Total body clearance
C_{max}	Plasma peak concentration
CNS	Central nervous system
CV	Coefficient of variation
CYP	Cytochrome P450

D

DAD	Diode array detector
DMEM	Dulbecco's Modified Eagle's Medium
DMSO	Dimethyl sulfoxide

E

EC_{50}	Half maximal effective concentration
EDTA	Ethylenediaminetetraacetic acid
EMA	European Medicines Agency
(-)-EPG	(-)-Epigallocatechin gallate

F

FBS	Fetal bovine serum
FDA	U.S. Food and Drug Administration

G

GABA	γ-Aminobutyric acid
$GABA_A$	GABA type A

H

HPLC	High-performance liquid chromatography
HPPH	5-(4-Hydroxyphenyl)-5-phenylhydantoin

I

ILAE	International League against Epilepsy
ip	Intraperitoneal
IS	Internal standard
iv	Intravenous

K

k_{el}	Apparent terminal rate constant

L

LIC	Licarbazepine
LLE	Liquid-liquid extraction
LLC-PK1	Porcine-kidney derived Lilly Laboratories cell line
LLC-PK1-MDR1	Porcine-kidney derived Lilly Laboratories cell line transfected with the *MDR1* gene
LLOQ	Lower limit of quantification
LOD	Limit of detection
LTG	Lamotrigine

M

MDCK	Madin-Darby canine kidney cell line
MDCK-MDR1	Madin-Darby canine kidney cell line transfected with the *MDR1* gene
MDR1	Human multidrug resistance-1 gene
mdr1	Rodent multidrug resistance-1 gene
MEPS	Microextraction by packed sorbent
MRP	Multidrug resistance-associated protein
MRT	Mean residence time
MTT	3-[4,5-Dimethylthiazol-2-yl]-2,5-diphbenyltetrazolium bromide

N

NBD	Nucleotide-binding domain

O

OXC	Oxcarbazepine

P

P_{app}	Apparent permeability coefficient
PB	Phenobarbital
PBS	Phosphate-buffered saline
P-gp	P-glycoprotein
PHT	Phenytoin
PP	Protein precipitation
PRM	Primidone

Q

QC	Quality control

R

r^2	Determination coefficient
Rh123	Rhodamine 123

S

SEM	Standard error of the mean
SPE	Solid-phase extraction

T

TDM	Therapeutic drug monitoring
TEER	Transepithelial electrical resistance
TM	Transmembrane α-helix segment
t_{max}	Time to reach C_{max}
TMD	Transmembrane domain
$t_{1/2el}$	Apparent terminal elimination half-life

U

UV	Ultraviolet

LIST OF PUBLICATIONS

List of publications

FERREIRA A *ET AL*. Isobolographic analysis of the neuro and hepatotoxic profile resulting from the combination of carbamazepine, oxcarbazepine or phenytoin with the flavonoid silymarin (*In preparation for publication*).

FERREIRA A *ET AL*. Impact of silymarin, a flavonoid-type P-glycoprotein inhibitor, on the pharmacokinetics of carbamazepine, oxcarbazepine and phenytoin in rats (*Submitted for publication*)

FERREIRA A *ET AL* (2018) Flavonoid compounds as reversing agents of the P-glycoprotein-mediated multidrug resistance: An *in vitro* evaluation with focus on antiepileptic drugs. *Food Res Int*. 103:110-120. doi: 10.1016/j.foodres.2017.10.010

FERREIRA A *ET AL* (2018) *In vitro* screening of dual flavonoid combinations for reversing P-glycoprotein-mediated multidrug resistance: Focus on antiepileptic drugs. *Food Chem Toxicol*. 111:84-93. doi: 10.1016/j.fct.2017.11.004

FERREIRA A *ET AL*. (2017) Influence of the dual combination of silymarin and (-)-epigallocatechin gallate, natural dietary flavonoids, on the pharmacokinetics of oxcarbazepine in rats. *Food Chem Toxicol*. 106: 446-454. doi: 10.1016/j.fct.2017.06.015

FERREIRA A *ET AL*. (**2016**) A Rapid and Sensitive HPLC–DAD Assay to Quantify Lamotrigine, Phenytoin and Its Main Metabolite in Samples of Cultured HepaRG Cells. *J Chromatogr Sci*. 54(8): 1352–1358. doi:10.1093/chromsci/bmw088

FERREIRA A *ET AL*. (**2016**) HPLC–DAD Method for the Quantification of Carbamazepine, Oxcarbazepine and their Active Metabolites in HepaRG Cell Culture Samples. *Chromatographia*. 79(9): 581–590. doi:10.1007/s10337-016-3063-7

FERREIRA A *ET AL*. (**2016**) Huperzine A from Huperzia serrata: a review of its sources, chemistry, pharmacology and toxicology. *Phytochem Rev*. 15(1): 51–85. doi:10.1007/s11101-014-9384-y

FERREIRA A *ET AL*. (**2015**) Flavonoid compounds as reversal agents of the P-glycoprotein-mediated multidrug resistance: biology, chemistry and pharmacology. *Phytochem Rev*. 14(2): 233–272. doi:10.1007/s11101-014-9358-0

FERREIRA A *ET AL*. (**2014**) Liquid chromatographic assay based on microextraction by packed sorbent for therapeutic drug monitoring of carbamazepine, lamotrigine, oxcarbazepine, phenobarbital, phenytoin and the active metabolites carbamazepine-10,11-epoxide and licarbazepine. *J Chromatogr B Anal Technol Biomed Life Sci*. 971: 20–29. doi:10.1016/j.jchromb.2014.09.010

CHAPTER I

General Introduction

The content of this chapter is included in the following manuscript:

FERREIRA A *ET AL*. (**2015**) Flavonoid compounds as reversal agents of the P-glycoprotein-mediated multidrug resistance: biology, chemistry and pharmacology. *Phytochem Rev*. 14(2): 233–272. doi:10.1007/s11101-014-9358-0

I.1. Epilepsy

Disease and pharmacological therapy

I.1.1. Historical background

Epilepsy is perhaps one of the oldest recorded medical illnesses in history (WAHAB 2010). In fact, the origin of the word "epilepsy", derived from Latin and Greek words for "seizure" or "to seize upon", evidence the ancient provenance of this disorder (WORLD HEALTH ORGANIZATION 2005; GOLDENBERG 2010). In all civilizations, epilepsy can be traced as far back as medical records exist (WORLD HEALTH ORGANIZATION 2005). As a disease entity, epilepsy has first been mentioned by the ancient Egyptians who called it *nesejet*, or by the ancient Babylonians who called it the *bennu* disease (WAHAB 2010). In these ancient times, the disease was described as a condition representing an evil state of mind or possession, requiring exorcism, incantations or other religious or social approaches, while on the other hand, in some cultures, patients with epilepsy were regarded as people who had mystical or spiritual powers, and it was even thought to be contagious (WORLD HEALTH ORGANIZATION 2005; WAHAB 2010). Nevertheless, although Hippocrates linked the seizures to a problem in brain function more than 2,000 years ago, the first modern definition of epilepsy was given in 1875 by Hughlings Jackson, who recognized a seizure as being due to disordered brain electricity, which can alter consciousness, sensation and behaviour (WORLD HEALTH ORGANIZATION 2005; WEIERGRÄBER ET AL. 2010; WAHAB 2010). The discovery of the human electroencephalography in the 1920s helped in correlating the neuronal activities to the behavioural disorders, and the remarkable advances in molecular biology, neurophysiology, genetics, functional imaging and numerous neurochemical techniques have contributed to deep the understanding of the basic mechanisms underlying seizures and epilepsy, allowing the exploitation of the concepts behind excitability, inhibition, modulation, neurotransmission and synchronisation (WORLD HEALTH ORGANIZATION 2005). Notwithstanding, although epilepsy is recognized as a neurological disorder since the 19th century, despite the considerable developments on neurophysiology and neurochemistry, the understanding of the molecular and cellular mechanisms underlying the genesis and progression of epileptic seizures (ictogenesis) remains unclear, as well as those mechanisms involved in transforming the normal brain tissue into a seizure-prone brain tissue (epileptogenesis) (BLAUWBLOMME ET AL. 2014; BOISON 2016). Nevertheless, it is recognised that γ-aminobutyric acid (GABA) and glutamate are the brain's most plentiful inhibitory and excitatory neurotransmitters, respectively, working together to control the brain's overall level of excitability. Regarding this, it is broadly acknowledged that an imbalance between inhibitory GABAergic system and excitatory glutamatergic system is a potential mechanism underlying seizure activity and cell death; on the other hand, changes in voltage- and receptor-gated ion channels also appear to be involved in the pathogenesis of epilepsy (KWAN ET AL. 2001; BRODIE 2010; LASOŃ ET AL. 2013).

I.1.2. Epidemiology and costs

With an increased risk of morbidity and mortality that significantly affects the patients' quality of life, epilepsy is one of the most prevalent non-communicable neurological conditions (LHATOO AND SANDER 2005; NGUGI ET AL. 2011) and the third most common neurological disorder, positioning itself just behind the stroke and Alzheimer's disease (SARMA ET AL. 2016; MULA AND SANDER 2016). This disorder affects almost 70 million people worldwide (KAUR ET AL. 2016).

The prevalence of epilepsy in low- and middle-income countries is about twice that of high-income countries, being estimated an overall prevalence of 0.7% (SCHMIDT AND SCHACHTER 2014). In Europe, the prevalence of this illness was reported to range between 4.3 and 7.8 per 1,000 (PUGLIATTI ET AL. 2007). On the other hand, the overall annual incidence of epilepsy ranges from 40 to 70 cases per 100,000 people in industrialised countries (SANDER 2003; DUNCAN ET AL. 2006; LAXER ET AL. 2014). The few incidence studies performed in developing countries show rates from 49.3 to 190 per 100,000 population (WORLD HEALTH ORGANIZATION 2005). The reported epilepsy incidence and prevalence vary widely despite this medical disorder is amongst the most common serious neurological conditions (BELL AND SANDER 2002). Epilepsy knows no geographical, ethnic or social boundaries (BELL AND SANDER 2002; WORLD HEALTH ORGANIZATION 2005). Nevertheless, prevalence and incidence of epilepsy differ by demographic factors including age, gender, race and socioeconomic status (DUNCAN ET AL. 2006; BANERJEE ET AL. 2009). Indeed, the incidence rate of epilepsy varies considerably with age showing a bimodal distribution characterized by steeply increases in childhood and in the elderly (BEGHI ET AL. 2009).

An initial estimative in Europe reported a total economic cost for epilepsy of €15.5 billion, with total costs per case ranging from €2,000 to €11,500 showing a high variability among countries. The costs are believed to be increased in western countries not only due to the overall number of cases, but also to the quality of their health system (PUGLIATTI ET AL. 2007). It is also recognised that drug-refractory epilepsy can increase the cost per patient, with indirect costs rising to more than three times when comparing with seizure-free patients (VAN HOUT ET AL. 1997; JACOBY ET AL. 1998).

I.1.3. Epilepsy and epileptic seizures

Epilepsy was conceptually defined in 2005 by the International League against Epilepsy (ILAE) as "a disorder of the brain characterized by an enduring predisposition to generate epileptic seizures and by the neurobiological, cognitive, psychological, and social consequences of this condition", requiring the occurrence of at least one epileptic seizure (FISHER ET AL. 2005). In general, the diagnosis of epilepsy was reported to imply a persistent epileptogenic abnormality of the brain that is able to spontaneously generate paroxysmal activity (ENGEL 2006). In turn, an epileptic seizure was defined by ILAE as "a transient occurrence of signs and/or symptoms due to abnormal excessive or synchronous neuronal activity in the brain" (FISHER ET AL. 2017a; FISHER ET AL. 2017b). Notwithstanding, some of the above definitions, created in a document

generated by an ILAE Task Force in 2005, are currently considered conceptual (theoretical) and not sufficiently detailed to provide guidance on how enduring predisposition should be defined, particularly for those individuals presenting a single unprovoked seizure. Therefore, new recommendations have recently been published and adopted as a position of the ILAE, where epilepsy is reported as "a disease of the brain defined by any of the following conditions: (1) at least two unprovoked (or reflex) seizures occurring greater than 24 h apart; (2) one unprovoked (or reflex) seizure and a probability of further seizures similar to the general recurrence risk (at least 60%) after two unprovoked seizures, occurring over the next 10 years; (3) diagnosis of an epilepsy syndrome" (FISHER ET AL. 2017a). Accordingly, epilepsy is considered to be resolved for individuals who had an age-dependent epilepsy syndrome but are now past the applicable age or those who have remained seizure-free for the last 10 years, with no seizure medicines for the last 5 years (FISHER ET AL. 2017a). In fact, patients may have seizures intermittently, with periods of months to years between seizures (GOLDENBERG 2010).

Seizures result from a shift in the normal balance of excitability and inhibition within the central nervous system (CNS) as well as from abnormal brain function. Nevertheless, because various factors control neuronal excitability, this normal balance can be disturbed in many different ways, and thus, there are many causes of seizures and epilepsy. Nonetheless, no cause can be found in about 70% of patients. The normal brain is capable of experiencing a seizure under certain circumstances, and individuals vary in their susceptibility or threshold for seizures. Accordingly, there are several possible causes of seizures in a given patient, epilepsy can be acquired as a result of an insult to the brain such as trauma, infection, stroke or a tumour, or can result from a genetic mutation in one or more of the ion channel or neurotransmitter genes or proteins that control brain excitability (BIALER AND WHITE 2010; GOLDENBERG 2010; PATI AND ALEXOPOULOS 2010; MARCHI ET AL. 2011; TSUKAMOTO ET AL. 2016).

I.1.4. Therapeutic approaches

After the diagnosis of seizures or epilepsy is made, the next step is to select the best form of treatment. Relatively few patients can be managed with nonpharmacological options namely surgery, vagus nerve stimulation or ketogenic diet. In fact, these options are primarily reserved for a few selected cases, usually upon antiepileptic drugs (AED) failure and, consequently, the AEDs continue to be the mainstay of epilepsy treatment (SHETH ET AL. 2005; SCHMIDT 2009; GOLDENBERG 2010; GSCHWIND AND SEECK 2016; SHORVON AND SCHMIDT 2016). AEDs also show therapeutic benefits to treat migraine headache, neuropathic pain and bipolar affective disorder, among other CNS conditions (ROGAWSKI AND LÖSCHER 2004; BIALER 2012a; CALLEGARI ET AL. 2016; SIDHU AND SADHOTRA 2016). Actually, the AEDs are among the most commonly prescribed centrally active agents (BROWN 2016). The primary goal of the treatment is to prevent the onset of seizures or reduce their frequency as much as possible, avoid adverse effects associated with long-term treatment, aid patients in maintaining or restoring their usual psychosocial and

vocational activities and in maintaining a normal lifestyle (SHETH ET AL. 2005). In effect, the resective surgery is restricted to patients with focal epilepsy in which the epileptogenic zone can be adequately identified (FOLDVARY ET AL. 2001).

The modern treatment of epilepsy began with potassium bromide, which was firstly mentioned in the Lancet of 23rd May, 1857, during the discussion of a paper presented at the Royal Medical and Chirurgical Society by Dr Edward Sieveking. Nevertheless, although there are no randomized clinical trials with bromide, there is enough clinical data to support its claim to be the first effective AED (CLOUSTON 1868). Actually, bromide has support to this day as a potential "drug of tertiary choice in the treatment of children with epilepsy" (BRODIE 2010). Nevertheless, the pharmacological age of AED therapy began with the serendipitous discovery by Alfred Hauptmann, in 1912, of the anticonvulsant properties of phenobarbital (PB) (PERUCCA 2001; BRODIE 2010; SHORVON AND SCHMIDT 2016). Indeed, this drug is still the most widely prescribed AED in the developing countries and remains a popular choice in many industrialized countries, in part because of its modest cost (BRODIE 2010). In the next years, several AEDs like phenytoin (PHT), primidone (PRM), ethosuximide, carbamazepine (CBZ), sodium valproate, and also a range of benzodiazepines, became available on the pharmaceutical market, and nowadays, they are regarded as "established" AEDs in clinical practice (BRODIE AND DICHTER 1996; BRODIE 2010). Nevertheless, although these older generations of AEDs continue to be widely used in the treatment of epilepsy, these drugs have important shortcomings such as a highly variable and nonlinear pharmacokinetics, a narrow therapeutic index, suboptimal response rates, and a propensity to cause significant adverse effects and drug interactions (PERUCCA 2001).

Indeed, the modern era of AED development began in 1975 with the establishment of the Anticonvulsant Drug Development Programme by the National Institute of Neurological Disorders and Stroke in the United States. Since then, more than 28,000 new chemical entities from academic and pharmaceutical chemists have been screened, which resulted in the license of an increasing list of AEDs (BRODIE 2010; JACOB AND NAIR 2016). Actually, since the beginning of the 1990s several new AEDs were approved by the U.S. Food and Drug Administration (FDA) and/or by the European Medicines Agency (EMA) [e.g., eslicarbazepine acetate, felbamate, gabapentin, lamotrigine (LTG), levetiracetam, oxcarbazepine (OXC), pregabalin, rufinamide, stiripentol, tiagabine, topiramate, vigabatrin and zonisamide] (BRODIE 2010; BIALER 2012b; ABRAHAM AND SHAJU 2013; SARMA ET AL. 2016). The majority of these AEDs offers appreciable advantages in terms of their favourable pharmacokinetics, improved tolerability and lower potential for drug interactions comparatively to the older AEDs (BRODIE 2010; BIALER 2012b; VENTOLA 2014; GSCHWIND AND SEECK 2016). Nonetheless, these newer AEDs are more expensive than the older drugs, and are also associated with the potential to cause birth defects (HILL ET AL. 2010; GOLDENBERG 2010; SARMA ET AL. 2016). In effect, although the ideal AED should suppress all seizures without causing any unwanted adverse effects, currently available AEDs not only fail to control seizure activity in some patients, but also frequently produce adverse effects that range in severity from minimal impairment of the CNS to death, or aplastic anaemia or hepatic failure (GOLDENBERG 2010). However, due to the limited clinical experience with new

agents, the mechanisms of action of individual AEDs may be an important criterion in this decision-making process (KWAN ET AL. 2001).

The AEDs currently marketed or those in today's AED pipeline were mainly discovered by one of the following pathways: a target/mechanism-oriented rational drug design; a serendipitous discovery by systematic screening of the anticonvulsant activity of new compounds; and a more-or-less rational drug design based on structural modification of existing AEDs (SMITH ET AL. 2007; BRODIE 2010; BROWN 2016). Considering the clinical impact of these three AED discovery approaches, Meir Bialer, a recognised scientist in the area, has pointed out that target-based drug design has not been as useful as would be expected in the development of AEDs. Indeed, the most successful AEDs have multiple mechanisms of action, and those developed by mechanism-based design are not widely used due to serious side effects related to the single mechanism of action. Moreover, it has been suggested that AEDs with multiple mechanisms of action have an enhanced probability of being efficacious in refractory epilepsy (BIALER 2012b).

The primary mechanisms of action of AEDs at excitatory and inhibitory synapses are represented in the Figure I.1.1. Actually, the selection of the most suitable AED, or a combination of AEDs, for individual patients has been complicated by the undoubtedly beneficial expansion of the pharmacological armamentarium for the treatment of epilepsy (KWAN ET AL. 2001; ST LOUIS ET AL. 2009).

DECKERS ET AL. (2000) proposed the classification of AEDs based upon the following mechanisms: (1) drugs which block sustained repetitive firing in individual neurons, mainly due to the blockade of voltage-dependent sodium or calcium channels (CBZ, gabapentin, LTG, OXC, PB, PHT, topiramate, valproate); (2) drugs enhancing inhibitory events mediated by GABA (benzodiazepines, gabapentin, PB, tiagabine, topiramate, vigabatrin, and valproate); (3) practically consists of one drug – ethosuximide - which blocks T-type calcium channels and is active against absences, but recent evidence also suggests that zonisamide may be a T-type calcium channel inhibitor; and (4) drugs that reduce events mediated by excitatory amino acids like glutamate (felbamate, PB, and topiramate).

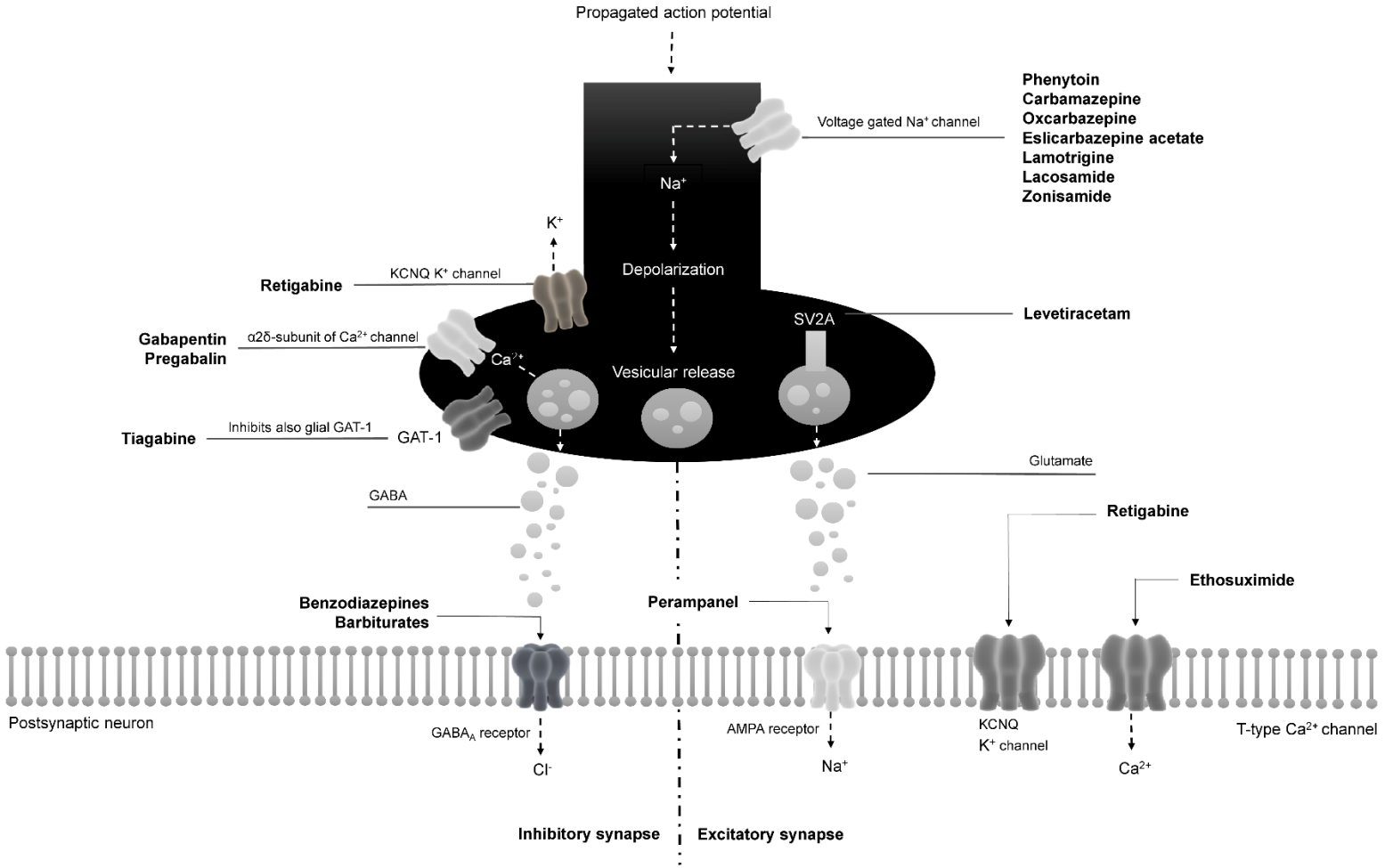

Figure I.1.1. Mechanisms of action of antiepileptic drugs at excitatory and inhibitory synapses. AMPA, α-amino-3-hydroxy-5-methyl-4-isoxazole-propionic acid; GABA, γ-aminobutyric acid; GAT-1, sodium- and chloride-dependent GABA transporter 1; SV2A, synaptic vesicle glycoprotein 2A. Adapted from Bialer and White (2010); Schmidt and Schachter (2014); and Singh and Brashier (2014).

In spite of monotherapy remains the treatment of choice for newly diagnosed epilepsy, polytherapy with more than one AED is considered after the failure of two or three AEDs given as monotherapy regimens (KAMINSKI ET AL. 2009; ST LOUIS ET AL. 2009; ABRAHAM AND SHAJU 2013). Nevertheless, combinations of AEDs should be carefully selected based on the potential for synergic effects that are not associated with unfavourable pharmacokinetic interactions and toxicity. Indeed, because lower doses of AEDs may be used, adverse effects can be expected to be reduced in combination treatments. Unfortunately, there is still a very limited clinical evidence on how and when combining AEDs. Consequently, preclinical studies could offer some experimental guidelines as to which AED combinations appear to be therapeutically advantageous (KAMINSKI ET AL. 2009). In fact, a large number of studies have been concentrated on AED interactions using nonclinical models of epilepsy (DECKERS ET AL. 2000; JONKER ET AL. 2007; STAFSTROM 2010; LEE AND DWORETZKY 2010; LÖSCHER 2011).

Given the current status, the effective therapy for epilepsy is undoubtedly an unmet clinical need and it is urgent to continue developing new AEDs. Therefore, the search for new anticonvulsant lead compounds among phytochemical constituents has emerged as a promissory and alternative drug discovery approach (NEWMAN AND CRAGG 2016). Actually, to discover natural compounds with fewer side effects and that decrease the frequency and intensity or duration of seizures would be extremely relevant in future AED development programs. It is noteworthy that natural products or derivatives of natural products account for more than half of the medically important pharmaceutical drugs (NEWMAN AND CRAGG 2012). In reality, natural products used in folk medicine represent a great deal of untapped reservoir of drugs and continue to contribute for the discovery of modern drugs worldwide, being a source of great value for the discovery of AEDs with novel structures as well as better pharmacokinetic, safety and efficacy profiles (JAMILU ET AL. 2007; NASSIRI-ASL ET AL. 2007; SAYYAH ET AL. 2011; YAZDI ET AL. 2011; VIJAYALAKSHMI ET AL. 2011; KHODAPARAST ET AL. 2012). For instance, according to the progress report on new AEDs published as a summary of the Thirteenth Eilat Conference on New Antiepileptic Drugs and Devices (EILAT XIII) that took place in Madrid (Spain) in 2016, at least three of the AEDs candidates in clinical development (cannabidiol, cannabidivarin and huperzine A) are herb-derived compounds; cannabidiol and cannabidivarin are components of the *Cannabis sativa* and huperzine A is a small naturally occurring alkaloid derived from the Chinese herb *Huperzia serrata*. More specifically, cannabidiol is under phase III clinical trials, while cannabidivarin and huperzine A are entering phase II clinical trials (BIALER ET AL. 2017). In this context, FERREIRA ET AL. (2016a) prepared and published an extensive review about the anticonvulsant properties of huperzine A from *Huperzia serrata*.

I.2. Pharmacoresistant Epilepsy

The concept of pharmacoresistance and P-glycoprotein

I.2.1. Pharmacoresistant epilepsy

Although the concept of pharmacoresistant epilepsy, often used interchangeably with drug resistant or medically refractory/intractable epilepsy, may appear self-explanatory and intuitive, there has been no uniformly accepted definition of this condition, and a precise definition has remained elusive (KWAN ET AL. 2010a; ALEXOPOULOS 2013; DALIC AND COOK 2016). Clinically, this condition is typically defined according to the number of anticonvulsant drugs that a patient has tried unsuccessfully, the frequency of seizures, the duration of the seizures, and the extent of any remission(s) (WEAVER 2013). Hence, a dedicated task force of the ILAE took a significant step forward by developing a global consensus-definition of drug-resistant epilepsy (KWAN ET AL. 2010a). According to this proposal, pharmacoresistant epilepsy may be defined as "failure of adequate drug trials of two tolerated and appropriately chosen and used AED regimens (whether as monotherapy or in combination) to achieve seizure freedom" (KWAN ET AL. 2010a). The definition is consistent with the clinical observation that if seizure freedom is not achieved with only two trials of appropriate AED regimens, the likelihood of therapeutic success with subsequent regimens declines sharply (KWAN ET AL. 2010a). Nevertheless, the definition of this condition will remain incomplete without a better understanding of the underlying cellular and molecular mechanisms (ALEXOPOULOS 2013; DALIC AND COOK 2016). Notwithstanding, the variability of its appearance across different types of epilepsy, as well as the variability of seizure control within a given patient over time, complicates the prospective identification of pharmacoresistance (BERG 2009).

Drug-resistant epilepsy is one of the most important challenges in epilepsy management (VENTOLA 2014; DALIC AND COOK 2016). Pharmacoresistant epilepsy has a great impact on the daily life of patients and their families, and has also a substantial impact on society due to the loss of employment potential and cost of medical care (ALEXOPOULOS 2013; WEAVER 2013; DE KINDEREN ET AL. 2014). Actually, neuropsychological, psychiatric and social impairments that reduce patients' quality of life, as well as increase morbidity and mortality, are consequences of the failure in response or partial response to AEDs in individuals who continue to experience incapacitating seizures. Indeed, the pharmacoresistant epilepsy is usually a lifelong condition strongly associated with psychiatric complications like depression and/or anxiety, feelings of lack of control and independence, and a host of AED-related adverse effects such as cognitive impairment, sexual dysfunction or weight gain (ALEXOPOULOS ET AL. 2007; ST LOUIS AND LOUIS 2009; BERG 2009; WEAVER 2013). Individuals with pharmacoresistant epilepsy are also at higher risk of suicide than the general population (LHATOO AND SANDER 2005; MEADOR 2008; VERROTTI ET AL. 2008). Nevertheless, despite the large therapeutic arsenal of old and new AEDs, approximately 55–60% of people with focal epilepsy and up to 20% of patients with primary generalized epilepsy develop drug resistance during the course of their condition (FAUGHT 2004; KWAN ET AL. 2010a; PATI AND ALEXOPOULOS 2010; WEAVER 2013). In fact, the proportion of patients failing to respond to drug treatment has not been changed to any significant extent in spite of the emergence a large number of new AEDs (LÖSCHER AND SCHMIDT 2002; GIDAL 2014; VENTOLA 2014; BAULAC ET AL.

2015; FRANCO ET AL. 2016). Hence, many patients are not seizure-free even under appropriate pharmacotherapy with the currently available AEDs, including under combination therapy with rational polytherapy regimens (BRODIE 2010).

While the reasons for this drug resistance are no doubt multifactorial, there is a growing body of evidence derived not only from animal models, but also by examinations of brain tissue of patients undergoing surgical resection, that the failure of AEDs to reach their molecular targets may explain the drug resistance in epilepsy (GIDAL 2014). Nevertheless, refractory epilepsy is generally reflects a complex multifactorial phenomenon to which genetic and acquired factors may contribute (BRODIE 2010). It has been suggested that AEDs with multiple mechanisms have an enhanced probability of being efficacious in refractory epilepsy (BIALER 2012b). Anyhow, none of the old or new AEDs appears to represent a 'cure' for epilepsy or an efficacious means for preventing epilepsy or its progression. Consequently, new concepts and original ideas for developing new AEDs, or for improving the therapeutic profile of the existing ones, are urgently needed (LÖSCHER AND SCHMIDT 2002; LÖSCHER AND SCHMIDT 2006). At this moment, the main use of new generation AEDs remains to be as adjunctive therapy in the management of patients refractory to older agents (PERUCCA 2001; KAUR ET AL. 2016).

Nevertheless, in the coming years, the recognition and validation of useful predictive markers to clinically identify resistant or responsive patient populations may gain a greater importance and strongly influence not only the initial therapy but also to increase the chance of success.

I.2.2. The pharmacoresistance phenomenon

The pharmacoresistance or multidrug resistance phenomenon was described for the first time in 1968 by Kessel and collaborators (KESSEL ET AL. 1968). Multidrug resistance refers to the phenomenon of simultaneous resistance to various structurally and functionally unrelated drugs, and it may be developed in response to a specific drug or drug combination (LING 1997; VAN DER KOLK ET AL. 2000; DEELEY ET AL. 2006). Moreover, it often encompasses agents to which individuals have not been previously exposed, and which may or may not share targets and mechanisms of action with those that elicited the development of drug resistance (DEELEY ET AL. 2006). The resistance to drug treatment still represents one of the major problems in the pharmacotherapy of several diseases. Actually, pharmacoresistance is not unique to epilepsy. Indeed, it is now recognized in diverse brain disorders including depression and schizophrenia, as well as in other diseases affecting the brain such as human immunodeficiency virus infection and many forms of cancer (BRANDT ET AL. 2006; PATI AND ALEXOPOULOS 2010).

Based on animal models and patients' findings, five hypotheses have been proposed to explain, at least in part, the pharmacoresistance phenomenon verified in epilepsy: the target hypothesis, which suggests that acquired alterations to the structure and/or functionality of target ion channels and neurotransmitter receptors lead to insufficient pharmacodynamic activity of AEDs in the brain; the network hypothesis, which proposes that structural brain

alterations and/or network changes (for example, hippocampal sclerosis) are involved in resistance to AEDs; the gene variant hypothesis, which suggests that there is an inherent resistance that is governed by genetic variants of proteins that are involved in the pharmacokinetics and pharmacodynamics of AED activity; the intrinsic severity hypothesis, which suggests that an increased disease severity leads to drug intractability; and the transporter hypothesis, which suggests an inadequate penetration of AEDs across the blood–brain barrier caused by the overexpression and/or increased activity of drug efflux transporters belonging to the adenosine triphosphate (ATP)-binding cassette (ABC) transporter superfamily, thus leading to insufficient drug levels in epileptogenic brain tissue.

Relatively to the network hypothesis, a clinical proof of concept has been achieved through demonstration that the surgical resection of the altered network counteracts AED resistance and may even cure epilepsy (WIEBE AND JETTE 2012; ROGAWSKI 2013; LÖSCHER ET AL. 2013; WANG ET AL. 2016). In what concerns the gene variant, the intrinsic severity, and the popular target hypothesis, evidence is currently more limited (LÖSCHER ET AL. 2013). Nevertheless, a reduction in the sensitivity of major therapeutic targets for many of the clinically established AEDs, namely the voltage-gated sodium channel and the γ-aminobutyric acid type A ($GABA_A$) receptor, has been suggested to have an important role in AED-resistant chronic human and experimental epilepsy (ROGAWSKI AND LÖSCHER 2004; SCHMIDT AND LÖSCHER 2005; REMY AND BECK 2006). Accordingly, those AEDs acting through other targets that are not downregulated in epilepsy could potentially offer important advantages.

Nonetheless, up to date, the transporter hypothesis is the mostly investigated theory and it is recognised as one of the most important mechanisms implicated in the pharmacoresistant epilepsy (GIRARDIN 2006; CHANG 2007; BORSKA ET AL. 2010; GIACOMINI ET AL. 2010; FELDMANN AND KOEPP 2016). Specifically, the role of the drug efflux transporter P-glycoprotein (P-gp) has been emphasized. The first evidence that supports this hypothesis was the overexpression of P-gp [the human multidrug resistance-1 gene *(MDR1)* product] and the up-regulation of *MDR1* gene itself in the brain tissue of pharmacoresistant epileptic patients when compared to drug-responsive patients (TISHLER ET AL. 1995; SISODIYA ET AL. 1999). The same observations were posteriorly reported in other studies (LAZAROWSKI ET AL. 1999; DOMBROWSKI ET AL. 2001; POTSCHKA AND LÖSCHER 2002; ARONICA ET AL. 2003; SISODIYA 2003; MARRONI ET AL. 2003; ARONICA ET AL. 2004; MARCHI ET AL. 2004; JÓŹWIAK 2007; KWAN ET AL. 2010b). Those findings in human epileptic patients have also been found in animal models of epilepsy. This kind of studies gives the possibility to select pharmacoresistant epileptic animals (non-responsive) and the responsive ones (BRANDT ET AL. 2004). Thus, an increased expression of P-gp in brain tissue of epileptic rats has been also observed, and it was shown to be higher in non-responsive animals (SEEGERS ET AL. 2002b; RIZZI ET AL. 2002; SEEGERS ET AL. 2002a; VAN VLIET ET AL. 2004; POTSCHKA ET AL. 2004; VOLK AND LÖSCHER 2005; LÖSCHER AND POTSCHKA 2005a; MARCHI ET AL. 2006; LIU ET AL. 2007; BAUER ET AL. 2008; NISHIMURA ET AL. 2008; BARTMANN ET AL. 2010). Moreover, it has also been described that P-gp overexpression involves seizure-relevant brain structures (SEEGERS ET AL. 2002b; VOLK ET AL. 2004b; VAN VLIET ET AL. 2007). Several preclinical studies revealed that the absence of the rodent multidrug

resistance-1 gene *(mdr1) a* or *b* genes is responsible by a significant increase in the brain uptake of various lipophilic drugs (SHARMA ET AL. 2015).

Many of the ABC drug efflux transporters are primarily located in the cell membrane where they can extrude a variety of structurally diverse drugs, drug conjugates and metabolites, and other compounds from the inside of cells (SCHINKEL AND JONKER 2012). In all mammalian species, these multidomain integral membrane proteins use energy of ATP hydrolysis to the translocation of solutes across cellular membranes against the concentration gradient (LÖSCHER AND POTSCHKA 2005b), reducing, consequently, the intracellular concentration of the substrates (DANTZIG ET AL. 2003; LÖSCHER AND POTSCHKA 2005b; SCHINKEL AND JONKER 2012). Indeed, drugs ability to cross cellular barriers and reach their therapeutic targets in appropriate concentrations is critical for their efficacy, and it may be considerably determined through the active efflux mediated by membrane proteins (CHAN ET AL. 2004; PÉREZ-TOMÁS 2006). Thus, transmembrane efflux proteins can be major determinants of the pharmacokinetics, safety and efficacy profiles of drugs (GIACOMINI ET AL. 2010). These membrane transporters are expressed in different cells and tissues such as lymphocytes, intestine, liver, kidney, testis, placenta, and CNS and, therefore, they are critical to the disposition of many xenobiotics (WANG ET AL. 2002; MCCORMICK ET AL. 2015; PRACHAYASITTIKUL AND PRACHAYASITTIKUL 2016). In fact, the pharmacological properties of many drugs in current use are affected by these membrane transporters, which may determine the rate and extent of the absorption, distribution and elimination processes. Furthermore, the ABC transporters can extensively limit the drug penetration into specific cells and tissue compartments, restricting the access of drugs into important pharmacological sanctuaries such as brain, testis and foetus. Therefore, the clinical efficacy and toxicity of many drugs may be determined on a large extent by drug interactions with ABC transporters (SCHINKEL AND JONKER 2012). Actually, although the family of mammalian ABC transporters is extensive and functionally highly diverse, the P-gp, the multidrug resistance-associated proteins (MRPs) 1–5 (MRP1, MRP2, MRP3, MRP4 and MRP5), and the breast cancer resistance protein (BCRP) have demonstrated a clinically significant role in the transport of relevant drugs (SCHINKEL AND JONKER 2012; CHEN ET AL. 2016). Indeed, apart from P-gp, the MRP1, MRP2 and BCRP were also found to be up-regulated and/or overexpressed in the blood-brain barrier endothelial cells, not only of rats but also of drug-resistant patients (ARONICA ET AL. 2003; VAN VLIET ET AL. 2006).

I.2.2.1. P-glycoprotein

P-gp is certainly the most studied drug efflux membrane transporter of the ABC transporter superfamily (SCHINKEL AND JONKER 2012; WILKENS 2015). P-gp was originally discovered in 1976 by Juliano and Ling as a surface glycoprotein, which was overexpressed in drug resistant ovary cells mutants from Chinese hamster (JULIANO AND LING 1976). The discovery of P-gp, more than 40 years ago, demonstrated that a single protein may confer resistance to a relatively large number of structurally diverse drugs with different mechanisms of action (DEELEY ET AL. 2006).

Consequently, the resistance conferred by P-gp efflux transporter is the best characterized process among the various putative mechanisms of multidrug resistance, and it is of considerable clinical importance (WANG ET AL. 2002; LÖSCHER AND POTSCHKA 2005b; BANSAL ET AL. 2009). This transmembrane active efflux system has been found in numerous species (insects, fish, amphibians, reptiles, birds and mammalians), although there are differences among them (LÖSCHER AND POTSCHKA 2002a; FORTUNA ET AL. 2011a).

The human gene encoding for multidrug resistance associated to P-gp is *MDR1* (*ABCB1*), while in mice are *mdr1a* (*abcb1a*) and *mdr1b* (*abcb1b*) (FORTUNA ET AL. 2011a). The combined tissue distribution of *mdr1a* and *mdr1b* transcripts in rodents roughly coincides with that of the *MDR1* mRNA transcripts in humans (KWAN AND BRODIE 2005; LINNET AND EJSING 2008; DEL AMO ET AL. 2009). Hence, it is believed that those two genes in rodents perform the same functions of the human *MDR1* gene (LÖSCHER AND POTSCHKA 2002a; CHAN ET AL. 2004; KWAN AND BRODIE 2005; LINNET AND EJSING 2008; ZHANG ET AL. 2012a). There is 82% homology between human *MDR1* and mouse *mdr1a* genes, and the corresponding value between human *MDR1* and mouse *mdr1b* is 79% (DEL AMO ET AL. 2009). The denomination P-gp usually refers to the protein encoded by *MDR1*, *mdr1a* and *1b* genes and, therefore, it will be herein followed.

The human P-gp is predominantly and physiologically expressed at the apical/luminal membrane of polarized cells in several normal tissues with secretory (small intestine, liver, kidney, adrenal gland) and barrier functions (small intestine, blood-brain barrier, blood-testis barrier, blood-ovarian barrier and placenta) (VOLK ET AL. 2004a; FROMM 2004; GIACOMINI ET AL. 2010; MARQUEZ AND VAN BAMBEKE 2011). Indeed, P-gp forms a functional barrier that protects the body by actively limiting the absorption and systemic distribution of xenobiotic compounds, and/or increasing their elimination together with xenobiotic-metabolizing enzymes (LÖSCHER AND POTSCHKA 2002b; DANTZIG ET AL. 2003; VOLK ET AL. 2004a; FROMM 2004; KWAN AND BRODIE 2005; DEL AMO ET AL. 2009). Thus, many xenobiotics are metabolized and/or excreted into bile, urine, and intestinal lumen, preventing their accumulation in body tissues (FROMM 2004; TANDON ET AL. 2006). In fact, the strategic physiological expression of P-gp in organs that play key roles in the processes of drug absorption and disposition suggests that P-gp has a relevant impact on the pharmacokinetics of its substrate molecules, including many clinically important therapeutic agents (TANDON ET AL. 2006; DEL AMO ET AL. 2009; FORTUNA ET AL. 2011a). Moreover, P-gp has also been associated to other physiological functions such as the transport of steroid hormones, transport of ions, and secretion of cytokines (DEL AMO ET AL. 2009). In addition, emerging evidence shows that P-gp expression is also changed at the level of blood-brain barrier during pathophysiology and/or therapy of CNS diseases such as epilepsy and stroke (LÖSCHER AND POTSCHKA 2002b; SEEGERS ET AL. 2002c; KUBOTA ET AL. 2006; MILLER ET AL. 2009), as well as in multidrug resistant tumour cells (ZHANG ET AL. 2012a).

The human P-gp contains two homologous and symmetrical distinct halves, called NH_2- and COOH-terminal halves (Figure I.2.1) (YANG ET AL. 2008; DEL AMO ET AL. 2009; SCHINKEL AND JONKER 2012; BREIER ET AL. 2013). Each half comprises a transmembrane domain (TMD) and a cytosolic nucleotide-binding domain (NBD) or ABC unit (BREIER ET AL. 2013; WILKENS 2015; CHEN ET AL. 2016).

The two halves are joined by a 60 amino acid linker region and each TMD is composed by six transmembrane α-helix segments (TMs) (PIETRO ET AL. 2002; RAMAKRISHNAN 2003; BREIER ET AL. 2013). The TMDs mediate the binding and efflux transport of P-gp substrates using energy derived from the hydrolysis of ATP at the NBD (SHEU ET AL. 2010). The NBDs are peripherally located at the cytoplasmic face of the cell membrane and they bind ATP and couple ATP hydrolysis with the drug transport process (CHAN ET AL. 2009). The twelve TMs fold together to form a barrel-like structure that crosses the plasma membrane (RAMAKRISHNAN 2003; LINNET AND EJSING 2008). The substrate specificity for P-gp is determined by the TM5, TM6, TM11 and TM12, which seem to be integrated to form a large drug binding pocket (BELLAMY 1996; BREIER ET AL. 2013). The drug recognition by P-gp, followed by ATP-binding and subsequent hydrolysis are essential to actively export relatively lipophilic substrates out of the lipid bilayer of the cell membrane to the extracellular medium (TANDON ET AL. 2006; BANSAL ET AL. 2009; DEL AMO ET AL. 2009).

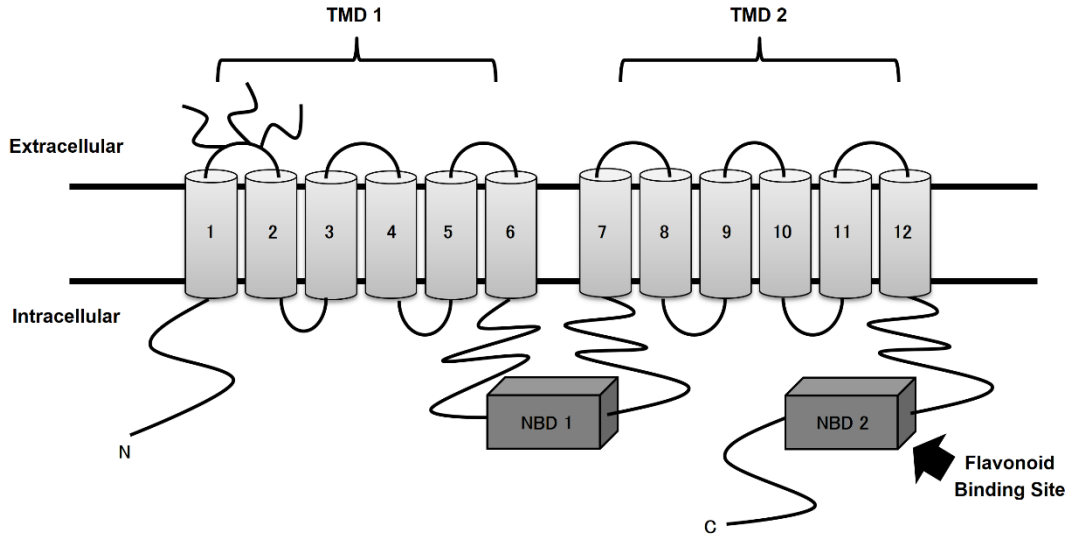

Figure I.2.1. Structure of P-glycoprotein (C, COOH; NBD, nucleotide-binding domain; N, NH2; TMD, transmembrane domain). Adapted from DEL AMO ET AL. (2009) and SCHINKEL AND JONKER (2012).

I.2.2.1.1. P-glycoprotein-mediated drug transport

Several models have been proposed to explain the mechanism of P-gp–mediated drug transport. The *pore*, the *flippase* and the *hydrophobic vacuum cleaner* are the most popular models of P-gp function (Figure I.2.2) (KRISHNA AND MAYER 2000; RAMAKRISHNAN 2003; VARMA 2003; HENNESSY AND SPIERS 2007; BANSAL ET AL. 2009; DEL AMO ET AL. 2009).

According to the *pore* model, in the absence of the nucleotide, both TMDs form a single barrel with a central pore that opens to the extracellular surface and spans much of the membrane depth. On the contrary, upon binding of nucleotides, the TMDs reorganize into three compact domains that open the central pore along its length, allowing the direct access of hydrophobic drugs from the lipid bilayer to the central pore of the transporter (Figure I.2.2a) (VARMA 2003; BANSAL ET AL. 2009). P-gp has also been suggested to function as a *flippase* that flips the substrate

from the inner leaflet of the lipid bilayer to the outer leaflet of the plasma membrane, or directly to the extracellular environment against the concentration gradient (Figure I.2.2b) (RAMAKRISHNAN 2003; HENNESSY AND SPIERS 2007; BANSAL ET AL. 2009; DEL AMO ET AL. 2009). The *flippase* model is based on the idea that after interaction of the substrate with the membrane, the substrate can access to the core of TMDs from the lipid bilayer and, then, P-gp flips the drug from the inner to the outer leaflet in an ATP hydrolysis-dependent manner (RAMAKRISHNAN 2003). The assumptions of the substrates partition into the lipid phase prior to interacting with P-gp and the location of a P-gp binding pocket in the internal part of the plasma membrane are considered in both models (HENNESSY AND SPIERS 2007; DEL AMO ET AL. 2009). These characteristics may explain the unusually broad substrate specificity of P-gp since the primary determinant for substrate specificity seems to be its ability to intercalate into the lipid bilayer appropriately, being the subsequent interaction with the substrate-binding site of secondary importance (HENNESSY AND SPIERS 2007). Finally, the *hydrophobic vacuum cleaner* (Figure I.2.2c) combines the features of *pore* and *flippase* models (VARMA 2003) and the designation of *hydrophobic* is due to the fact that the majority of P-gp substrates have been found to be hydrophobic compounds with a planar ring system, and often carrying a positive charge at physiological pH (BANSAL ET AL. 2009). This model suggests that P-gp binds directly to the hydrophobic compounds embedded in the inner leaf of the plasma membrane and transports the substrate from the lipid bilayer to the extracellular medium through a protein channel (KRISHNA AND MAYER 2000; RAMAKRISHNAN 2003; HENNESSY AND SPIERS 2007; BANSAL ET AL. 2009; DEL AMO ET AL. 2009). Structural data indicate that the substrates could access to their binding sites through *gates* formed between TMs 5/8 and 2/11 (HENNESSY AND SPIERS 2007). However, other mechanisms are also suggested particularly because uncharged hydrophilic molecules with planar ring systems (e.g., colchicine) are also effluxed out by P-gp. The change in electric potential and pH across membrane seems to contribute to that process (BANSAL ET AL. 2009) as well as the conformational changes that P-gp undergoes when nucleotide binds to the intracellular NBDs (VARMA 2003; BANSAL ET AL. 2009).

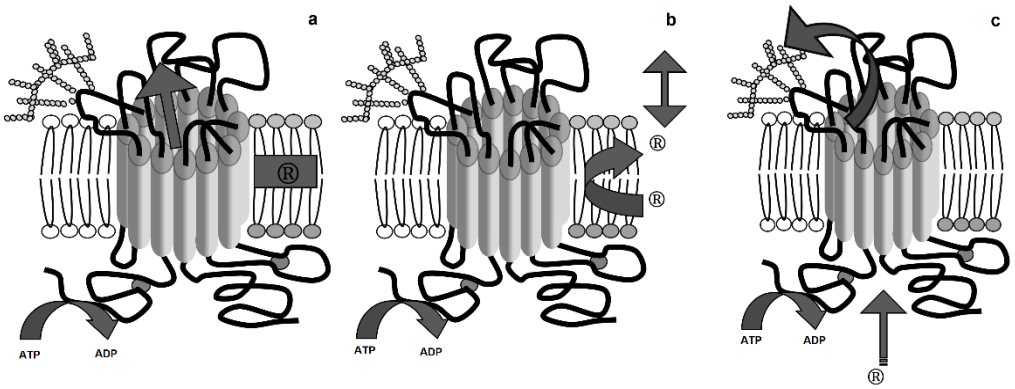

Figure I.2.2. Models proposed to explain the P-glycoprotein function: the pore (a), the flippase (b) and the hydrophobic vacuum cleaner model (c). Adapted from VARMA (2003).

Structurally, human P-gp is a 170 kDa transmembrane glycoprotein composed by 1280 amino acids (KWAN AND BRODIE 2005; LINNET AND EJSING 2008; MCCORMICK ET AL. 2015). This well-known drug efflux transporter contains more than one substrate binding domain and extrudes a wide range of structurally and functionally unrelated compounds. P-gp is unique in its ability to recognize and transport a plethora of diverse substrates with variable chemical properties and pharmacological actions. Indeed, P-gp substrates include several clinically important drugs from different pharmacotherapeutic or pharmacological classes (Table I.2.1) (HENNESSY AND SPIERS 2007; MILLER ET AL. 2009; BORSKA ET AL. 2010; FORTUNA ET AL. 2011a). However, the ability of P-gp to transport such enormous variety of chemical compounds is still poorly understood (RAUB 2006). Moreover, it has been shown that drug–drug interactions involving P-gp may decrease the therapeutic efficacy and/or potentiate toxic effects. This problem results from the large number of compounds that may interact with P-gp either as a substrate, inhibitor or inducer (FORTUNA ET AL. 2011a). Therefore, one of the key points that are increasingly considered in programs of drug discovery and development consists on testing new chemical entities as P-gp substrates. Indeed, drug candidates that are substrates of P-gp may be "victims" of drug–drug interactions where this transporter is inhibited or induced (LIN AND YAMAZAKI 2003b; DORAN ET AL. 2005; CHANG ET AL. 2006; SUGIMOTO ET AL. 2011; PALMEIRA ET AL. 2011). Hence, this type of studies are recommended and may be useful in the decision-making processes for optimization and selection of the most promissory drug candidates (MIZUNO ET AL. 2003; BALAYSSAC ET AL. 2005; GIACOMINI ET AL. 2010; U.S. FOOD AND DRUG ADMINISTRATION 2012).

Furthermore, the understanding of the physiological role of P-gp as a natural detoxification mechanism in various human tissues (LIN 2003; BALAYSSAC ET AL. 2005; ZHANG ET AL. 2006; CHANG ET AL. 2006) and the recognition of the involvement of P-gp in multidrug resistance (MATHENY ET AL. 2001) have motivated the search of P-gp inducers and inhibitors with potential interest respectively in cases of poisoning and therapeutic inefficacy (HUISMAN ET AL. 2003; DINIS-OLIVEIRA ET AL. 2006).

Table I.2.1. Representative P-glycoprotein substrates (SAUNA ET AL. 2001; STOUCH AND GUDMUNDSSON 2002; SUN ET AL. 2003; LÖSCHER AND POTSCHKA 2005b; KWAN AND BRODIE 2005; BALAYSSAC ET AL. 2005; TANDON ET AL. 2006; HENNESSY AND SPIERS 2007; BANSAL ET AL. 2009; FORTUNA ET AL. 2011a; SCHINKEL AND JONKER 2012; CHEN ET AL. 2016).

Therapeutic Class	Drugs
Analgesics	Asimadoline, Morphine
Antibiotics	Erythromycin, Gramicidin D, Fluoroquinolones, Tetracyclines, Valinomycin
Antiemetics	Domperidone, Ondansetron
Antiepileptics	Carbamazepine, Felbamate, Gabapentin, Lamotrigine, Phenobarbital, Phenytoin, Topiramate
Antigout agents	Colchicine
Anthelmintics	Abamectin, Ivermectin
Antidepressants	Amitriptyline, Citalopram, Doxepin, Nortriptyline, Paroxetine, Venlafaxine
Antipsychotics	Risperidone
Antidiarrheal agents	Loperamide
Antifungals	Itraconazole, Ketoconazole
Anticancer drugs	Anthracenes (Bisanthrene, Mitoxantrone), Anthracyclines (Daunorubicin, Doxorubicin, Epirubicin, Idarubicin), Camptothecins (Irinotecan, Topotecan), Epipodophyllotoxins (Etoposide, Teniposide), Miscellaneous (Actinomycin D, Amsacrine, Colchicine, Dactinomycin, Imatinib, Methotrexate, Mithramycin, Mitomycin C, Tamoxifen, Trimetrexate), Taxanes (Docetaxel, Paclitaxel), Vinca alkaloids (Vinblastine, Vincristine, Vindesine, Vinorebline)
Antituberculosis agents	Rifampicin
Beta blockers	Bunitrolol, Carvediol, Celiprolol, Talinolol
Calcium channel blocker	Diltiazem, Felodipine, Nicardipine, Verapamil
Cardiac drugs	Digitoxin, Digoxin, Quinidine
Corticoids	Corticosterone, Dexamethasone, Hydrocortisone, Methylprednisolone, Triamcinolone
Histamine H_1-receptor antagonists	Fexofenadine, Terfenadine
Histamine H_2-receptor antagonists	Cimetidine, Ranitidine
Human immunodeficiency virus protease inhibitors	Amprenavir, Indinavir, Lopinavir, Nelfinavir, Ritonavir, Saquinavir
Hormones	Progesterone, Testosterone, Estradiol
Immunosuppressants	Cyclosporin A, Sirolimus, Tacrolimus
Lipid-lowering agents (Statins)	Atorvastatin, Lovastatin
Proton pump inhibitors	Lansoprazole, Omeprazole, Pantoprazole

I.2.2.2. P-glycoprotein inhibitors: an overview

The recognition that P-gp–mediated multidrug resistance is clinically important in several diseases has been followed by concerted efforts to search for therapeutically useful P-gp inhibitors in order to overcome that functional barrier and allow drug penetration into the target tissue (TANDON ET AL. 2006; HENNESSY AND SPIERS 2007). The pharmacokinetics, efficacy and safety of P-gp substrates can be affected by the level of expression and functionality of P-gp,

which can be modulated by inhibition and induction (GIACOMINI ET AL. 2010). If P-gp inhibitors or reversal agents become available, it might be possible, for example, to administer drugs targeted to the brain concomitantly with reversal agents, which would overcome the extrusion of P-gp substrates from the brain, increasing its concentration at the biophase and, consequently, the intended therapeutic effects (RAMAKRISHNAN 2003).

Although initial thoughts on the clinical application of P-gp inhibitors were focused on reversing multidrug resistance in chemo-resistant tumour cells that express significant amounts of P-gp, more recent insights indicated that such inhibitors might also be useful to modulate the general pharmacokinetic behaviour of drugs in the body (SCHINKEL AND JONKER 2012). Therefore, P-gp inhibitors are currently in development not only to increase drug penetration into malignant tissues in order to optimize chemotherapy, but also to increase brain penetration of CNS-active drugs to circumvent the pharmacoresistance associated with several CNS diseases (e.g., epilepsy) (THOMAS AND COLEY 2003; KEMPER ET AL. 2003; MILLER ET AL. 2009; BANSAL ET AL. 2009; COLEY 2010).

A P-gp inhibitor should have a high propensity for binding to P-gp without inhibiting other ABC transporters or interacting with cytochrome P450 (CYP) isoenzymes. Furthermore, it should be selectively targeted to P-gp in non-physiological tissues with a high affinity and individually adapted to the recipient's genotype. Thus, a non-toxic compound which does not have any pharmacological activity by its own is considered the ideal P-gp inhibitor (BANSAL ET AL. 2009). P-gp inhibitors, even though structurally divergent, are responsible for decreased drug extrusion and reversal of cellular multidrug resistance (DE WET ET AL. 2001). Considering their physicochemical properties, P-gp inhibitors apparently are hydrophobic molecules, with a molecular weight ranging from 200 to almost 1900 Da (CHAN ET AL. 2004; FROMM 2004; SCHINKEL AND JONKER 2012), with a planar ring system and weak positive charge at physiologic pH (SCHINKEL 1999; KWAN AND BRODIE 2005; MILLER ET AL. 2009; GIACOMINI ET AL. 2010; ZHANG ET AL. 2012a). Some investigators suggest a general pharmacophore with two or three hydrogen bond acceptor (or electron donor) groups in a fixed spatial separation (SUN ET AL. 2003; CHAN ET AL. 2004; KWAN AND BRODIE 2005). The general features of a substrate/inhibitor include also a planar aromatic domain, as well as the existence of at least one tertiary basic nitrogen atom on the drug molecule in deprotonated state at neutral pH (SUN ET AL. 2003; BREIER ET AL. 2013). Thus, based on their chronological development, specificity and affinity to the efflux transporter, the P-gp inhibitors are now categorized into three generations (DANTZIG ET AL. 2003; VARMA 2003; BANSAL ET AL. 2009).

The first-generation of P-gp inhibitors are pharmacologically active and they are in clinical use for other indications beyond the inhibition of P-gp (DANTZIG ET AL. 2003; VARMA 2003; HENNESSY AND SPIERS 2007; YANG ET AL. 2008; BANSAL ET AL. 2009; POTSCHKA 2012). It includes calcium channel blockers such as verapamil (Figure I.2.3), anti-hypertensives like reserpine and yohimbine, the immunosuppressant cyclosporin A (Figure I.2.3), anti-oestrogens like tamoxifen and toremifene, and antiarrhythmic agents such as quinidine (DANTZIG ET AL. 2003; VARMA 2003; HENNESSY AND SPIERS 2007; BANSAL ET AL. 2009; POTSCHKA 2012). However, these compounds have

low potency and lack of selectivity for P-gp inhibition. Indeed, the clinical use of these agents at the concentrations necessary to inhibit P-gp is associated with severe toxicity (KRISHNA AND MAYER 2000; DANTZIG ET AL. 2003; VARMA 2003; CHUNG ET AL. 2005; HENNESSY AND SPIERS 2007; BANSAL ET AL. 2009; POTSCHKA 2012). For instance, the use of verapamil to inhibit P-gp leads to cardiotoxicity and the use of cyclosporin A induces an increase of hepatic, renal, myeloid, and neurological toxicity (RAMAKRISHNAN 2003).

The second-generation of P-gp inhibitors was developed as derivatives of the first-generation compounds in order to retain the ability of the lead compound to inhibit P-gp, but decreasing the pharmacological activity and, consequently, the toxicity (KRISHNA AND MAYER 2000; DANTZIG ET AL. 2003; VARMA 2003; HENNESSY AND SPIERS 2007; BANSAL ET AL. 2009; POTSCHKA 2012). For example, the P-gp modulator valspodar lacks the immunosuppressive effect of cyclosporin A, although it is a close structural analogue of this drug (Figure I.2.3). On the other hand, dexverapamil (*R*-isomer of verapamil; Figure I.2.3) retains the ability to inhibit P-gp, but lacks the cardiovascular effects of its precursor (verapamil) (DANTZIG ET AL. 2003; HENNESSY AND SPIERS 2007). Although these compounds have been developed to be less toxic, some of their characteristics still limit their clinical usefulness. Indeed, the affinity of these compounds towards P-gp was shown to be too low to produce significant P-gp inhibition *in vivo* at tolerable doses (BANSAL ET AL. 2009). Additionally, first- and second-generation P-gp inhibitors also lack specificity as they inhibit two or more ABC transporters, which leads to complicated drug–drug interactions (VARMA 2003; HENNESSY AND SPIERS 2007). For instance, valspodar inhibits not only P-gp but also MRP2 and the bile acid export protein (*ABCB11*) (HENNESSY AND SPIERS 2007). Moreover, P-gp also has overlapping substrate specificity with CYP3A. Therefore, numerous studies have demonstrated clinically important drug–drug interactions when a P-gp inhibitor is coadministered with another drug metabolised by CYP3A4; as example, valspodar interferes with CYP enzyme activity thereby affecting clearance and systemic exposure of coadministered compounds (HENNESSY AND SPIERS 2007; POTSCHKA 2012). Thus, in spite of the early expected favourable contributions of the first- and second-generations of P-gp inhibitors, compounds have failed to yield the desired clinical benefit (DANTZIG ET AL. 2003). Besides that, many first- and second-generation P-gp inhibitors are just competitive inhibitors, competing as substrates for the P-gp (YANG ET AL. 2008).

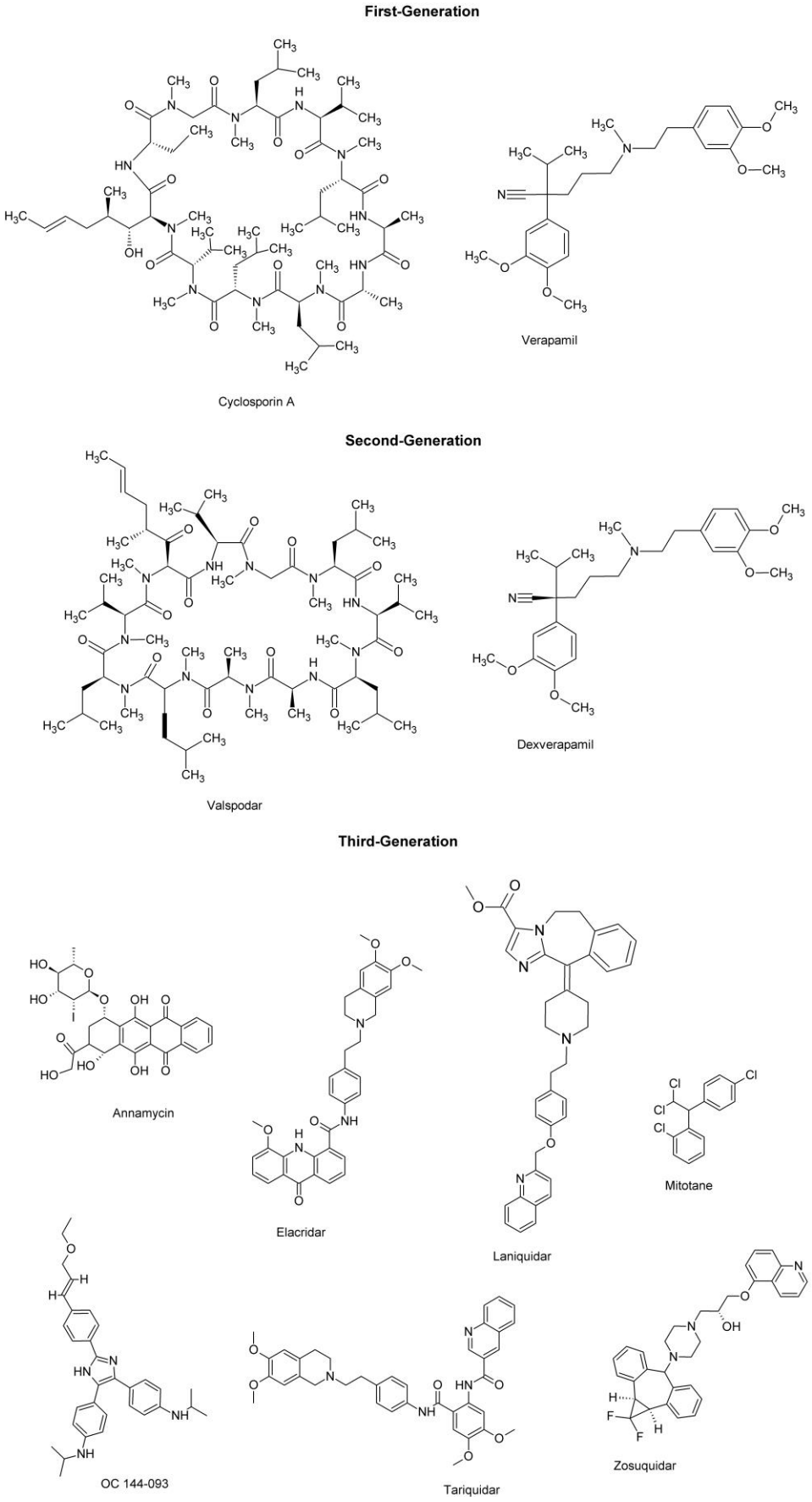

Figure I.2.3. Chemical structure of some P-glycoprotein inhibitors belonging to the first-, second- and third-generation (PUBCHEM COUMPOUND DATABASE).

In contrast to first- and second-generation compounds, the third-generation of P-gp modulators has been designed to have an increased potency, inhibiting P-gp at concentrations in the nanomolar ranges, and to exhibit an increased specificity being simultaneously devoid of additional effects on drug metabolic enzymes. These include compounds as annamycin, elacridar, laniquidar, mitotane, OC 144-093, tariquidar and zosuquidar (Figure I.2.3) (KRISHNA AND MAYER 2000; DANTZIG ET AL. 2003; HENNESSY AND SPIERS 2007; POTSCHKA 2012). BANSAL ET AL. (2009) presented a list of P-gp modulators belonging to different classes, which includes compounds that are inducers and inhibitors of P-gp. In the third-generation of P-gp inhibitors are included not only synthetic compounds, but also pharmaceutical excipients like polysorbates (Tween 20 or 80), herbs and fruits like curcumin or orange, and herbal constituents like flavonoids (BANSAL ET AL. 2009).

Competitive inhibitors, which are P-gp substrates themselves, and non-competitive inhibitors, are included in the three generations of P-gp modulators. Non-competitive inhibitors can interfere with the activation and transport cycle of P-gp and induce alterations in the conformation of the transporter molecule that affects transport efficacy (POTSCHKA 2012). Different mechanisms by which these inhibitors might interact with the transport proteins have been suggested (BRAND ET AL. 2006). In general, P-gp can be inhibited by (a) blocking drug binding site either competitively, non-competitive or allosterically; (b) interfering with ATP hydrolysis; or (c) changing integrity of cell membrane lipids (VARMA 2003; BRAND ET AL. 2006). However, most of the drugs inhibits P-gp function by blocking drug binding sites (VARMA 2003). Furthermore, many of the inhibitors have their potential use reduced in clinical settings probably because they seem to be relatively nonspecific and participate in unwanted drug–drug interactions or interfere with other physiological systems (BRAND ET AL. 2006). Thereby, it is urgent the emergence of new agents with potential to reverse the multidrug resistance mediated by P-gp. These drug candidates should be potent, non-cytotoxic, and have minimal adverse effects (HADJERI ET AL. 2003).

Over the last years, phytochemicals are gaining a great attention as P-gp modulators because, as potentially non-toxic compounds, they present characteristics of ideal P-gp inhibitors (BANSAL ET AL. 2008; BANSAL ET AL. 2009). Herbal products are taken by about 10% or more of the general population, and by 30-70% of individuals with specific diseases (CHUNG ET AL. 2005). Hence, it has also been reported that some phytochemicals found in vegetables, fruits and some plants, which have, among others, anticancer, antiviral, and antioxidant properties, may modulate or inhibit P-gp activity and may have potential to be developed as multidrug resistance reversing agents (CHUNG ET AL. 2005). Accordingly, herbal constituents are considered good candidates for increasing the bioavailability and tissue-penetration (e.g., overpass the blood-brain barrier) or decreasing biliary excretion of P-gp substrates, reversing thus the multidrug resistance; although there are also safety concerns related to the phytochemical compounds, their continuous and long history of use in large amounts as a part of normal daily diet constitutes a favourable feature (BANSAL ET AL. 2009).

I.3. Flavonoids as P-glycoprotein Inhibitors

I.3.1. Flavonoids

For a long time, flavonoids have been consumed in order to improve health status of humans (BANSAL ET AL. 2009); indeed, the medicinal use of natural products, such as extracts of plants, is now a common practice worldwide (ASZALOS 2008). Since several flavonoids share some of the optimal properties of an ideal P-gp inhibitor, the interest on testing whether they inhibit P-gp has significantly increased during the search for selective and non-cytotoxic P-gp inhibitors (BRAND ET AL. 2006; BANSAL ET AL. 2009). Currently, they are considered good drug candidates (or lead compounds) as modulators of multidrug resistance due to their inhibitory activities on P-gp function and because of their physiological safety (KITAGAWA ET AL. 2005).

Flavonoids consist on a large group of polyphenolic herbal constituents, which integrate the third-generation, non-pharmaceutical category of P-gp inhibitors (ROSS AND KASUM 2002; BRAND ET AL. 2006; BANSAL ET AL. 2009). Some of these compounds produced effects that are found to be comparable to those of the classic P-gp inhibitors, verapamil and cyclosporin A (Figure I.2.3) (BANSAL ET AL. 2009; SCHINKEL AND JONKER 2012). Actually, flavonoids and/or their metabolites are considered interesting modulators or substrates of intestinal membrane bound transport proteins, including P-gp (BRAND ET AL. 2006; CHAN ET AL. 2009).

The flavonoids are herbal secondary metabolites (KITAGAWA 2006; SHOHAI ET AL. 2011; THILAKARATHNA AND RUPASINGHE 2013; ROMANO ET AL. 2013). According to KITAGAWA (2006) and SHEU ET AL. (2010), flavonoids comprise more than 4,000 known compounds, resulting from the various combinations of multiple hydroxyl and methoxyl group substituents of the basic flavonoid skeleton (Figure I.3.1).

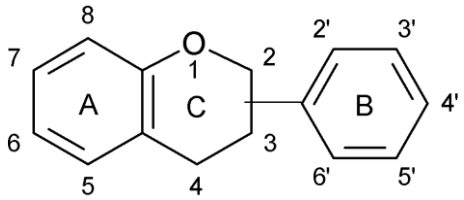

Figure I.3.1. Basic chemical structure of flavonoids. Adapted from MOON ET AL. (2006); VAUZOUR ET AL. (2008) and CROZIER ET AL. (2009).

MOON ET AL. (2006) reported more than 8,000 compounds with a flavonoid structure. Although occasionally they are found in nature as aglycones, most of the flavonoids are attached to sugars (glycosides) (ROSS AND KASUM 2002; MORRIS AND ZHANG 2006). Many of the flavonoids have a very limited bioavailability because of high intestinal metabolism or poor absorption *in vivo* (TSUJI ET AL. 2013). In humans and animals, these compounds are absorbed from the gastrointestinal tract and are excreted in the urine and faeces, either unchanged or as flavonoid metabolites (COOK AND SAMMAN 1996; MORRIS AND ZHANG 2006; BRAND ET AL. 2006). In the small intestine and liver, dietary flavonoids are substrates for phase I and phase II metabolizing enzymes (WASOWSKI AND MARDER 2012). Upon ingestion, and before oral absorption, flavonoid glycosides are deglycosylated by lactase phlorizin hydrolase or cytosolic ß-glucosidase. The

compounds that are not absorbed in the intestine will reach the colon, where the enzymes of the gut microflora degrade flavonoids to simple phenolic acids, that may undergo absorption and further hepatic metabolism (SPENCER 2007; VAUZOUR ET AL. 2008; THILAKARATHNA AND RUPASINGHE 2013). The absorbed aglycone is metabolized into glucuronide-, sulphate- and methoxylated conjugates (BRAND ET AL. 2006; SPENCER 2007; VAUZOUR ET AL. 2008; BANSAL ET AL. 2009; JÄGER AND SAABY 2011; WASOWSKI AND MARDER 2012).

I.3.1.1. Flavonoids chemistry

The term flavonoid is used to describe herbal pigments mostly derived from benzo-γ-pyrone (rings A and C; Figure I.3.1), with an assortment of basic structures (HENDRICH 2006). These compounds are found in all vascular plants and have low molecular weights (WASOWSKI AND MARDER 2012; ROMANO ET AL. 2013). The basic structure of flavonoids consists of two benzene moieties (rings A and B, Figure I.3.1), which are linked in the middle through a heterocyclic pyran or pyrone with a double bond (ring C; Figure I.3.1) (PIETRO ET AL. 2002; ROSS AND KASUM 2002; SHOHAI ET AL. 2011; WASOWSKI AND MARDER 2012; TSUJI ET AL. 2013). Hence, the flavonoids can be divided into several classes depending on their structure (KITAGAWA 2006; JÄGER AND SAABY 2011), namely the oxidation status of ring C, the hydroxylation pattern of the ring structure and the substituent located on the 3rd position (MORRIS AND ZHANG 2006; SPENCER 2007; BANSAL ET AL. 2009; ALVAREZ ET AL. 2010; TSUJI ET AL. 2013). Taking into account the chemical nature of each molecule and the positions of moieties substituting rings A, B, and C, the flavonoids are divided into six major subclasses that are particularly well known and characterized and they correspond to the main dietary groups of flavonoids (ROSS AND KASUM 2002; SPENCER 2007). These subclasses include the anthocyanidines (Figure I.3.2); the flavanols or catechins, in which the 2,3-bond is reduced, contain an additional hydroxyl substituent at position 3 of the ring C, and the carbonyl at position 4 is absent (Figure I.3.3); the flavanones, where the 2,3-bond is reduced, losing electron conjugation and ring planarity (Figure I.3.4); the flavones (Figure I.3.5); the flavonols, which contain an additional hydroxyl substituent at the position 3 of the ring C and where the 4',5'-bond is reduced (Figure I.3.6); and the isoflavones, where the ring B is branched at position 3 of the ring C (Figure I.3.7) (ROSS AND KASUM 2002; DEFERME AND AUGUSTIJNS 2003; HENDRICH 2006; KITAGAWA 2006; MOON ET AL. 2006; SPENCER 2007; CROZIER ET AL. 2009; SHEU ET AL. 2010; THILAKARATHNA AND RUPASINGHE 2013). Indeed, flavonoids and isoflavonoids (e.g., isoflavones) are distinguished by the position at which the ring B is attached into the benzo-γ-pyrone core of the molecule. Thus, in flavonoids the ring B is bound at position 2 of ring C, whereas in isoflavonoids the ring B is bound at position 3 of ring C (Figure I.3.2-Figure I.3.7) (HENDRICH 2006). Minor dietary flavonoids include dihydroflavonols, flavan-3,4-diols, coumarins, chalcones, dihydrochalcones, and aurones (CROZIER ET AL. 2009). Although a modified number system is used for chalcones and isoflavones derivatives, the individual carbon atoms are identified with ordinary numerals for the ring A and the ring C, and "primed numerals" for the ring B (Figure I.3.1) (TAPAS ET AL. 2008; WASOWSKI AND MARDER 2012).

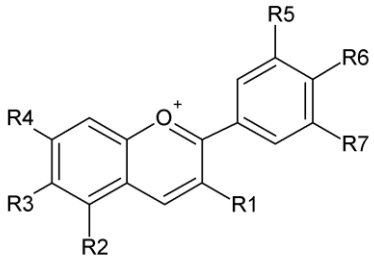

	R1	R2	R3	R4	R5	R6	R7
Aurantinidin	H	OH	OH	OH	H	OH	H
Cyanidin	OH	OH	H	OH	OH	OH	H
Delphinidin	OH	OH	H	OH	OH	OH	OH
Diosmetinidin	H	OH	H	OH	OH	OCH_3	H
Europinidin	OH	OCH_3	H	OH	OCH_3	OH	OH
Fisetinidin	OH	H	H	OH	OH	OH	H
Kuromanin	O-Glu	OH	H	OH	OH	OH	H
Luteolinidin	H	OH	H	OH	OH	OH	H
Malvidin	OH	OH	H	OH	OCH_3	OH	OCH_3
Peonidin	OH	OH	H	OH	OCH_3	OH	H
Pelargonidin	OH	OH	H	OH	H	OH	H
Petunidin	OH	OH	H	OH	OCH_3	OH	OH
Quercetagetinidin	OH	OH	OH	OH	OH	OH	H
Rosinidin	OH	OH	H	OCH_3	OCH_3	OH	H

Substituents

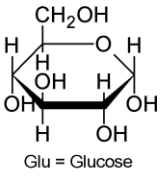

Glu = Glucose

Figure I.3.2. Chemical structures of the compounds belonging to the anthocyanidines subgroup of flavonoids and their glycosides (anthocyanins) (PUBCHEM COUMPOUND DATABASE; TOKI ET AL. 2008; VAUZOUR ET AL. 2008; SHOHAI ET AL. 2011; JÄGER AND SAABY 2011; KELLENBERGER ET AL. 2011).

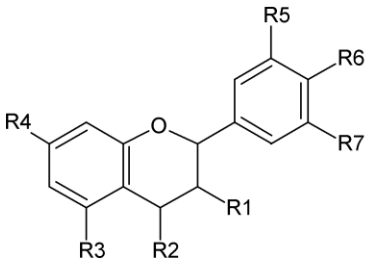

	R1	R2	R3	R4	R5	R6	R7
Catechin	OH	H	OH	OH	OH	OH	H
Catechin gallate	Gallic acid	H	OH	OH	OH	OH	H
Epicatechin	OH	H	OH	OH	OH	OH	H
Epicatechin gallate	Gallic acid	H	OH	OH	OH	OH	H
Epigallocatechin	OH	H	OH	OH	OH	OH	OH
Epigallocatechin gallate	Gallic acid	H	OH	OH	OH	OH	OH
Gallocatechin	OH	H	OH	OH	OH	OH	OH
Leucocyanidol	OH	OH	OH	OH	H	OH	OH

Substituents

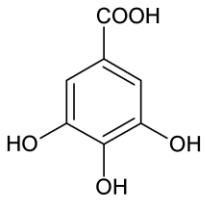

Gallic Acid

Figure I.3.3. Chemical structures of the compounds belonging to the flavanols or catechins subgroup of flavonoids (PUBCHEM COUMPOUND DATABASE; COOK AND SAMMAN 1996; VAUZOUR ET AL. 2008; CROZIER ET AL. 2009; SHOHAI ET AL. 2011; JÄGER AND SAABY 2011; DU ET AL. 2012).

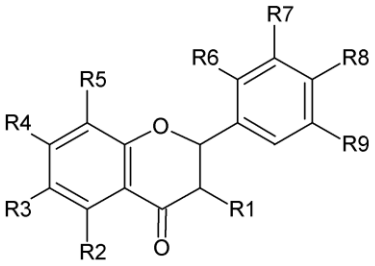

	R1	R2	R3	R4	R5	R6	R7	R8	R9
Butin	H	H	H	OH	H	H	H	OH	OH
Butrin	H	H	H	O-Glu	H	H	H	OH	O-Glu
Eriocitrin	H	OH	H	O-Glu-Rh	H	H	OH	OH	H
Eriodictyol	H	OH	H	OH	H	H	OH	OH	H
Hesperidin	H	OH	H	O-Glu-Rh	H	H	OH	OCH_3	H
Hesperetin	H	OH	H	OH	H	H	H	OCH_3	H
Homoeriodictoyl	H	OH	H	OH	H	H	OCH_3	OH	H
Isomonospermoside	H	H	H	OH	H	H	H	OH	O-Glu
Isosakuranetin	H	OH	H	OH	H	H	H	OCH_3	H
Liquiritigenin	H	H	H	OH	H	H	H	OH	H
Lonchocarpol A	H	OH	Prenyl group	OH	Prenyl group	H	H	OH	H
Naringenin	H	OH	H	OH	H	H	H	OH	H
Naringin	H	OH	H	O-Glu-Rh	H	H	H	OH	H
Neohesperidin	H	OH	H	O-Glu-Rh	H	H	OH	OCH_3	H
Pinocembrim	H	OH	H	OH	H	H	H	H	H
Ponciretin	H	OH	H	OH	H	H	H	OCH_3	H
Poncirin	H	OH	H	O-Glu-Rh	H	H	H	OCH_3	H
Sakuranetin	H	OH	H	OCH_3	H	H	H	OH	H
Sakuranin	H	O-Glu	H	OCH_3	H	H	H	OH	H
Sophoraflavanone G	H	OH	H	OH	Lavandulyl	OH	H	OH	H
Sterubin	H	OH	H	OCH_3	H	H	OH	OH	H
Taxifolin	OH	OH	H	OH	H	H	OH	OH	H

Substituents

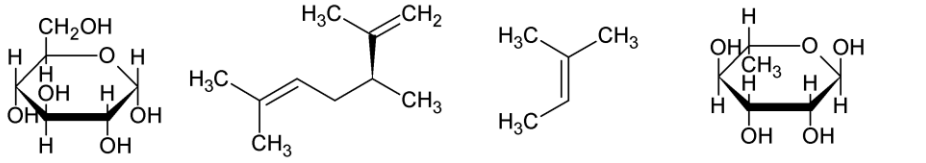

Figure I.3.4. Chemical structures of the compounds belonging to the flavanones subgroup of flavonoids and their glycosides (PUBCHEM COUMPOUND DATABASE; HOROWITZ AND GENTILI 1960; WAGNER ET AL. 1969; SACCO AND MAFFEI 1997; RAKWAL ET AL. 2000; LEY ET AL. 2005; OGAWA ET AL. 2006; MIYAKE ET AL. 2007; CHOKCHAISIRI ET AL. 2009; SHEU ET AL. 2010; SHOHAI ET AL. 2011; JÄGER AND SAABY 2011; TRAN ET AL. 2011; WESOŁOWSKA 2011).

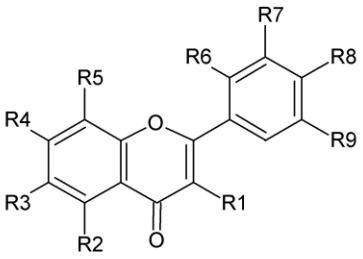

	R1	R2	R3	R4	R5	R6	R7	R8	R9
Acacetin	H	OH	H	OH	H	H	H	OCH_3	H
Apigenin	H	OH	H	OH	H	H	H	OH	H
Apigetrin	H	OH	H	O-Glu	H	H	H	OH	H
Baicalin	H	OH	OH	O- Glucuronic acid	H	H	H	H	H
Baicalein	H	OH	OH	OH	H	H	H	H	H
Bayin	H	H	H	OH	Glu	H	H	OH	H
Chrysin	H	OH	H	OH	H	H	H	H	H
Chrysoeriol	H	OH	H	OH	H	H	OCH_3	OH	H
Cirsiliol	H	OH	H	OCH_3	H	H	OH	OH	H
Cirsimaritin	H	OH	OCH_3	OCH_3	H	H	H	OH	H
Diosmetin	H	OH	H	OH	H	H	OH	OCH_3	H
Diosmim (synthetic)	H	OH	H	O-Glu-Rh	H	OH	OH	OH	H
Eupafolin	H	OH	OCH_3	OH	H	H	OH	OH	H
Eupatilin	H	OH	OCH_3	OH	H	H	OCH_3	OCH_3	H
Flavoxate (synthetic)	CH_3	H	H	H	PEF	H	H	H	H
Gardenin A (demethylated)	H	OH	OH	OH	OH	H	OH	OH	OH
Gardenin D	H	OH	OCH_3	OCH_3	OCH_3	H	OH	OCH_3	H
Genkwanin	H	OH	H	OCH_3	H	H	H	OH	H
Hispidulin	H	OH	H	OH	H	H	H	OCH_3	H
Hypolactin	H	OH	H	OH	OH	H	OH	OH	H
Isoorientin	H	OH	Glu	OH	H	H	OH	OH	H
Luteolin	H	OH	H	OH	H	H	OH	OH	H
Luteolin 7-glucoside	H	OH	H	O-Glu	H	H	OH	OH	H
Nobiletin	H	OCH_3	OCH_3	OCH_3	OCH_3	H	OCH_3	OCH_3	H
Orientin	H	OH	H	OH	Glu	H	OH	OH	H
Oroxylin A	H	OH	OCH_3	OH	H	H	H	H	H
Pedalitin	H	OH	H	OCH_3	H	H	OH	OH	H
Rhoifolin	H	OH	H	O-Glu-Rh	H	H	H	OH	H
Scutellarein	H	OH	OH	OH	H	H	H	OH	H
Sideritoflavone	H	OH	OCH_3	OCH_3	OCH_3	H	OH	OH	H
Sinensetin	H	OCH_3	OCH_3	OCH_3	H	H	OCH_3	OCH_3	H
Tangeretin	H	OH	OCH_3	OCH_3	OCH_3	H	H	OCH_3	H
Techtochrysin	H	OH	H	H	OCH_3	H	H	H	H
Vicenin-2	H	OH	H	Glu	Glu	H	H	OH	H
Vitexin	H	OH	H	OH	Glu	H	H	OH	H
Wogonin	H	OH	H	OH	OCH_3	H	H	H	H
Xanthomicrol	H	OH	OCH_3	OCH_3	OCH_3	H	H	OH	H
8-Methoxycirisilincol	H	OH	OCH_3	OCH_3	OCH_3	H	OCH_3	OH	H

Substituents

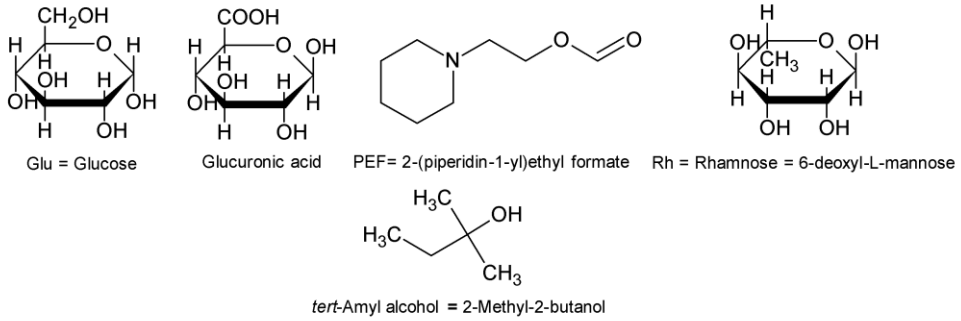

Figure I.3.5. Chemical structures of the compounds belonging to the flavones subgroup of flavonoids and their glycosides (PubChem Coumpound Database; Cook and Samman 1996; Kim et al. 2004; Tapas et al. 2008; Crozier et al. 2009; Kim et al. 2010; Shohai et al. 2011; Rao et al. 2011; Tran et al. 2011; Wasowski and Marder 2012; Moreno Escobosa et al. 2012; Lam et al. 2012; Kumar et al. 2013).

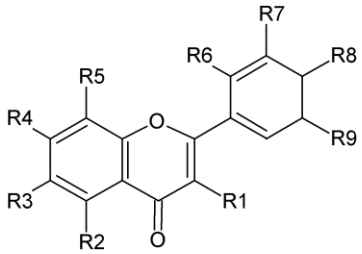

	R1	R2	R3	R4	R5	R6	R7	R8	R9
Amurensin	OH	OH	H	O-Glu	tert-amyl alcohol	H	H	OH	H
Azalein	O-Rh	OCH_3	H	OH	H	H	OH	OH	H
Azaleatin	OH	OCH_3	H	OH	H	H	OH	OH	H
Datiscetin	OH	OH	H	OH	OH	H	H	H	H
Fisetin	OH	H	H	OH	H	H	OH	OH	H
Galangin	OH	OH	H	OH	H	H	H	H	H
Gossypetin	OH	OH	H	OH	OH	H	OH	OH	H
Hyperoside	O-Gal	OH	H	OH	H	H	OH	OH	H
Isoquercetrin	O-Glu	OH	H	OH	H	H	OH	OH	H
Isorhamnetin	OH	OH	H	OH	H	H	OCH_3	OH	H
Kaempferide	OH	OH	H	OH	H	H	H	OCH_3	H
Kaempferitrin	O-Rh	OH	H	O-Rh	H	H	H	OH	H
Kaempferol	OH	OH	H	OH	H	H	H	OH	H
Morin	OH	OH	H	OH	H	OH	H	OH	H
Myricitin	OH	OH	H	OH	H	H	OH	OH	OH
Myricitrin	O-Rh	OH	H	OH	H	H	OH	OH	OH
Natsudaidain	OH	OCH_3	OCH_3	OCH_3	OCH_3	H	H	OCH_3	OCH_3
Quercetagetin	OH	OH	OH	OH	H	H	OH	OH	H
Quercetin	OH	OH	H	OH	H	H	OH	OH	H
Quercitrin	O-Rh	OH	H	OH	H	H	OH	OH	H
Pachypodol	OCH_3	OH	H	OCH_3	H	H	OCH_3	OH	H
Rhamnetin	OH	OH	H	OCH_3	H	H	OH	OH	H
Rhamnazin	OH	OH	H	OCH_3	H	H	H	OH	OCH_3
Robinetin	OH	H	H	OH	H	H	OH	OH	OH
Robinin	O-Rh-Glu	OH	H	O-Rh	H	H	OH	OH	H
Rutin	O-Rh-Glu	OH	H	OH	H	H	OH	OH	H
Spiraeoside	OH	OH	H	OH	H	H	H	O-Glu	OH
Spirenoside	OH	OH	H	OH	H	H	OH	O-Glu	H
Tamarixetin	OH	OH	H	OH	H	H	OH	OCH_3	H
Troxerutin	O-Rh-Glu	OH	H	O-He	H	H	O-He	O-He	H
Vitexecarpin	OCH_3	OH	OCH	OCH_3	H	H	OH	OCH_3	H

Substituents

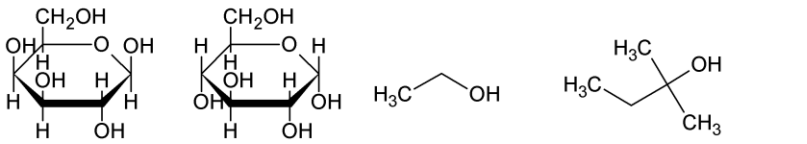

Gal = Galactose Glu = Glucose He = Hydroxyethyl *tert*-amyl alcohol = 2-Methyl-2-butanol

Figure I.3.6. Chemical structures of the compounds belonging to the flavonols subgroup of flavonoids and their glycosides (PubChem Coumpound Database; Harborne 1962; Cook and Samman 1996; Raj 2001; Hasegawa and Shirato 2002; Boumendjel et al. 2002; Tapas et al. 2008; Ali et al. 2008; Matsui et al. 2009; Zhou et al. 2009; Crozier et al. 2009; Sheu et al. 2010; Shohai et al. 2011; Jäger and Saaby 2011; Tran et al. 2011; Wasowski and Marder 2012; Alonso-Castro et al. 2013; Yang et al. 2013; Makino et al. 2013).

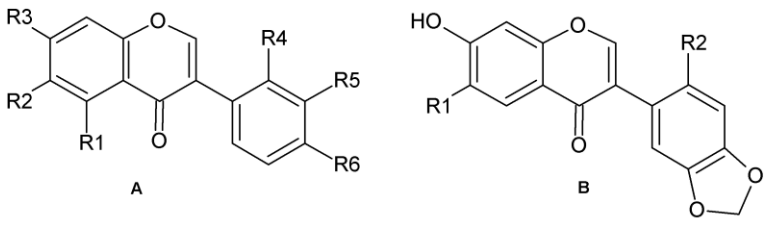

	R1	R2	R3	R4	R5	R6
A						
Afrormosin	H	OCH_3	OH	H	H	OCH_3
Biochanin A	OH	H	OH	H	H	OCH_3
Calycosin	H	H	OH	H	OH	OCH_3
Castanin	H	OCH_3	OH	H	H	OCH_3
Daidzein	H	H	OH	H	H	OH
Daidzin	H	H	O-Glu	H	H	OH
Formononetin	H	H	OH	H	H	OCH_3
Genistein	OH	H	OH	H	H	OH
Genistin	OH	H	O-Glu	H	H	OH
Glycitein	H	OCH_3	OH	H	H	OH
Odoratin	H	OCH_3	OH	H	OH	OCH_3
Ononin	H	H	O-Glu	H	H	OCH_3
Sophoraisoflavone A	OH	H	OH	#	#	OH
Sissotrin	OH	H	O-Glu	H	H	OCH_3
Tectorigenin	OH	OCH3	OH	H	H	OH
B						
Cuneatin	H	OCH_3	--	--	--	--
Fujikinetin	OCH_3	H	--	--	--	--
Pseudobaptogenin	H	H	--	--	--	--

- pyran ring between positions 2' (R4) and 3' (R5)

Substituents

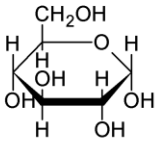

Glu = Glucose

Figure I.3.7. Chemical structures of the compounds belonging to the isoflavones subgroup of flavonoids and their glycosides (PUBCHEM COUMPOUND DATABASE; KEUNG AND VALLEE 1993; KHAN ET AL. 2000; TAPAS ET AL. 2008; CHOKCHAISIRI ET AL. 2009; SHEU ET AL. 2010; TRAN ET AL. 2011; WESOŁOWSKA 2011; ZHANG ET AL. 2011b; ZOU ET AL. 2012; SHAJIB ET AL. 2012).

I.3.1.1.1. Structure-activity relationship

Specifically, there are structural requirements necessary for the inhibitory effects of flavonoids on P-gp function (KITAGAWA ET AL. 2005). The structure-activity relationships for flavonoid–P-gp interaction have been extensively studied mainly evaluating the binding affinity of different flavonoids with mouse NBD2 (Figure I.2.1) (MORRIS AND ZHANG 2006). The presence of the 5-hydroxyl group, the 3-hydroxyl group, and the 2,3-double bond appears to be important for potent flavonoid-NBD2 interaction and are required for the P-gp inhibitory activity (Figure I.3.1; Figure I.3.8) (CONSEIL ET AL. 1998; BOUMENDJEL ET AL. 2002; HENDRICH 2006; MORRIS AND ZHANG 2006; BANSAL ET AL. 2009). Isoflavonoids have lower P-gp interaction activity due to the different position where the ring B is branched (BOUMENDJEL ET AL. 2002; MORRIS AND ZHANG 2006). BOUMENDJEL ET AL. (2002) evaluate the binding affinity toward the NBD2 of P-gp of a set of naturally occurring

flavones, isoflavones, flavonols, flavanones and chalcones. The structure-activity relationship analysis of flavonoids–P-gp concluded that flavonols, chalcones and flavones are the most active and the binding affinities are lower for flavanones and isoflavones (BOUMENDJEL ET AL. 2002; SHEU ET AL. 2010). On the other hand, SHEU ET AL. (2010) conducted a study aiming to establish the qualitative and quantitative structure-activity relationships of flavonoids modulation effects on P-gp, using the human colorectal adenocarcinoma cells (HCT15) as an *in vitro* model and fexofenadine as a P-gp substrate probe. Accordingly, the flavonoid compounds with hydroxyl groups attached at the 5- and 7-positions of the ring A and with the total number of hydroxyl groups, at an optimal of three, possess a high inhibitory effect on P-gp activity (Figure I.3.8). However, flavonoids with four hydroxyl groups such as kaempferol (3,5,7,4'-tetrahydroxyflavone; Figure I.3.6) and fisetin (3,7,3',4'-tetrahydroxyflavone; Figure I.3.6) have not shown this high inhibitory effect on P-gp activity, whereas flavonoids with a greater number of hydroxyl groups such as quercetin (3,5,7,3',4-pentahydroxyflavone; Figure I.3.6) and taxifolin (3,5,7,3',4'-pentahydroxyflavanone; Figure I.3.4), were able to enhance P-gp activity (SHEU ET AL. 2010).

WESOŁOWSKA (2011) besides stating that flavonoids should possess hydroxyl groups at positions 3 and 5 of ring A and the 2,3-double bond to exhibit high affinity for NBD2 of P-gp, also described the importance of the carbonyl group at position 4 and a hydrophobic motif on either ring A or B (Figure I.3.8). The planar structure of flavonoids also seems to be important for their interaction with P-gp (Figure I.3.8). As a result, for flavanones which lack the double-bond between the 2- and 3-position in ring C, the stereoscopic relationship of the ring B with other rings (A and C) is different from that of flavones (with the double-bond in that position) (Figure I.3.4; Figure I.3.5). This double bond confers a special structure on flavonoids molecules that are largely planar so that they may readily intercalate between the hydrophobic amino acid residues of P-gp (KITAGAWA ET AL. 2005).

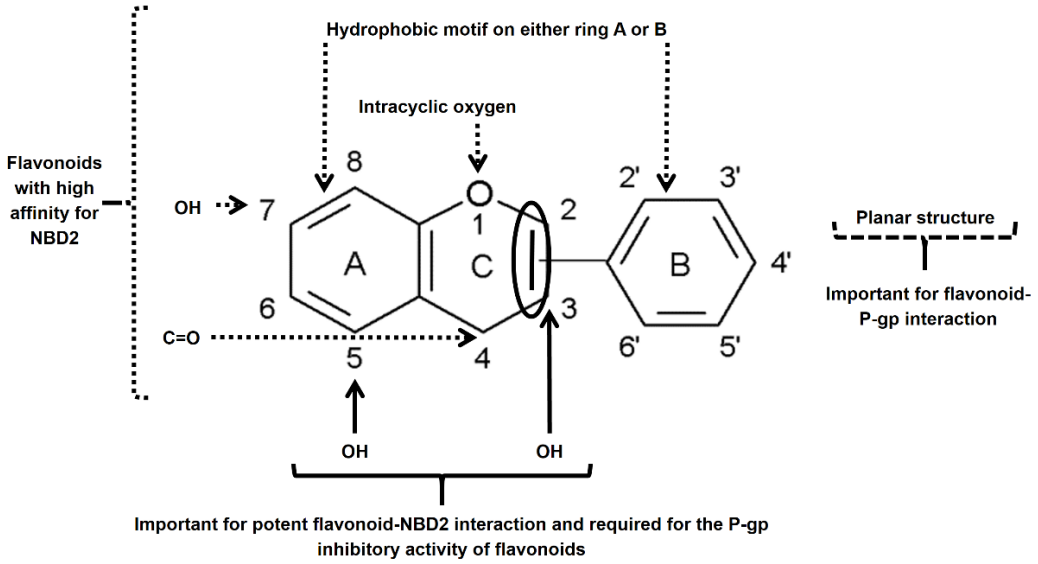

Figure I.3.8. Structure-activity relationship of flavonoids (NBD, nucleotide-binding domain; P-gp, P-glycoprotein) (BOUMENDJEL ET AL. 2002; KITAGAWA ET AL. 2005; HENDRICH 2006; MORRIS AND ZHANG 2006; BANSAL ET AL. 2009; SHEU ET AL. 2010; WESOŁOWSKA 2011).

Over the years, flavonoids have been subjected to various chemical modifications in order to obtain improved chemical entities as P-gp inhibitors. In general, it was found that chemical modifications that increased hydrophobicity of the flavonoid molecules, such as prenylation, geranylation, or a linear sequence of two isoprenyl residues, significantly increased the modulatory activity of P-gp (WESOŁOWSKA 2011). Therefore, in some cases, prenylated flavonoids bind with high affinity to P-gp and show an increased inhibitory potency (PIETRO ET AL. 2002; HENDRICH 2006). In this context, it was demonstrated that the introduction of alkoxy groups at position 4 of chalcones resulted in compounds much more actives, being recognised that the binding affinity increases as a function of the chain length (BOIS ET AL. 1999); on the other side, it was reported that halogenated chalcones exhibited high-affinity binding to P-gp and that the increase in binding affinity is related to the increase in hydrophobicity of the halogenate substituent (BOIS ET AL. 1998). The intracyclic oxygen may be also required, since, when it was replaced by a nitrogen atom, the P-gp inhibitory activity was dramatically reduced (Figure I.3.8) (KITAGAWA ET AL. 2005). The hydroxyl groups in polyphenols, such as those in the gallic acid moiety of tea catechins and alkyl gallates may be important in polar interactions with P-gp, possibly at the ATP-binding site. Accordingly, the hydrophobic moiety of polyphenols may be important for interaction at the steroid-interacting hydrophobic sequence of P-gp (KITAGAWA 2006). Thus, the hydrophobicity of flavonoid compounds is a critical parameter for binding affinity towards NBD2 and consequently for their inhibitory effects on P-gp–mediated efflux of substrates (PIETRO ET AL. 2002; KITAGAWA ET AL. 2005; KITAGAWA 2006). Thereby, the P-gp inhibitory activity of flavonoids increases as their molecular hydrophobicity increases (KITAGAWA ET AL. 2005). Additionally, WESOŁOWSKA (2011) underlined the role of the hydrophobicity of ring substituents because the compounds containing geranyl groups are more active than those substituted by halogen atoms, which are followed by flavonoids with methoxy and hydroxyl groups. On the other hand, the results of a virtual screening of flavonoids as P-gp inhibitory agents indicated that glutamine-47, tyrosine-53, serine-83, isoleucine-87, glycine-100 and arginine-154 of the P-gp molecule are determinant residues for binding interactions as they establish strong hydrogen bonding with flavonoid molecules (UDAYA KUMAR ET AL. 2011). UDAYA KUMAR ET AL. (2011) also referred that for the stability of the complex an important role is played by hydrogen bonding interactions.

Although detailed studies have been performed only on the interaction of flavonoids with NBD2, a similar binding site certainly also exists on NBD1 since flavonoids compete with ATP. Indeed, TROMPIER ET AL. (2003) reported that a series of flavonoids bind to both NBDs (1 and 2) of the human MRP1, being stated that isoprenylation of flavonoid molecules leads to a preferential binding to NBD1. Thus, it is expected that additional binding(s) is(are) also found within the TMDs' drug-binding sites, as described for MRP1 (TROMPIER ET AL. 2003).

I.3.1.2. Sources of flavonoids

The flavonoids are among the most ubiquitous groups of polyphenolic compounds found in foods and beverages of herbal origin (BOUMENDJEL ET AL. 2002; KITAGAWA ET AL. 2005; BADHAN AND PENNY 2006; BRAND ET AL. 2006; WESOŁOWSKA ET AL. 2009; CHAN ET AL. 2009). These compounds, diverse in chemical structure and characteristics, are found in high levels in fruits, vegetables, nuts, stems, flowers, red wine, soybeans and tea (COOK AND SAMMAN 1996; DEFERME AND AUGUSTIJNS 2003; BADHAN AND PENNY 2006; BRAND ET AL. 2006; ASZALOS 2008; CHAN ET AL. 2009). The anthocyanidines are mainly found in berries, cherries, grapes, red cabbage and red wine; the flavanols or catechins in apples, black tea, chocolate, bilberry, cocoa, grapes, hawthorn, motherwort, red wine and tea; the flavanones in tomato and citrus fruits and juices; the flavones in celery, honey, parsley, peppers, propolis, sweet red and thyme; the flavonols in apples, berries, broccoli, cherries, kale, leeks, lettuce, onions, red wine, tea and tomato; and, finally, the isoflavones can be found in legumes like peas, red clover and soy (MOON ET AL. 2006; ALVAREZ ET AL. 2010; SHOHAI ET AL. 2011; THILAKARATHNA AND RUPASINGHE 2013; TOH ET AL. 2013).

Apart from food components, flavonoids are also present in medicinal herbs or dietary supplements including silybin, which is extracted from milk thistle, *Silybum marianum, Alpina officinarum, Soy Isoflavones, Ginkgo biloba or Hypericum perforatum* (HENDRICH 2006; MOON ET AL. 2006; SHEU ET AL. 2010). Although in the usual human diet, the intake level of these compounds can be up to several hundred milligrams a day (WANG ET AL. 2005; BADHAN AND PENNY 2006; BRAND ET AL. 2006) in people consuming over-the-counter botanical and dietary supplements the intake may be considerably higher (LOHNER ET AL. 2007).

I.3.1.3. Biological properties and flavonoid-P-glycoprotein interactions

Flavonoids are water-soluble pigments and play diverse functions in the plant kingdom including defence, growth, development, photosensitization, ultraviolet (UV) protection, auxin transport inhibition, allelopathy and flower colouring (BUER ET AL. 2010; SHOHAI ET AL. 2011; JÄGER AND SAABY 2011). In 1936, Rusznyak and Szent-Gyorgyi reported the first observation regarding the biological activities of flavonoids (ROSS AND KASUM 2002). As integral constituents of the diet, they may exert a wide range of beneficial effects on human health in a multitude of disease states including cancer, cardiovascular diseases, neurodegenerative disorders and osteoporosis (BOUMENDJEL ET AL. 2002; BADHAN AND PENNY 2006; MORRIS AND ZHANG 2006; BRAND ET AL. 2006; WESOŁOWSKA ET AL. 2009; CHAN ET AL. 2009; WASOWSKI AND MARDER 2012). Moreover, there is recent evidence of an inverse relationship between dietary flavonoid intake and cardiovascular disease mortality and its risk factors (TOH ET AL. 2013). These broad spectrum of biological activities also include anti-inflammatory, antimicrobial, antiviral, anti-proliferative, pro-apoptotic, free-radical scavenging, antioxidant and hormonal effects (BOUMENDJEL ET AL. 2002; DEFERME AND AUGUSTIJNS 2003; HENDRICH 2006; BADHAN AND PENNY 2006; BRAND ET AL. 2006; WESOŁOWSKA ET AL. 2009; CHAN ET AL. 2009; BUER ET AL. 2010; WASOWSKI AND MARDER 2012). However, CHOI ET AL. (2011a) also referred that the protective defence mechanism against oxidants can be overcome by the

inadvertent overproduction of reactive oxygen species. Interactions with key enzymes, signalling cascades involving cytokines and transcription factors, or antioxidant systems, may originate the health-promoting effects of flavonoids (BUER ET AL. 2010; WASOWSKI AND MARDER 2012). Flavonoids have also attracted interest as new chemical entities with activity on the CNS. These actions can result from their binding to the benzodiazepine site on the $GABA_A$ receptor resulting in sedation, anxiolytic or anticonvulsant effects, or from their action as inhibitors of monoamine oxidase A or B, working as antidepressants or antiparkinsonian agents (ROMANO ET AL. 2013). However, although some of these activities have been demonstrated by FERNÁNDEZ ET AL. (2005), the antidepressant effects were not observed in rodents.

Flavonoids produce their modulating effects by a number of possible mechanisms (CHAN ET AL. 2009). Some of them are good inhibitors of a variety of ATP-binding proteins including protein kinases such as cyclic adenosine monophosphate dependent protein kinase, protein kinase C, serine/threonine kinases, tyrosine kinase, topoisomerase II, and myosin. They also inhibit various membrane ATPases, such as mitochondrial H^+-ATPase, Na^+/K^+-ATPase, Ca^{2+}-ATPase, and H^+/K^+-ATPase (PIETRO ET AL. 2002; BOUMENDJEL ET AL. 2002; CHAN ET AL. 2009). Moreover, the activities of many other enzymes are also inhibited by flavonoids, for instance ß-glucuronidase, lipoxygenase, cyclooxygenase, inducible nitric oxide synthase, monooxygenase, thyroid peroxidase, xanthine oxidase, mitochondrial succinoxidase and nicotinamide adenine dinucleotide-oxidase, phosphodiesterase and phospholipase A2 (MOON ET AL. 2006).

Although the molecular mechanisms particularly underlying flavonoid–P-gp interactions are not clear, several hypotheses have been proposed (CHAN ET AL. 2009; GO ET AL. 2009; CASSIDY AND SETZER 2010). Among the proposed mechanisms are the following: (a) flavonoids modulate P-gp by interacting with the vicinal ATP-binding site and the steroid binding site; (b) flavonoids act as substrate and may interact with P-gp directly either by competitive binding to the substrate-binding site or by binding to other drug-binding sites and changing the P-gp conformation; and (c) flavonoids may bind to the allosteric site or other binding sites (MORRIS AND ZHANG 2006; LOHNER ET AL. 2007; GO ET AL. 2009; ALVAREZ ET AL. 2010). Thus, due to the complexity of interactions between P-gp and its modulators, and also because the interactions of flavonoids with P-gp may be different for specific flavonoids, the elucidation of the exact interaction mechanism between these polyphenolic compounds and P-gp is difficult (ZHANG AND MORRIS 2003a; GO ET AL. 2009). Therefore, it has been shown that flavonoids, such as flavonols (e.g., quercetin; Figure I.3.6), flavanones (e.g., naringenin; Figure I.3.4), isoflavones (e.g., genistein; Figure I.3.7) and glycosylated flavonol derivatives (e.g., rutin; Figure I.3.6), directly interact with the ATP-binding site and the vicinal steroid binding site, leading to the inhibition of P-gp function (MORRIS AND ZHANG 2006; LOHNER ET AL. 2007; CHEN ET AL. 2010). Others flavonoids compounds, like epicatechin (Figure I.3.3) from green tea, activate P-gp by a heterotropic allosteric mechanism (LOHNER ET AL. 2007). In addition, MORRIS AND ZHANG (2006) reported that flavonoids may also directly bind to the C-terminal NBD2 of the purified recombinant mouse P-gp; for instance chrysin (Figure I.3.5), quercetin (Figure I.3.6) and kaempferol (Figure I.3.6) directly bound to the NBD2 cytosolic domain of mouse P-gp (CHAN ET

AL. 2009). According to BADHAN AND PENNY (2006) flavonoids have also shown to interact with NBDs of ATPase transporters. The inhibition of the ATPase activity and direct binding of flavonoids to the C-terminal NBD2 of murine Abcb1 has been demonstrated using saturation transfer difference-nuclear magnetic resonance spectroscopy (BADHAN AND PENNY 2006).

Thus, the use of flavonoids as potential modulators of P-gp–mediated drug efflux is highly attractive and NBDs represent potential targets for therapeutic intervention (BADHAN AND PENNY 2006). Flavonoids bind to NBD of P-gp by overlapping simultaneously both binding sites of the cytosolic domains (TROMPIER ET AL. 2003; KITAGAWA 2006). As a result, these compounds have been suggested to be modulators with bifunctional interactions at vicinal ATP-binding sites and steroid-interacting regions of the P-gp, which are expected to be in close proximity to the ATP-binding site, within a cytosolic domain of P-gp (CONSEIL ET AL. 1998; KITAGAWA ET AL. 2005; KITAGAWA 2006; MORRIS AND ZHANG 2006; TRAN ET AL. 2011). In such situation, the hydrophobic ring B would bind to the steroid-binding region, whereas rings A and C would bind to the ATP pocket (KITAGAWA ET AL. 2005). The results presented by SHEU ET AL. (2010) confirm that flavonoids have bifunctional interactions in their rings A and C at the ATP-binding site, and the hydrophobic ring B at the steroid-interacting hydrophobic sequence of P-gp. Thus, flavonoids may induce their binding affinity towards NBD2 of P-gp through their ability to mimic the adenine moiety of ATP (PIETRO ET AL. 2002; BOUMENDJEL ET AL. 2002; KITAGAWA 2006). However, it is also postulated that these compounds may also interact with P-gp by other mechanisms once opposite effects on P-gp ATPase activity have been observed for different flavonoids (MORRIS AND ZHANG 2006).

Although chalcones, flavones and flavonols have demonstrated to possess multidrug resistance reversing activity through their high affinity to bind P-gp, the isoflavones have been reported as inactive as modulators of the P-gp functioning (HADJERI ET AL. 2003). Overall, the concentrations of flavonoids required to produce a significant modulation of P-gp activity seem to be 10 μM or higher. These concentrations appear to be easily achievable in the intestine after food ingestion and, especially, in the course of dietary supplementation (MORRIS AND ZHANG 2006; BANSAL ET AL. 2009).

Many of the flavonoid glycosides may not potently interact with P-gp. However, the aglycones released from these glycosides could be present in intestine at high enough concentrations to inhibit intestinal P-gp, resulting in potential drug interactions (MORRIS AND ZHANG 2006; BANSAL ET AL. 2009). Nevertheless, except for the more potent flavonoids, the concentration of flavonoid aglycones in the systemic circulation may not be high enough for the occurrence of significant P-gp interactions in other tissues (MORRIS AND ZHANG 2006). Moreover, because the main metabolites of flavonoids (glucuronides and sulphate conjugates) are organic anions, these may not interact with P-gp. Hence, even after regular supplementation the systemic inhibition of P-gp by flavonoids or their metabolites may be, in general, insignificant. However, a significant interaction could occur after administration of an extremely high dose, especially by intravenous (iv) injection (MORRIS AND ZHANG 2006; BANSAL ET AL. 2009). In that way, flavonoid modulators also have limitations besides their moderate activity as P-gp inhibitors. Thus, they have a broad spectrum of biological activities including anti-estrogenic activity and the

inhibition of other ATPases (CHAN ET AL. 2009); they can also inhibit the absorption of some nutrients, change the pharmacokinetics of certain drugs, and affect neurobehavioral development (WANG ET AL. 2007).

I.3.1.3.1. Interactions of flavonoids with P-glycoprotein

Currently, with the resurgence of the use of medicinal herbs in the western world, the combined use of modern and traditional therapies is increasingly becoming more common (PATHAK AND UDUPA 2010; NEWMAN AND CRAGG 2016). Although many ingredients in the dietary supplements are not thoroughly studied, a significant number of people regularly consume them in the hope of improving their health and prevent or treat specific diseases (PENG ET AL. 2006). However, either harmful or beneficial food–drug interactions can occur, particularly due to changes in drug bioavailability. Therefore, the interactions of dietary supplements with drugs may be exploited as a way to improve the pharmacokinetic properties of the coadministered drug (PENG ET AL. 2006; BANSAL ET AL. 2008; PATHAK AND UDUPA 2010). In the process of drug discovery and development, several drug candidates have been found to be potent, safe, selective and affordable, but often do not have a favourable pharmacokinetic profile. Thus, the coadministration of another drug or molecule may improve the drug's pharmacokinetic properties. In this way, a promising approach to overcome the P-gp–mediated drug resistance can be the coadministration of safe dietary phytochemicals that are inhibitors of known drug transporters or metabolizing enzymes which are determinants for drug biodisposition (PENG ET AL. 2006). This strategy can result in a more cost-effective therapy, by saving additional amounts of drugs due to the optimization of drug delivery (AMIN 2013).

The resistance against a variety of chemically unrelated drugs may be due to the overexpression of P-gp in the plasma membrane (BREIER ET AL. 2013). The dietary flavonoids have gained a great attention in respect of the discovery of effective P-gp inhibitors owing to their various health promoting effects and favourable safety profiles. Indeed, because some of these compounds appear to inhibit P-gp–mediated drug efflux, they have potential value to enhance the cellular availability of diverse drugs (GO ET AL. 2009; ABDALLAH ET AL. 2015; MOHANA ET AL. 2016). Hence, through an effect on the ATPase activity, the flavonoids can modulate ABC transporters by inhibition (e.g., genistein and quercetin) or induction (e.g., glabridin) (ALVAREZ ET AL. 2010).

Many prototypic inhibitors and inducers affect both CYP3A4 and P-gp and thus many drug interactions caused by these inhibitors and inducers involve these two systems. Nevertheless, although the P-gp participates in drug efflux phenomena affecting absorption, distribution and elimination of numerous drugs, the CYP enzymes are only involved in drug metabolism (LIN 2003). Due to their beneficial pharmacological activities and their additional ability to modulate both CYP3A4 and P-gp, flavonoids have attracted much attention in recent years (HSIU ET AL. 2002; FANG ET AL. 2005; CHOI AND LI 2005; RAO ET AL. 2007; CHO ET AL. 2011; LI ET AL. 2011). To eliminate foreign compounds, P-gp co-localizes with CYP3A4 in the polarized epithelial cells of excretory organs, such as the liver, kidney and intestine (LI ET AL. 2011). Since CYP3A4 and P-gp share a substantial overlap in substrate specificity, their function can modulate the

bioavailability of many drugs, affecting their pre-systemic metabolism (CHOI AND BURM 2006; CHOI AND KANG 2008; LI ET AL. 2009; LI ET AL. 2011) and promoting the circulation of P-gp substrates between the lumen and epithelial cells. These facts prolong the drug exposure to CYP3A4, reducing the systemic absorption (CHOI AND LI 2005; CHOI AND BURM 2006; CHOI AND KANG 2008). Thus, it seems important to understand the actions of flavonoids not only on the function of P-gp, but also at the P-gp expression levels (LOHNER ET AL. 2007).

Actually, the effects of flavonoids compounds on the level of P-gp expression and/or P-gp activity in cells and tissues may globally change the pharmacokinetic parameters of many drugs. Obviously, this can lead to modifications in drug bioavailability, as well as in biodisposition and toxicity (CHIELI ET AL. 2009). However, many phytochemicals have poor bioavailability and show limited efficacy *in vivo* (GO ET AL. 2009). With the great interest in herbal components as alternative medicines, more preclinical and clinical investigation of interactions between herbal constituents and drugs needs to be performed to prevent potential adverse reactions, or to utilize those interactions for therapeutic benefit (PIAO AND CHOI 2008a; SHIN ET AL. 2009; PATHAK AND UDUPA 2010; SINGH ET AL. 2012). However, there is far less information on the pharmacokinetic interactions between herbal products and drugs (SHIN ET AL. 2009; PATHAK AND UDUPA 2010; SINGH ET AL. 2012) and several efforts are currently being expended to identify natural phytocompounds that modulate P-gp and metabolic enzymes (SHIN ET AL. 2009; CHO ET AL. 2011).

Due to the popular use of flavonoid-containing dietary supplements, flavonoid–drug interactions have been increasingly reported (SINGH ET AL. 2012). Therefore, the discover of promising compounds for P-gp inhibition among flavonoids still continuous (GO ET AL. 2009). The literature cites various examples of flavonoids as inhibitors of P-gp transport, which affect the bioavailability and uptake of many drugs. These include in *vitro studies* on the effect of flavonoids on intracellular accumulation, efflux or transport of P-gp substrates using cells overexpressing P-gp, or a variety of animal and clinical studies (BANSAL ET AL. 2009). Then, several *in vitro*, *in vivo* non-clinical and clinical assays performed with different flavonoids are presented below, constituting a summary of the literature data and a starting point for new studies.

I.3.1.3.1.1. Cell-based in vitro models

Over the years, a great diversity of flavonoid compounds has been tested in *in vitro* conditions, particularly in cell-based models, aiming to assess their effects on the expression levels and functional activity of P-gp (Table A.1, Appendix A). In many studies, molecular biology assays prior to functional tests were performed either as confirmatory tests to effectively verify the presence of P-gp in the cells, or as quantization assays to determine the effects of the flavonoids on the expression levels of P-gp.

In order to evaluate the potential effect that a flavonoid may have in the P-gp activity (as inhibitor or inducer), at least one P-gp probe substrate must be used in the *in vitro* functional

assays which include accumulation/efflux and/or transport assays. However, the selection of the adequate P-gp probe substrate is not easy, especially because such compounds may interact with other transport proteins and metabolizing enzymes. Thus, according to a FDA draft guidance for drug interaction studies, an *in vitro* P-gp probe substrate should be selective for the P-gp transporter, exhibit low to moderate passive membrane permeability through the cell monolayer, not suffer significant metabolism, be commercially available, and be suitable to be also used as an *in vivo* P-gp probe substrate (U.S. FOOD AND DRUG ADMINISTRATION 2006).

Analysing Table A.1 (Appendix A), there are flavonoids that stand out as being simultaneously inducers and inhibitors of P-gp. For example, the flavanol (-)-epigallocatechin gallate [(-)-EPG] (Figure I.3.3) appeared to be a strong inducer of P-gp expression in Caco-2 cells when used at a concentration of 10 μM (LOHNER ET AL. 2007); however, its uses at concentrations levels in the order of 100 μM inhibited P-gp function in the same cell model (JODOIN ET AL. 2002). AN AND MORRIS (2010) and MITSUNAGA ET AL. (2000) also reported a biphasic effect of biochanin A (Figure I.3.7) and quercetin (Figure I.3.6) in the P-gp function. MITSUNAGA ET AL. (2000) concluded that low concentrations of quercetin indirectly activate the efflux transport of [^{3}H]-vincristine by enhancing the phosphorylation and thus the activity of P-gp, whereas high concentrations of quercetin lead to P-gp inhibition. Thus, the uptake of [^{3}H]-vincristine by MBEC4 cells in the steady-state was decreased by 10 μM quercetin, but increased by 50 mM quercetin (MITSUNAGA ET AL. 2000). Likewise, SCAMBIA ET AL. (1994) reported that 10 μM of quercetin reduces the expression of the immunoreactive P-gp in MCF-7/ADR-resistant cells as evaluated by flow cytofluorimetry. In the study performed by AN AND MORRIS (2010), the intracellular fluorescence of mitoxantrone, a P-gp substrate, decreased when co-incubated with 10 μM of biochanin A while there was no significant difference in mitoxantrone cell accumulation in the presence of 50 μM biochanin A. These results indicate that biochanin A may induce the P-gp activity at lower concentrations, and, hence, decreasing the intracellular concentration of mitoxantrone. Actually, several studies summarized in Table A.1 (Appendix A) revealed that the inhibitory effects of various flavonoids on P-gp function were concentration-dependent (e.g., diosmin, fisetin, naringin, silymarin, tangeritin) (ROMITI ET AL. 2004; KITAGAWA ET AL. 2005; CASTRO ET AL. 2007; MERTENS-TALCOTT ET AL. 2007; YOO ET AL. 2007). The increase in P-gp expression levels caused by some flavonoids such as catechin (Figure I.3.3), naringenin (Figure I.3.4) or chrysin (Figure I.3.5) in *in vitro* intestinal epithelial cells may represent an adaptation or defence mechanism limiting the entry of lipophilic xenobiotics into the organism (LOHNER ET AL. 2007).

The *in vitro* results shown by OFER ET AL. (2005) also demonstrated that the flavonoids hesperetin, naringin (Figure I.3.4), isoquercetin, kaempferol, quercetin and spiraeoside (Figure I.3.6) bear the ability to interfere with processes of secretory intestinal transport. These effects may occur due to the interaction of flavonoids with P-gp, but apparently not via competition at the talinolol (P-gp probe substrate) binding site of P-gp as demonstrated by the radioligand binding assay, where none of the tested flavonoids showed to induce the displacement of talinolol. Another mode of interaction may be the inhibition of members of the organic cation transporters family, which are located at the basolateral membrane of

intestinal epithelial cells. These organic cation transporters are mainly located in the basolateral membranes of kidney and liver and usually mediate the uptake of compounds with a transiently or permanently positive net charge into the cells of these excretory organs (OFER ET AL. 2005).

In some cases, the use of distinct *in vitro* systems and/or assays yielded slightly different results. Therefore, it is important to test flavonoid compounds in different cell lines and using different assays in order to increase the confidence in their classification as inhibitors or inducers of P-gp. The inhibition of P-gp activity by many flavonoids and the increased cell accumulation of many drugs (P-gp substrates) suggests the possibility of important changes in absorption/bioavailability of such drugs by the coadministration of these compounds (ZHANG AND MORRIS 2003b). In this context, despite the valuable evidence often obtained from these *in vitro* studies on the modulation of P-gp by flavonoids, more conclusive results are only achieved through interaction studies conducted in *in vivo* conditions (CHOI ET AL. 2010; CHOI ET AL. 2011a).

I.3.1.3.1.2. In vivo animal models

Table A.2 (Appendix A) summarizes the main features regarding the *in vivo* studies conducted to assess the effects of flavonoids in the bioavailability of different drugs (P-gp substrates) administered orally and/or iv. Indeed, it has been reported that pharmacokinetic interaction between herbal constituents and drugs may be mediated by CYP metabolizing enzymes and also by drug transporters such as P-gp (CHO ET AL. 2009). Based on the broad overlap in their substrate specificities as well as their co-localization in the small intestine (the primary site of absorption for orally administered drugs), CYP3A4 and P-gp have been recognized as a concerted barrier to drug intestinal absorption (SHIN ET AL. 2009). Since P-gp is co-localized with CYP3A4 in the small intestine, P-gp and CYP3A4 may act synergically in pre-systemic metabolism, limiting the absorption of drugs which are substrates of both proteins (PIAO ET AL. 2008; CHO ET AL. 2009; LI ET AL. 2011). Therefore, dual inhibitors against CYP3A4 and P-gp can have a great impact on the bioavailability of many drugs (SHIN ET AL. 2009). Bearing this in mind, several studies using flavonoids have been performed in order to develop P-gp inhibitors that reduce the drug efflux in the intestine and, hence, enhance oral bioavailability of P-gp substrate drugs (PARK ET AL. 2012). The dosage of drug should be also considered in case of the increased drug toxicity following the combination with flavonoids (LI ET AL. 2009). In most studies included in the Table A.2 (Appendix A), the pretreatment of the animals with a flavonoid (10-30 minutes before drug administration) is sufficient to significantly increase the oral drug bioavailability. For instance, the oral bioavailability of diltiazem was increased in male Sprague-Dawley rats submitted to a pretreatment with the flavanone hesperidin (Figure I.3.4). LI ET AL. (2011) also describe the higher bioavailability of tamoxifen in male Sprague-Dawley rats pretreatment with the flavone baicalein (Figure I.3.5). According to the authors, this increase might be mainly due to the flavonoid-mediated inhibition of CYP3A metabolism and P-gp efflux (CHOI ET AL. 2004a; YEUM AND CHOI 2006; CHOI ET AL. 2006; LI ET AL. 2007; SHIN ET AL. 2008; PIAO AND CHOI 2008a; LI AND CHOI 2008;

Choi and Kang 2008; Li et al. 2009; Cho et al. 2009; Shin et al. 2009; Lee and Choi 2010; Cho et al. 2011).

In addition, some studies also compared the effect of the flavonoid pretreatment on the bioavailability of a drug administered either orally or iv; as expected, in the majority of these studies the impact of the flavonoid pretreatment on pharmacokinetics of the drug administered intravenously was less significant than after oral administration (Choi et al. 2006; Li et al. 2007; Piao and Choi 2008a; Bansal et al. 2008; Li et al. 2009; Shin et al. 2009; Pathak and Udupa 2010; Lee and Choi 2010; Cho et al. 2011). Accordingly, the enhanced oral drug exposure in the presence of the flavonoid, together with insignificant changes on drug pharmacokinetics after iv administration, supposes that the increased intestinal absorption occurs via flavonoid-mediated P-gp inhibition rather than reduction in drug elimination (Choi et al. 2006; Lee and Choi 2010). As shown in Table A.2 (Appendix A), the study performed by Li and Choi (2007), in which genistein (Figure I.3.7) was pre-administered at a dose of 10 mg/kg, the area under the concentration-time curve (AUC) significantly increased and the total body clearance (CL_t) was reduced for iv paclitaxel. This study is consistent with the results reported by Lim and Choi (2006) where a dose of 10 mg/kg of naringin (Figure I.3.4), a dual inhibitor of CYP3A and P-gp, significantly increased the AUC and reduced the CL_t of paclitaxel administered by iv route to rats. According to the authors, the significantly greater value of AUC could be due mainly to an inhibition of metabolism of paclitaxel via CYP3A1/2 by oral naringin, but the inhibition of hepatic P-gp by oral naringin could also contribute (Lim and Choi 2006).

In other studies, the animals were not pretreated with the flavonoid, but a simultaneous coadministration with the target drug was performed. The results obtained after oral and/or iv administration of the drug are similar to the aforementioned (Choi and Han 2005; Shin et al. 2006; Piao and Choi 2008b; de Castro et al. 2008; Li and Choi 2009; Go et al. 2009). In other words, overall, the oral drug bioavailability significantly increased after coadministration of the flavonoid, but the same was not true when the drug was administered iv. However, the results reported by Choi and Li (2005) and Choi and Burm (2006) disagree with this theory. Indeed, in male New Zealand white rabbits pretreated with the flavanone morin (Figure I.3.4), the oral bioavailability of nimodipine was significantly increased, but the same did not occur when the drug was simultaneously coadministered with the flavonoid (Choi and Li 2005; Choi and Burm 2006). Accordingly, the morin can interact with nimodipine in the gastrointestinal lumen forming a flavonoid-drug complex that is not absorbed, or the absorption of morin in the gastrointestinal mucosa is early enough to inhibit nimodipine-CYP3A4 metabolizing enzyme and P-gp efflux pump by a pretreatment period of 30 min before nimodipine administration (Choi and Burm 2006). The same results were obtained by Choi and Li (2005) wherein the bioavailability of diltiazem in rabbits pretreated with quercetin (Figure I.3.6) is significantly increased, but not in the rabbits coadministered with quercetin. The coadministration of naringenin (Figure I.3.4) with talinolol in male Sprague-Dawley rats also did not result in a significant increase of the oral drug bioavailability (de Castro et al. 2008).

As biochanin A (Figure I.3.7) is an inhibitor of CYP3A and P-gp and tamoxifen a well-known substrate of CYP3A4/P-gp, after their coadministration an increase of the oral bioavailability of tamoxifen was expected; however this was not observed, and a significant decrease in the relative bioavailability of tamoxifen after the coadministration of the flavonoid was reported by SINGH ET AL. (2012). This isoflavone also caused a significant decrease in oral bioavailability of fexofenadine that is not metabolized by CYP isoenzymes at a large extent (PENG ET AL. 2006). Similarly, HSIU ET AL. (2002) reported the decrease in the oral bioavailability of cyclosporin when coadministered with quercetin (Figure I.3.6) in male Sprague-Dawley rats and in male Yorkshire pigs. Finally, PARK ET AL. (2012) studied the effect of the coadministration of silymarin [a flavonoid composed mainly by silybin (90%), as silybin A, silybin B and isosilybin A, and also by silydianin, and silychristin (Figure I.3.9)] on oral bioavailability of paclitaxel, and the results obtained demonstrated an increased oral bioavailability of the drug (a P-gp substrate). Actually, all the previously reported results suggest that the concurrent use of flavonoids or flavonoids-containing dietary supplements or herbs with medications whose absorption and metabolism are mediated by P-gp and/or CYP3A4 should be given with special attention (HSIU ET AL. 2002).

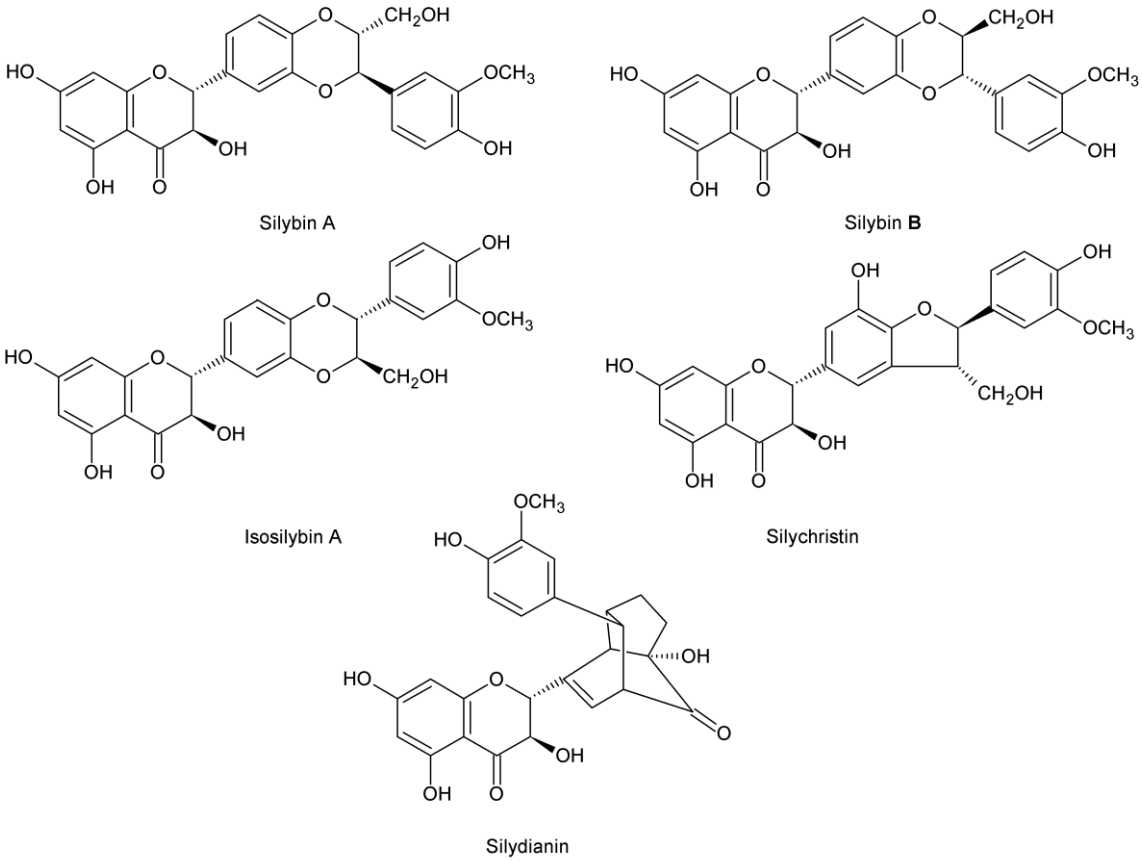

Figure I.3.9. Some constituents of the flavonoid silymarin (GAZÁK ET AL. 2007; KATIYAR ET AL. 2008).

I.3.1.3.1.3. Clinical studies

Up to date there are few clinical studies published in literature documenting the effect of a particular flavonoid on the pharmacokinetics of a given drug. Two of those studies were developed by RAO ET AL. (2007) and KIM ET AL. (2009) testing the flavonoids silymarin (Figure I.3.4) and quercetin (Figure I.3.6) respectively. RAO ET AL. (2007) investigated the effect of silymarin pretreatment on the pharmacokinetics of ranitidine in twelve healthy male human volunteers (age range 19-26 years, weight 50-68 kg). The study design involved the administration of 150 mg ranitidine to the volunteers, either alone, or after a 7 days pretreatment period with thrice-daily dose of 140 mg silymarin, after an overnight fast. The washout period between each ranitidine treatment was 7 days and the serum levels of the drug were determined by high-performance liquid chromatography (HPLC) with UV detection. The results showed that the pharmacokinetics of ranitidine was not influenced by silymarin. The plasma peak concentration (C_{max}), the plasma AUC from zero to 12 h (AUC_{0-12}), the plasma AUC from zero to infinity ($AUC_{0-\infty}$), elimination rate constant (K_{el}), terminal elimination half-life ($t_{1/2el}$) and time to reach C_{max} (t_{max}) were not significantly altered after pretreatment with silymarin. However, the area under the first moment curve (AUMC) and the mean residence time (MRT) showed a significant increase after the silymarin pretreatment. Indeed, despite ranitidine is a substrate of CYP3A4 and P-gp, and silymarin a flavonoid compound that has potential to influence drug biodisposition by decreasing the metabolic activity of CYP3A4 and by inhibiting P-gp function, important changes were not evidenced in the majority of the pharmacokinetic parameters of ranitidine. RAO ET AL. (2007) suggested that silymarin was so poorly absorbed after oral administration that its blood concentrations were too low to cause an appreciable effect on CYP3A4 or P-gp.

In turn, KIM ET AL. (2009) developed a study aimed at evaluating whether quercetin exhibited any inhibitory effect on P-gp–mediated drug disposition in humans using fexofenadine as a P-gp probe substrate. In this study, twelve healthy male subjects (age range 24–31 years, weight 67–82 kg) were treated for 7 days with 500 mg quercetin or placebo three times daily. Subsequently, a single dose of 60 mg fexofenadine was administered orally on day 7. Afterwards, the fexofenadine drug concentrations in plasma and urine samples were quantified using HPLC coupled to fluorescence detection. After a pharmacokinetic analysis of the concentration-time profiles, a significant increase in the mean plasma concentrations of fexofenadine after quercetin treatment was registered; more specifically, the AUC of plasma fexofenadine was increased by 55% and the C_{max} was elevated by 68% during the quercetin treatment. Nevertheless, no differences were observed in the renal clearance or apparent terminal elimination half-life ($t_{1/2el}$) of fexofenadine between placebo and quercetin phases, but the oral clearance of the drug was significantly decreased (37%) under quercetin treatment. The results of this clinical study showed that the short-term use of quercetin elevated the plasma concentrations of fexofenadine and it may occur due to the inhibition of P-gp–mediated drug efflux (KIM ET AL. 2009). Hence, more clinical trials are needed to reliably assess the effects of flavonoids in modulating P-gp function in humans.

I.4. Aims

I.4.1. Aims of this thesis

Regardless the large number of currently available AEDs, and albeit their broad spectrum of efficacy, the pharmacoresistance remains a major problem in the therapeutics of epilepsy. The hypothesis of the efflux transporters is one of the theories pointed out to explain this phenomenon, being recognised, in particular, the contribution of the P-gp as an important drug efflux transporter. In this context, the main goal of this thesis was to carry out an integrated non-clinical pharmacometric evaluation of the potential of coadministration of AEDs and flavonoid compounds as a strategy to reverse the drug resistance verified in epilepsy. Actually, in addition to their potential efficacy and safety as P-gp inhibitors, flavonoids appear to exert some other beneficial activities in the CNS. Hence, these agents may not only help to optimise the pharmacokinetics of AEDs that are P-gp substrates, but also to potentiate their anticonvulsant activity as well as reduce their systemic toxicity. Therefore, the conduction of several *in vitro* and *in vivo* studies designed to compare the pharmacokinetic properties of CBZ, LTG, OXC and PHT in the absence and presence of flavonoids is fully justified. These AEDs are widely used in the clinical practice as first- or second-line drug therapies for the management of a variety of different seizure types and epileptic syndromes.
In order to obtain accurate and reliable quantitative data, it was necessary to develop and validate appropriate bioanalytical methods to quantify the target analytes in the biological matrices of interest. Accordingly, the development of new bioanalytical tools was required to quantify CBZ, LTG, OXC, PHT and some of their metabolites; when justified other analytes of interest, such as PB, were also included in order to extend the applicability of the each technique.

Regarding this, the following specific objectives were outlined for the implementation of this doctoral work:

- Development and validation of an HPLC method coupled with diode array detection (DAD) based on microextraction by packed sorbent (MEPS) to simultaneously quantify five AEDs (CBZ, LTG, OXC, PHT and PB) and the pharmacologically active metabolites of CBZ [carbamazepine-10,11-epoxide (CBZ-E)] and OXC [licarbazepine (LIC)] in human plasma.

- Development and validation of appropriate HPLC-DAD methodologies to quantify CBZ, CBZ-E, LTG, OXC, LIC, PHT and the main PHT metabolite [5-(4-hydroxyphenyl)-5-phenylhydantoin (HPPH)] in cell culture matrices, and in rat plasma and brain tissue homogenate. These quantitative bioanalytical tools were essential to support the *in vitro* and *in vivo* experiments mentioned in the following aims.

- Characterization of the target AEDs (CBZ, LTG, OXC and PHT) and the active metabolites (CBZ-E and LIC) as P-gp substrates and/or inhibitors or inducers in a suitable *in vitro* cell model.

- *In vitro* evaluation of several individual flavonoid compounds as potential P-gp inhibitors through rhodamine 123 (Rh123, a classic P-gp probe) intracellular accumulation assays. Then, the effects of the most promising flavonoids on the intracellular accumulation of the AEDs and active metabolites were also investigated.

- Investigation of the *in vitro* profile of dual flavonoid combinations on the inhibition of the P-gp activity, through the comparison of their individual and combined effects in the intracellular accumulation of Rh123 (P-gp probe). These assays were followed by an evaluation of the potential of the most promising flavonoid combinations in increasing the intracellular accumulation of the AEDs and metabolites characterized as P-gp substrates.

- *In vivo* non-clinical assessment of the impact of the most promising flavonoid compound and dual flavonoid combination, selected as P-gp inhibitors in the previous *in vitro* screening assays, on the pharmacokinetics of the target AEDs that prove to be P-gp substrates.

CHAPTER II

Drug Analysis

The content of this chapter is included in the following manuscripts:

FERREIRA A ***ET AL.*** (**2014**) Liquid chromatographic assay based on microextraction by packed sorbent for therapeutic drug monitoring of carbamazepine, lamotrigine, oxcarbazepine, phenobarbital, phenytoin and the active metabolites carbamazepine-10,11-epoxide and licarbazepine. *J Chromatogr B Anal Technol Biomed Life Sci*. 971: 20–29. doi:10.1016/j.jchromb.2014.09.010

FERREIRA A ***ET AL.*** (**2016**) A Rapid and Sensitive HPLC–DAD Assay to Quantify Lamotrigine, Phenytoin and Its Main Metabolite in Samples of Cultured HepaRG Cells. *J Chromatogr Sci*. 54(8): 1352–1358. doi:10.1093/chromsci/bmw088

FERREIRA A ***ET AL.*** (**2016**) HPLC–DAD Method for the Quantification of Carbamazepine, Oxcarbazepine and their Active Metabolites in HepaRG Cell Culture Samples. *Chromatographia* 79(9): 581–590. doi:10.1007/s10337-016-3063-7

II.1. General Considerations

II.1.1. Quantitative drug analysis

The measurement of a compound (drug) or their metabolites in biological samples such as blood, plasma, serum, urine, other fluids (e.g., saliva, cerebrospinal fluid) or tissues, employing fast, cost-effective, sensitive, well-characterized and fully validated analytical methods, is the key determinant in generating reproducible and reliable data used in the evaluation and interpretation of bioavailability, bioequivalence, pharmacokinetic and toxicokinetic findings (SHAH ET AL. 2000; VISWANATHAN ET AL. 2007; NOVÁKOVÁ AND VLCKOVÁ 2009; TIWARI AND TIWARI 2010; PANDEY ET AL. 2010). Actually, bioanalysis can be considered the cornerstone of the whole drug discovery and development process (KORFMACHER 2011), as well as in the therapeutic drug monitoring (TDM) after drug approval (SHAH ET AL. 2000; NOVÁKOVÁ AND VLCKOVÁ 2009).

A bioanalytical method consists of two main components, the sample preparation and the instrumental detection of the target analytes. The sample preparation step aims to clean up the sample before instrumental analysis and/or to concentrate the analytes of interest to improve its detection (PANDEY ET AL. 2010). In the sample preparation procedure multiple techniques can be applied, the conventional ones such as protein precipitation (PP), liquid-liquid extraction (LLE) and solid-phase extraction (SPE), and the most recent and innovative methodologies as solid-phase microextraction, liquid-phase microextraction, microextraction by packed sorbent (MEPS), stir-bar sorptive extraction, and single-drop microextraction. Of course all the techniques have their own advantages and disadvantages, and the choice of most suitable will depend on the intended purposes (FARHADI ET AL. 2012; ALVES ET AL. 2013; KATAOKA ET AL. 2016). With regard to the instrumental analysis, the high-performance liquid chromatography (HPLC) coupled to several types of detection systems remains the standard methodology for drug analysis due to its ability to separate quite complicated mixtures of low and high molecular weight compounds, with different polarities and acid–base properties, in various matrices (NOVÁKOVÁ AND VLCKOVÁ 2009). Although the mass spectrometry detectors are those of choice, the diode array detector (DAD) is one of the most widely used detection systems in the analytical laboratories due to its versatility and cost-effectivity (PANDEY ET AL. 2010).

A bioanalytical method must be conveniently developed, optimised and validated before its implementation for a routine use. Nevertheless, each methodology has its own characteristics that vary from analyte to analyte, being the appropriateness of the technique influenced by the ultimate goal of the study (SHAH ET AL. 2000; TIWARI AND TIWARI 2010).

The development of a bioanalytical methodology is an inherently laborious and complex process that can be conducted in multiple ways depending on its specific requirements, the stage of drug discovery and development process and the analyst's experience (PANDEY ET AL. 2010; FORTUNA ET AL. 2014). Thus, the development of and analytical method may simply involve, in one extreme, the adaptation of an existing method by making minor changes so that it is suitable for a new application; but, at the other extreme, the analyst may start out with a few sketchy ideas and apply expertise to develop a proper method (EURACHEM 2014). After

developing and optimising the sample preparation and instrumental conditions, the analytical method needs to be properly validated. Indeed, the success of validation is a reflection of a well performed bioanalytical method development and optimisation (CHANDRAN AND SINGH 2007). The validation of a bioanalytical method includes a systematic process which permit to demonstrate that a particular method for the quantitative determination of the concentration of an analyte (or series of analytes) in a particular biological matrix is acceptable and reliable for the intended application (SHAH ET AL. 2000; CHANDRAN AND SINGH 2007). Generally, a reliable bioanalytical method should fulfil the acceptance criteria of the international guidelines on bioanalytical method validation for a set of reliability parameters as selectivity, linearity, precision, accuracy, limits of quantification and detection, recovery and stability of the analyte(s) in the biological matrix (U.S. FOOD AND DRUG ADMINISTRATION 2001; EUROPEAN MEDICINES AGENCY 2011).

This chapter sets up the beginning of the experimental work underlying the present thesis. In order to support the *in vitro* and *in vivo* studies that were intended to develop, the first requirement was the availability of appropriate and reliable analytical assays to quantify the antiepileptic drugs (AEDs) and their respective main metabolites in different biological matrices that include cell culture samples and rat plasma and brain samples.

Accordingly, a bioanalytical method that would allow the simultaneous quantification of all the compounds of interest was initially developed and validated in human plasma, which can be a useful tool to support the TDM of phenytoin (PHT), phenobarbital (PB), carbamazepine (CBZ), oxcarbazepine (OXC) and lamotrigine (LTG) in routine clinical practice. This strategy was also considered as a starting point due to the characteristics of the human plasma as biological matrix. Indeed, human plasma is a complex biological matrix, easily accessible, available in large quantities and whose existing ethical constraints are easily overcome, thus making it the ideal matrix for the optimisation of various analytical conditions that could be applied in the subsequent techniques used for the quantitative drug analysis in cellular and animal matrices.

The next steps included the development and validation of two HPLC-DAD assays for the quantification of the AEDs of interest (CBZ, LTG, OXC and PHT) and their main metabolites [carbamazepine-10,11-epoxide (CBZ-E), licarbazepine (LIC) and 5-(4-hydroxyphenyl)-5-phenylhydantoin **(**HPPH)] in cell culture samples.

The analytical methodologies used to quantify the intended AEDs and metabolites in the rat plasma and brain matrices were only partially validated based on the knowledge obtained through these first HPLC techniques. Therefore, the validation results of such bioanalytical HPLC-DAD assays are not presented herein, but they are summarily reported in the following chapter describing the *in vivo* studies (*Chapter IV*).

II.2. Experimental

Liquid chromatographic assay based on microextraction by packed sorbent for therapeutic drug monitoring of carbamazepine, lamotrigine, oxcarbazepine, phenobarbital, phenytoin and the active metabolites carbamazepine-10,11-epoxide and licarbazepine

II.2.1. Introduction

Epilepsy is one of the most common serious chronic neurological disorders and it is estimated to affect more than 50 million people worldwide (PERUCCA 2001; GALANOPOULOU ET AL. 2012; ZHANG ET AL. 2012a). The pharmacotherapy with AEDs is currently the therapeutic approach of choice regarding epilepsy (FRANCO ET AL. 2016) as it controls the occurrence of unpredictable epileptic seizures on approximately two thirds of the patients (PERUCCA 2001). Even though, and besides the fact of more than twenty AEDs are today clinically available (ZHANG ET AL. 2012a), the truth is that the monotherapy with AEDs often fails, requiring polytherapy regimens in an attempt to achieve better seizure control and fewer side effects (DECKERS ET AL. 2000; BUGAMELLI ET AL. 2002; GARNETT ET AL. 2009; FORTUNA ET AL. 2011b). At this moment, the clinicians may opt among AEDs of the first-generation, namely PHT, CBZ or PB, and/or among newer 'second-generation' AEDs such as LTG or OXC (LÖSCHER 2002; GHAFFARPOUR ET AL. 2013). Although these newer drugs are not necessarily more effective than the traditional drugs, the new AEDs are safer and better tolerated than the classic ones, namely due to their improved tolerability profile, broader therapeutic ranges, linear pharmacokinetics, less inter- and intra-individual pharmacokinetic variability and, consequently, less propensity to be involved in pharmacokinetic interactions (LEVERT ET AL. 2002; FORTUNA ET AL. 2010; GHAFFARPOUR ET AL. 2013). Due to these advantages, some of the second-generation AEDs are increasingly used for the first-line management in certain subgroups of patients including those that are refractory to the classic AEDs; in addition, they can also be used as add-on therapy with other AEDs. Unfortunately, it is incontestable that these clinical practice of poly- and add-on therapies frequently lead to complex and unpredictable pharmacokinetic and pharmacodynamic interactions, with possible clinical consequences in terms of toxicity or even therapeutic inefficacy (BUGAMELLI ET AL. 2002). All these shortcomings coupled to fact that the pharmacotherapy with AEDs is usually prophylactic and lifelong, and the relationship between dose and drug concentrations is unpredictable, the effectiveness of AEDs therapy frequently requires TDM procedures. Based on the measurement of drug concentrations in plasma (BUGAMELLI ET AL. 2002; PATIL AND BODHANKAR 2005; BUDAKOVA ET AL. 2008), TDM is therefore largely employed with the purpose of avoiding the risks of acute and chronic toxicity (NEELS ET AL. 2004) and to optimize the patient's clinical outcome (BUGAMELLI ET AL. 2002; PATSALOS ET AL. 2002; PATIL AND BODHANKAR 2005; BUDAKOVA ET AL. 2008; PATSALOS ET AL. 2008). Indeed, AEDs can be used more safely if the clinician is aware of the concentrations the patient is exposed to and adjusts the dose as necessary. Therefore, the availability of rapid, simple, sensitive, accurate and reliable analytical methods is essential to support TDM in clinical routine.

Up to date, several HPLC methods coupled to ultraviolet (UV) detection or DAD have been developed and validated for the determination of AEDs and some of their main metabolites in human plasma or serum, employing distinct sample preparation procedures which included PP (KHOSCHSORUR ET AL. 2001), SPE (BUGAMELLI ET AL. 2002; FRANCESCHI AND FURLANUT 2005; FORTUNA ET AL. 2010; SERRALHEIRO ET AL. 2013), LLE (MEYLER ET AL. 1993) and MEPS (SARACINO ET AL. 2010; RANI

ET AL. 2012). The MEPS is one of the latest achievement in the field of sample preparation; it is directed toward miniaturization and automation, and it has been successfully used for qualitative and quantitative bioanalysis of a vast number of drugs and metabolites (NOVÁKOVÁ AND VLCKOVÁ 2009; ALVES ET AL. 2013; RODRIGUES ET AL. 2013). Specifically, regarding the application of MEPS in bioanalysis of AEDs, to the best of our knowledge only two HPLC-UV/DAD methods (SARACINO ET AL. 2010; RANI ET AL. 2012) and a gas chromatography–mass spectrometry assay (RANI AND MALIK 2012) were developed and none of them included all the AEDs and the metabolites considered in the current work.

Hence, this MEPS/HPLC-DAD assay was planned, aiming at developing a sensitive, fast and reliable bioanalytical tool for the simultaneous determination of the plasma concentrations of CBZ, LTG, OXC, PB, PHT and the active metabolites CBZ-E and LIC (Figure II.2.1). The inclusion of CBZ-E in this bioanalytical method is justified because it is the main pharmacologically active metabolite of CBZ, showing anticonvulsant properties, and many of the toxic effects associated to CBZ are ascribed to the metabolite CBZ-E. Therefore, the quantification of CBZ-E in plasma should be considered during TDM of CBZ in order to optimize both efficacy and toxicological profiles (MINKOVA AND GETOVA 2001). Furthermore, the determination of CBZ-E concentrations may be also important due to the dose-dependent metabolic auto-induction phenomenon displayed by the parent drug (CBZ), particularly on the cytochrome P450 (CYP) 3A4 isoenzyme (PATSALOS ET AL. 2002). On the other hand, LIC was also herein considered because, in humans, LIC represents the main pharmacologically active entity responsible for the anticonvulsant activity observed after the administration of OXC (a prodrug) (FORTUNA ET AL. 2010).

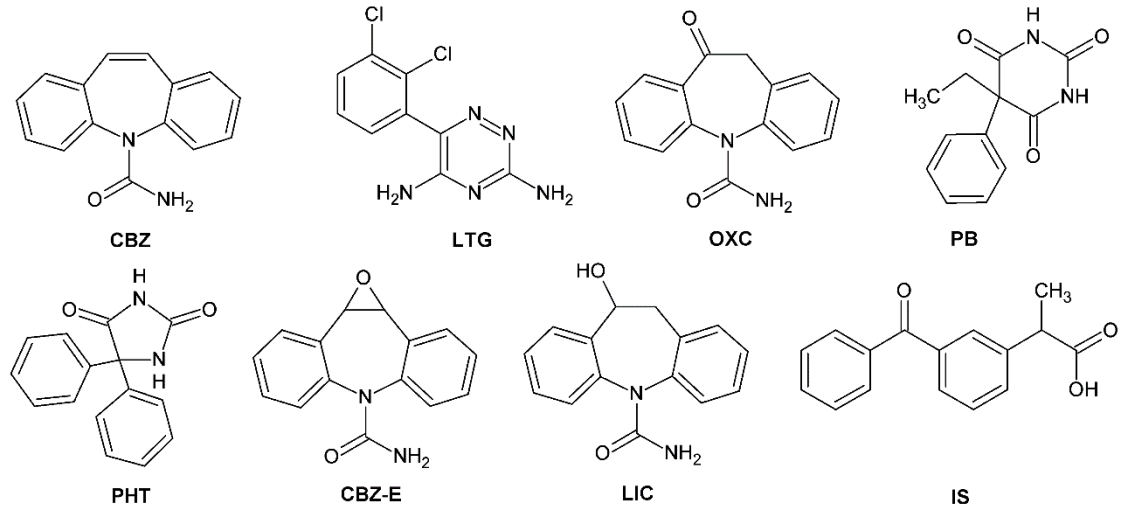

Figure II.2.1. Chemical structures of carbamazepine (CBZ), lamotrigine (LTG), oxcarbazepine (OXC), phenobarbital (PB), phenytoin (PHT), carbamazepine-10,11-epoxide (CBZ-E), licarbazepine (LIC) and ketoprofen which was used as internal standard (IS).

II.2.2. Material and methods

II.2.2.1. Materials and reagents

CBZ, CBZ-E, OXC, PHT, and ketoprofen, used as internal standard (IS), were purchased from Sigma–Aldrich (St Louis, MO, USA). LIC and PB were kindly supplied by BIAL - Portela & C^{a}, S.A. (S. Mamede do Coronado, Portugal). LTG was gently provided by Bluepharma (Coimbra, Portugal). Methanol and acetonitrile, both of HPLC gradient grade, were purchased from Fisher Scientific (Leicestershire, United Kingdom) and the ultra-pure water (HPLC grade, >18 MΩ.cm) was prepared by means of a Milli-Q water apparatus from Millipore (Milford, MA, USA). Triethylamine was acquired from Merck KGaA (Darmstadt, Germany) and the 85% *ortho*-phosphoric acid from Panreac Química SA (Barcelona, Spain). MEPS 250 µL syringe and MEPS BIN (barrel insert and needle) containing ~4 mg of solid-phase silica – C_{18} material (SGE Analytical Science, Australia) were purchased from ILC (Porto, Portugal). Blank human plasma from healthy blood donors was kindly provided by the Portuguese Blood Institute after the written consent of each subject.

II.2.2.2. Stock solutions, calibrations standards and quality control samples

Stock solutions of CBZ (15 mg/mL), LTG (10 mg/mL), OXC (5 mg/mL), PB (40 mg/mL), PHT (30 mg/mL), CBZ-E (5 mg/mL) and LIC (40 mg/mL) were individually prepared by dissolving the appropriate amount of each compound in methanol. From these solutions, working standard solutions were prepared by appropriate dilution in water-methanol (50:50, v/v). Subsequently, six combined spiking solutions with final concentrations of 0.5, 1, 3, 10, 30 and 75 µg/mL for CBZ; 0.5, 1, 3.5, 15, 62.5 and 100 µg/mL for LTG; 0.5, 1, 2, 4, 10 and 25 µg/mL for OXC and CBZ-E; 1, 2, 7.5, 37.5, 125 and 200 µg/mL for PB; 1.5, 3, 7.5, 25, 90 and 150 µg/mL for PHT; and 2, 4, 12.5, 50, 125 and 200 µg/mL for LIC were prepared by mixing the stock and working solutions of the drugs and metabolites.

Six calibration standards in the concentration ranges of 0.1-15 µg/mL for CBZ; 0.1-20 µg/mL for LTG; 0.1-5 µg/mL for OXC and CBZ-E; 0.2-40 µg/mL for PB; 0.3-30 µg/mL for PHT; and 0.4-40 µg/mL for LIC were daily prepared by spiking aliquots of blank human plasma with each one of these combined solutions. The stock solution of the IS was also prepared in methanol (1 mg/mL) and the working solution (25 µg/mL) was obtained after diluting an appropriate volume of the stock solution with water-methanol (50:50, v/v). The stock, working and combining solutions were protected from light, being the stock solutions stored at −80 °C, and the working and combining solutions at 4 °C. An exception was the IS working solution which was daily prepared.

Quality control (QC) samples at three representative concentration levels, representing the low (QC_1) medium (QC_2) and high (QC_3) ranges of the calibration curves, were also independently prepared in plasma. With that purpose, aliquots of blank human plasma were spiked to achieve final concentrations of 0.3, 7.5 and 13.5 µg/mL for CBZ; 0.3, 10 and 18 µg/mL for LTG; 0.3, 2.5

and 4.5 µg/mL for OXC and CBZ-E; 0.6, 20 and 36 µg/mL for PB; 0.9, 15 and 27 µg/mL for PHT; and 1.2, 20 and 36 µg/mL for LIC. Another QC sample at the concentration of the lower limit of quantification (LLOQ; QC_{LLOQ}) was also prepared.

II.2.2.3. Apparatus and chromatographic conditions

Chromatographic analysis was carried out using an UHPLC system (Agilent 1260 Infinity Binary LC system) coupled to a DAD detector (Agilent 1260 Infinity; G4212B DAD). All instrumental parts were automatically controlled by Agilent ChemStation software (Agilent Technologies). A reversed-phase LiChroCART® Purospher Star column (C_{18}, 55 mm × 4 mm; 3 µm particle size) at 35 °C, purchased from Merck KGaA (Darmstadt, Germany), was used to perform the chromatographic separation of all drugs, metabolites and IS. The mobile phase consisted of acetonitrile (6%) and a mixture (94%) of water–methanol–triethylamine (73.2:26.5:0.3, v/v/v), pH 6.5 adjusted with 85% *ortho*-phosphoric acid, being an isocratic elution applied at a flow rate of 1.0 mL/min. The injection volume was 20 µL and the wavelengths of 215, 237 and 280 nm were selected for the detection of all compounds.

II.2.2.4. Sample preparation and extraction

The sample preparation was previously optimized and the final conditions were as follows. Each aliquot (100 µL) of human plasma samples, spiked with 20 µL of the IS working solution, was added of 400 µL of ice-cold acetonitrile in order to precipitate plasma proteins. The mixture was vortex-mixed for 30 s and centrifuged at 14,000 rpm (equivalent to 18,620 rcf) for 10 min at 4 °C. Afterwards the resulting supernatant was evaporated under a gentle nitrogen stream at 45 °C and the dry residue reconstituted with 200 µL of 0.1 M phosphate buffer (pH 5.5). The resulting sample mixture was then submitted to the MEPS procedures. Firstly, the MEPS sorbent (C_{18}) was manually activated/conditioned with methanol (3 x 200 µL) and ultra-pure water (3 x 200 µL). After that, the whole sample volume was drawn through the sorbent and ejected at a flow rate of approximately 10 µL/s; this procedure was performed ten times. Then, the sorbent was washed with 200 µL of ultra-pure water in order to remove interferences and, at the end, the analytes were eluted with methanol (2 x 30 µL) and diluted with 90 µL of ultra-pure water. An aliquot (20 µL) of this final sample was injected into the chromatographic system. To reuse the MEPS device and avoid carry-over phenomena the MEPS sorbent was sequentially washed/reconditioned with 12 x 200 µL of methanol followed by 5 x 200 µL of ultra-pure water after each sample extraction. This procedure allowed each MEPS device to be reused in about 200 extractions before being discarded.

II.2.2.5. Method validation

The international accepted recommendations for bioanalytical method validation (SHAH ET AL. 2000; U.S. FOOD AND DRUG ADMINISTRATION 2001; EUROPEAN MEDICINES AGENCY 2011) were followed in the validation of the developed method and considering the acceptance criteria proposed for specific validation parameters including selectivity, linearity, precision, accuracy, limits of quantification and detection, recovery and stability.

The selectivity was evaluated analysing blank human plasma samples from six different subjects to ascertain the existence of matrix endogenous substances which retention times interfere with those of CBZ, LTG, OXC, PB, PHT, CBZ-E, LIC, and IS. In addition, interferences from drugs potentially coadministered to epileptic patients in the clinical practice were also assessed by the injection, under the optimized chromatographic conditions, of the standard solutions of those compounds. The tested drugs included analgesics/antipyretics (acetylsalicylic acid, ibuprofen, paracetamol, nimesulide), antiarrhythmics (flecainide, diltiazem), anticoagulants (warfarin), antidepressants (amitriptyline, citalopram, clomipramine, dosulepine, duloxetine, escitalopram, fluoxetine, fluvoxamine, maprotiline, mianserine, mirtazapine, nortriptyline, paroxetine, protriptyline, sertraline, trazadone), antihypertensives (amiloride, nifedipine), antiparkinsonians (selegiline), antipsychotics (chlorpromazine, clozapine, droperidol, haloperidol, levopromazine, olanzapine, promazine, quetiapine, risperidone), histamine H_2 receptor antagonists (cimetidine), proton pump inhibitors (omeprazole), sedative/hypnotics (alprazolam, clorazepate, diazepam, mexazolam, oxazepam, zolpidem) and others like caffeine.

To evaluate the linearity of the analytical method for each analyte within the concentration ranges defined in s*ection II.2.2.2*, calibration curves were prepared using the six spiked plasma calibration standards and assayed on five different days (n = 5). These curves were constructed by plotting analyte-IS peak area ratio as function of the corresponding nominal concentrations. The data were subjected to a weighted linear regression analysis using $1/x^2$ as weighting factor, being the plots and the sums of absolute percentage of relative error taking into account (ALMEIDA ET AL. 2002).

The LLOQ, defined as the lowest concentration of the calibration curve that can be measured with adequate intra e interday precision and accuracy, was evaluated by analysing plasma samples prepared in five replicates (n = 5) (U.S. FOOD AND DRUG ADMINISTRATION 2001; EUROPEAN MEDICINES AGENCY 2011). The precision, which is given by the value of coefficient of variation (CV), cannot exceed 20%; while accuracy, given by the deviation from nominal concentration value (*bias*), must be within ±20%. The limit of detection (LOD), which is the lowest concentration that can be reliably distinguished from background noise, was defined as the concentration which affords a signal-to-noise ratio of 3:1 (U.S. FOOD AND DRUG ADMINISTRATION 2001).

The interday precision and accuracy of the assay were investigated using plasma QC samples analysed on five consecutive days (n = 5) at the four concentration levels (QC_{LLOQ}, QC_1, QC_2 and

QC_3) representative of the calibration range. Similarly, the intraday precision and accuracy were also assessed analysing four sets of the QC samples in a single day (*n* = 5). Bioanalytical method validation guidelines define that intra and interday precision (expressed as percentage of CV) must be lower than or equal to 15% (or 20% in the LLOQ) and intra and interday accuracy (expressed as percentage of *bias*) must be within ±15% (or ±20% in the LLOQ).

The absolute recovery of the analytes from human plasma samples submitted to the treatment previously described in the s*ection II.2.2.4* was calculated for the three QC samples (QC_1, QC_2 and QC_3), comparing the analytes peak areas from extracted QC plasma samples with those obtained after direct injection of non-extracted solutions at the same nominal concentrations (*n* = 5). Likewise, the calculation of the ratio of IS peak areas in extracted samples and non-extracted solutions, determined at the concentration used in sample analysis, was used to define the absolute recovery of the IS.

Human plasma stability of the seven analytes was investigated for QC_1 and QC_3 (*n* = 5). The data of the QC samples analysed before (reference samples) were compared with those obtained after being exposed to the experimental conditions for stability assessment (stability samples). As stability criterion (*n* = 5), a stability/reference samples ratio of 85-115% was accepted (CHEN ET AL. 2005; EUROPEAN MEDICINES AGENCY 2011). With the aim of simulating sample handling and storage time in the refrigerator and freezer before analysis, the short- and long-term stability were evaluated at room temperature for 4 h, 4 °C for 24 h and −20 °C for 30 days (*n* = 5). The post-preparative stability of the analytes in processed samples was also studied at room temperature during 12 h in an attempt of simulating the time that samples can be in the auto-sampler before analysis. Additionally, the effect of three freeze-thaw cycles on the stability of the compounds in human plasma samples was studied at −20 °C. For this purpose, aliquots of spiked plasma samples (QC_1 and QC_3) were stored at −20 °C for 24 h, thawed unassisted at room temperature, and when completely thawed. The samples were refrozen for 24 h under the same conditions until completing the three cycles.

II.2.2.6. Clinical application

With the purpose of demonstrating the applicability of the bioanalytical method herein developed and validated, a set of real plasma samples obtained from epileptic patients under treatment at the Hospital Centre of Cova da Beira (CHCB) were analysed. The analysis of these samples in order to quantify the plasma levels of AEDs and metabolites also enable to assess one more time the selectivity of the method, since other drugs from distinct pharmacological groups are coadministered to the patients. The blood samples were taken at the morning, before the daily administration of the AEDs, being the protocol approved by the local Independent Ethics Committee and the informed consent obtained from each subject.

II.2.3. Results and discussion

II.2.3.1. Development and optimization of chromatographic conditions

As it was intended to apply this technique during TDM on epileptic patients, one of the most usual detection systems (DAD) and the simplest chromatographic elution conditions (isocratic elution) were preferred as they are commonly used in clinical laboratories. Chromatographic conditions were optimized aiming at providing a symmetric peak shape and achieving the best resolution of all the analytes and the IS within the shortest running time. The optimized mobile phase was composed by acetonitrile (6%) and a mixture (94%) of water–methanol–triethylamine (73.2:26.5:0.3, v/v/v), pH 6.5, adjusted with 85% *ortho*-phosphoric acid. Different percentages of acetonitrile were tested. However, the use of lower percentages of acetonitrile increased the run time, whereas higher percentages did not allow a good separation of the peaks of the analytes. The influence of mobile phase pH on peaks shape, resolution and retention times was also evaluated. Considerable differences were observed in the pH range of 3.5-7.5. Thus, due to the more favourable retention times, peaks separation and peak shape obtained for all the analytes, the pH 6.5 was chosen. The triethylamine was incorporated in the mobile phase due to the fact that the compound saturates the free silanol groups of the stationary phase, allowing the decrease of the asymmetry and peak tailing phenomenon (KUHN ET AL. 2010).

The influence of column temperature was also tested, being the temperature of 35 °C chosen. Although a temperature of 20 °C permitted a better resolution between the peaks, it increased significantly the run time, making the technique less practical. On the other hand, the opposite occurred when the temperature was enhanced to 40 °C, compromising peaks resolution. Under these chromatographic conditions the order of elution of the compounds was LTG, PB, LIC, CBZ-E, OXC, IS, PHT and CBZ (Figure II.2.2). Although several wavelength values ranging from 195 nm to 306 nm were assessed, the best compromise in terms of sensitivity and selectivity was achieved at 215 nm for CBZ, LTG, PB, PHT, CBZ-E and LIC, at 237 nm for OXC, and at 280 nm for IS. Thus, the simple chromatographic conditions herein employed enable the analysis of all the analytes in a short and adequate period of time.

Although some compounds were tested to select the appropriate IS, ketoprofen was chosen taking into account its adequate retention time, chromatographic behaviour and absolute recovery values that were similar to those displayed by the AEDs considered.

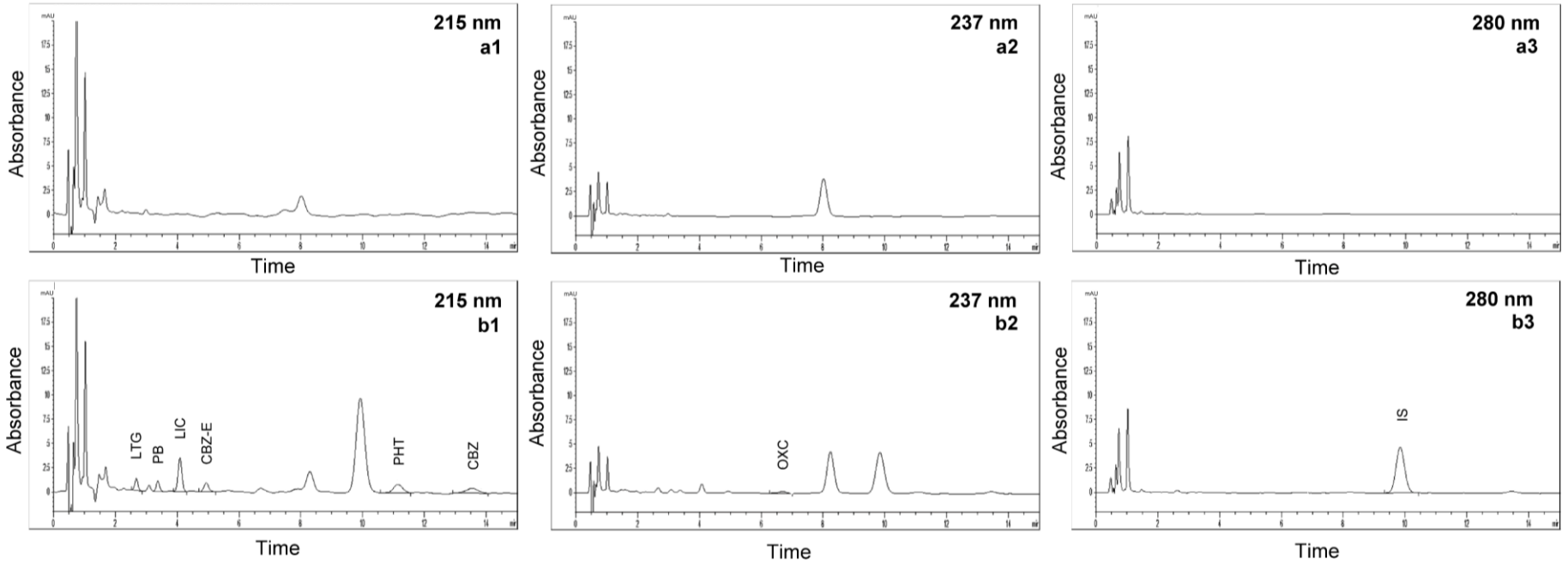

Figure II.2.2. Typical chromatograms of extracted human plasma samples obtained by the MEPS/HPLC-DAD assay developed: blank plasma at 215 nm (a1), at 237 nm (a2) and at 280 nm (a3); and plasma spiked with internal standard (IS) and the analytes at concentrations of the lower limit of quantification at 215 nm (b1), at 237 nm (b2) and at 280 nm (b3). CBZ, carbamazepine; LTG, lamotrigine; OXC, oxcarbazepine; PB, phenobarbital; PHT phenytoin; CBZ-E, carbamazepine-10,11-epoxide; LIC, licarbazepine.

II.2.3.2. Optimization of sample preparation: MEPS conditions

Sample preparation, which typically takes 80% of the total analysis time, affects nearly all the posterior bioanalysis steps and, therefore, it is essential for an unequivocal identification and quantification of analytes (NOVÁKOVÁ AND VLCKOVÁ 2009; MERCOLINI ET AL. 2014). Due to the fact that conventional sample preparation approaches are labour intensive and time-consuming (like the LLE), or often are not sufficiently efficient (like the PP), several new sample preparation techniques have been developed over the last decade (NOVÁKOVÁ AND VLCKOVÁ 2009; MERCOLINI ET AL. 2014). MEPS was herein selected due to its several advantages. The MEPS cartridges can be reused several times, more than 100 times using plasma or urine samples, in contrary to the conventional SPE column, making the cost of analysis minimal in comparison to SPE. Moreover, MEPS is easily adaptable to several analytical systems, offers the opportunity for full automation, is rapid and requires very small sample volumes, which may be as small as 10 µL (ABDEL-REHIM 2010; ALVES ET AL. 2013; RODRIGUES ET AL. 2013). During the development of MEPS protocols, several factors should be cautiously studied such as sample pretreatment, the conditioning/activation of the sorbent, sample loading, sorbent washing, analytes elution and sorbent cleaning/reconditioning (ALVES ET AL. 2013). At the beginning of the optimization of MEPS conditions, the dilution of human plasma samples with ultra-pure water was tested as sample pretreatment approach. This option was taken into account as it had been previously used for the quantification of AEDs (SARACINO ET AL. 2010; RANI ET AL. 2012). However, this procedure was not efficient and originated a rapid clogging of the MEPS cartridge. To overcome this problem, strong precipitation agents like perchloric and trichloroacetic acids were tested. Although they avoided sample dilution, the final recoveries obtained for all the analytes were very low, probably due to the degradation of the analytes and therefore this procedure was discarded (BUGAMELLI ET AL. 2002; FORTUNA ET AL. 2010). Zinc sulphate, which has been reported as an effective precipitation agent (ANNESLEY AND CLAYTON 2004; BUCHWALD ET AL. 2012) was also tested, but the resulting processed samples were relatively unclean and the recoveries obtained were also disappointing. Due to the aforementioned results, the PP with methanol, acetonitrile and methanol/acetonitrile (50:50, v/v) was tested. At this step, 400 µL of acetonitrile were chosen for sample pretreatment before MEPS sample loading because cleaner chromatograms were obtained. This procedure permitted a large-scale increase in the useful life of each MEPS cartridge.

After plasma sample pretreatment, the resulting supernatant was collected and evaporated to dryness in order to remove the organic solvent (acetonitrile), which would lead to the low retention of the compounds in the MEPS sorbent, determining consequently low absolute recovery. For the reconstitution of the dry residue, ultra-pure water, mobile phase and 0.1 M phosphate buffer at pH 5.5 were tried (200 µL). The last one revealed greater recovery values as it was expected taking into account that pH 5.5 is regarded as the optimum pH to enhance the extraction yields of the AEDs (RANI ET AL. 2012). This pH adjustment seems to reduce the ionization of the analytes, promoting their sorption to the MEPS sorbent (ABDEL-REHIM 2011).

The MEPS protocols usually involve multiple drawn-ejected cycles during the sample loading step (RANI ET AL. 2012) and, particularly for the AEDs, the influence of the number of extraction cycles on the analyte extraction efficiency has shown to be significant (SARACINO ET AL. 2010; RANI ET AL. 2012). According to RANI ET AL. (2012), the analytes recovery increased as the number of extraction cycles enhanced up to ten. Therefore, due to the good results obtained, ten draw-eject pump cycles were selected in this bioanalytical assay.

The effect of different washing solutions [ultra-pure water, methanol (5-10%), acetic acid (5%) and formic acid (1%)] on analytes recovery was herein investigated. This step follows the sample loading and it is essential to remove endogenous interferences and improve the selectivity of the method, but it may also determine a significant leakage of the target compounds (ALVES ET AL. 2013). Therefore, taking into account the obtained results, a good compromise between selectivity and absolute recovery was achieved using 200 µL of ultra-pure water as washing solution. Concerning the elution step, the use of methanol as elution solvent was the first option to be considered. Indeed, pure methanol is the elution solution most frequently reported in MEPS protocols, since it provides good extraction yields. Actually, the retention mechanism of the AEDs in the MEPS sorbent (C_{18}) is mainly based on hydrophobic interactions, thus a non-polar solvent such as methanol appears to be strong enough to efficiently elute the target compounds (ALVES ET AL. 2013). At this stage, different elution volumes of methanol were tested, but the direct injection of pure methanolic eluate into the chromatographic system impaired the peak shape, symmetry and resolution. Hence, after elution of the compounds (AEDs and IS) with 2 x 30 µL of methanol, that yielded good absolute recoveries and higher recoveries than those obtained with a single elution with 60 µL of methanol, a dilution step of the methanolic elute with ultra-pure water was incorporated before HPLC injection to avoid peak distortion.

Finally, the carry-over phenomenon was investigated. Indeed, the presence of carry-over effects is one of the major concerns in MEPS procedures because each cartridge is reused several times before being discarded. Therefore, the occurrence of memory effects must be carefully assessed to reuse MEPS cartridges with high accuracy and precision (ALVES ET AL. 2013). Thus, the obtained data showed that significant carry-over effects are avoided through the cleaning/reconditioning of the MEPS sorbent with 12 x 200 µL of methanol followed by 5 x 200 µL of ultra-pure water before the extraction of the following sample. The evaluation of the carry-over was performed by the preparation and analysis of blank samples after high concentration samples. In that way, the accuracy and reliability of the results obtained were assured by the fact that the carry-over in the blank samples was not greater than 20% of the LLOQ and 5% for the IS.

II.2.3.3. Method validation

II.2.3.3.1. Selectivity

The analysis of blank human plasma samples from six healthy volunteers confirmed the absence of endogenous interferences at the retention times of the compounds of interest (CBZ, LTG, OXC, PB, PHT, CBZ-E, LIC and IS). In the Figure II.2.2 are depicted typical chromatograms of the extracts obtained from blank and spiked human plasma samples. Moreover, most of the tested drugs potentially coadministered with the AEDs under investigation were not found to interfere at the retention times of the analytes (CBZ, LTG, OXC, PB, PHT, CBZ-E and LIC) and IS, using the chromatographic and detection conditions previously established. In Table II.2.1 are specifically indicated the tested drugs that interfered with the analytes or IS.

Table II.2.1. Tested drugs that interfered at the retention times of the analytes [carbamazepine (CBZ), lamotrigine (LTG), oxcarbazepine (OXC), phenobarbital (PB), phenytoin (PHT), carbamazepine-10,11-epoxide (CBZ-E), licarbazepine (LIC) and internal standard (IS)].

Pharmacological group **Drugs**	**Target compounds (analytes and IS)**
Antidepressants	
Venlafaxine	IS
Antipsychotics	
Melperone	OXC
Histamine H_1 receptor antagonists	
Hydroxyzine	PHT, CBZ
Prometazine	LTG, PB
Vasodilators and inhibitors of platelet aggregation	
Dipyridamole	LTG, PB, LIC, CBZ-E, OXC

II.2.3.3.2. Calibration curves, LLOQs and LODs

The calibration curves obtained in human plasma for all the analytes were linear ($r^2 \geq 0.9946$; Table II.2.2) in the concentration ranges defined in *section II.2.2.2*, and showed a consistent correlation between analyte-IS peak area ratios and corresponding nominal plasma concentrations. A weighted linear regression analysis was used due to the wide calibration range and in order to compensate for heteroscedasticity. A weighting factor of $1/x^2$ was chosen to subject the calibration curves to weighted linear regression analysis. Actually, this was shown to be the best-fit weighting factor for all analytes (CBZ, LTG, OXC, PB, PHT, CBZ-E and LIC), considering the plots and the sums of absolute percentage relative error as statistical criteria, and taking into account all the factors commonly tested in heteroscedasticity conditions, namely, $1/\sqrt{x}$, $1/x$, $1/x^2$, $1/\sqrt{y}$, $1/y$ and $1/y^2$.

The Table II.2.2 summarizes the regression equations of the calibration curves and the corresponding determination coefficients (r^2) achieved for each AED and metabolites. The applicability of this method for both pharmacokinetics and toxicological studies is also

supported by the fact that the analytical target concentration ranges of each compound are wider than the corresponding plasma/serum therapeutic windows (PATSALOS ET AL. 2008; HOYLAND ET AL. 2013).

Table II.2.2. Mean calibration parameters obtained for carbamazepine (CBZ), lamotrigine (LTG), oxcarbazepine (OXC), phenobarbital (PB), phenytoin (PHT), carbamazepine-10,11-epoxide (CBZ-E) and licarbazepine (LIC) in human plasma (n = 5).

Analyte	Calibration parameters		
	Concentration range (μg/mL)	Equation[a]	r^2
CBZ	0.1-15	y = 1.3311x + 0.0137	0.9968
LTG	0.1-20	y = 0.8698x + 0.0021	0.9969
OXC	0.1-5	y = 0.3191x − 0.0033	0.9959
PB	0.2-40	y = 0.3528x + 0.0071	0.9946
PHT	0.3-30	y = 0.5965x + 0.0374	0.9964
CBZ-E	0.1-5	y = 1.2976x − 0.0061	0.9979
LIC	0.4-40	y = 0.7887x + 0.0647	0.9952

[a] *y, represents analyte-IS peak area ratio; x, represents analyte concentration (μg/mL).*

As shown in Table II.2.2, the LLOQs were experimentally defined as 0.1 μg/mL for CBZ, LTG, OXC and CBZ-E, 0.2 μg/mL for PB, 0.3 μg/mL for PHT and 0.4 μg/mL for LIC, with suitable precision (CV ≤ 17.7%) and accuracy (*bias* varied from 0.6% to 17.8%). Importantly, this LLOQs are often lower than those achieved by other HPLC–UV/DAD methods reported in the literature even herein employing a smaller volume of sample (KHOSCHSORUR ET AL. 2001; BUGAMELLI ET AL. 2002; LEVERT ET AL. 2002; FRANCESCHI AND FURLANUT 2005; PATIL AND BODHANKAR 2005; JUENKE ET AL. 2006; GREINER-SOSANKO ET AL. 2007; BUDAKOVA ET AL. 2008; DZODIC ET AL. 2012). The LODs were established as being 0.015 μg/mL for CBZ and PB, 0.025 μg/mL for LTG, 0.03 μg/mL for OXC, 0.05 μg/mL for PHT, 0.010 μg/mL for CBZ-E, and 0.09 μg/mL for LIC.

II.2.3.3.3. Precision and accuracy

The Table II.2.3 displays the data for intra and interday precision and accuracy obtained from QC plasma samples at the four different concentration levels (QC_{LLOQ}, QC_1, QC_2 and QC_3). The overall intra and interday CV values lower than or equal to 9.7% (17.7% for QC_{LLOQ}), and the overall intra and interday *bias* values ranging from −4.1 to 14.8% (0.6 to 17.8% for QC_{LLOQ}) clearly demonstrates that the HPLC–DAD method herein described is reliable and accurate.

Table II.2.3. Intra and interday precision (% CV) and accuracy (% *bias*) values obtained for carbamazepine (CBZ), lamotrigine (LTG), oxcarbazepine (OXC), phenobarbital (PB), phenytoin (PHT), carbamazepine-10,11-epoxide (CBZ-E) and licarbazepine (LIC) in human plasma samples at the concentrations of the lower limit of quantification (*) and at the low (QC1), middle (QC2) and high (QC3) concentrations representative of the calibration ranges (*n* = 5).

Analyte	Nominal concentration (μg/mL)	Intraday		Interday	
		Precision (% CV)	Accuracy (% *bias*)	Precision (% CV)	Accuracy (% *bias*)
CBZ	0.1*	5.6	3.6	5.0	2.8
	0.3	3.8	12.4	3.7	10.3
	7.5	2.9	14.2	1.0	5.6
	13.5	0.7	13.7	3.9	7.2
LTG	0.1*	3.2	11.0	4.8	6.0
	0.3	4.3	12.4	4.8	8.5
	10	3.5	7.1	1.8	−1.9
	18	1.1	9.4	4.2	3.0
OXC	0.1*	17.7	9.2	9.0	7.1
	0.3	9.7	−4.1	6.4	7.0
	2.5	5.2	−1.5	2.1	1.1
	4.5	3.4	11.0	4.4	8.4
PB	0.2*	3.7	5.9	4.5	0.6
	0.6	5.8	9.7	4.1	6.2
	20	3.8	7.3	5.0	−2.0
	36	1.6	0.9	6.1	−3.0
PHT	0.3*	6.2	13.7	3.1	0.9
	0.9	5.7	14.3	3.0	11.5
	15	3.3	9.6	1.3	2.1
	27	0.8	7.8	4.3	2.8
CBZ−E	0.1*	5.4	17.8	14.0	15.8
	0.2	1.7	13.6	8.3	11.3
	2.5	3.2	12.6	1.6	4.3
	4.5	0.7	11.5	3.9	5.3
LIC	0.4*	3.5	12.9	3.5	5.9
	1.2	1.7	14.8	3.6	8.5
	20	3.0	9.2	1.5	1.5
	36	0.6	6.8	4.3	1.4

CV, coefficient of variation; bias, deviation from nominal concentration value.

II.2.3.3.4. Recovery

The results of the overall absolute recovery of the analytes from human plasma samples spiked at the three different concentration levels (QC_1, QC_2 and QC_3) are presented in Table II.2.4. In that way, the absolute mean recoveries ranged from 57.8 to 98.1%, and exhibited CV values lower than 13.3% for all analytes (AEDs and metabolites). Similarly to the yields achieved for the analytes, the absolute recovery of the IS was 82.3 ± 9.1%, with a CV value of 11.1%. These results undoubtedly corroborate that the IS was well chosen, and that the sample preparation

procedure guarantees a consistent average recovery over the evaluated concentration ranges, since the values of CV achieved are lower than 15%.

Table II.2.4. Absolute recovery of carbamazepine (CBZ), lamotrigine (LTG), oxcarbazepine (OXC), phenobarbital (PB), phenytoin (PHT), carbamazepine-10,11-epoxide (CBZ-E) and licarbazepine (LIC) from human plasma.

Analyte	Nominal concentration (μg/mL)	Absolute recovery (%)[a]	Precision (% CV)
CBZ	0.3	89.2 ± 8.6	9.7
	7.5	86.3 ± 3.7	4.3
	13.5	88.8 ± 10.4	11.7
LTG	0.3	83.8 ± 6.1	7.3
	10	77.0 ± 3.1	4.0
	18	77.5 ± 8.8	11.4
OXC	0.3	63.9 ± 8.5	13.3
	2.5	68.5 ± 3.1	4.5
	4.5	77.2 ± 9.6	12.4
PB	0.6	64.0 ± 4.4	6.8
	20	59.3 ± 3.0	5.0
	36	57.8 ± 6.8	11.7
PHT	0.9	82.8 ± 8.4	10.1
	15	82.1 ± 3.3	4.1
	27	83.7 ± 9.8	11.8
CBZ-E	0.3	98.1 ± 10.6	10.8
	2.5	86.8 ± 3.5	4.0
	4.5	88.3 ± 10.0	11.4
LIC	1.2	87.6 ± 8.8	10.1
	20	83.0 ± 3.3	4.0
	36	84.5 ± 9.6	11.4

[a] *Mean ± standard deviation, n = 5.*

II.2.3.3.5. Stability

The stability of the AEDs and metabolites in human plasma was evaluated under the different conditions previously described in *section II.2.2.5*, which simulate the handling and sample storage conditions to be likely encountered during the analytical process. The analytes demonstrated to be stable in human plasma at room temperature for 4 h, at 4 ºC for 24 h, at −20 ºC for 30 days and after three freeze–thaw cycles at −20 ºC, and in processed plasma samples at room temperature during 12 h. The stability data are shown in Table II.2.5.

Table II.2.5. Stability (values in mean percentage) of carbamazepine (CBZ), lamotrigine (LTG), oxcarbazepine (OXC), phenobarbital (PB), phenytoin (PHT), carbamazepine-10,11-epoxide (CBZ-E) and licarbazepine (LIC) in unprocessed and processed human plasma samples under the conditions that mimic sample handling and storage (*n* = 5).

Analyte	Nominal concentration (µg/mL)	Human plasma				
		Unprocessed sample				Processed sample
		Room temperature (4 h)	4 °C (24 h)	−20 °C (30 days)	Freeze-thaw (3 cycles; −20 °C)	Room temperature (12 h)
CBZ	0.3	97.2	95.9	101.8	94.7	89.0
	13.5	94.6	95.4	99.3	94.2	104.5
LTG	0.3	90.6	91.2	110.6	93.4	87.7
	18	92.2	94.4	96.5	92.0	102.6
OXC	0.3	96.7	98.2	90.9	103.6	89.0
	4.5	92.6	92.7	92.8	91.5	108.0
PB	0.6	87.7	94.1	87.8	89.3	86.1
	36	89.8	93.2	95.9	85.6	97.1
PHT	0.9	94.4	94.8	98.9	94.5	89.0
	27	94.3	96.0	98.1	93.8	104.2
CBZ-E	0.3	94.0	92.9	99.7	95.2	89.2
	4.5	94.3	95.3	99.1	94.5	104.9
LIC	1.2	92.4	93.0	99.4	93.5	87.5
	36	93.7	95.1	98.0	92.8	102.8

II.2.3.3.6. Clinical application

It is today well recognized that the effectiveness of the AEDs therapy is considerably dependent of the achievement and maintenance of plasma drug concentrations within the established therapeutic range. Therefore, the clinical availability of a reliable bioanalytical method to determine the plasma/serum concentrations of AEDs is determinant to support the TDM procedures required for optimization and individualization of the pharmacotherapy. Other important bioanalytical characteristics for the routine laboratory analysis of a large number of samples are the ease of sample preparation, simple instrumentation and analytical conditions, and short sample analysis time (FRANCESCHI AND FURLANUT 2005; FORTUNA ET AL. 2010).

Because the main purpose for the development of this new analytical assay is to apply it for TDM in hospitals and clinical pharmacokinetic departments, a set of real plasma samples obtained from patients undergoing therapy with the selected AEDs were analysed. These real plasma samples were collected immediately before the next oral dose of the drug (trough concentrations), which is the ideal blood sampling time for TDM of AEDs (PATSALOS ET AL. 2008). The chromatograms achieved with the analysis of these real plasma samples revealed good peak shape and resolution, similarly to those obtained after the analysis of spiked human plasma samples. Representative chromatograms are shown in

Figure II.2.3.

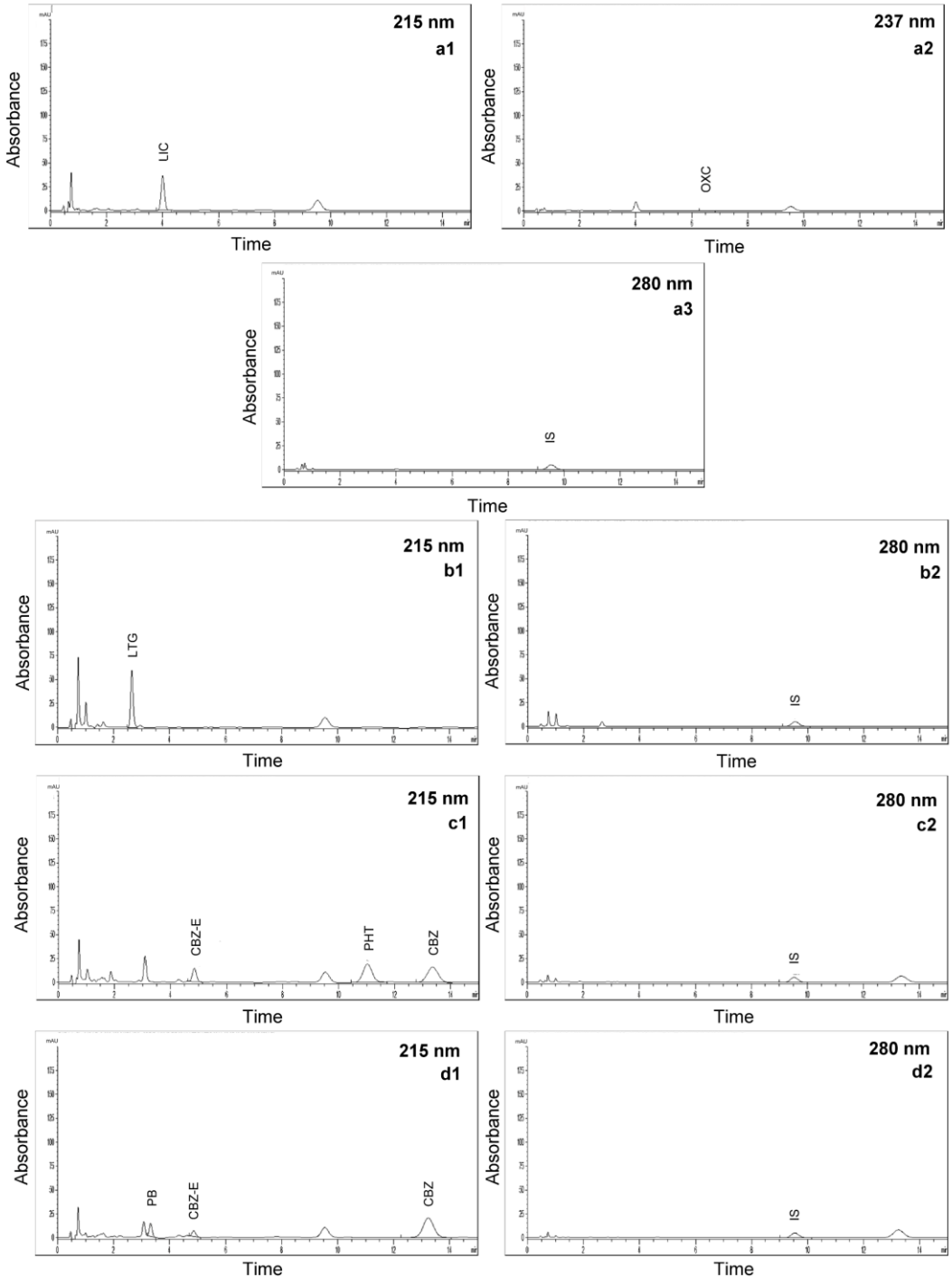

Figure II.2.3. Representative chromatograms of the analysis of real plasma samples obtained from patients treated with oxcarbazepine (ID4; a1, a2 and a3); lamotrigine (ID9; b1 and b2); carbamazepine and phenytoin (ID12; c1 and c2); and carbamazepine and phenobarbital (ID13; d1 and d2). CBZ, carbamazepine; LTG, lamotrigine; OXC, oxcarbazepine; PB, phenobarbital; PHT, phenytoin; CBZ-E, carbamazepine-10,11-epoxide; LIC, licarbazepine; IS, internal standard.

Indeed, despite the presence of co-medication in some patients (Table II.2.6), no significant interfering peaks were detected during the analysis of the authentic samples. In addition, as shown in Table II.2.6, the plasma drug concentrations measured in the samples of these epileptic patients are within the corresponding therapeutic ranges referred to in the literature (PATSALOS ET AL. 2008), except for LTG in subject ID7, for CBZ and PHT in subject ID12, and for PB in subject ID13. As a result, the reported MEPS/HPLC-DAD method seems to be appropriate to support the TDM of the AEDs and metabolites under investigation.

Table II.2.6. Plasma concentrations of carbamazepine (CBZ), lamotrigine (LTG), oxcarbazepine (OXC), phenobarbital (PB) and phenytoin (PHT), and the metabolites carbamazepine-10,11-epoxide (CBZ-E) and licarbazepine (LIC) in real plasma samples obtained from epileptic patients under treatment with different therapeutic regimens.

Patients	AED therapy, mg/day	Concentrations, µg/mL	Co-medication
ID1	CBZ, 800	CBZ, 6.1; CBZ-E, 0.7	---
ID2	OXC, 300	OXC, 0.1; LIC, 5.8	Olanzapine, Omeprazole, Lormetazepam
ID3	LTG, 25	LTG, 3.9	Pregabaline
ID4	OXC, 300	OXC, 0.1; LIC, 4.6	---
ID5	CBZ, 800	CBZ, 5.3; CBZ-E, 0.4	---
ID6	OXC, 600	OXC, 0.1; LIC, 9.0	Valproic acid
ID7	LTG, 100	LTG, 0.9	Cloxazolam, Escitalopram, Levetiracetam
ID8	LTG, 200	BLQ	Olanzapine, Sertraline
ID9	LTG, 300	LTG, 5.6	---
ID10	OXC, 600	OXC, BLQ; LIC, 7.6	---
ID11	PHT, 300	PHT, 10.8	Diazepam, Valproic acid
ID12	CBZ, 1200 PHT, 300	CBZ, 3.7; CBZ-E, 1.4 PHT, 8.4	Topiramate
ID13	CBZ, 800 PB, 100	CBZ, 5.0; CBZ-E, 0.8 PB, 2.9	Haloperidol Decanoate

BLQ, below the lower limit of quantification (<0.1 µg/mL); ID, individual.

II.2.4. Conclusion

In conclusion, a novel MEPS/HPLC-DAD method was developed, fully validated and successfully applied to the simultaneous determination of five commonly prescribed AEDs (CBZ, LTG, OXC, PB, PHT) and two main active metabolites (CBZ-E and LIC) from a small volume of human plasma (100 µL). Furthermore, the method was validated for the quantitative analysis of these analytes within a wide concentration range, which includes the corresponding therapeutic concentrations. Therefore, this bioanalytical assay represents a cost-effective tool, which can be used in TDM of epileptic patients (including children) under mono or polytherapy with CBZ, LTG, OXC, PB and/or PHT.

II.3. Experimental

A new HPLC-DAD method for the quantification of carbamazepine, oxcarbazepine and their active metabolites in HepaRG cell culture samples

II.3.1. Introduction

Epilepsy is one of the most common serious chronic neurological disorders, affecting 50 million people worldwide (PERUCCA 2001; GALANOPOULOU ET AL. 2012; ZHANG ET AL. 2012a). It is characterized by recurrent unprovoked seizures and the main goal of epilepsy treatment is the achievement of a complete seizure-freedom without deleterious effects. For that, a continuous antiepileptic activity is required, which will be achieved only if plasma and brain drug concentrations remain continuously at therapeutic levels (SCHMIDT 2009).

Since the beginning of the 1990s several new AEDs were approved by the U.S. Food and Drug Administration (FDA) and/or by the European Medicines Agency (EMA) (e.g., eslicarbazepine acetate, felbamate, gabapentin, LTG, levetiracetam, OXC, pregabalin, rufinamide, stiripentol, tiagabine, topiramate, vigabatrin and zonisamide). The majority of these AEDs offers appreciable advantages in terms of their favourable pharmacokinetics, improved tolerability and lower potential for drug interactions comparatively to the older AEDs (e.g., PB, PHT, ethosuximide, CBZ and valproic acid) (BRODIE 2010; BIALER 2012b). However, despite the large therapeutic arsenal of old and new AEDs, approximately 55–60% of people with focal epilepsy and up to 20% of patients with primary generalized epilepsy develops drug resistance (WEAVER 2013). Hence, many patients are not seizure-free even under appropriate pharmacotherapy with the currently available AEDs, including under combination therapy with rational polytherapy regimens (BRODIE 2010). Thus, the search for novel AEDs with better efficacy and a safer therapeutic index is clearly warranted (BRODIE 2010; BIALER 2012b; WEAVER 2013; WEAVER AND POHLMANN-EDEN 2013).

CBZ and OXC are clinically well-established AEDs, presenting a substantial overlap in terms of pharmacological and therapeutic properties (FRENCH AND GAZZOLA 2011). CBZ and OXC are structurally related drugs that share the dibenzazepine nucleus but they differ at the 10,11-position (Figure II.3.1). These molecular differences are possibly on the basis of their different metabolic profiles. In humans, whereas CBZ undergoes oxidative metabolism to CBZ-E, OXC is rapidly reduced to its pharmacologically active LIC metabolite (Figure II.3.1) (BENES ET AL. 1999; FLESCH 2004; ALVES ET AL. 2010).

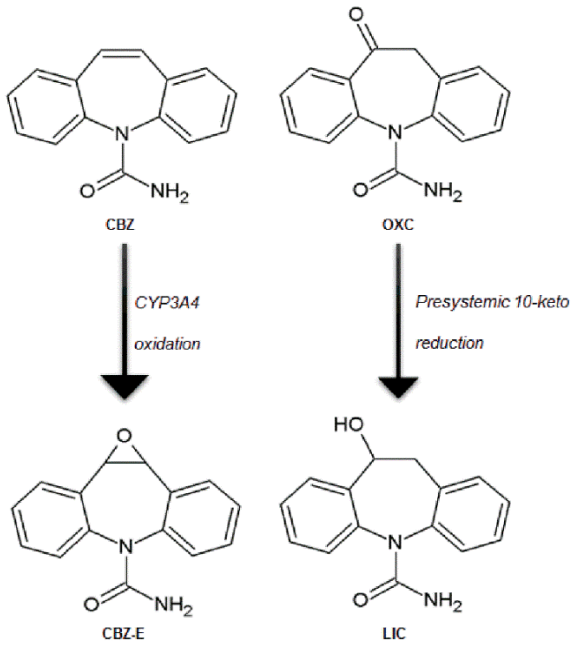

Figure II.3.1. Metabolic pathways of carbamazepine (CBZ) and oxcarbazepine (OXC) to their active metabolites carbamazepine-10,11-epoxide (CBZ-E) and licarbazepine (LIC), respectively.

Although clinical benefits are not expected with long-term CBZ and OXC cotherapy, the switching from CBZ to OXC is a common practice in patients unsatisfactorily treated with CBZ (Albani and Baruzzi 2006; Vaisleib and Neft 2008; Lee et al. 2010). Nevertheless, these drugs are commonly used in combination therapy regimens with other AEDs in refractory patients (Guberman 1998; French and Faught 2009; Giussani and Beghi 2013); actually, when monotherapy fails add-on therapy is an alternative option and there are many possible AED combinations based on their mechanisms of action and pharmacokinetic interactions. Nowadays, polytherapy regimens with AEDs are prevalent and the potential for AEDs to interact results in many challenges (Johannessen Landmark and Patsalos 2012; Giussani and Beghi 2013). These concerns were recently reviewed by Johannessen Landmark and Patsalos (2012) and the importance of the availability of appropriate *in vitro* models to characterize potential interactions involving AEDs was also highlighted.

Accordingly, as CBZ and OXC are widely used in the clinical practice and taking into account the valuable characteristics of the HepaRG cell line, which constitutes a new and promising alternative model to the primary human hepatocytes ("*gold standard*" model) for the evaluation of the hepatic drug metabolism in *in vitro* conditions (Andersson 2010), this work was planned to make available a useful bioanalytical method to support future *in vitro* pharmacokinetic-based studies in cultured HepaRG cells involving CBZ and/or OXC. Among other advantages, HepaRG cells possess the metabolic capacity characteristic of primary human hepatocytes and the indefinite proliferation property of hepatoma cell lines, constituting a promising *in vitro* tool to assess the drug metabolite profiling, the hepatic kinetics of drugs and to foresee drug–drug interactions (Guillouzo 2008; Anthérieu et al. 2010; Darnell et al. 2011). In fact, the use of *in vitro* data for the assessment of potential drug–drug interactions is also a

practice widely accepted by the regulatory authorities in the development of new drugs (WALSKY AND BOLDT 2008).

Hence, to the best of our knowledge, it is herein reported for the first time an HPLC method with DAD to quantify CBZ, OXC, and their pharmacologically active metabolites (CBZ-E and LIC, respectively) in HepaRG cell culture samples.

II.3.2. Material and methods

II.3.2.1. Reagents and cells

CBZ, CBZ-E, OXC and primidone (PRM), used as IS, were purchased from Sigma–Aldrich (St Louis, MO, USA). LIC was supplied by Tocris Bioscience (Bristol, United Kingdom). Methanol and acetonitrile, both of HPLC gradient grade, were purchased from Fisher Scientific (Leicestershire, United Kingdom) and the ultra-pure water (HPLC grade, >18 MΩ.cm) was prepared by means of a Milli-Q water apparatus from Millipore (Milford, MA, USA). Ethyl acetate were purchased from Fisher Scientific (Leicestershire, United Kingdom). HepaRG cells (lot no. #48588) were obtained from Life Technologies – Invitrogen™ (through Alfagene, Portugal). All cell culture reagents including Williams' E medium, fetal bovine serum (FBS), hydrocortisone hemisuccinate, dimethyl sulfoxide (DMSO) and trypsin–ethylenediaminetetraacetic acid (EDTA) were purchased from Sigma–Aldrich (St Louis, MO, USA).

II.3.2.2. Stock solutions, calibration standards and quality control samples

Stock solutions of CBZ (15 mg/mL), CBZ-E (30 mg/mL), OXC (10 mg/mL) and LIC (10 mg/mL) were individually prepared by dissolving the appropriate amount of each compound in methanol. These solutions were then adequately diluted in water-methanol (50:50, v/v) to obtain the corresponding working solutions. Afterwards, stock and working solutions of drugs and metabolites were properly mixed to afford six combined spiking solutions with final concentrations 1, 2, 6, 20, 80 and 150 µg/mL for CBZ; 1, 2, 5, 10, 30 and 50 µg/mL for CBZ-E and OXC; and 1, 2, 10, 50, 250 and 400 µg/mL for LIC. Each one of these combined solutions was daily used for spiking aliquots of blank supplemented Williams' E medium in order to prepare six calibration standards in the concentration ranges of 0.1-15 µg/mL for CBZ; 0.1-5 µg/mL for CBZ-E and OXC; and 0.1-40 µg/mL for LIC. Regarding the IS, the stock solution was also prepared in methanol (2 mg/mL) and the working solution (500 µg/mL) was obtained through the dilution of an appropriate volume of the stock solution with water-methanol (50:50, v/v). With exception of the IS working solution which was daily prepared, all the stock, working and combining solutions were stored at 4 °C and protected from light.

QC samples at three representative concentration levels, representing the low (QC_1), medium (QC_2) and high (QC_3) ranges of the calibration curves, were also independently prepared in supplemented Williams' E medium. With that purpose, aliquots of blank supplemented

Williams' E medium were spiked to attain final concentrations of 0.3, 7.5 and 13.5 µg/mL for CBZ; 0.3, 2.5 and 4.5 µg/mL for CBZ-E and OXC; and 0.3, 20 and 36 µg/mL for LIC. One additional QC sample was also prepared at the concentration of the LLOQ (QC_{LLOQ}).

II.3.2.3. Apparatus and chromatographic conditions

Chromatographic analysis was carried out using an HPLC system (Shimadzu LC-2010A HT Liquid Chromatography) coupled with DAD (Shimadzu SPD-M20A). All instrumental parts were automatically controlled by LabSolutions software (Shimadzu, Kyoto, Japan). The chromatographic separation of CBZ, CBZ-E, OXC, LIC and IS was carried out at 35 °C on a reversed-phase LiChroCART® Purospher Star column (C_{18}, 55 mm × 4 mm; 3 µm particle size) purchased from Merck KGaA (Darmstadt, Germany). An isocratic elution was applied at a flow rate of 1.0 mL/min with a mobile phase composed of water/methanol/acetonitrile (69:25:6 v/v/v). The mobile phase was filtered through a 0.2 µm filter and degassed ultrasonically for 15 min before use. The injection volume was 20 µL and the wavelength of 215 nm was selected for the detection of all compounds.

II.3.2.4. Sample preparation and extraction

Each aliquot (200 µL) of supplemented Williams' E culture medium was added with 20 µL of IS working solution, 300 µL of acetonitrile and then with 1 mL of ethyl acetate. Afterwards, the mixture was vortex-mixed for 30 s and centrifuged at 13500 rpm (3 min). The organic layer was transferred to a glass tube and the aqueous layer was re-extracted twice more with ethyl acetate (1 mL each time) using the conditions previously described. The combined organic phases were evaporated to dryness under a gentle nitrogen stream at 45 °C and then reconstituted with 100 µL of mobile phase. An aliquot (20 µL) of this final sample was injected into the chromatographic system.

II.3.2.5. Method validation

The developed method was appropriately validated taking into account the international accepted recommendations for bioanalytical method validation (SHAH ET AL. 2000; U.S. FOOD AND DRUG ADMINISTRATION 2001; EUROPEAN MEDICINES AGENCY 2011). The validation was carried out considering the acceptance criteria proposed for specific validation parameters including selectivity, linearity, precision, accuracy, LLOQ, recovery and stability.

II.3.2.5.1. Selectivity

Aiming at testing the chromatographic similarity between the supplemented Williams' E medium collected after the culture of HepaRG cells, in order to reproduce in the best way what happens in real metabolic studies, and the simple supplemented Williams' E medium, a set of samples from these two related matrices was analysed and compared. To obtain aliquots of

medium from cultured HepaRG cells the following procedures were conducted. HepaRG cells were maintained in the Williams' E medium supplemented with 10% FBS, 100 IU/mL penicillin, 100 µg/mL streptomycin, 5 µg/mL insulin, 2 mM glutamine and 5 x 10^{-5} M hydrocortisone hemisuccinate during 15 days. After this period of time the confluence was reached and cells were then maintained in the same culture medium but supplemented with 2% DMSO (differentiation medium) for more 15 days to obtain differentiated HepaRG cell cultures. It is worthy to mention that HepaRG cell cultures were maintained at 37 °C in humidified air incubator with 5% CO_2 and the medium was renewed each 3 days. Then, the differentiated HepaRG cells were seeded at a high density (4.5 x 10^5 cells/cm^2) in 96-well plates and maintained during 48 h. After that, the cells were exposed to 200 µL of supplemented Williams' E medium for 12 h and then the total volume of each well was collected and 300 µL of acetonitrile were immediately added.

II.3.2.5.2. Calibration curve

The linearity of this chromatographic assay was evaluated for each analyte within the concentration ranges defined in *section II.3.2.2*. For this purpose, calibration curves were prepared using six spiked supplemented Williams' E medium calibration standards and assayed on three different days (*n = 3*). Calibration curves were constructed by plotting the analyte-IS peak area ratio as function of the corresponding nominal concentrations. The data were fitted to a weighted linear regression analysis and the weighting factor that yields the best fit of peak-area ratios *versus* concentration is selected (ALMEIDA ET AL. 2002).

II.3.2.5.3. Lower limit of quantification

The LLOQ, defined as the lowest concentration of the calibration curve which can be measured with adequate inter and intraday precision and accuracy (U.S. FOOD AND DRUG ADMINISTRATION 2001; EUROPEAN MEDICINES AGENCY 2011) was evaluated by analysing supplemented Williams' E medium samples prepared in replicates. The precision, expressed as percentage of the CV, cannot exceed 20%; whereas accuracy, expressed by the *bias*, should be within ±20%.

II.3.2.5.4. Precision and accuracy

QC samples analysed on three consecutive days (*n* = 3) at the four concentration levels (QC_{LLOQ}, QC_1, QC_2 and QC_3) representative of the calibration range were used to investigate the interday precision and accuracy of the assay. Similarly, the intraday precision and accuracy were also assessed by analysing five sets of QC samples in a single day (*n* = 5). According to the acceptance criteria defined by the bioanalytical method validation guidelines the intra and interday precision (expressed as percentage of CV) should be lower than or equal to 15% (or 20% in the LLOQ) and the intra and interday accuracy (expressed as percentage of *bias*) should be within ±15% (or ±20% in the LLOQ) (U.S. FOOD AND DRUG ADMINISTRATION 2001).

II.3.2.5.5. Recovery

The absolute recovery of the analytes from the samples submitted to the treatment previously described in the *section II.3.2.4* was determined using three QC samples (QC_1, QC_2 and QC_3). The recovery was calculated comparing the analytes peak areas from extracted QC supplemented Williams' E medium samples with those obtained after direct injection of non-extracted solutions at the same nominal concentrations (*n = 5*). Similarly, the recovery of IS was also evaluated at the concentration used in sample analysis, calculating the ratio of its peak areas in extracted samples and non-extracted solutions.

II.3.2.5.6. Stability

The stability of the analytes in supplemented Williams' E medium was investigated for QC_1 and QC_3 (*n* = 5). The data of the QC samples analysed before (reference samples) were compared with those obtained after being exposed to the experimental conditions for stability assessment (stability samples). As stability criterion (*n* = 5), a stability/reference samples ratio of 85-115% was accepted (CHEN ET AL. 2005; EUROPEAN MEDICINES AGENCY 2011). The short- and long-term stability were evaluated respectively at room temperature for 4 h and −20 °C for 8 days (*n* = 5), aiming at simulating sample handling and storage time in the freezer before analysis. Moreover, in an attempt to simulate the time that samples can remain in the auto-sampler before analysis, the post-preparative stability of the analytes in processed samples was also studied at room temperature during 12 h.

II.3.3. Results

II.3.3.1. Method validation

The chromatographic separation of CBZ, CBZ-E, OXC and LIC in spiked supplemented Williams' E medium culture samples was successfully achieved using the chromatographic conditions previously described. Under these analytical conditions the last-eluting analyte was CBZ, being the run time of approximately 15 min. The order of elution of the compounds was the following: PRM (IS), LIC, CBZ-E, OXC and CBZ. Representative chromatograms of blank and spiked supplemented Williams' E culture medium samples are shown in Figure II.3.2.

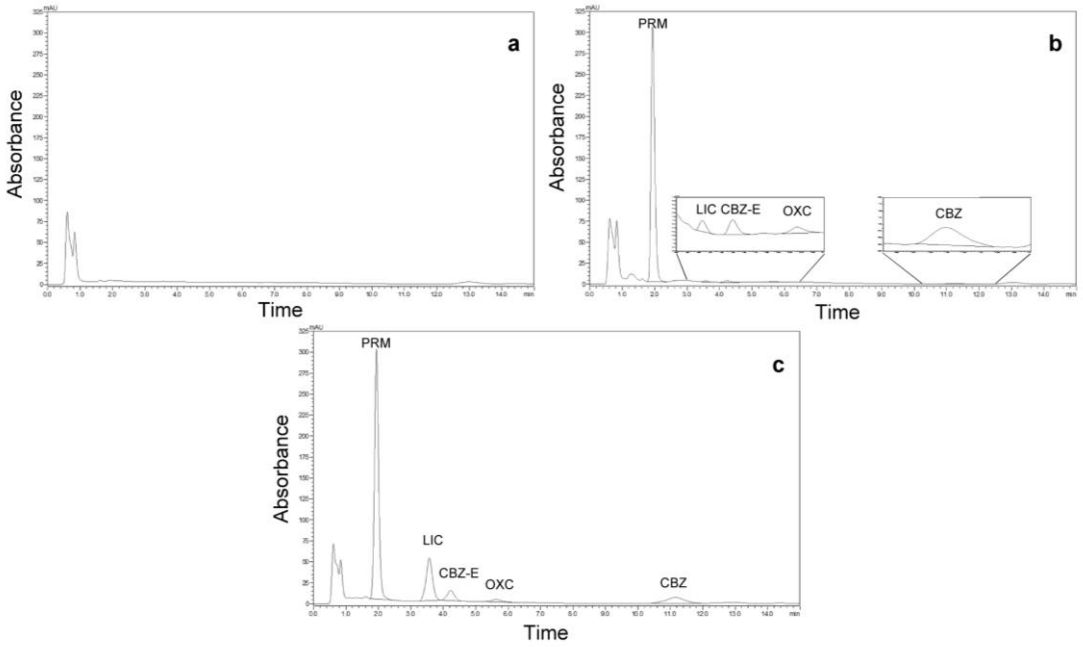

Figure II.3.2. Typical chromatograms of extracted supplemented Williams' E medium samples generated by the HPLC-DAD assay developed: blank supplemented Williams' E medium (a); supplemented Williams' E medium spiked with internal standard (IS) and the analytes at concentrations of the lower limit of quantification (b); and supplemented Williams' E medium spiked with IS and the analytes at intermediate concentrations of the calibration ranges (c). CBZ, carbamazepine; CBZ-E, carbamazepine-10,11-epoxide; PRM, Primidone; LIC, licarbazepine; OXC, oxcarbazepine.

II.3.3.1.1. Selectivity

The chromatograms obtained by the analysis of blank samples of supplemented Williams' E medium collected after the culture of HepaRG cells (to reproduce the metabolic studies) and those generated by the analysis of blank samples of the simple supplemented Williams' E medium were broadly comparable. As result, the most convenient blank matrix (the simple supplemented Williams' E medium) was chosen to the development and validation of this HPLC-DAD assay.

II.3.3.1.2. Calibration curves and LLOQs

The calibration curves obtained in supplemented Williams' E culture medium were linear ($r^2 \geq 0.9901$; Table II.3.1) for all the analytes over the concentration range defined in *section II.3.2.2* and showed a consistent correlation between analyte-IS peak area ratios and the corresponding nominal concentrations. The calibration curves for all the analytes were subjected to weighted linear regression analysis using $1/x^2$ as the weighting factor, due to the wide calibration range and in order to compensate for heteroscedasticity detected. This factor was chosen taking into account the plots and the sums of absolute percentage of relative error as statistical criteria. The regression equations of the calibration curves and the corresponding r^2 achieved for each analyte are summarized in the Table II.3.1.

The LLOQs were experimentally defined as 0.1 µg/mL for all the analytes (CBZ, CBZ-E, OXC and LIC) with acceptable precision (CV ≤17.3%) and accuracy (*bias* varied from −12.3% to 10.1%).

Table II.3.1. Mean calibration parameters obtained for carbamazepine (CBZ), carbamazepine-10,11-epoxide (CBZ-E), oxcarbazepine (OXC) and licarbazepine (LIC) in supplemented Williams' E culture medium (*n* = 3).

Analyte	Calibration parameters		
	Concentration range (µg/mL)	Equation[a]	r^2
CBZ	0.1-15	y = 0.0949 x + 0.0038	0.9901
CBZ-E	0.1-5	y = 0.1022x + 0.0010	0.9913
OXC	0.1-5	y = 0.0493x + 0.0021	0.9924
LIC	0.1-40	y = 0.0615x + 0.0031	0.9905

[a] *y, represents analyte-IS peak area ratio; x, represents analyte concentration (µg/mL).*

II.3.3.1.3. Precision and accuracy

The data for intra and interday precision and accuracy obtained from QC supplemented Williams' E medium samples at the four different concentration levels (QC_{LLOQ}, QC_1, QC_2 and QC_3) are shown in the Table II.3.2. All the data fulfilled the acceptance criteria established. Accordingly, the overall inter and intraday CV values did not exceed 13.1% (or 17.7% in the QC_{LLOQ}), and the overall inter and intraday *bias* values varied between −12.8 to 14.6% (or 12.3% to 10.1% in the QC_{LLOQ}), which supports that the HPLC–DAD method herein described is precise and accurate.

Table II.3.2. Inter and intraday precision (% CV) and accuracy (% *bias*) values obtained for carbamazepine (CBZ), carbamazepine-10,11-epoxide (CBZ-E), oxcarbazepine (OXC) and licarbazepine (LIC) in supplemented Williams' E culture medium samples at the concentrations of the lower limit of quantification (*) and at low (QC_1), medium (QC_2) and high (QC_3) concentrations representative of the calibration ranges.

Analyte	Nominal concentration (µg/mL)	Interday		Intraday	
		Precision (% CV)	Accuracy (% *bias*)	Precision (% CV)	Accuracy (% *bias*)
CBZ	0.1*	17.3	2.5	6.8	−2.8
	0.3	8.0	12.7	0.8	13.8
	7.5	4.6	−1.4	3.2	−6.7
	13.5	3.5	3.1	5.9	−6.9
CBZ−E	0.1*	6.3	−1.6	9.2	10.1
	0.3	3.4	5.6	3.7	12.6
	2.5	12.2	0.6	1.8	14.6
	4.5	4.2	−2.3	6.7	−5.6
OXC	0.1*	10.3	−5.1	10.3	3.3
	0.3	4.0	−9.0	4.6	−11.5
	2.5	13.1	−0.2	4.9	11.0
	4.5	6.1	−2.0	2.5	−11.2
LIC	0.1*	1.3	−12.3	4.7	−5.1
	0.3	6.8	6.2	4.3	13.6
	20	10.0	−3.5	10.4	−0.2
	36	3.2	−10.7	2.8	−12.8

CV, coefficient of variation; bias, deviation from nominal concentration value.

II.3.3.1.4. Recovery

The overall absolute recovery of CBZ, CBZ-E, OXC and LIC from supplemented Williams' E culture medium samples was determined at three concentration levels (QC1, QC2 and QC3) by repeated analysis (n = 5). These data are shown in Table II.3.3. The mean absolute recoveries ranged from 64.5% to 96.9% and showed CV values lower than 14.8% for all analytes (AEDs and metabolites). The recovery of the IS (PRM) was also evaluated, being its absolute recovery of 70.2 ± 8.6% with a CV value of 12.2%. These data undoubtedly support a consistent recovery over the evaluated concentration ranges by the sample preparation procedure implemented.

Table II.3.3. Absolute recovery of carbamazepine (CBZ), carbamazepine-10,11-epoxide (CBZ-E), oxcarbazepine (OXC) and licarbazepine (LIC) in supplemented Williams' E culture medium.

Analyte	Nominal concentration (µg/mL)	Absolute recovery (%)[a]	Precision (% CV)
CBZ	0.3	79.5 ± 4.8	6.1
	7.5	68.7 ± 7.1	12.2
	13.5	69.4 ± 8.8	14.8
CBZ-E	0.3	87.5 ± 8.0	9.1
	2.5	65.1 ± 8.2	12.6
	4.5	66.8 ± 6.4	9.6
OXC	0.3	96.9 ± 6.2	6.4
	2.5	85.2 ± 2.3	2.7
	4.5	82.4 ± 2.5	3.0
LIC	0.3	88.3 ± 8.5	9.6
	20	65.1 ± 9.0	13.8
	36	64.5 ± 8.8	13.7

[a] *Mean ± standard deviation, n = 5.*

II.3.3.1.5. Stability

The stability of the CBZ, CBZ-E, OXC and LIC in supplemented Williams' E culture medium was evaluated under the different conditions previously described, which simulate the handling and sample storage conditions to be likely required during the analytical process. The analytes demonstrated to be stable in unprocessed samples at room temperature for 4 h and at −20 ºC for 8 days and also in processed samples at room temperature during 12 h. The stability data are shown in Table II.3.4.

Table II.3.4. Stability (values in mean percentage) of carbamazepine (CBZ), carbamazepine-10,11-epoxide (CBZ-E), oxcarbazepine (OXC) and licarbazepine (LIC) in unprocessed and processed samples of supplemented Williams' E culture medium under the expected sample handling and storage conditions (*n* = 5).

Analyte	Nominal concentration (µg/mL)	Supplemented Williams' E culture medium		
		Unprocessed sample		Processed sample
		Room temperature (4 h)	−20 ºC (8 days)	Room temperature (12 h)
CBZ	0.3	102.8	106.9	102.5
	13.5	98.4	95.2	94.1
CBZ-E	0.3	102.8	108.5	109.2
	4.5	99.7	105.7	97.9
OXC	0.3	96.2	105.6	108.1
	4.5	98.6	94.5	90.6
LIC	0.3	106.4	110.5	110.8
	36	99.7	102.3	92.6

II.3.3.1.6. Method application

HepaRG cells were seeded in Williams' E medium supplemented with 10% FBS, 100 IU/mL penicillin, 100 µg/mL streptomycin, 5 µg/mL insulin, 2 mM glutamine and 5 x 10^{-5} M hydrocortisone hemisuccinate (basal growth medium) and maintained at 37 °C in a humidified air incubator with 5% CO_2. The medium was renewed every 2-3 days until cells reach confluence, which were expanded by gentle trypsinization and maintain in culture by serial passages and then used when appropriate for the specific studies. For the metabolic studies, HepaRG cells were maintained in the basal growth medium during 15 days. After this period of time the confluence was reached and the cells were maintained in the same culture medium supplemented with 2% DMSO (differentiation medium) for more 15 days to obtain differentiated HepaRG cell cultures. In both cases, cell cultures were maintained at 37 °C in humidified air incubator with 5% CO_2 and the medium was renewed each 3 days. The differentiated HepaRG cells were then seeded at a high density (4.5 x 10^5 cells/cm^2) on 96-well plates. After a period of cell adhesion of 24 h, the cells were incubated with 200 µL OXC 2.5 µg/mL prepared in FBS-free basal growth medium (0.25% DMSO). After 2, 4, 6, 12 and 24 h, the culture medium (200 µL) was collected and 300 µL of ice-cold acetonitrile was added to each sample in order to stop the metabolic reactions. During the incubation times, the cell cultures were maintained at 37 °C in humidified air incubator with 5% CO_2. Thereafter, the samples were frozen at −20 °C until analysis of OXC and its metabolite (LIC). The obtained results are presented in the Figure II.3.3a, showing an increasing formation of LIC over the time while the concentration of OXC (parent drug) is gradually reduced. In the Figure II.3.3b is shown a chromatogram resulting of the analysis of a real sample obtained at 6 h after incubation of OXC (2.5 µg/mL) with the HepaRG cells.

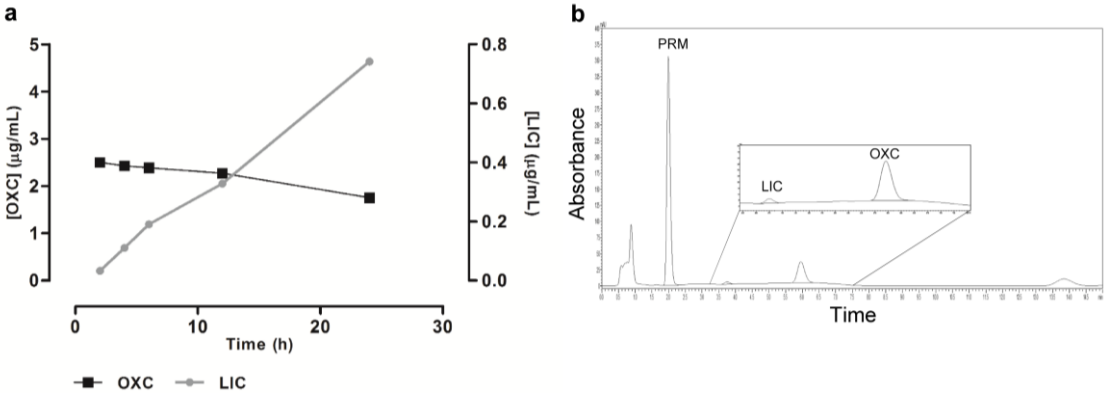

Figure II.3.3. Concentration-time profiles for the metabolism of OXC in its active metabolite LIC after 2, 4, 6, 12 and 24 h of incubation of the parent drug (OXC) at 2.5 µg/mL in differentiated HepaRG cells (a); and a representative chromatogram of the analysis of a real sample obtained after 6 h of incubation of OXC (2.5 µg/mL) in the differentiated HepaRG cells (b). OXC, oxcarbazepine; LIC, licarbazepine; PRM, Primidone.

II.3.4. Discussion

As previously mentioned, besides the availability of more than twenty AEDs (ZHANG ET AL. 2012a), the truth is that the monotherapy with AEDs often fails, requiring polytherapy regimens in an attempt to achieve better seizure control and fewer side effects (DECKERS ET AL. 2000; BUGAMELLI ET AL. 2002; GARNETT ET AL. 2009; FORTUNA ET AL. 2011b). Unfortunately, the implementation of polytherapy regimens in the clinical practice frequently originates complex and unpredictable pharmacokinetic and pharmacodynamic interactions, leading to possible clinical consequences in terms of toxicity or even therapeutic inefficacy (BUGAMELLI ET AL. 2002; PERUCCA 2006). In fact, patients with epilepsy are particularly affected by clinically relevant drug interactions (RIVA ET AL. 1996; PERUCCA 2006; JOHANNESSEN AND LANDMARK 2010). This can be explained not only by the long administration periods of AEDs, often required for a lifetime, increasing the probability of coprescription, but also due to the narrow therapeutic index of some AEDs (e.g., PB, PHT, CBZ, valproic acid); in fact, some of these older AEDs (e.g., CBZ, valproic acid) are still widely prescribed today and have marked effects on the activity of CYP isoenzymes, which also metabolize the majority of existing medication, including the new generation AEDs (PERUCCA 2006). Although other drug interaction mechanisms can occur, such as pharmacodynamic-based interactions, the majority of clinically significant AED interactions are result of induction or inhibition of drug-metabolizing CYP isoenzymes (PERUCCA 2006). The enzyme inducers as CBZ, PHT and PB increase the activity of a variety of CYP isoenzymes (CYP1A2, CYP2C9, CYP2C19 and CYP3A4), as well as glucuronyl transferases and epoxide hydrolase, which may enhance the drug metabolism and reduce the serum concentrations of other concurrently administered drugs (including AEDs) (PERUCCA 2006; JOHANNESSEN AND LANDMARK 2010; BRODIE ET AL. 2013). Actually, although none of the newer AEDs shares the broad spectrum enzyme-inducing activity of those older generation agents, they are also cleared fully or partly by inducible CYP isoenzymes, making them a target for drug interactions mediated by enzyme induction (PERUCCA 2006). On the other hand, several drugs from other therapeutic classes have also been found to increase the serum concentration of AEDs, presumably by inhibiting their metabolism. For example, several antidepressants like fluoxetine, fluvoxamine or trazodone and antimicrobials like clarithromycin, erythromycin or fluconazole have been reported to interfere in the serum concentrations of CBZ (PERUCCA 2006). Consequently, whenever possible, these drug interactions should be prevented and early identified (RIVA ET AL. 1996). Indeed, drug-drug interactions are an essential aspect to be considered in the process of new drug development, representing a major concern for pharmaceutical industry and regulatory agencies and at clinical level for healthcare professionals and their patients. Therefore, *in vitro* models are being increasingly used during preclinical drug development, arising as screening tools to predict drug-drug interactions (FABRE ET AL. 1990; LIN AND LU 1997; WIENKERS AND HEATH 2005; COSTA ET AL. 2014). In fact, there is increasing evidence that appropriate *in vitro* drug interaction studies can accurately reflect what happens in *in vivo* conditions (LIN AND LU 1997; COSTA ET AL. 2014). Indeed, in the decision making process during the development of new drug candidates,

the evaluation of induction and inhibition of CYP isoenzymes is one of the major points of concern (McGinnity and Riley 2001; Anthérieu et al. 2012). Although in the last years numerous *in vitro* and/or *ex vivo* models have been developed to investigate drug metabolism, the HepaRG cells represent perhaps nowadays the most relevant *in vitro* model as surrogate to the primary human hepatocytes, evidencing a great value to foresee drug–drug interactions (Anthérieu et al. 2010; Darnell et al. 2011).

Several metabolic interactions involving AEDs have been identified by means of *in vitro* models. For instance, it is the case of the metabolic interaction between imipramine (Daniel and Netter 1988) or felbamate (Egnell et al. 2003) with CBZ. Taking into account the experimental advantages of HepaRG cells, the availability of a rapid, sensitive and reliable analytical method is critical to support subsequent metabolic drug interaction studies in this kind of biological samples. Up to date, several HPLC methods have been developed and validated for the determination of these AEDs and some of their main metabolites in several matrices. Most of the methodologies described in the literature for the simultaneous determination of CBZ and OXC are HPLC assays using DAD or UV detection (Khoschsorur et al. 2001; Bugamelli et al. 2002; Franceschi and Furlanut 2005; Fortuna et al. 2010; Rani et al. 2012; Serralheiro et al. 2013; Ferreira et al. 2014a). Nevertheless, the extraction procedures that were applied in the preparation of the samples were diversified and included not only the LLE (Meyler et al. 1993), that was also applied in this assay, but also SPE (Bugamelli et al. 2002; Franceschi and Furlanut 2005; Fortuna et al. 2010; Serralheiro et al. 2013), MEPS (Rani et al. 2012; Ferreira et al. 2014a) and PP (Khoschsorur et al. 2001). The matrices used in these methodologies included human plasma (Khoschsorur et al. 2001; Bugamelli et al. 2002; Franceschi and Furlanut 2005; Fortuna et al. 2010; Rani et al. 2012; Ferreira et al. 2014a) or urine (Rani et al. 2012), for example. However, none of the HPLC assays described permitted the quantification of CBZ or/and OXC, and their main metabolites, in culture mediums or even in supernatants of cell cultures. Actually, the HPLC-DAD assay herein described is the first one to quantify CBZ, OXC, and their relevant pharmacologically active metabolites (CBZ-E and LIC, respectively) in HepaRG cell culture medium.

During the process of drug discovery and development the bioanalysis was recognised to be a critical tool, essential for the pharmacokinetic/pharmacodynamics characterization of a drug. Indeed, there is a continuous need of development of analytical methodologies, which permit the quantification of not only the drug but also its metabolites in several biological samples, supporting various stages of the drug discovery and development (Pandey et al. 2010; Korfmacher 2011). However, it is accepted that in the latter stages of the process the levels of analytical acceptance criteria become stricter, and it is supposed that the results were confirmed by appropriate validation assays, which permit to attest the reliability, robustness and accuracy of the methods (Srinivas 2006; Pandey et al. 2010; Korfmacher 2011). Nevertheless, the degree of development and quality of bioanalytical assays used in the discovery and development of novel chemical entities tends to increase as the lead candidates progress to more advanced stages. Actually, the various validation criteria defined by the international guidelines are not

usually applied in the early stages of drug discovery and development, being used only minimal standards in the higher throughput assays performed in these steps (SRINIVAS 2006; PANDEY ET AL. 2010; KORFMACHER 2011). All these points could explain the lack of HPLC methodologies in the literature describing a full bioanalytical method validation regarding the *in vitro* studies. Nonetheless, as we intended to develop a robust technique that could provide a high level of confidence in the results obtained, the HPLC-DAD method herein described was extensively validated taking into account the international criteria of the FDA and by the EMA guidelines.

II.3.5. Conclusion

Until now, to the best of our knowledge, there is no reported methodology in the literature to simultaneously determine the considered analytes CBZ, CBZ-E, OXC and LIC in HepaRG cell culture medium samples. Therefore, the present work describes the first HPLC-DAD assay developed and fully validated according to the international requirements for bioanalytical purposes. Hence, this methodology represents a useful bioanalytical tool to support future *in vitro* metabolic, drug interaction and other pharmacokinetic-based studies involving these AEDs and metabolites in the new and promising *in vitro* model HepaRG cell line.

II.4. Experimental

A rapid and sensitive HPLC-DAD assay to quantify lamotrigine, phenytoin and its main metabolite in samples of cultured HepaRG cells

II.4.1. Introduction

The *in vitro* studies play a crucial role during the discovery of drug candidates (ZHANG ET AL. 2012b). In fact, the high-throughput approaches for the early assessment of potential drug candidates are important tools providing a key direction in the choice of the most promising chemical series to pursue (WALSKY AND BOLDT 2008). Hence, the need of early predictive data became essential the development of several *in vitro* approaches to study drug disposition and pharmacokinetic properties. Among these *in vitro* tools are those which permit to assess the metabolite profiling and the potential for CYP drug interactions in various species, including human-based *in vitro* models (BAJPAI AND ESMAY 2002; ZHANG ET AL. 2012b; FERREIRA ET AL. 2014b). Undoubtedly, the CYP isoenzymes mediate the metabolism of the majority of drugs available today. Actually, serious clinical drug-drug interactions could be prevented by knowledge of the potential for inhibition and/or induction of CYP isoenzymes in early stages of drug discovery programs. Even the regulatory authorities widely accept the use of *in vitro* data for assessment of the potential for drug–drug interactions in the development of new drugs (WALSKY AND BOLDT 2008). Accordingly, several *in vitro* metabolism models have been developed and are now available to study the hepatic drug metabolism (ANTHÉRIEU ET AL. 2010). However, it should be highlighted that only those models which involve human liver cells have the capacity to express the complete metabolic pathways similarly to what occurs in man (JOSSÉ ET AL. 2008; GUILLOUZO AND GUGUEN-GUILLOUZO 2008). Nevertheless, despite the primary human hepatocytes are considered the "*gold standard*" model for these purposes, some pitfalls that have to be taken into account (e.g., scarce and erratic availability, poor stability of functions in culture, limited growth activity and life span) make them not as appropriate as would be desired for high-throughput screening (DONATO AND CASTELL 2003; ANINAT ET AL. 2006b; JOSSÉ ET AL. 2008; TURPEINEN ET AL. 2009; ANDERSSON 2010; ANTHÉRIEU ET AL. 2010; SZABO ET AL. 2013). Hence, other models have been proposed as an alternative to primary human hepatocytes like the immortalized human hepatic tumour cell lines such as HepG2, Huh-7 and HepaRG cells (ANINAT ET AL. 2006b; ANDERSSON 2010; LÜBBERSTEDT ET AL. 2011; PERNELLE ET AL. 2011). In fact, it is believed nowadays that the development of HepaRG cells, a new human cell line derived from a hepatocellular carcinoma, constitutes a promising achievement to improve the evaluation of hepatic drug metabolism in *in vitro* conditions (ANDERSSON 2010). Indeed, among several other advantages, the HepaRG cell line possesses the metabolic capacity characteristic of primary human hepatocytes and the indefinite proliferation property of hepatoma cell lines, making them a useful *in vitro* tool to study the hepatic kinetics of drugs and to foresee drug–drug interactions (GUILLOUZO 2008; ANTHÉRIEU ET AL. 2010; DARNELL ET AL. 2011).

Thus, aiming at evaluating the potential for drug-drug interactions involving the AEDs LTG and PHT (Figure II.4.1), a rapid, simple, sensitive, accurate and reliable analytical assay was herein developed, which enable the quantitative determination of LTG, PHT and its main metabolite in samples of cultured HepaRG cells. Whereas PHT is extensively *para*-hydroxylated to the inactive metabolite HPPH (Figure II.4.1), mainly through CYP2C9 and CYP2C19 isoenzymes, LTG

undergoes extensive metabolism to an inactive glucuronide metabolite (PATSALOS ET AL. 2008). Therefore, this HPLC assay with DAD is a useful bioanalytical tool to support future *in vitro* metabolic, drug interaction and/or pharmacokinetic studies in HepaRG cell cultures incubated with PHT and/or LTG in the presence of other chemical entities (e.g., new drug candidates) to be tested.

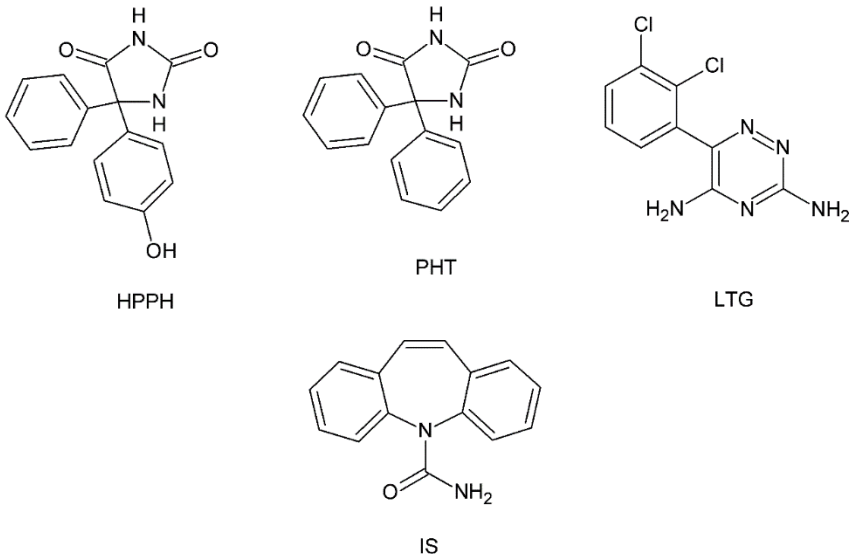

Figure II.4.1. Chemical structures of 5-(4-hydroxyphenyl)-5-phenylhydantoin (HPPH), phenytoin (PHT), lamotrigine (LTG) and carbamazepine which was used as internal standard (IS).

II.4.2. Experimental

II.4.2.1. Reagents and cells

PHT, HPPH and CBZ, used as IS, were purchased from Sigma–Aldrich (St Louis, MO, USA). LTG was gently provided by Bluepharma (Coimbra, Portugal). Methanol and acetonitrile, both of HPLC gradient grade, were purchased from Fisher Scientific (Leicestershire, United Kingdom) and the ultra-pure water (HPLC grade, >18 MΩ.cm) was prepared by means of a Milli-Q water apparatus from Millipore (Milford, MA, USA). Triethylamine was acquired from Merck KGaA (Darmstadt, Germany), the 85% ortho-phosphoric acid from Panreac Química SA (Barcelona, Spain) and ethyl acetate were purchased from Fisher Scientific (Leicestershire, United Kingdom). HepaRG cells (lot no. #48588) were obtained from Life Technologies – Invitrogen™ (through Alfagene, Portugal). The cell culture components including Williams' E medium, FBS, hydrocortisone hemisuccinate, DMSO and trypsin–EDTA were purchased from Sigma–Aldrich (St Louis, MO, USA).

II.4.2.2. Stock solutions, calibration standards and quality control samples

Stock solutions of PHT (30 mg/mL), HPPH (15 mg/mL) and LTG (10 mg/mL) were individually prepared by dissolving the appropriate amount of each compound in methanol. In order to obtain the corresponding working solutions, the stock solutions were then adequately diluted in water-methanol (50:50, v/v). Then, stock and working solutions of the individual compounds were properly mixed to afford six combined spiking solutions with final concentrations of 1.5, 3, 15, 60, 180, and 300 µg/mL for PHT, 1, 2, 5, 20, 80 and 150 µg/mL for HPPH, and 2, 4, 15, 50, 125 and 200 µg/mL for LTG. Each one of these combined solutions was daily used for spiking aliquots of supplemented Williams' E medium in order to prepare six calibration standards in the concentration ranges of 0.15-30 µg/mL for PHT, 0.1-15 µg/mL for HPPH, and 0.2-20 µg/mL for LTG. The stock solution of the IS was also prepared in methanol (2 mg/mL) and the working solution (200 µg/mL) was obtained after diluting an appropriate volume of the stock solution with water-methanol (50:50, v/v). The stock, working and combining solutions were stored at 4 °C and protected from light, with exception of the IS working solution which was daily prepared.

QC samples at three representative concentration levels, representing the low (QC_1) medium (QC_2) and high (QC_3) ranges of the calibration curves, were independently prepared in supplemented Williams' E medium. With this purpose, aliquots of supplemented Williams' E medium were spiked to attain final concentrations of 0.45, 15 and 27 µg/mL for PHT, 0.3, 7.5 and 13.5 µg/mL for HPPH, and 0.6, 10 and 18 µg/mL for LTG. One other QC sample at the concentration of the LLOQ (QC_{LLOQ}) was also prepared.

II.4.2.3. Apparatus and chromatographic conditions

Chromatographic analysis was carried out using an HPLC system (Shimadzu LC-2010A HT Liquid Chromatography) coupled with a DAD (Shimadzu SPD-M20A). All instrumental parts were automatically controlled by LC solution software (Shimadzu, Kyoto, Japan). The chromatographic separation of LTG, HPPH, PHT and IS was carried out at 35 °C on a reversed-phase LiChroCART® Purospher Star column (C_{18}, 55 mm × 4 mm; 3 µm particle size) purchased from Merck KGaA (Darmstadt, Germany). An isocratic elution was applied using acetonitrile (6%), methanol (25%) and a mixture (69%) of water–triethylamine (99.7:0.3, v/v; pH 6.0), pumped at 1 mL/min. The mobile phase was filtered through a 0.2 µm filter and degassed ultrasonically for 15 min before use. The injection volume was 20 µL and the wavelengths of 215 nm and 235 nm were selected for detection of the compounds.

II.4.2.4. Sample preparation and extraction

Each aliquot (200 µL) of supplemented Williams' E medium was added to 20 µL of IS working solution, 300 µL of acetonitrile and 1 mL of ethyl acetate. Then, this mixture was vortex-mixed for 30 s and centrifuged at 13500 rpm (3 min). The organic layer was transferred to a glass

tube, being the aqueous layer re-extracted twice more with ethyl acetate (1 mL each time) using the conditions previously described. The combined organic phases were evaporated to dryness under a gentle nitrogen stream at 45 °C and then reconstituted with 100 µL of mobile phase. Finally, an aliquot (20 µL) of the final sample was injected into the chromatographic system.

II.4.2.5. Method validation

The international accepted recommendations for bioanalytical method validation (SHAH ET AL. 2000; U.S. FOOD AND DRUG ADMINISTRATION 2001) were followed to the validation of the developed method. Accordingly, the acceptance criteria proposed for specific validation parameters including selectivity, linearity, precision, accuracy, limits of quantification and recovery were considered.

II.4.2.5.1. Selectivity

To reproduce in the best way what happens in the real metabolic and pharmacokinetic studies, samples of supplemented Williams' E medium collected from cultured HepaRG cells were analysed and compared with samples of the simple supplemented Williams' E medium. In real experimental conditions, HepaRG cells were maintained in the Williams' E medium supplemented with 10% FBS, 100 IU/mL penicillin, 100 µg/mL streptomycin, 5 µg/mL insulin, 2 mM glutamine and 5 x 10^{-5} M hydrocortisone hemisuccinate during 15 days. Afterwards, cells were then maintained in the same culture medium but supplemented with 2% DMSO (differentiation medium) for more 15 days to obtain differentiated HepaRG cell cultures. In both phases HepaRG cell cultures were maintained at 37 °C in humidified air incubator with 5% CO_2 and the medium was renewed each 3 days. Subsequently, the differentiated HepaRG cells were seeded at a high density (4.5 x 10^5 cells/cm^2) in 96-well plates and maintained during 48 h. After this period, the cells were exposed to 200 µL of supplemented Williams' E medium for 12 h. The total volume of each well was collected to an eppendorf and 300 µL of acetonitrile were immediately added.

II.4.2.5.2. Calibration curve

The linearity of the developed method for each analyte (PHT, HPPH and LTG) was evaluated in the concentration ranges previously defined using calibration curves prepared with six spiked supplemented Williams' E medium calibration standards and assayed on three different days ($n = 3$). Calibration curves were constructed by plotting the analyte-IS peak area ratio *versus* the corresponding nominal concentrations. The data were subjected to a weighted linear regression analysis using $1/x^2$ as weighting factor for all analytes, taking the plots and the sums of absolute percentage of relative error into account. This weighting factor yielded the best fit of peak-area ratios *versus* concentration for all compounds (ALMEIDA ET AL. 2002).

II.4.2.5.3. Limits of quantification

The LLOQ is defined as the lowest concentration of the calibration curve which can be measured with adequate inter/intraday precision and accuracy (U.S. FOOD AND DRUG ADMINISTRATION 2001; EUROPEAN MEDICINES AGENCY 2011). This parameter was evaluated by analysing supplemented Williams' E medium samples prepared in replicates. The precision, expressed as percentage of CV, cannot exceed 20%; whereas accuracy, expressed by the *bias*, must be within ±20%.

II.4.2.5.4. Precision and accuracy

In order to investigate the interday precision and accuracy of the assay, QC samples analysed on three consecutive days (n = 3) at the four concentration levels (QC_{LLOQ}, QC_1, QC_2 and QC_3) representative of the calibration range were used. On the other hand, the intraday precision and accuracy were assessed analysing five sets of the QC samples in a single day (n = 5). Taking into account the acceptance criterion defined by the bioanalytical method validation guidelines the intra and interday precision (expressed as percentage of CV) must be lower than or equal to 15% (or 20% in the LLOQ) and intra and interday accuracy (expressed as percentage of *bias*) must be within ±15% (or ±20% in the LLOQ) (U.S. FOOD AND DRUG ADMINISTRATION 2001; EUROPEAN MEDICINES AGENCY 2011).

II.4.2.5.5. Recovery

Three QC samples (QC_1, QC_2 and QC_3) were used to test the absolute recovery of the analytes from the samples submitted to the treatment previously described in *the section II.4.2.4*. The recovery was calculated comparing the analytes peak areas from extracted QC supplemented Williams' E medium samples with those obtained after direct injection of non-extracted solutions at the same nominal concentrations (n = 5). Likewise, the calculation of the ratio of IS peak areas in extracted samples and non-extracted solutions, evaluated at the concentration used in sample analysis, was used to define its absolute recovery.

II.4.3. Results

II.4.3.1. Method validation

The previously described chromatographic conditions enabled the separation of HPPH, PHT and LTG in spiked supplemented William's E culture medium samples. The order of elution of the compounds was the following: LTG, HPPH, PHT and CBZ (IS), with a running time of 15 min. In Figure II.4.2 are shown representative chromatograms of the analysis of blank and spiked supplemented William's E culture medium samples.

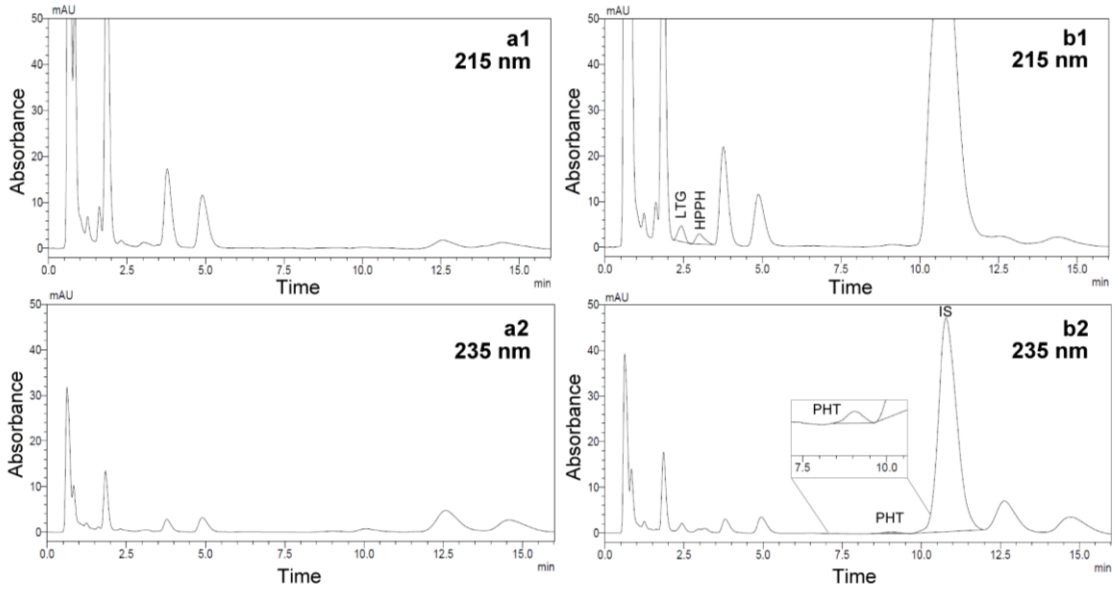

Figure II.4.2. Typical chromatograms of extracted supplemented Williams' E medium samples obtained by the HPLC-DAD assay developed: supplemented Williams' E medium at 215 nm (a1) and 235 nm (a2) and supplemented Williams' E medium spiked with the analytes at the lower limit of quantification of the calibration ranges at 215 nm (b1) and 235 nm (b2). HPPH, 5-(4-hydroxyphenyl)-5-phenylhydantoin; IS, internal standard; LTG, lamotrigine; PHT phenytoin.

II.4.3.1.1. Selectivity

Taking into account the chromatographic similarity of the blank samples of supplemented Williams' E medium collected from cultured HepaRG cells and those of simple supplemented Williams' E medium, the latter was chosen as matrix to the development and validation of this HPLC-DAD methodology.

II.4.3.1.2. Calibration curves and LLOQs

Over the concentration ranges established for all the analytes (PHT, HPPH and LTG), the calibration curves obtained in supplemented Williams' E culture medium were linear ($r^2 \geq 0.9941$; Table II.4.1), showing a consistent correlation between analyte-IS peak area ratios and the corresponding nominal concentrations in supplemented Williams' E culture medium. Regarding the wide calibration range and in order to compensate for heteroscedasticity, the calibration curves were subjected to weighted linear regression analysis using $1/x^2$ as the weighting factor for all the analytes. The choice of this factor took into account the plots and the sums of absolute percentage relative error as statistical criteria. In Table II.4.1 are summarized the regression equations of the calibration curves and the corresponding r^2 achieved for each analyte. The LLOQs were experimentally defined as 0.1 µg/mL for HPPH, 0.15 µg/mL for PHT and 0.2 µg/mL for LTG with acceptable precision (CV ≤15.4%) and accuracy (*bias* varied from 17.6% to 12.0%).

Table II.4.1. Mean calibration parameters obtained for 5-(4-hydroxyphenyl)-5-phenylhydantoin (HPPH), phenytoin (PHT) and lamotrigine (LTG) in supplemented Williams' E culture medium (n = 3).

Analyte	Calibration parameters		
	Concentration range (μg/mL)	Equation[a]	r^2
HPPH	0.1-15	y = 0.01288x + 0.0001	0.9953
PHT	0.15-30	y = 0.0248x + 0.0007	0.9941
LTG	0.2-20	y = 0.0172x + 0.0016	0.9973

[a] *y, represents analyte-IS peak area ratio; x, represents analyte concentration (μg/mL).*

II.4.3.1.3. Precision and accuracy

The Table II.4.2 contains the data for intra and interday precision and accuracy obtained from QC supplemented Williams' E medium samples at the four different concentration levels (QC_{LLOQ}, QC_1, QC_2 and QC_3). It is worthy to mention that all the data fulfilled the acceptance criteria. Therefore, the overall inter and intraday CV values lower than or equal to 8.1% (or 15.4% in the QC_{LLOQ}), and the overall inter and intraday *bias* values ranging from −9.4 to 10.5% (or −17.6%-12.0% in the QC_{LLOQ}) clearly demonstrates that the HPLC–DAD method herein described is reliable, accurate and reproducible.

Table II.4.2. Inter and intraday precision (% CV) and accuracy (% *bias*) values obtained for 5-(4-hydroxyphenyl)-5-phenylhydantoin (HPPH), phenytoin (PHT) and lamotrigine (LTG) in samples of supplemented Williams' E culture medium at the concentrations of the lower limit of quantification (*) and at the low (QC_1), middle (QC_2) and high (QC_3) concentrations representative of the calibration ranges.

Analyte	Nominal concentration (μg/mL)	Interday		Intraday	
		Precision (% CV)	Accuracy (% *bias*)	Precision (% CV)	Accuracy (% *bias*)
HPPH	0.1*	1.8	12.0	15.4	0.6
	0.3	3.3	1.5	0.5	1.5
	7.5	3.6	−10.0	4.4	−9.2
	13.5	4.7	−3.2	0.3	5.0
PHT	0.15*	7.9	−16.2	3.7	−17.6
	0.45	3.6	0.1	1.9	−2.5
	15	3.5	−9.4	4.3	−8.5
	27	8.1	−1.3	0.4	10.5
LTG	0.2*	3.9	−4.1	3.9	1.2
	0.6	4.1	−5.5	1.8	−0.2
	10	3.2	−6.6	5.3	−3.8
	18	6.1	1.8	0.2	1.8

CV, coefficient of variation; bias, deviation from nominal concentration value.

II.4.3.1.4. Recovery

Five repeated analysis (*n = 5*) at the three concentration levels (QC_1, QC_2 and QC_3) for HPPH, PHT and LTG were used to determine the overall absolute recovery of each analyte. The Table II.4.3 exhibits the absolute recovery data. As noted, the absolute mean recoveries ranged from 62.5% to 96.9% with CV values lower than 10.9% for all analytes (PHT, HPPH and LTG). On the other hand, the absolute recovery value of the IS (CBZ) was 82.4% with a CV value of 9.9%.

Table II.4.3. Absolute recovery of 5-(4-hydroxyphenyl)-5-phenylhydantoin (HPPH), phenytoin (PHT) and lamotrigine (LTG) in supplemented Williams' E culture medium.

Analyte	Nominal concentration (µg/mL)	Absolute recovery (%)[a]	Precision (% CV)
HPPH	0.3	85.8 ± 9.4	10.9
	7.5	80.4 ± 3.9	3.9
	13.5	62.5 ± 1.4	2.2
PHT	0.45	85.1 ± 8.9	10.5
	15	80.1 ± 3.5	4.4
	27	66.2 ± 3.4	5.2
LTG	0.6	96.9 ± 6.2	6.4
	10	85.2 ± 2.3	2.7
	18	82.4 ± 2.5	3.0

[a] *Mean ± standard deviation, n = 5.*

II.4.4. Discussion

Epilepsy is a serious chronic neurological disorder affecting approximately 50 million people worldwide (ZHANG ET AL. 2012a; SAVAGE 2014; ZHAO ET AL. 2015). LTG and PHT are two AEDs commonly used in clinical practice. LTG has been widely used in epilepsy treatment due to its broad spectrum of activity and it is also effective as a mood stabilizer agent (LEES AND LEACH 1993; WERZ 2008). In turn, the therapeutic value of PHT could be attested by its inclusion in the World Health Organization's List of Essential Medicines, which contains the most important medication needed in a basic health system (WORLD HEALTH ORGANIZATION 2013).

Even though interactions may occur under AED polytherapy regimens, such drugs are commonly prescribed for long periods of time making possible the cotherapy and, consequently, the occurrence of drug-drug interactions with other kind of therapeutic agents used for usual comorbidities (PATSALOS AND PERUCCA 2003; PERUCCA 2006). Actually, several comorbid health conditions are common among people with epilepsy, mainly psychiatric disorders (e.g., depression, psychosis, attention deficit hyperactivity, anxiety, and panic disorder), increasing the likelihood of co-prescription (SAVAGE 2014). This fact, added to the narrow therapeutic index of several AEDs and their marked effects on the activity of CYP isoenzymes (inhibition or induction) (PERUCCA 2006) make the patients with epilepsy especially susceptible to complex and unpredictable pharmacokinetic and also pharmacodynamic interactions (BUGAMELLI ET AL. 2002; PERUCCA 2006; JOHANNESSEN AND LANDMARK 2010; BRODIE ET AL. 2013).

As it is well-known, PHT is extensively involved in drug interactions with other AEDs (felbamate, OXC and valproic acid), and also with many other drugs such as antidepressants (fluoxetine, fluvoxamine, imipramine, paroxetine, sertraline, trazodone and viloxazine), antimicrobials (chloramphenicol, fluconazole, isoniazid, miconazole and sulfaphenazole), antineoplastic drugs (doxifluridine, fluorouracil, tamoxifen and tegafur) and several compounds from miscellaneous classes like allopurinol, amiodarone, azapropazone, cimetidine, chlorpheniramine, dextropropoxyphene, diltiazem, disulfiram, omeprazole, tacrolimus and ticlopidine (SCHMIDER ET AL. 1997; PERUCCA 2006). On the other hand, although there are fewer interactions described in literature involving LTG, the AED valproic acid and the antidepressant sertraline have been found to increase its serum concentrations (PERUCCA 2006).

Nowadays, it is well-recognized the value of the early identification of potential drug interactions in the development process of new drug candidates (RIVA ET AL. 1996). In this context, *in vitro* methodologies are being increasingly used during preclinical drug development for the prediction of drug-drug interactions, providing useful data to extrapolate to human (FABRE ET AL. 1990; LIN AND LU 1997; WIENKERS AND HEATH 2005; COSTA ET AL. 2014). Indeed, several *in vitro* models have demonstrated ability to identify relevant drug interactions. For instance, the metabolic interactions between valproic acid and LTG (ROWLAND ET AL. 2006), and those involving the PHT and the selective serotonin reuptake inhibitors, norfluoxetine or paroxetine (SCHMIDER ET AL. 1997), have been identified and studied in *in vitro* conditions. Therefore, bearing in mind the valuable characteristics of HepaRG cells, this *in vitro* model arises as a valuable tool to foresee drug–drug interactions (ANTHÉRIEU ET AL. 2010; DARNELL ET AL. 2011).

Thus, bioanalysis emerged as a critical tool in the process of drug discovery and development, being essential for pharmacokinetic/pharmacodynamics characterization of a drug compound. In fact, a plethora of assays has been continuously developed for novel chemical entities in order to support the various stages of discovery and development programs, involving quantitative bioanalytical methods for the measurement of parent compounds and their metabolites in several biological samples (PANDEY ET AL. 2010; KORFMACHER 2011). However, the degree of development and quality of the bioanalytical assays used tends to increase as the lead drug candidates progress to more advanced stages. Accordingly, the levels of analytical acceptance criteria become stricter in the latter stages, being the results confirmed by appropriate validation assays, which attest its reliability, robustness and accuracy (SRINIVAS 2006; PANDEY ET AL. 2010; KORFMACHER 2011). This aspect explains the scarcity of HPLC methodologies fully validated in literature to support *in vitro* studies. Notwithstanding, the HPLC-DAD assay herein reported to quantify LTG, PHT and its main metabolite was extensively validated taking into account the international criteria of FDA and EMA guidelines.

Apart from other methodologies like, for example, gas chromatography (QUEIROZ ET AL. 2002), several HPLC assays have been developed for the simultaneous determination of PHT and LTG in human plasma or urine using mainly DAD or UV detection (MEYLER ET AL. 1993; KHOSCHSORUR ET AL. 2001; BUGAMELLI ET AL. 2002; PATIL AND BODHANKAR 2005; RANI ET AL. 2012; SERRALHEIRO ET AL. 2013; FERREIRA ET AL. 2014a; ASADI ET AL. 2015). For instance, an HPLC-DAD assay which enables

the simultaneous quantification of PHT and LTG in human plasma has been previously developed by our group (FERREIRA ET AL. 2014a). Nevertheless, the PHT metabolite (HPPH) was not considered in such bioanalytical assay; moreover, it is desirable the availability of less expensive, faster and simpler analytical methodologies to support drug interaction screening studies, and thus, the MEPS used therein for sample preparation was not considered to be the most easy-to-use approach in this case. On the other hand, although the differences in terms of selectivity and sensitivity between DAD and mass spectrometry detectors used by other authors are incontestable (KADI ET AL. 2013), for screening purposes the current technique employing a more accessible and cheaper DAD detector is considered to be appropriate. Taking also into account the liquid chromatography-tandem mass spectrometry method published by KADI ET AL. (2013), which was developed to the simultaneous determination of LTG and PHT in human plasma, it is also evident that our HPLC-DAD assay requires a more environmentally friendly chromatographic mobile phase due to the different nature of the column stationary phase employed (reversed-phase *vs*. normal-phase liquid chromatography). Additionally, it should not be neglected the lack of HPLC assays fully validated for the quantification of LTG or/and PHT in culture media or even in supernatants of cell cultures. Actually, the HPLC-DAD method herein described is the first one which permits the quantification of LTG, PHT and its main metabolite in samples of cultured HepaRG cells. In fact, we intended to develop a robust technique, which will provide results with a high level of confidence that could be properly interpreted.

II.4.5. Conclusion

In recent years, HepaRG cells emerged as a very promising model to evaluate the hepatic drug metabolism in *in vitro* conditions. Consequently, analytical methodologies to support the studies conducted with this model are extremely relevant. Thus, the reported HPLC-DAD method, validated according to the international requirements of EMA and FDA, will be suitable to support future metabolic, drug interaction and pharmacokinetics studies involving PHT and LTG in cultured HepaRG cells.

CHAPTER III

In Vitro Studies

The content of this chapter is included in the following manuscripts:

FERREIRA A *ET AL* (2018) Flavonoid compounds as reversing agents of the P-glycoprotein-mediated multidrug resistance: An in vitro evaluation with focus on antiepileptic drugs. *Food Res Int*. 103:110-120. doi: 10.1016/j.foodres.2017.10.010

FERREIRA A *ET AL* (2018) In vitro screening of dual flavonoid combinations for reversing P-glycoprotein-mediated multidrug resistance: Focus on antiepileptic drugs. *Food Chem Toxicol*. 111:84-93. doi: 10.1016/j.fct.2017.11.004

III.1. General Considerations

III.1.1. *In vitro* assays

The price tag for drug discovery and development is still raising with no signs of decreasing or even stabilizing, mainly due to the high failure rate of drug candidates in clinical trials (LI 2005; VISK 2015). The drug discovery and development process involves the conduction of both *in vitro* and *in vivo* studies, ranging from test tube assays to cell culture models, tissue experiments, whole-animal models, healthy humans and even patients to prove the drug's efficacy and safety (ZHANG ET AL. 2012b).

The early study of the pharmacokinetic properties of drug candidates is a trend that began about 15–20 years ago and it has improved the success rates in the process of drug discovery and development (ZHANG ET AL. 2012b). Undoubtedly, a drug candidate with desirable drug-like properties will have an increased probability to be successful in clinical trials (LI 2005). In this context, over the last decades, several alternatives to animal testing have been proposed in order to overcome some of the drawbacks associated with animal experiments and to avoid unethical procedures. Thus, a variety of medium and high-throughput *in vitro* methodologies, predictive of the absorption, distribution, metabolism, excretion and toxicity (ADMET), have been routinely used to generate early *in vitro* comparative data for the most relevant pharmacokinetic and toxicity endpoints (LI 2005; ZHANG ET AL. 2012b; DOKE AND DHAWALE 2015). In addition, the *in vitro* evaluation of the potential for pharmacokinetic-based drug interactions is also an integral part of drug development programs. Indeed, many of these drug interactions involve inhibition or induction of drug-metabolizing cytochrome P450 (CYP) isoenzymes and transporters, resulting in increased or reduced systemic exposure that can lead to toxicity or loss of efficacy of coadministered drugs, respectively (PELKONEN ET AL. 2005; ZHANG ET AL. 2012b). Actually, one of the aspects that should be evaluate in the early stages of preclinical drug development is the occurrence of interactions of test compounds with drug efflux transporters, which may have impact in terms of pharmacokinetics and toxicity (BJORNSSON ET AL. 2003; SCHWAB ET AL. 2003; PRACHAYASITTIKUL AND PRACHAYASITTIKUL 2016). Among several well-characterised drug efflux transporters [e.g., P-glycoprotein (P-gp), multidrug resistance-associated proteins (MRPs) and breast cancer resistance protein (BCRP)], P-gp is certainly the most important one and thus it is useful to assess potential interactions with this biological target in order to optimize the decision-making process during drug development. Moreover, P-gp has been recognised to be implicated in the phenomenon of multidrug resistance that represents a major obstacle in the successful therapy of many diseases (LÖSCHER AND POTSCHKA 2005c; THUERAUF AND FROMM 2006; HOOSAIN ET AL. 2015).

In fact, drug regulatory agencies recommend that the screening of target bioactive compounds against the P-gp should be conducted as early as possible during drug discovery pipeline (PRACHAYASITTIKUL AND PRACHAYASITTIKUL 2016). Thus, P-gp probe substrates should be used to assess the potential liability that a new chemical entity may pose toward P-gp, either as substrate, inhibitor or inducer (FORTUNA ET AL. 2011a). According to the U.S. Food and Drug Administration (FDA), an *in vitro* P-gp substrate should have some features including selectivity

for this transporter, low to moderate passive permeability through the cell monolayer, not suffer significant metabolism, be commercially available and be suitable to be also used in *in vivo* conditions (U.S. FOOD AND DRUG ADMINISTRATION 2006). In this context, rhodamine 123 (Rh123), a specific and fluorescent dye, has been successfully applied in early drug discovery and non-clinical development stages to assess the functional activity of P-gp in a variety of *in vitro* and *in vivo* studies (FOGER ET AL. 2006; DUPUY ET AL. 2010; IQBAL ET AL. 2010; MARIANA ET AL. 2011). Actually, apart from its non-toxic *in vitro* profile (CHO ET AL. 2000), Rh123 is a well-established P-gp substrate and its selective binding site was already identified (SHAPIRO AND LING 1997; SHAPIRO ET AL. 1999).

Nowadays, a variety of *in vitro* cell-based models expressing P-gp are available to investigate the P-gp activity, which can be employed in different formats including intracellular accumulation assays and unidirectional or bidirectional transport studies across a cell monolayer (BENTZ ET AL. 2013). Among such cell-based models, the most used to evaluate interactions with the P-gp efflux transporter are the human colon adenocarcinoma (Caco-2) cell line and the epithelial kidney cell lines as the Madin-Darby canine kidney (MDCK) cells and the porcine-kidney derived Lilly Laboratories cell line (LLC-PK1), either untransfected or transfected with the *MDR1* (MDCK-MDR1 and LLC-PK1-MDR1 cells) (KUTEYKIN-TEPLYAKOV ET AL. 2010; BENTZ ET AL. 2013; GAMEIRO ET AL. 2017). Particularly, the MDCK-MDR1 is a well-established model for the identification of interactions with the human P-gp, which has been considered a useful tool that can aid drug candidate selection and optimization (GARTZKE AND FRICKER 2014). Actually, MDCK cells grow and differentiate quickly than Caco-2 cell line, which significantly reduces the time required to perform the *in vitro* P-gp screening assays (JIN ET AL. 2014). On the other hand, in comparison to LLC-PK1-MDR1 cells, the MDCK-MDR1 cell line has a low expression of endogenous (canine) *Mdr1,* which is an advantage in identifying substrates of the human P-gp (KUTEYKIN-TEPLYAKOV ET AL. 2010).

Considering all the aforementioned aspects, and taking also into account the aim of this work regarding the evaluation of a strategy to reverse the P-gp–mediated multidrug resistance, this chapter reports the *in vitro* screening assays performed to find promising flavonoids as P-gp inhibitors. Hence, the potential of a series of flavonoid compounds were firstly evaluated through a set of intracellular accumulation assays conducted in MDCK-MDR1 cells and using Rh123 as P-gp probe substrate. Then, those flavonoids exhibiting a higher capacity to inhibit the functional activity of P-gp were evaluated regarding their effects on the intracellular accumulation of commonly used antiepileptic drugs (AEDs) and their active metabolites. Additional studies were also performed in order to explore the potential of some AEDs as substrates and also as inducers of the P-gp activity, a topic that still remains controversial and dubious in our days. In a second part of this work, an evaluation of the effects of dual combinations of flavonoid-type P-gp inhibitors was also performed through intracellular accumulation assays and transepithelial permeability assays. This large set of initial *in vitro* screening tests was planned to minimize the subsequent *in vivo* studies, thus respecting the principles of 3Rs underlying the humane use of animals in scientific research.

III.2. Experimental

Flavonoid compounds as reversing agents of the P-glycoprotein-mediated multidrug resistance: Focus on antiepileptic drugs

III.2.1. Introduction

Despite the clinical availability of more than twenty AEDs with different pharmacokinetic profiles, mechanisms of action and potential for drug interactions, the development of drug-resistant epilepsy is a major, unresolved problem, affecting 30–40% of all patients (GIDAL 2014; VENTOLA 2014; BAULAC ET AL. 2015; FRANCO ET AL. 2016). Although several pathomechanisms have been advocated to explain the drug resistance to AEDs, two major hypotheses have been gaining emphasis: the target hypothesis and the multidrug transporter hypothesis (ROGAWSKI 2013; LÖSCHER ET AL. 2013; WANG ET AL. 2016). The former postulates that AEDs loose efficacy due to changes in the structure/functionality of their target ion channels and neurotransmitter receptors; while the multidrug transporter hypothesis suggests an overexpression of multidrug efflux transporters, such as P-gp, in capillary endothelial cells of the blood–brain barrier, restricting AEDs penetration into the brain tissue of non-responsive epileptic patients (LÖSCHER ET AL. 2013; GIDAL 2014; XIONG ET AL. 2015; FERREIRA ET AL. 2015). This hypothesis has been supported by important clinical findings that demonstrated a greater expression of P-gp in drug-resistant patients, being this expression significantly higher in patients with recurrent seizures than in those who have been seizure-free (LAZAROWSKI ET AL. 1999; SISODIYA ET AL. 1999; DOMBROWSKI ET AL. 2001; MARCHI ET AL. 2004; JÓŹWIAK 2007; KWAN ET AL. 2010b). Similar evidence has also been obtained from several animal models (SEEGERS ET AL. 2002b; RIZZI ET AL. 2002; SEEGERS ET AL. 2002a; VAN VLIET ET AL. 2004; POTSCHKA ET AL. 2004; VOLK AND LÖSCHER 2005; MARCHI ET AL. 2006; LIU ET AL. 2007; BAUER ET AL. 2008; NISHIMURA ET AL. 2008; BARTMANN ET AL. 2010). Furthermore, there are clinical case reports of patients with drug-resistant epilepsy in which verapamil, a classic P-gp inhibitor, was successfully used as an add-on agent to conventional AEDs therapy, suggesting that P-gp inhibition could be one of the reasons underlying the improved seizure control (SUMMERS ET AL. 2004; IANNETTI ET AL. 2005).

Thus, the multidrug transporter hypothesis has become particularly plausible in the context of drug-resistant epilepsy given that, similarly to other drug classes, several AEDs have been found to be substrates of the P-gp efflux pump (STOUCH AND GUDMUNDSSON 2002; WEISS ET AL. 2003; LUNA-TORTÓS ET AL. 2008). Additionally, the exposure to certain AEDs themselves has been proposed as a potential cause for P-gp upregulation; actually, some AEDs have been identified as P-gp inducers in both *in vitro* and *in vivo* conditions (ZHANG ET AL. 2012a; GIDAL 2014).

Given the relevance of the aforementioned P-gp–mediated multidrug resistance, efforts have been made to search for therapeutically useful P-gp inhibitors in order to overcome this functional barrier and reach higher drug concentrations into the target tissue for a longer period of time (CHEN ET AL. 2016). Nowadays, the limited therapeutic success of the first- and second-generation P-gp inhibitors is widely recognised, particularly due to their low potency, affinity and selectivity, requiring so high concentrations to inhibit P-gp that severe toxic effects are developed, compromising their clinical use (BANSAL ET AL. 2009; PALMEIRA ET AL. 2012). In turn, the search for non-toxic third-generation P-gp inhibitors, which include herbal constituents like flavonoids, has gained a great attention (BANSAL ET AL. 2008; BANSAL ET AL. 2009; FERREIRA ET AL.

2015). As several flavonoids share some of the properties of an ideal P-gp inhibitor, their interest as P-gp modulators has significantly increased in the last decade (ABDALLAH ET AL. 2015; FERREIRA ET AL. 2015; MOHANA ET AL. 2016). As a result, compounds of this large group of polyphenolic constituents have been recognised to exhibit P-gp inhibitory effects comparable to those of the classic P-gp inhibitors (verapamil and cyclosporine A) (BANSAL ET AL. 2009; SCHINKEL AND JONKER 2012; FERREIRA ET AL. 2015). In fact, some evidence of the potential of flavonoid compounds as P-gp inhibitors is supported by *in vitro* and *in vivo* studies as reviewed by FERREIRA ET AL. (2014).

Hence, aware that the P-gp overexpression can be mediated by seizures activity and prolonged AEDs therapy, together with the fact that several AEDs are P-gp substrates, is of paramount importance the evaluation of the effect of multiple flavonoids on the activity of P-gp efflux pump and their influence on AEDs transportation. For this purpose, MDCK cell line transfected with the *MDR1* (*ABCB1*) gene encoding P-gp (MDCK-MDR1) and its respective wild-type MDCK II cells were used to identify P-gp inhibitors among several flavonoids and evaluate their effect on cell uptake of AEDs and their active metabolites. In parallel, P-gp substrates were identified among these drugs as well as the ability of AEDs/metabolites to interfere with the P-gp activity. The compounds under investigation included flavonoids as apigenin, baicalein, (+)-catechin, (-)-epicatechin, (-)-epigallocatechin gallate [(-)-EPG], fisetin, hesperetin, kaempferol, naringin, quercetin and silymarin, and some of the most commonly prescribed AEDs [carbamazepine (CBZ), phenytoin (PHT), oxcarbazepine (OXC) and lamotrigine (LTG)] and pharmacologically active metabolites [carbamazepine-10,11-epoxide (CBZ-E) and licarbazepine (LIC)].

III.2.2. Material and methods

III.2.2.1. Compounds and reagents

CBZ, CBZ-E, PHT, OXC, baicalein, (+)-catechin hydrate, fisetin, quercetin, silymarin, verapamil (a reference P-gp inhibitor used as positive control), Rh123 (a P-gp fluorescent probe substrate), and primidone [PRM; used as internal standard (IS) in chromatographic analysis] were purchased from Sigma–Aldrich (St Louis, MO, USA). Silymarin is composed of silybinin, silydianin and silychristin, and the molar concentration was calculated based on the molecular weight of silybinin because this is the main flavonoid component present (ZHANG AND MORRIS 2003a; ZHANG AND MORRIS 2003b). Apigenin, (-)-EPG, kaempferol, hesperetin and naringin were obtained from Santa Cruz Biotechnology (Heidelberg, Germany) and (-)-epicatechin from Fluka (St Louis, MO, USA). LIC was supplied by Tocris Bioscience (Bristol, United Kingdom) and LTG was gently provided by Bluepharma (Coimbra, Portugal). All cell culture reagents including Dulbecco's Modified Eagle's Medium - high glucose (DMEM), fetal bovine serum (FBS), penicillin, streptomycin, 3-[4,5-dimethylthiazol-2-yl]-2,5-diphbenyltetrazolium bromide (MTT), dimethyl sulfoxide (DMSO), trypsin-ethylenediaminetetraacetic acid (EDTA) (0.5 g/L porcine trypsin,

0.2 g/L EDTA) and phosphate-buffered saline (PBS) were acquired from Sigma-Aldrich (St Louis, MO, USA). Methanol and acetonitrile, both of high-performance liquid chromatography (HPLC) gradient grade, and ethyl acetate were purchased from Fisher Scientific (Leicestershire, United Kingdom), and the ultra-pure water (HPLC grade, >18 MΩ.cm) was prepared by means of a Milli-Q water apparatus from Millipore (Milford, MA, USA).

III.2.2.2. Cell lines and culture conditions

MDCK II (passages 8-10) and MDCK-MDR1 (passages 18-30) cells, originally obtained from The Netherlands Cancer Institute (NKI-AVL; Amsterdam, Netherlands), were cultured in 75-cm^2 culture flasks in DMEM supplemented with 10% FBS, 100 IU/mL penicillin and 100 µg/mL streptomycin and maintained at 37°C in a humidified air incubator with 5% CO_2, renewing the medium every 2-3 days. Cells were seeded (density of 7.9 x 10^4 cells/cm^2) in 96-well plates for cytotoxicity and Rh123 accumulation assays and in 24-well plates for the AEDs/metabolites accumulation assays, and maintained in culture for 4 days at 37 °C in an atmosphere of 5% CO_2 before being subjected to the experiments.

III.2.2.3. Cytotoxicity assays

The *in vitro* cell viability was determined by the MTT assay, according to the procedure described by FRESHNEY (2010), for the combination of each flavonoid (50-200 µM) or verapamil (50 µM) with Rh123 (5 µM), the co-incubation of each AED/metabolite [CBZ (20-50 µM), CBZ-E (2-16 µM), PHT (40-75 µM), OXC (2-20 µM), LIC (16-140 µM), LTG (12-55 µM)] and Rh123 (5 µM), and for each AED/metabolite alone (at the highest concentration level of the previously mentioned ranges) and their combination with those flavonoids (200 µM) which revealed higher potential of P-gp inhibition [baicalein, (-)-EPG, kaempferol, quercetin and silymarin] or verapamil (50 µM, positive control).

Briefly, after incubating the cells for 4 h with the compounds of interest at the designated concentration levels, medium was removed and 100 µL of FBS- and antibiotic-free DMEM medium containing MTT (1 mg/mL) was loaded to each well, followed by incubation for 3 h under the same conditions. In the untreated control cells was used the drug vehicle with the same final percentage of DMSO. Thereafter, the MTT-containing medium was removed and replaced with DMSO to dissolve the formazan crystals. Afterwards, the content of the wells was transferred to a reading 96-well plate and the absorbance was measured at 570 nm using a microplate spectrophotometer xMark™ (Bio-Rad). Cell viability was expressed as a percentage relatively to the absorbance determined in the untreated control cells.

III.2.2.4. Intracellular rhodamine 123 accumulation assays

To identify the flavonoid compounds that are P-gp inhibitors and the AEDs/metabolites that are inducers of the P-gp activity, intracellular Rh123 accumulation assays were performed

according to BARTHOMEUF ET AL. (2005) with some modifications. At confluence, MDCK-MDR1 cells were washed once with PBS (pH 7.4) at 37 °C and pre-incubated for 30 min with FBS-free DMEM medium, containing the test compounds as described in s*ections II.2.4.1* and *II.2.4.2*. Subsequently, 5 µM Rh123, prepared in FBS-free DMEM medium (1% DMSO, v/v), was added to each well and cells were maintained at 37 ºC/5% CO_2 for 2 h. These conditions were common through all studies. Finally, cells were washed with cold PBS in order to stop the accumulation of Rh123, and then the cells were lysed with 100 µL 0.1% Triton X-100 for 30 min at room temperature, protected from light. The fluorescence of cell lysates was measured with a SpectraMax Gemini spectrofluorometer (Molecular Devices) at excitation/emission wavelengths of 485 nm/538 nm. Untreated control cells, exposed only to the drug vehicle with the same percentage of DMSO (1%, v/v), were also incubated with 5 µM Rh123 in order to estimate the baseline levels of intracellular Rh123 accumulation. A Rh123 standard curve (0.00625-5 µM) was generated to quantify the total amount of Rh123 accumulated in each sample.

III.2.2.4.1. Identification of flavonoid compounds as P-glycoprotein inhibitors

MDCK-MDR1 cells were pre-incubated for 30 min with FBS-free DMEM medium, supplemented with penicillin and streptomycin, containing apigenin, baicalein, (+)-catechin, (-)-epicatechin, (-)-EPG, fisetin, hesperetin, kaempferol, naringin, quercetin or silymarin. The positive control consisted of incubating the cells with verapamil instead of flavonoid. The flavonoid compounds were tested at 50, 100 and 200 µM, and the verapamil was incubated at 50 µM, all prepared in FBS-free DMEM medium (1% DMSO, v/v).

III.2.2.4.2. Identification of antiepileptic drugs/metabolites as inducers of P-glycoprotein activity

MDCK-MDR1 cells were pre-incubated for 30 min with FBS-free DMEM medium, containing each AED or active metabolite. These compounds were tested at three concentrations, corresponding to the low, medium and high level of their therapeutic ranges: 20, 30 and 50 µM for CBZ; 2, 8 and 16 µM for CBZ-E; 12, 65 and 140 µM for LIC; 12, 35 and 55 µM for LTG; 2, 10 and 20 µM for OXC; and 40, 55 and 75 µM for PHT.

III.2.2.5. Intracellular antiepileptic drugs accumulation assays

III.2.2.5.1. Identification of antiepileptic drugs/metabolites as P-glycoprotein substrates

Confluent and washed MDCK II and MDCK-MDR1 cells were incubated for 2 h with FBS-free DMEM medium, containing each AED or active metabolite. The AEDs and active metabolites were tested at therapeutic concentrations (50 µM for CBZ, 16 µM for CBZ-E, 140 µM for LIC, 55 µM for LTG, 20 µM for OXC and 75 µM for PHT) and were prepared in FBS-free DMEM (1% DMSO, v/v). After incubation, cells were washed and lysed as described above in s*ection III.2.2.4,* and

the total content of each well was collected individually and frozen at −20 °C until HPLC analysis.

III.2.2.5.2. Effects of flavonoid compounds on the intracellular accumulation of antiepileptic drugs/metabolites

The flavonoids identified as P-gp inhibitors [baicalein, (-)-EPG, kaempferol, quercetin and silymarin] were selected to evaluate their effects on the intracellular accumulation of each AED or active metabolite. For that, confluent and washed MDCK-MDR1 cells were pre-incubated for 30 min with FBS-free DMEM, in the presence of flavonoids or the positive control, verapamil. The flavonoids were tested at 200 µM and verapamil at 50 µM, all prepared in FBS-free DMEM (1% DMSO, v/v). Untreated control cells were exposed only to P-gp inhibitor vehicle (FBS-free DMEM) with the same percentage of DMSO (1%, v/v), in order to estimate the baseline level of intracellular AED/metabolite accumulation. Then, untreated and P-gp inhibitor treated cells were incubated with the AEDs or metabolites at the highest tested concentrations (CBZ 50 µM, CBZ-E 16 µM, LIC 140 µM, LTG 55 µM, OXC 20 µM and PHT 75 µM) for 2 h. After incubation, cells were washed and lysed as described above in s*ection III.2.2.4* and the total content of each well was collected separately and frozen at −20 °C until HPLC analysis.

III.2.2.6. HPLC analysis

The quantitative HPLC analysis of AEDs and their active metabolites was performed based on the methods previous reported by FERREIRA ET AL. (2016b, 2016c). For the determination of CBZ, CBZ-E, LIC, LTG and PHT in MDCK II or MDCK-MDR1 cell lysate, two HPLC methods were used after sample preparation by liquid-liquid extraction (LLE). Briefly, to each aliquot (200 µL) of 0.1% Triton X-100 samples were added 20 µL of the IS working solution, 300 µL of acetonitrile and 1 mL of ethyl acetate. The mixture was vortex-mixed for 30 s and centrifuged at 13500 rpm (3 min). Then, the sample was re-extracted twice more with ethyl acetate (1 mL each time) using the same conditions. The whole organic extract was evaporated to dryness under a nitrogen stream at 45 °C and then reconstituted with 100 µL of mobile phase. An aliquot (20 µL) of this final sample was injected into the HPLC system.

Chromatographic analysis was carried out using an HPLC system (Shimadzu LC-2010A HT Liquid Chromatography) coupled with a diode array detector (DAD; Shimadzu SPD-M20A). All instrumental parts were automatically controlled by LabSolutions software (Shimadzu, Kyoto, Japan). The chromatographic separation was carried out at 35 °C on a reversed-phase LiChroCART® Purospher Star column (C_{18}, 55 mm × 4 mm; 3 µm particle size) purchased from Merck KGaA (Darmstadt, Germany). For the determination of CBZ, CBZ-E, OXC and LIC an isocratic elution was applied at a flow rate of 1.0 mL/min with a mobile phase composed of water/methanol/acetonitrile (69:25:6, v/v/v), and PRM was used as IS (working solution at 500 µg/mL). The wavelength of 215 nm was selected for detection of all compounds. On the other hand, the chromatographic analysis of LTG and PHT was carried out using an isocratic elution

with acetonitrile (6%), methanol (25%) and a mixture (69%) of water–triethylamine (99.7:0.3, v/v; pH 6.0), pumped at 1 mL/min; in this case, CBZ was used as IS (working solution at 200 µg/mL). The compounds were detected at 215 nm (LTG and CBZ) and 235 nm (PHT). The mobile phases were filtered through a 0.2 µm filter and degassed ultrasonically for 15 min before use and the injected sample volume was always 20 µL.

III.2.2.7. Statistical analysis

Data were reported as mean ± standard error of the mean (SEM). The statistical analysis was performed using GraphPad Prism 5.0 (GraphPad Software, La Jolla, CA, USA.). The analysis of the effect of each treatment *versus* the control group was performed by one-way ANOVA with the *post hoc* Dunnett's test for multiple comparisons. To check for statistically significant differences of the effects produced by different concentrations of the same treatment a one-way ANOVA with the *post hoc* Tukey's test was performed. In some specific cases, a Student's *t*-test was applied to compare two groups. A difference was considered to be statistically significant for a *p*-value lower than 0.05 ($p < 0.05$). The statistical tests used were appropriately identified in the figure legends.

III.2.3. Results

III.2.3.1. Cytotoxicity assays

The effects of the different combinations of each flavonoid (or verapamil) with Rh123 on the cell viability was investigated during 4 h. As shown in Figure III.2.1, few flavonoid concentrations produced a statistically significant loss of cell viability when compared to the untreated control cells [fisetin, (+)-catechin and (-)-epicatechin at 200 µM; and silymarin and (-)-epicatechin at 100 µM], but without a very marked effect. It is worthy of note that the cytotoxic effect of verapamil at 50 µM was similar or higher than that observed with the highest tested concentration of flavonoids (200 µM). Actually, although this concentration of verapamil has been widely used in this kind of studies (Crivellato et al. 2002; Konsoula and Jung 2009; Jouan et al. 2016), and even in this cell line (Barthomeuf et al. 2005), the impact of 50 µM verapamil (positive control) on the cell viability was also tested herein, and a relatively high cell viability was found (82.6%). In turn, baicalein did not reduce cell viability, but appeared to slightly increase cell proliferation at 200 µM (Figure III.2.1).

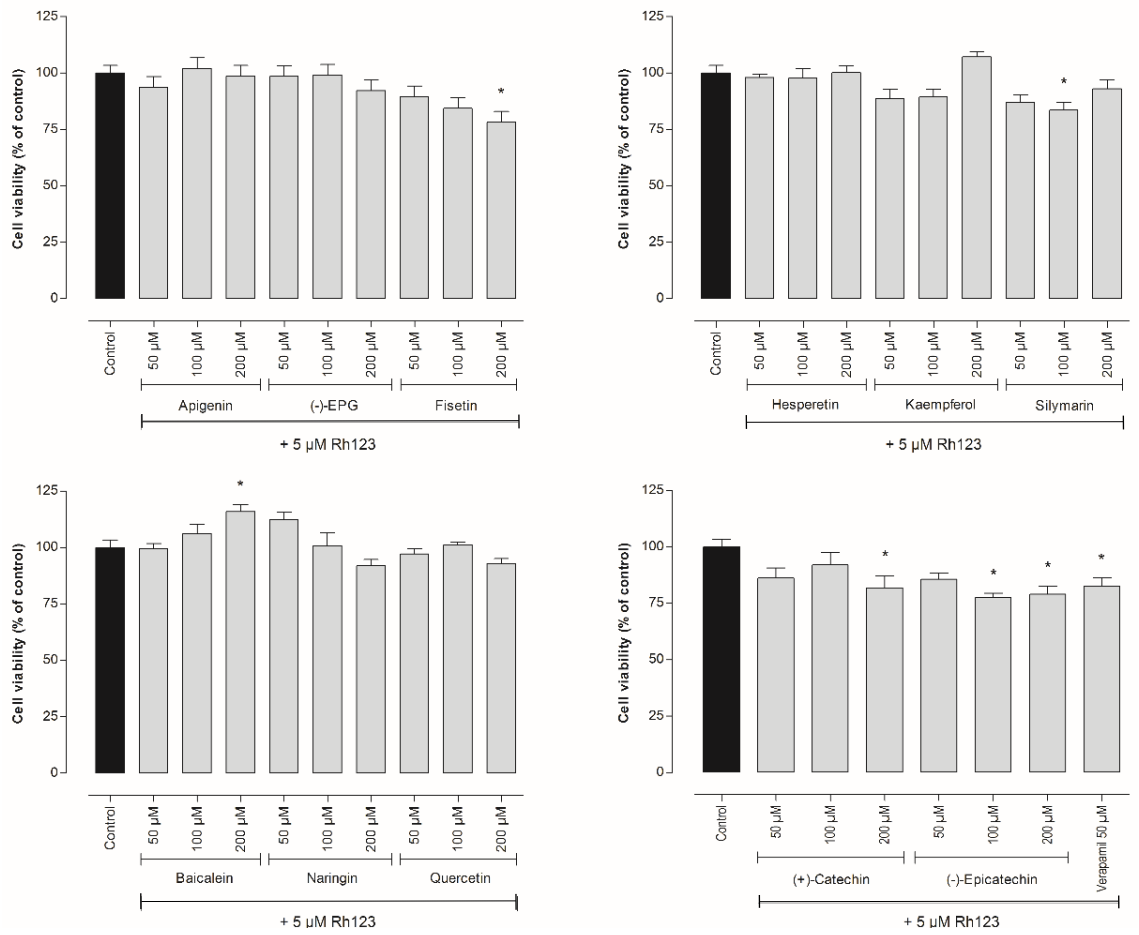

Figure III.2.1. Cell viability data for flavonoids or verapamil together with 5 µM rhodamine 123 (Rh123) after 4 h of incubation in MDCK-MDR1 cells. Data are expressed as the mean ± standard error of the mean (n = 6). Comparisons between treated cells *vs.* untreated control cells were performed by one-way ANOVA with the *post hoc* Dunnett's test ($^{*}p < 0.05$). (-)-EPG, (-)-epigallocatechin gallate.

Regarding the combination of AEDs or metabolites and Rh123 at 5 µM (Figure III.2.2), statistically significant differences in the reduction of cell viability were observed for OXC over the tested concentration range (2-20 µM) and also for LTG at the lower concentrations assayed (12 and 35 µM); however, no statistically significant cytotoxicity was found for LTG at 55 µM. In addition, analysing the data obtained on the cell viability for the three tested concentrations of LTG and OXC, no statistically significant differences were found ($p > 0.05$), supporting the use of the highest concentration levels of LTG and OXC in the following intracellular Rh123 accumulation studies.

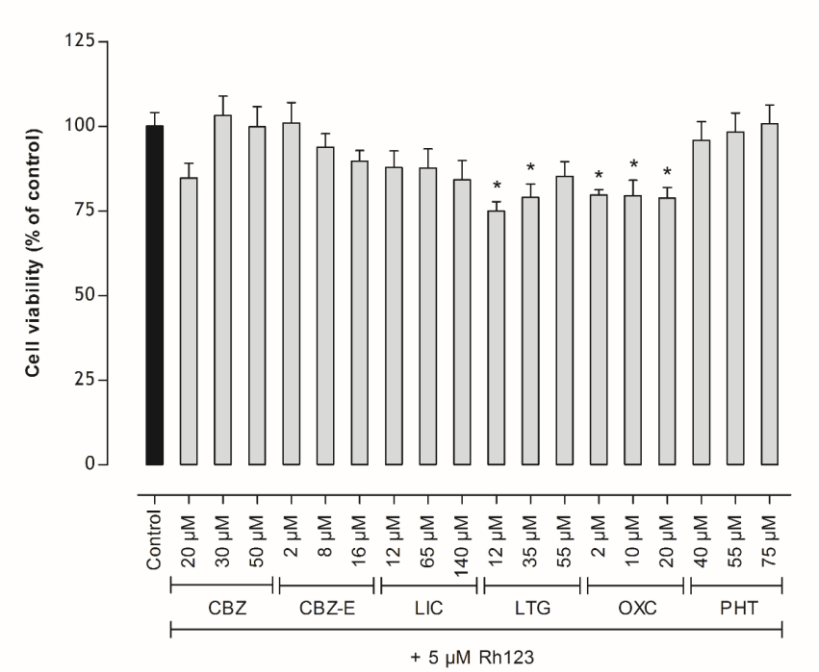

Figure III.2.2. Cell viability data for antiepileptic drugs (or metabolites) together with 5 µM rhodamine 123 (Rh123) after 4 h of incubation in MDCK-MDR1 cells. Data are expressed as the mean values ± standard error of the mean (n = 6). Comparisons between treated cells *vs.* untreated control cells were performed by one-way ANOVA with the *post hoc* Dunnett's test ($^{*}p < 0.05$). Comparisons among the data obtained for the three different tested concentrations of lamotrigine (LTG) and oxcarbazepine (OXC) were also carried out by one-way ANOVA with the *post hoc* Tukey's test ($p > 0.05$, no statistically significant differences were found). CBZ, carbamazepine; CBZ-E, carbamazepine-10,11-epoxide; LIC, licarbazepine; PHT, phenytoin.

Figure III.2.3 represents the data of cell viability obtained for each AED (or metabolite) alone and in combination with each one of the selected flavonoid compounds as P-gp inhibitors or verapamil. Overall, the AED (or metabolite)/flavonoid combinations appeared to originate no important cytotoxicity effects, which supports the use of these compound concentrations in the subsequent studies. Once again, in general, no marked loss of cell viability was promoted by the combinations of verapamil (50 µM) and AEDs or metabolites.

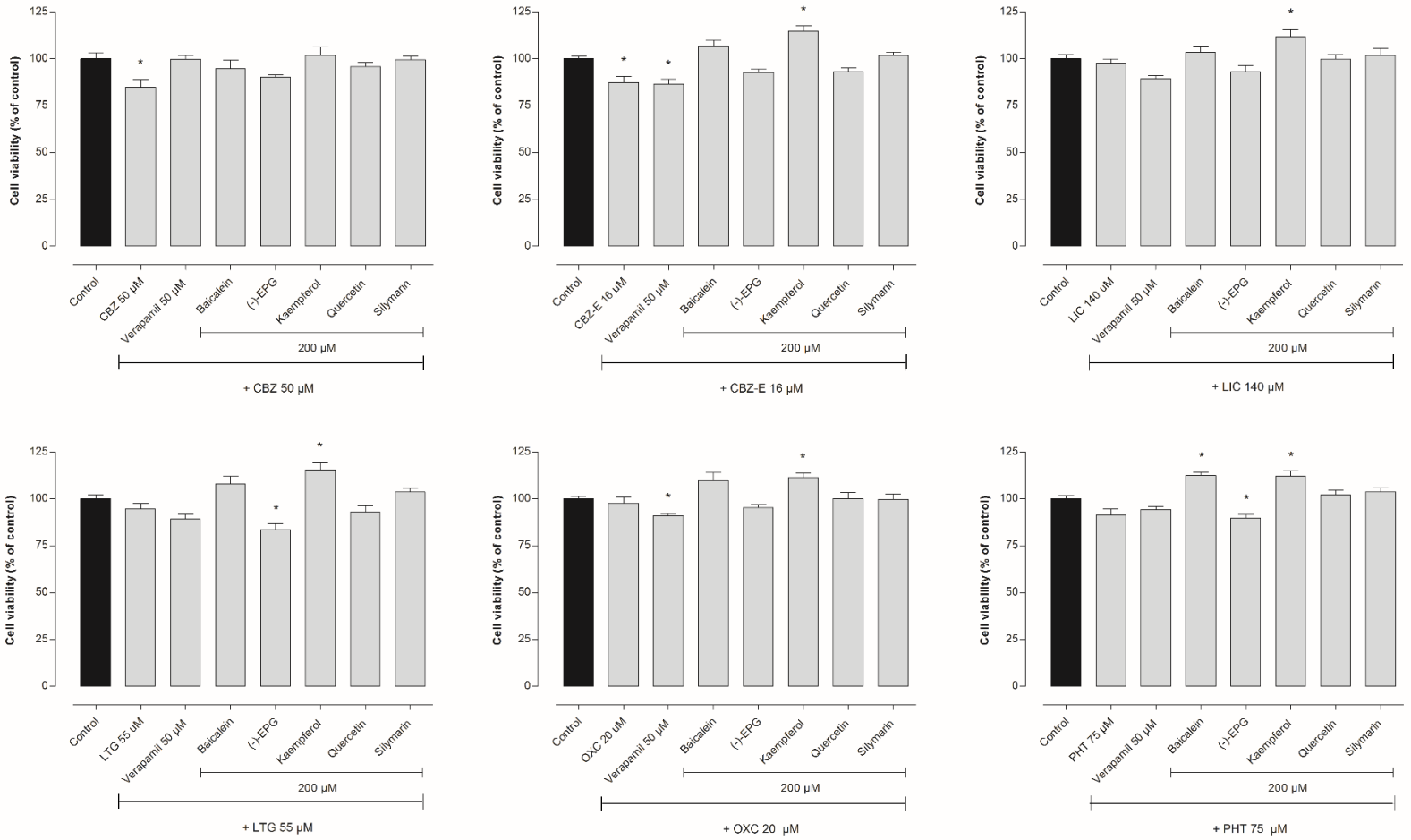

Figure III.2.3. Cell viability data for antiepileptic drugs (or metabolites) alone and together with verapamil or flavonoids after 4 h of incubation in MDCK-MDR1 cells. Data are expressed as the mean values ± standard error of the mean (n = 6). Comparisons between treated cells *vs.* untreated control cells were performed by one-way ANOVA with the *post hoc* Dunnett's test ($^{*}p < 0.05$). CBZ, carbamazepine; CBZ-E, carbamazepine-10,11-epoxide; (-)-EPG, (-)-epigallocatechin gallate; LIC, licarbazepine; LTG, lamotrigine; OXC, oxcarbazepine; PHT, phenytoin.

III.2.3.2. Identification of flavonoid compounds as P-glycoprotein inhibitors

According to the results depicted in Figure III.2.4, five [baicalein, (-)-EPG, kaempferol, quercetin and silymarin] of the eleven flavonoids induced a marked increase on the intracellular Rh123 accumulation in MDCK-MDR1 cells. The obtained results showed statistically significant differences in almost all the range of tested concentrations between flavonoid treated cells and untreated control cells (*p < 0.05), the last representing the baseline intracellular Rh123 accumulation (negative control). Moreover, as it can be seen in Figure III.2.4, the effects of baicalein, (-)-EPG, kaempferol, quercetin and silymarin on the intracellular Rh123 accumulation occurred in a concentration-dependent manner ($^{\#}p$ < 0.05). Actually, the Rh123 accumulation increases as the concentration of these five flavonoids increases (predictive of P-gp inhibition). Specifically, for the highest concentration of 200 μM, (-)-EPG produced an increase in the intracellular accumulation of Rh123 in a similar extent to that exhibited by verapamil (positive control as P-gp inhibitor). On the other hand, apigenin, (+)-catechin, (-)-epicatechin and fisetin decreased the intracellular accumulation of Rh123, suggesting to be inducers of the P-gp activity, whereas no effect was found for hesperetin and naringin.

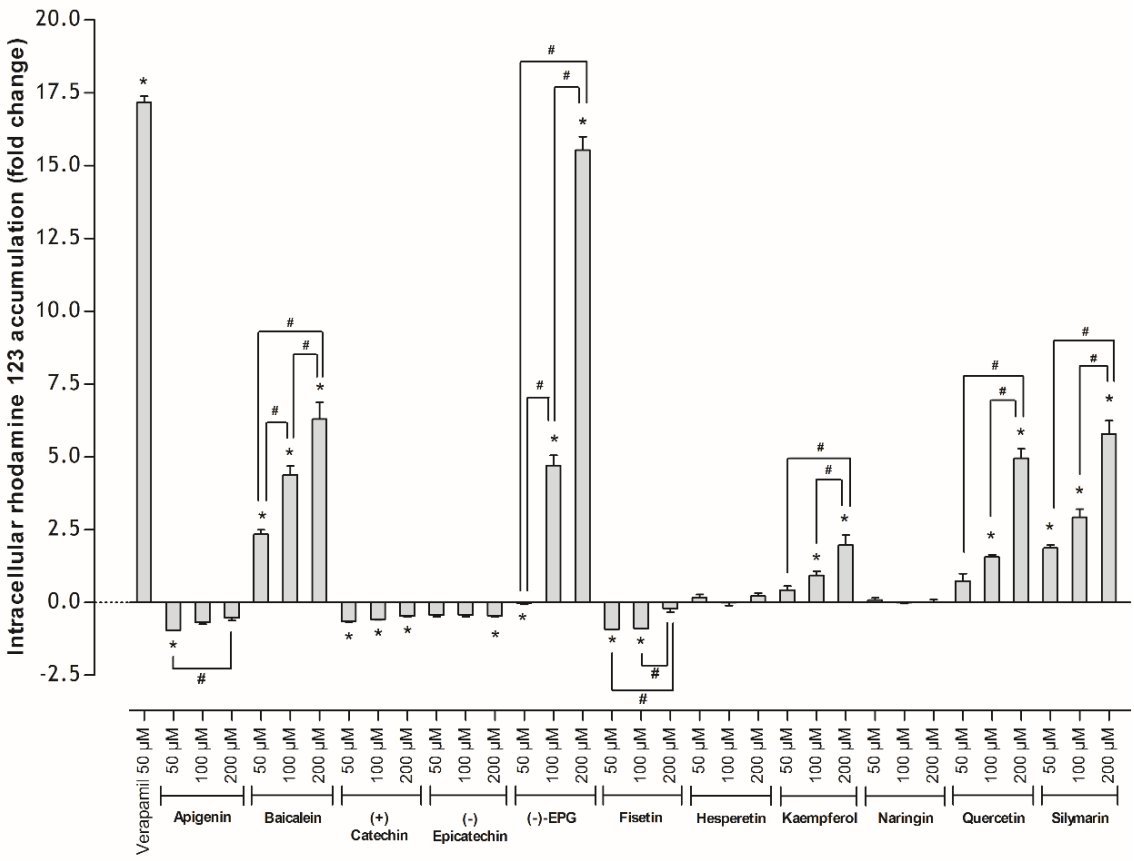

Figure III.2.4. Effect of flavonoids on the intracellular accumulation of rhodamine 123 (Rh123) in MDCK-MDR1 cells. The results were obtained by comparing the flavonoid (or verapamil) pretreated cells vs. untreated cells (control). Data are expressed as the mean values ± standard error of the mean (n = 6). The basal intracellular accumulation of Rh123 in the control group was 0.0097 ± 0.0026 μM. Comparisons between flavonoids/verapamil group *vs.* control group were performed by one-way ANOVA with the *post hoc* Dunnett's test ($^{*}p$ < 0.05). Comparisons among the different concentrations of flavonoids were performed by one-way ANOVA with the *post hoc* Tukey's test ($^{\#}p$ < 0.05). (-)-EPG, (-)-epigallocatechin gallate.

Taking into account the aforementioned results, the highest concentration (200 μM) of baicalein, (-)-EPG, kaempferol, quercetin and silymarin was selected to be evaluated in the subsequent experiments involving the combination with AEDs or their active metabolites.

III.2.3.3. Identification of antiepileptic drugs/metabolites as inducers of P-glycoprotein activity

Although with different magnitudes, the AEDs or metabolites, with the exception of CBZ-E and OXC at 2 μM, promoted a statistically significant decrease in the accumulation of Rh123 into MDCK-MDR1 cells, appearing to exhibit an inducer effect on the P-gp activity (Figure III.2.5). Overall, it is noteworthy the concentration-dependent effect found for OXC on the intracellular accumulation of Rh123, which significantly decreases as the concentration of OXC increases ($^{\#}p < 0.05$). In contrast to OXC, no statistically significant difference was detected among the different concentrations of the other AEDs or metabolites tested.

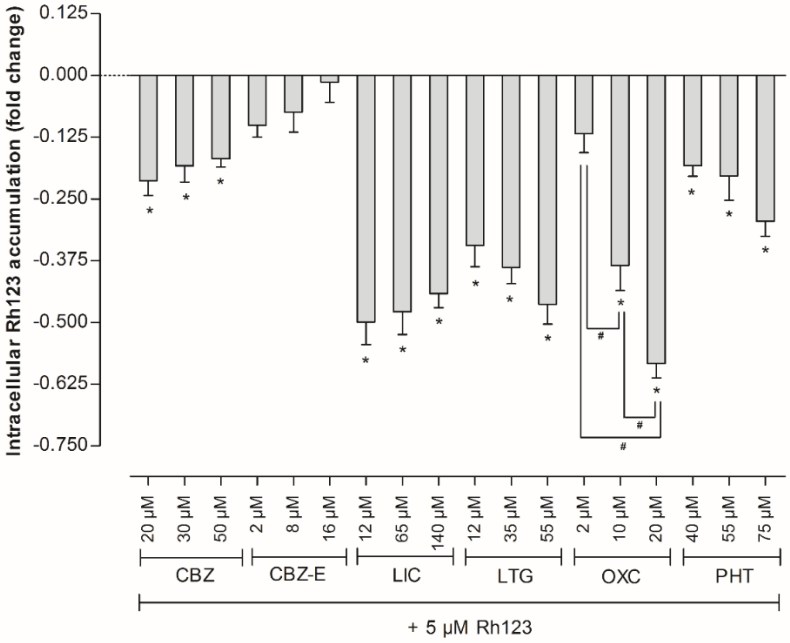

Figure III.2.5. Identification of P-glycoprotein inducers among the antiepileptic's/metabolites through rhodamine 123 (Rh123) accumulation assays performed in MDCK-MDR1 cells. The results were obtained by comparing the intracellular Rh123 accumulation in antiepileptic drugs (AEDs) or metabolites pretreated cells vs. untreated cells (control). Data are expressed as the mean values ± standard error of the mean (n = 6). The basal intracellular accumulation of Rh123 in the control group was 0.0091 ± 0.0016 μM. Comparisons between AEDs/metabolite group *vs.* control group were performed by one-way ANOVA with the *post hoc* Dunnett's test ($^{*}p < 0.05$). Comparisons among the different concentrations of AEDs/metabolites were performed by one-way ANOVA with the *post hoc* Tukey's test ($^{\#}p < 0.05$). CBZ, carbamazepine; CBZ-E, carbamazepine-10,11-epoxide; (-)-EPG, (-)-epigallocatechin gallate; LIC, licarbazepine; LTG, lamotrigine; OXC, oxcarbazepine; PHT, phenytoin.

III.2.3.4. Identification of antiepileptic drugs/metabolites as P-glycoprotein substrates

The intracellular accumulation of the AEDs or metabolites was compared in MDCK II cells and those overexpressing the P-gp, MDCK-MDR1 cells. Taking into account the results presented in Figure III.2.6, the intracellular accumulation of CBZ (p = 0.0011), CBZ-E (p = 0.0254), LIC (p = 0.0060) and PHT (p = 0.0071) was 1.2 to 1.5 times higher in MDCK II than in MDCK-MDR1 cells. Nevertheless, the degree of intracellular accumulation of OXC was very much steeper in MDCK II (a 16-fold increase) than in MDCK-MDR1 cells (p = 0.0003). On the contrary, no relevant differences were observed in the intracellular accumulation of LTG between the two cell lines. Contrarily to the LTG, the lower intracellular accumulation of CBZ, CBZ-E, LIC, OXC and PHT in the MDCK-MDR1 cells than in MDCK II cells indicates that these AEDs and metabolites are P-gp substrates in this cell model.

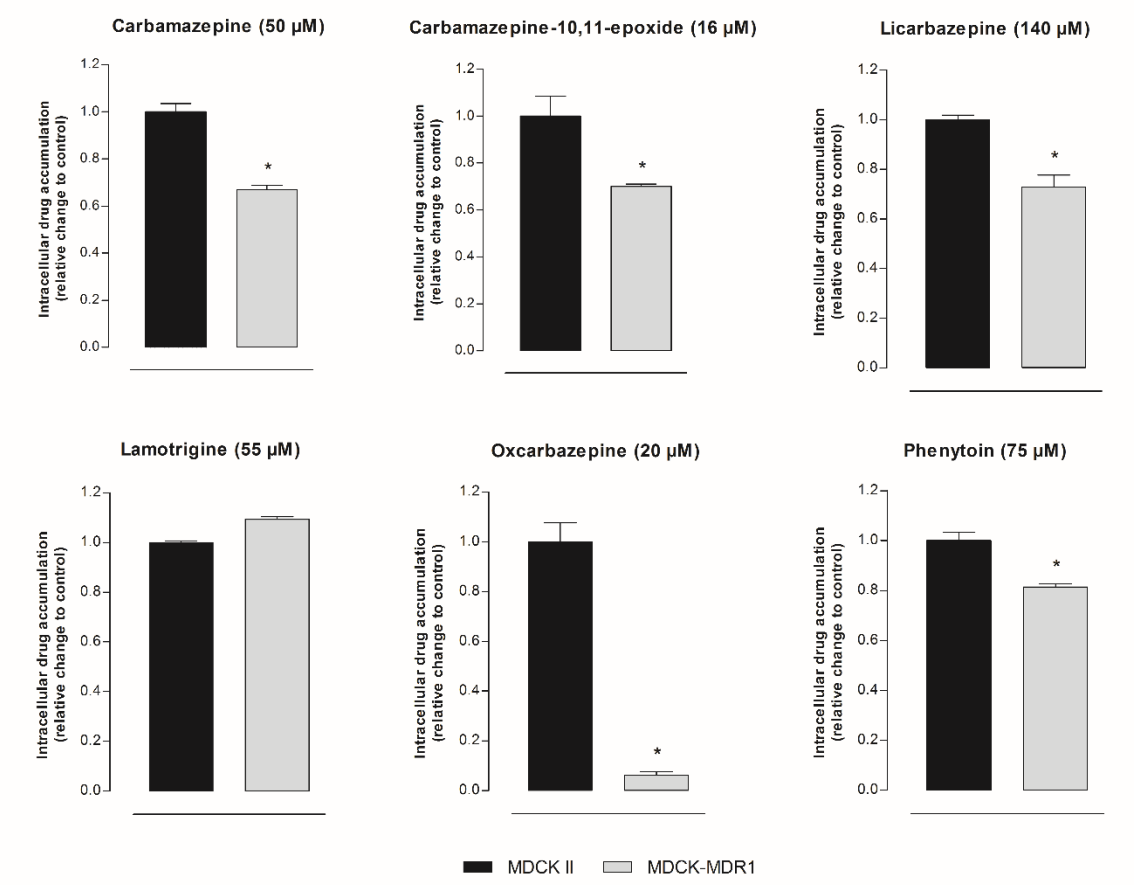

Figure III.2.6. Comparison of the intracellular accumulation of antiepileptic drugs/metabolites between MDCK II and MDCK-MDR1 cells. Data are expressed as the mean values ± standard error of the mean (n = 3). Comparisons between MDCK II *vs.* MDCK-MDR1 group were performed by Student's t-test. $^{*}p < 0.05$, compared to control group (MDCK II cell line).

III.2.3.5. Effects of flavonoid compounds on the intracellular accumulation of antiepileptic drugs/metabolites

In these set of studies, the concentrations used for each of the AEDs and metabolites correspond to values of the highest part of the therapeutic range (PATSALOS ET AL. 2008; HOYLAND ET AL. 2013), and the most promising flavonoids as P-gp inhibitors were tested at 200 μM. According to the results shown in Figure III.2.7, the majority of flavonoids significantly increased the intracellular accumulation of the AEDs and their active metabolites in MDCK-MRD1 cells comparatively to the untreated control cells ($p < 0.05$). LTG was the unique compound, among the AEDs and metabolites, for which intracellular accumulation was not affected by any of the flavonoids (Figure III.2.7). Overall, silymarin was the flavonoid compound that most increased the AED/metabolite accumulation, suggesting being the most promising flavonoid as P-gp inhibitor. Actually, in some of the cases, the effect of silymarin on the intracellular accumulation of AEDs/metabolites was very close to that produced by verapamil. In opposition, kaempferol was the flavonoid that less increased the intracellular accumulation of AEDs/metabolites. Regarding LTG, the results obtained are in accordance with the fact that this drug has not been identified as P-gp substrate in MDCK-MDR1 cells. Thus, as expected, the flavonoids did not substantially affect the intracellular accumulation of LTG into MDCK-MDR1 cells.

III.2.4. Discussion

The research of new therapeutic options continues to be pursued in order to overpass the pharmacoresistance in epilepsy. The recognition of P-gp as a major factor responsible for drug resistance that may restrict the penetration or accumulation of AEDs into the epileptic brain tissue has increased the demand for P-gp inhibitors that could enhance the AEDs concentration in the site of action (ROBEY ET AL. 2008; ZHANG ET AL. 2012a; LÖSCHER ET AL. 2013). These efforts are particularly justified by the fact that this glycoprotein is overexpressed in patients with drug-resistant epilepsy, who are resistant to several, if not all, AEDs despite their different mechanisms of action. Moreover, evidence has been reported documenting the inducer effects of AEDs on the P-gp activity. All these findings support the transporter hypothesis of AED-resistant epilepsy and emphasize the potential of P-gp inhibitors in an attempt to reverse this drug resistance phenomenon (LUNA-TORTÓS ET AL. 2008; ZHANG ET AL. 2012a; GIDAL 2014).

Bearing in mind this possible therapeutic approach, the current study had as a starting point the evaluation of the potential of a series of flavonoids to inhibit the P-gp. According to our results, five flavonoids [baicalein, (-)-EPG, kaempferol, quercetin and silymarin] were identified as the most promising P-gp inhibitors due to their ability to increase the intracellular accumulation of Rh123 in MDCK-MRD1 cells. Although we expected to find some flavonoid compounds capable of inhibiting P-gp, the increase on the intracellular accumulation of Rh123

promoted by (-)-EPG was truly remarkable at 200 μM (a 16-fold increase), a similar effect to that found for verapamil, the standard P-gp inhibitor (Figure III.2.4).

The exact mechanisms underlying flavonoid–P-gp interactions are not yet clear. Nevertheless, several hypotheses have been proposed: (1) flavonoids can directly bind to the C-terminal nucleotide-binding domain of P-gp (NBD2) and modulate P-gp by interacting in a bifunctional way with the vicinal ATP-binding site and the steroid binding site within a cytosolic domain of P-gp (chrysin, flavone, quercetin, rutin, apigenin, 3-hydroxyflavone, genistein, kaempferide, and kaempferol) (CONSEIL ET AL. 1998); (2) flavonoids can act as substrate and may directly interact with P-gp either by competitive binding to the substrate-binding site or by binding to other drug-binding sites and changing the P-gp conformation [genistein, epicatechin gallate, catechin gallate, (-)-EPG and silymarin] (CASTRO AND ALTENBERG 1997; SHAPIRO AND LING 1997; JODOIN ET AL. 2002; ZHANG AND MORRIS 2003b); and (3) flavonoids may bind to an allosteric site (epicatechin) (WANG ET AL. 2002). It is worthy to mention that in our studies the inhibitory activity of baicalein, (-)-EPG, kaempferol, quercetin and silymarin appeared to be concentration-dependent, increasing with flavonoids concentrations. These results are in accordance with the literature (FERREIRA ET AL. 2015).

In addition, other pharmacological properties that have been exhibited by flavonoid compounds can also contribute to enhance the interest in these agents to reverse the AED-resistant epilepsy. Indeed, the potential of flavonoids as antiepileptic/anticonvulsant drugs has been widely debated. For instance, baicalein (YOON ET AL. 2011) and quercetin (BALUCHNEJADMOJARAD ET AL. 2010; NASSIRI-ASL ET AL. 2013; NASSIRI-ASL ET AL. 2014) demonstrated some anticonvulsant activity in rodent models of acute and chronic seizures. However, as regards the (-)-EPG, kaempferol and silymarin, to the best of our knowledge, no data are available in the literature concerning their anticonvulsant activity. Furthermore, the therapeutic potential of flavonoid compounds for frequent epilepsy comorbidities, due to their activity on cognition and neurodegeneration, inflammation and depression, emphasizes, even more, the interest in these multi-target compounds for complex central nervous system (CNS) disorders such as epilepsy. Particularly, quercetin demonstrated to have neuroprotective effects on hippocampal injury post status epilepticus (HU ET AL. 2011), whereas baicalein evidenced a protective role against global ischemia (ROMANO ET AL. 2013). Moreover, quercetin demonstrated to inhibit both cyclooxygenase and lipoxygenase activities, diminishing the formation of inflammatory mediators. Additionally, flavonoids also appear to inhibit eicosanoid biosynthesis, such as cytosolic and membrane tyrosine kinase, and neutrophil degranulation (NIJVELDT ET AL. 2001). Some flavonoids like quercetin and kaempferol also revealed antidepressant activity thorough their effects by the stimulation of brain-derived neurotrophic factor and the reduction of Aß toxicity (HOU ET AL. 2010).

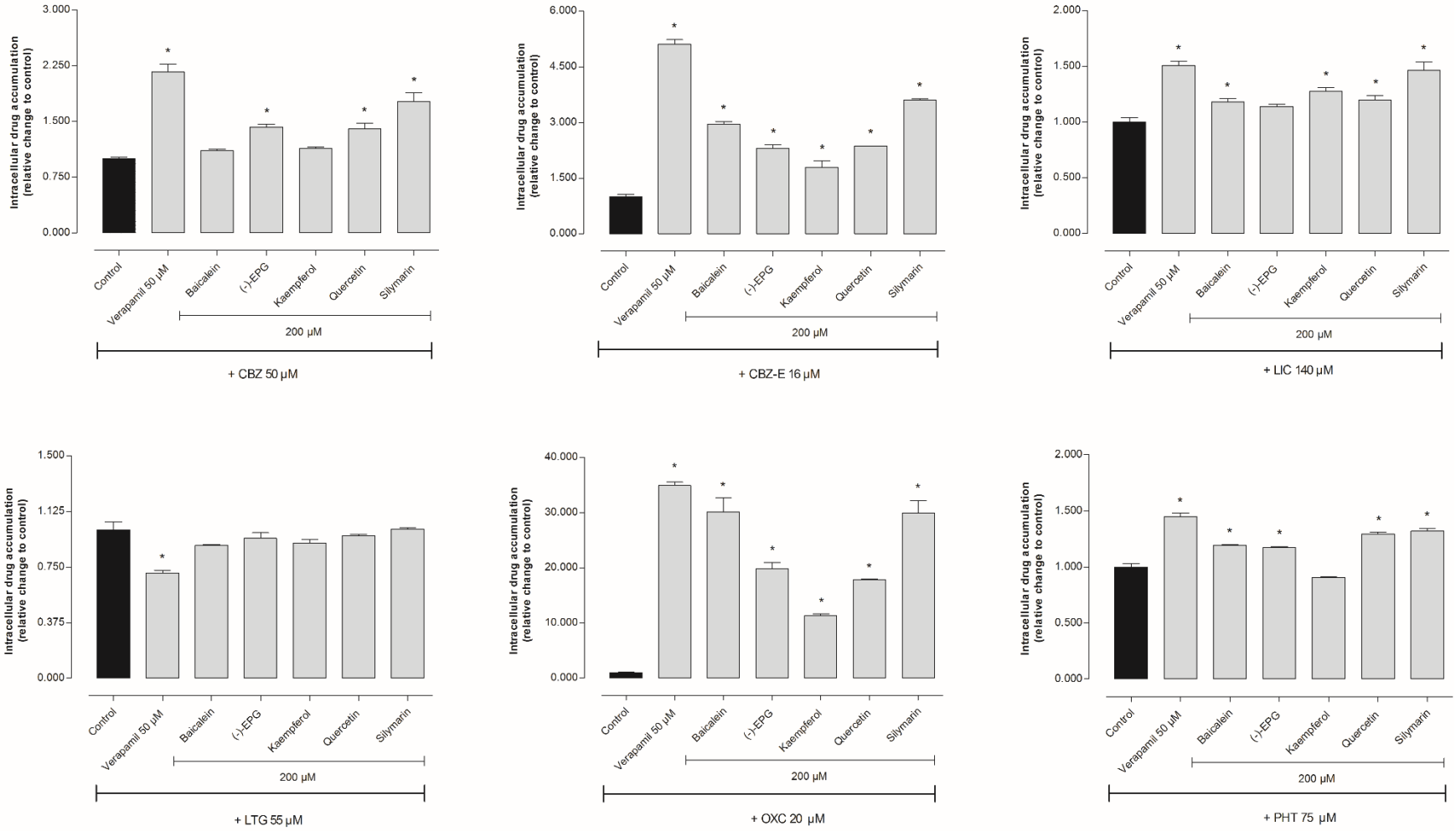

Figure III.2.7. Effect of selected flavonoid compounds or verapamil in the intracellular accumulation of antiepileptic drugs/metabolites in MDCK-MDR1 cells. Data are expressed as the mean values ± standard error of the mean (n = 3). Comparisons between flavonoids and verapamil groups vs. control (basal drug accumulation) group were performed by one-way ANOVA with the post hoc Dunnett's test. *p < 0.05, compared to control group. CBZ, carbamazepine; CBZ-E, carbamazepine-10,11-epoxide; (-)-EPG, (-)-epigallocatechin gallate; LIC, licarbazepine; LTG, lamotrigine; OXC, oxcarbazepine; PHT, phenytoin.

Although there are studies reporting some AEDs as P-gp substrates, herein this point was also investigated, using MDCK II and MDCK-MDR1 cells, because there is still no consensus on this subject (ZHANG ET AL. 2012a). Taking into account our results, only the LTG did not demonstrated to be a P-gp substrate in MDCK-MDR1 cell model; in contrast, OXC appears to have been subjected to a strong P-gp–mediated efflux transport (Figure III.2.6). According to the results of other *in vitro* and *in vivo* studies, including clinical trials, the AEDs as LTG, PHT and OXC are classified as definite P-gp substrates, while CBZ, CBZ-E and S-LIC are classified only as probable P-gp substrates as deeply reviewed by ZHANG ET AL. (2012a). The main divergence between our results and those of the literature involves the LTG, which has not yet been investigated in MDCK-MDR1 cells; however, LTG previously demonstrated to be a P-gp substrate in LLC-PK1-MDR1 and OS2.4/Doxo cells, but not in the Caco-2 cell line (ZHANG ET AL. 2012a). According to an *in vitro* transportation study performed by ZHANG ET AL. (2011), the CBZ analogues (eslicarbazepine acetate, OXC, S-LIC and CBZ-E) demonstrated to be P-gp substrates. Indeed, there are few *in vitro* studies in the literature evaluating OXC as P-gp substrate but, in this particular one, OXC exhibited a higher P-gp–mediated transport level than its derivatives (except for the eslicarbazepine acetate) (ZHANG ET AL. 2011a). Although there are available some studies which evaluated the structure-activity relationship of multiple P-gp substrates (EKINS ET AL. 2002; WANG ET AL. 2003; RAUB 2006), the reports analysing the structure-activity relationship regarding the interactions between AEDs and P-gp are highly limited (KNIGHT AND WEAVER 1998). Nevertheless, CBZ as well as its analogues have the identical dibenzazepine (iminostilbene) nucleus, differing at the 10,11-position. Actually, this planar structure is reported to be very important for the interaction with P-gp (FERREIRA ET AL. 2015). Consequently, the ketone group exhibited by OXC at the 10,11-position can be responsible for the higher affinity evidenced by OXC for the P-gp when comparing to CBZ and its structural analogues (Figure III.2.6).

After identifying the most promising flavonoids as P-gp inhibitors, and classifying the AEDs and their active metabolites as P-gp substrates or not in MDCK-MDR1 cells, the potential of the flavonoids to increase the intracellular accumulation of the AEDs was also herein assessed. Although with different degrees of potency, almost all the selected flavonoids [baicalein, (-)-EPG, kaempferol, quercetin and silymarin] demonstrated to enhance the intracellular accumulation of AEDs or their active metabolites into MDCK-MDR1 cells. As expected, only the intracellular accumulation of LTG was not changed in the presence of flavonoids once it does not appear to be a P-gp substrate (Figure III.2.7). The extremely high effect produced by the tested flavonoids and verapamil in the intracellular OXC accumulation is in accordance with its profile as P-gp substrate. Actually, other studies have demonstrated that huge differences observed in the OXC transportation in MDCK-MDR1-transfected and LLC-PK1-MDR1-transfected *versus* non-transfected cells were almost completely nullified by verapamil and tariquidar, both P-gp inhibitors (ZHANG ET AL. 2011a). Indeed, the positive effect on the OXC bioavailability promoted by verapamil was also reported in healthy volunteers (ANTUNES ET AL. 2016).

The set of tested flavonoid compounds did not seem to importantly compromise the cell viability. This is important when remembering that the first- and second-generation P-gp

inhibitors are associated with severe toxicity at the concentrations necessary to significantly inhibit the P-gp (KRISHNA AND MAYER 2000; DANTZIG ET AL. 2003; VARMA 2003; CHUNG ET AL. 2005; HENNESSY AND SPIERS 2007; BANSAL ET AL. 2009; COREA ET AL. 2009; POTSCHKA 2012). Moreover, several flavonoid preparations are already found on the market as herbal medicines, or dietary supplements, alleged without nontoxic effects. A variety of flavonoid-containing dietary supplements and herbal products are nowadays marketed for their antioxidant, anticarcinogenic, anti-inflammatory, antiproliferative, antiangiogenic and antiestrogenic (or estrogenic) effects, with no evidence of toxicity (BANSAL ET AL. 2009; FERREIRA ET AL. 2015). Additionally, in some animal studies flavonoid compounds have revealed a weak potential of toxicity. Notwithstanding, to document the clinical value of these compounds as P-gp inhibitors capable of reversing the drug-resistant epilepsy requires the conduction of well-designed clinical trials.

In addition to the identification of the AEDs/metabolites as P-gp substrates, the recognition of AEDs as P-gp inducers also highlights the importance of this strategy to reverse the drug resistance mediated by the P-gp. In fact, the investigated AEDs and their active metabolites induced the P-gp activity (herein assessed by the decrease in intracellular Rh123 accumulation; Figure III.2.5). Hence, besides our recognition that all the AEDs tested, exception for CBZ-E, had an inducer effect on the P-gp activity, the existing literature is not extensive regarding the characterization of these compounds as P-gp inducers. In the literature, only PHT and CBZ are particularly recognised as P-gp inducers (GEICK ET AL. 2001; GIESSMANN ET AL. 2004; LÜ ET AL. 2004; OWEN ET AL. 2006; CHHUN ET AL. 2009; U.S. FOOD AND DRUG ADMINISTRATION 2011; AKAMINE ET AL. 2012). In conclusion, this strategy of coadministration of AEDs with safe and potent P-gp inhibitors should continue to be exploited to reverse the pharmacoresistance in epilepsy and flavonoids such as baicalein, (-)-EPG, kaempferol, quercetin and silymarin can be promising drug candidates as adjuvant therapy for refractory epilepsy.

III.3. Experimental

Synergic effects of dual flavonoid combinations for reversing P-glycoprotein-mediated multidrug resistance: focus on phenytoin, carbamazepine, oxcarbazepine and their active metabolites

III.3.1. Introduction

Flavonoids are a diverse group of herbal pigments found in almost all fruits and vegetables, constituting an important class of polyphenol phytonutrients present in the human diet. Structurally, flavonoid compounds are benzo-γ-pyrone derivatives and they can be divided into six major subclasses, namely anthocyanins, flavanols or catechins, flavanones, flavones, flavonols and isoflavones (Ferreira et al. 2015; Cassidy and Minihane 2016). The structural chemical diversity presented by flavonoids is certainly responsible for their wide range of bioactivities, including anti-inflammatory, antiproliferative, pro-apoptotic, free-radical scavenging, antioxidant, antitumoral, antimicrobial, antiviral, hormonal and anticonvulsant properties (Baluchnejadmojarad et al. 2010; Buer et al. 2010; Yoon et al. 2011; Wasowski and Marder 2012; Nassiri-Asl et al. 2013; Nassiri-Asl et al. 2014; Hoensch and Oertel 2015).

Nowadays, with the resurgence of the use of medicinal herbs in the Western world, it has become increasingly more common the combined use of modern and traditional therapies (Pathak and Udupa 2010; Ekor 2014; Newman and Cragg 2016). Indeed, the exploitation of potentially beneficial interactions between dietary supplements and drugs could be a valuable strategy in certain circumstances, including to overcome some mechanisms of multidrug resistance (Boumendjel et al. 2002; Thomas and Coley 2003; Peng et al. 2006; Bansal et al. 2008; Pathak and Udupa 2010). The overexpression of multidrug efflux transporters in the cell membrane, such as the P-gp, is one of the major pathomechanisms underlying the resistance against a variety of chemically unrelated drugs, as is the case of AEDs (Breier et al. 2013; Xiong et al. 2015; Wang et al. 2016; Chen et al. 2016). Consequently, the use of inhibitors of these drug efflux transporters could help to overcome the P-gp–mediated drug resistance, resulting in a more cost-effective therapy (Peng et al. 2006; Amin 2013).

Over the last decade, several herbal constituents, including flavonoids, have gained much attention as effective and safe compounds in reversing the P-gp–mediated multidrug resistance (Bansal et al. 2009; Schinkel and Jonker 2012; Abdallah et al. 2015; Ferreira et al. 2015; Mohana et al. 2016). In fact, there is a large amount of studies, not only *in vitro* but also *in vivo*, describing flavonoid compounds as potential P-gp inhibitors (Ferreira et al. 2015). The P-gp inhibitory effect produced by some flavonoids appears to be comparable to those of classic P-gp inhibitors, like verapamil and cyclosporine A, showing additionally a more favorable safety profile (Bansal et al. 2009; Abdallah et al. 2015; Ferreira et al. 2015; Mohana et al. 2016).

The search for compounds of herbal origin as a new category of P-gp inhibitors is a consequence of the disappointing results achieved with the first, second and third-generations of synthetic P-gp inhibitors. On one hand, P-gp inhibitors of first and second-generations require high concentrations to substantially inhibit P-gp, which are associated with severe toxicity; this is explained by their low potency and affinity as well as selectivity towards P-gp (Bansal et al. 2009; Palmeira et al. 2012; Potschka 2012; Ferreira et al. 2015). On the other hand, the third-generation P-gp inhibitors as biricodar, elacridar, laniquidar, tariquidar or zosuquidar, although promising in some clinical trials, they ended up evidencing undesirable side effects in non-

target organs (BANSAL ET AL. 2009). Thus, all the aforementioned aspects have further triggered the interest in flavonoids during the research of selective and non-cytotoxic P-gp inhibitors (BANSAL ET AL. 2008; BANSAL ET AL. 2009; FERREIRA ET AL. 2015).

The synergic pharmacological potential of flavonoids cannot be ignored taking into account that highly complex mixtures of flavonoid compounds are abundantly found in our daily diet (HARASSTANI ET AL. 2010; CHOI ET AL. 2013; YU ET AL. 2013; JARAMILLO-CARMONA ET AL. 2014). In this context, the study of flavonoid combinations regarding their P-gp inhibitory activity is fully justified. Indeed, this could be a valuable strategy to decrease the effective concentration of a single P-gp inhibitor, avoiding potential side effects and enhancing their value against the multidrug resistance mediated by P-gp. The fact that there are multiple binding sites for substrates and inhibitors on P-gp also highlights the potential of the combination of different flavonoids as P-gp inhibitors (YANG AND LIU 2004). In the chemotherapy field, for example, the combined chemosensitization with classic P-gp inhibitors (verapamil and quinine) demonstrated to increase the accumulation and retention of anthracycline in the resistant cells to a greater extent, proving to be a potentially useful approach for overcoming multidrug resistance in cancer (LEHNERT ET AL. 1991).

In the path to develop a strategy capable of reversing the P-gp interference in the brain delivery of CNS-active drugs, including AEDs, we aimed to explore whether the combined use of flavonoids would be more promising than their individual use. In this work, the MDCK-MDR1 cells were used for the identification of the most promising flavonoid combinations as P-gp inhibitors. This approach was tested targeting AEDs and their pharmacologically active metabolites widely recognized as P-gp substrates, namely CBZ, PHT, OXC, and their active metabolites, CBZ-E (main CBZ active metabolite) and LIC (main OXC active metabolite).

III.3.2. Experimental section

III.3.2.1. Reagents

CBZ, CBZ-E, PHT, OXC, baicalein, quercetin, silymarin, verapamil (a P-gp reference inhibitor, used as positive control), Rh123 (a P-gp fluorescent probe substrate) and PRM (used as IS in chromatographic analysis) were purchased from Sigma–Aldrich (St Louis, MO, USA). Silymarin is composed of silybinin, silydianin and silychristin (Figure III.3.1), and the molar concentration was calculated based on the molecular weight of silybinin because this is the main flavonoid component present (ZHANG AND MORRIS 2003a; ZHANG AND MORRIS 2003b). (-)-EPG and kaempferol were obtained from Santa Cruz Biotechnology (Heidelberg, Germany). LIC was supplied by Tocris Bioscience (Bristol, United Kingdom). All cell culture reagents including DMEM, FBS, penicillin, streptomycin, DMSO, trypsin-EDTA and PBS were acquired from Sigma-Aldrich (St Louis, MO, USA). Methanol and acetonitrile, both of HPLC gradient grade, were purchased from Fisher Scientific (Leicestershire, United Kingdom) and the ultra-pure water (HPLC grade,

>18 MΩ.cm) was prepared by means of a Milli-Q water apparatus from Millipore (Milford, MA, USA). Ethyl acetate were purchased from Fisher Scientific (Leicestershire, United Kingdom).

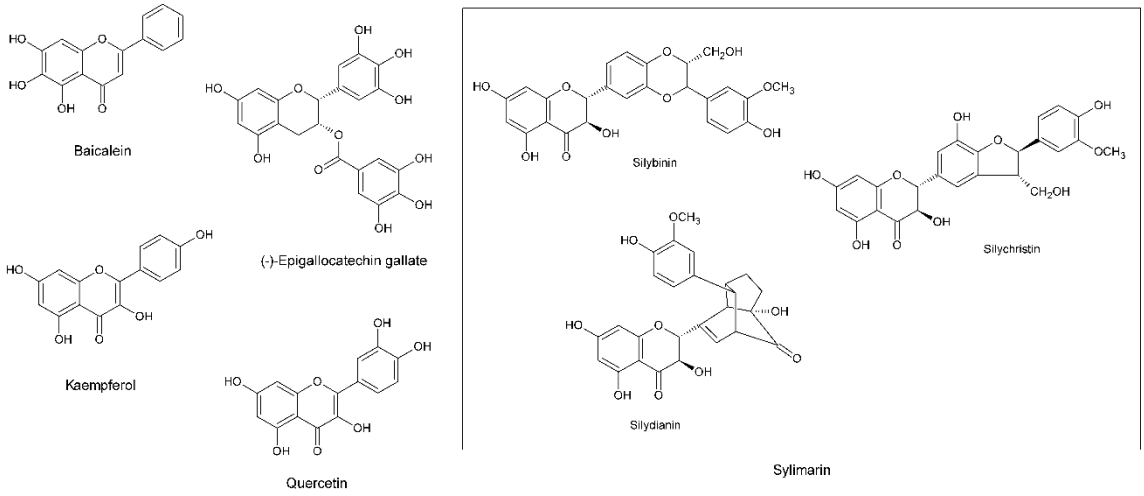

Figure III.3.1. Chemical structures of baicalein, (-)-epigallocatechin gallate, kaempferol and quercetin and of some constituents of the flavonoid silymarin (PUBCHEM COUMPOUND DATABASE; FERREIRA ET AL. 2015).

III.3.2.2. Cell culture

MDCK-MDR1 cells were obtained from The Netherlands Cancer Institute (NKI-AVL; Amsterdam, Netherlands). Cultures of MDCK-MDR1 cells (passages 22-38) were maintained as monolayers in 75 cm^2 culture flasks in DMEM supplemented with 10% FBS, 100 IU/mL penicillin and 100 µg/mL streptomycin. The cells were grown at 37 °C in a humidified air incubator with 5% CO_2 and the medium was renewed every 2-3 days. Cells were seeded (density of 7.9 x 10^4 cells/cm^2) in 96-well plates for Rh123 accumulation assays and in 24-well plates for the AEDs/metabolites accumulation assays, and cultured for 4 days at 37 °C in an atmosphere of 5% CO_2 before being used in the previously mentioned experiments. Both the Rh123 and AEDs/metabolites accumulation assays were performed based on the work of BARTHOMEUF ET AL. (2005) with some modifications.

III.3.2.3. Rhodamine 123 accumulation assays

At confluence, cells were washed once with PBS (150 mM NaCl, 2.7 mM KCl, 1.3 mM KH_2PO_4, 8.1 mM Na_2HPO_4, pH 7.4) at 37 °C. Then, the cells were pre-incubated for 30 min with FBS-free DMEM medium containing the test compounds as described in the following subsections. Subsequently, 5 µM Rh123, prepared in FBS-free DMEM medium (1% DMSO, v/v), was added to each well for 2 h. In both the phases, the cells were maintained at 37 °C in an atmosphere containing 5% CO_2. Finally, the cells were washed three times with cold PBS in order to stop the Rh123 accumulation, and then the cells were lysed with 100 µL 0.1% Triton X-100 at room temperature for 30 min. The fluorescence of cell lysates was measured with a SpectraMax Gemini spectrofluorometer (Molecular Devices) at the wavelengths of 485 nm (excitation) and

538 nm (emission). Untreated control cells, exposed only to the test compound vehicle (FBS-free DMEM medium) with the same percentage of DMSO (1%, v/v) were also incubated with 5 μM Rh123 in order to estimate the baseline levels of intracellular Rh123 accumulation. A Rh123 standard curve (0.00625-5 μM) was generated to quantify the total amount of Rh123 accumulated in each sample.

III.3.2.3.1. Concentration-response curves for individual flavonoids in the intracellular accumulation of rhodamine 123

MDCK-MDR1 cells were pre-incubated for 30 min with FBS-free DMEM medium in the presence of increasing concentrations of baicalein, (-)-EPG, kaempferol, quercetin or silymarin. All the flavonoids were prepared in FBS-free DMEM medium (1% DMSO, v/v). Half maximal effective concentration (EC_{50}) values (the concentration of flavonoid originating 50% of its maximum effect in Rh123 accumulation) were calculated using sigmoidal dose-response (variable slope) fit, with the bottom parameter constant and equal to 1 (GraphPad Prism).

III.3.2.3.2. Concentration-response curves for dual combinations of flavonoids in the intracellular accumulation of rhodamine 123.

MDCK-MDR1 cells were pre-incubated for 30 min with FBS-free DMEM medium in the presence of baicalein, (-)-EPG, kaempferol, quercetin or silymarin combined at three fixed-concentration ratios of 1:1, 1:3 and 3:1 of their EC_{50} values previously calculated. For instance, a fixed-concentration ratio combination of 1:3 of two flavonoids means that the test mixture is composed of the first flavonoid at the concentration equal to 1/4 of its EC_{50} value and the second one at the concentration corresponding to 3/4 of its EC_{50}. For all the combinations the final concentration of DMSO was 1% (v/v).

III.3.2.4. Antiepileptic drugs accumulation assays

III.3.2.4.1. Effects of the most promising flavonoid combinations on the intracellular accumulation of antiepileptic drugs/metabolites

At confluence, cells were washed once with PBS (150 mM NaCl, 2.7 mM KCl, 1.3 mM KH_2PO_4, 8.1 mM Na_2HPO_4, pH 7.4) at 37 °C. Then, the cells were pre-incubated for 30 min with FBS-free DMEM medium in the presence of the two most promising dual combinations of flavonoids [198 μM (-)-EPG/500 μM silymarin (1:1); and 167 μM kaempferol/183 μM baicalein (1:3)]. The positive control consisted of incubating the cells with 50 μM verapamil (a P-gp reference inhibitor) instead of flavonoid combinations. For all the combinations, or the positive control verapamil, the final concentration of DMSO in the medium was 1% (v/v). Untreated control cells were pre-exposed only to P-gp inhibitor vehicle with the same percentage of DMSO (1%, v/v), in order to estimate the baseline levels of intracellular accumulation of AEDs/metabolites. Then, the cells were added for 2 h with FBS-free DMEM medium in the presence of AEDs or their

active metabolites. The AEDs/metabolites were tested at therapeutic concentrations (CBZ 50 μM, CBZ-E 16 μM, LIC 140 μM, OXC 20 μM and PHT 75 μM) all prepared in FBS-free DMEM medium (1% DMSO, v/v). Subsequently, the cells were washed three times with cold PBS and the cells were lysed with 100 μL 0.1% Triton X-100 at room temperature for about 30 min. Finally, the total volume of each well was separately collected and frozen at −20 °C until HPLC analysis of AEDs/metabolites.

III.3.2.4.2. MDCK-MDR1 monolayer permeability assays to licarbazepine

LIC was selected as the target drug compound for a set of permeability assays through MDCK-MDR1 cell monolayers. For the permeability experiments, the MDCK-MDR1 cells were seeded onto Corning® Costar® Snapwell™ cell culture inserts (12 mm diameter, 0.4 mm pore-sized polycarbonate membranes) at a density of 4 x 10^5 cells/cm^2. The cells were incubated at 37 °C with 95% humidity and 5% CO_2 for 4 days in order to form polarized cell monolayers. Then, the bottom section of the Snapwell™ was detached from its upper assembly, washed with prewarmed PBS and mounted in the diffusion Ussing chambers thermostated at 37 ºC. The experiment was started by pre-incubation the diffusion chambers for 30 min with prewarmed FBS-free DMEM medium fortified with vehicle or the selected flavonoid combination [(-)-EPG (198 μM) and silymarin (500 μM), 1:1, prepared in FBS-free DMEM medium (1% DMSO, v/v)]. Afterwards, the medium was replaced in the receiver and donor compartments as follows: in the receiver compartment with similar flavonoid solutions or the corresponding vehicle (FBS-free DMEM medium with 1% DMSO, v/v), and in the donor compartment with the solutions added of LIC 140 μM. A 200 μL sample was taken from the donor compartment at t = 0 min to measure the initial concentration of LIC (C_0). At 30, 90, 120, 180 and 240 min, 200 μL samples were also removed from the receiver compartments followed by the immediate addition of an equal volume of preheated FBS-free DMEM medium with 1% DMSO (v/v) or the (-)-EPG/silymarin combination, prepared in FBS-free DMEM medium (1% DMSO, v/v). The collected samples were immediately added with 300 μL of acetonitrile and frozen at −20 °C until HPLC analysis of LIC.
To evaluate the integrity of the cell monolayers during permeability study, transepithelial electrical resistance (TEER) values were monitored during the assay using an EVOM^2 Epithelial Volt/Ohm meter and its STX2 “chopstick” electrodes from World Precision Instruments Inc. (Sarasota, Florida, USA). The background resistance values of an Ussing chamber without Snapwell™ insert were subtracted from the resistance values of Ussing chambers with Snapwell™ inserts containing cells.
The apparent permeability coefficients (P_{app}) of LIC, in 10^{-6} cm/s, was computed using the Equation (1):

$$P_{app} = \frac{10^6 Q}{C_0 \times t \times A}$$

where Q (μmol) is the total amount of LIC that permeated to the receiver compartment throughout the incubation time, C_0 (μmol/ml) is the initial drug concentration in the donor

side, A (cm^2) is the diffusion area of the Ussing chamber, and t (s) is the duration of the incubation. The successive dilution due to medium replacement was taken into account, and the Q was calculated according to the following Equation (2):

$$Q = C_t \times V_{chamber} + \Sigma(C_{t-1} \times V_{sample})$$

where C_t (µmol/ml) is the LIC concentration at each sampling time, C_{t-1} (µmol/ml) is the LIC concentration at the previous sampling time, $V_{chamber}$ is the chamber volume (3800 µL) and V_{sample} is the sample volume (200 µL).

III.3.2.5. HPLC analysis

The quantitative HPLC analysis of AEDs and their active metabolites was performed based on the methods previous reported by FERREIRA ET AL. (2016b, 2016c). For the determination of CBZ, CBZ-E, LIC, and PHT in MDCK-MDR1 cell lysate samples and LIC in the samples collected during the permeability assays, the samples were processed by LLE previously to HPLC analysis. Briefly, to each sample aliquot (200 µL) were added 20 µL of the IS working solution, 300 µL of acetonitrile and 1 mL of ethyl acetate (LLE solvent). The mixture was vortex-mixed for 30 s and centrifuged at 13500 rpm (3 min). Then, the sample was re-extracted twice more with ethyl acetate (1 mL each time) using the conditions previously described. The whole organic extract was evaporated to dryness under a nitrogen stream at 45 °C and then reconstituted with 100 µL of mobile phase. An aliquot (20 µL) of this final extract was injected into the HPLC system.

Chromatographic analysis was carried out using an HPLC system (Shimadzu LC-2010A HT Liquid Chromatography) coupled with diode array detection (Shimadzu SPD-M20A). All instrumental parts were automatically controlled by LabSolutions software (Shimadzu, Kyoto, Japan). The chromatographic separation was carried out at 35 °C on a reversed-phase LiChroCART® Purospher Star column (C_{18}, 55 mm × 4 mm; 3 µm particle size) purchased from Merck KGaA (Darmstadt, Germany). For the determination of CBZ, CBZ-E, OXC and LIC an isocratic elution was applied at a flow rate of 1.0 mL/min with a mobile phase composed of water/methanol/acetonitrile (69:25:6, v/v/v), and PRM was used as IS. The wavelength of 215 nm was selected for the detection of all compounds. On the other hand, the chromatographic analysis of PHT, using CBZ as the IS, was carried out by isocratic elution with a mobile phase of acetonitrile (6%), methanol (25%) and a mixture (69%) of water–triethylamine (99.7:0.3, v/v; pH 6.0), also pumped at a flow rate of 1 mL/min. In this case, the wavelengths of 215 nm and 235 nm were selected for the detection of the CBZ (IS) and PHT respectively. The mobile phases were filtered through a 0.2 µm filter and degassed ultrasonically for 15 min before use and the injected volume of the final extract was always 20 µL.

III.3.2.6. Statistical analysis

Data were reported as mean ± standard error of the mean. The statistical analysis was performed using GraphPad Prism 5.0 (GraphPad Software, La Jolla, CA, USA). The analysis of the effect of each treatment *versus* the control group was performed by one-way ANOVA with the *post hoc* Dunnett's test for multiple comparisons. To check for statistically significant differences among treatments with similar effects one-way or two-way ANOVA with the *post hoc* Bonferroni's test were performed. The statistical tests used were appropriately identified in the figure legends. A minimum *p*-value of 0.05 was used as the significance level for all the tests.

III.3.3. Results and discussion

III.3.3.1. Flavonoid combinations increase the intracellular accumulation of the P-glycoprotein probe substrate rhodamine 123

Five flavonoids [baicalein, (-)-EPG, kaempferol, quercetin and silymarin; Figure III.3.1] were selected in preceding *in vitro* experiments using the model of intracellular accumulation of Rh123, a known and fluorescent substrate of P-gp (*Chapter III, section III.2*). Moreover, these flavonoids have also been previously identified as P-gp inhibitors by several accumulation or efflux (SCAMBIA ET AL. 1994; MITSUNAGA ET AL. 2000; JODOIN ET AL. 2002; ZHANG AND MORRIS 2003a; ZHANG AND MORRIS 2003b; KHANTAMAT ET AL. 2004; KITAGAWA ET AL. 2004; ROMITI ET AL. 2004; CHUNG ET AL. 2005; CHUNG ET AL. 2007; SHIN ET AL. 2009; CHIELI ET AL. 2009; LEE AND CHOI 2010; BORSKA ET AL. 2010; CHO ET AL. 2011; CHOI ET AL. 2011a; LI ET AL. 2011) and transport (WANG ET AL. 2001; ZHANG AND MORRIS 2003b) *in vitro* assays. Numerous *in vivo* studies using animals also revealed a significant increase of drug bioavailability of several P-gp substrates like paclitaxel, doxorubicin, tamoxifen, irinotecan or verapamil with the administration of baicalein (SHIN ET AL. 2009; CHO ET AL. 2011; LI ET AL. 2011), kaempferol (PIAO ET AL. 2008; LI ET AL. 2009), quercetin (HSIU ET AL. 2002; CHOI ET AL. 2004b; CHOI AND LI 2005; SHIN ET AL. 2006; BANSAL ET AL. 2008; LI AND CHOI 2009; CHOI ET AL. 2011a) or silymarin (PARK ET AL. 2012).

To determine the concentrations of flavonoids to be use in fixed-ratio dual combinations, individual concentration-response curves were generated for baicalein, (-)-EPG, kaempferol, quercetin and silymarin (Figure III.3.2). All the studied flavonoids increased the intracellular accumulation of Rh123 in the MCDK-MDR1 cell line in a concentration-dependent manner (predictive of the inhibition of P-gp–mediated efflux). The EC_{50} values obtained were 120.0 μM [95% confidence interval ($CI_{95\%}$) = 99.1 to 145.2 μM] for baicalein, 132.3 μM ($CI_{95\%}$ = 121.1 to 143.9 μM) for (-)-EPG, 332.5 μM ($CI_{95\%}$ = 310.5 to 356 μM) for kaempferol, 241.2 μM ($CI_{95\%}$ = 226.0 to 257.4 μM) for quercetin, and 352.3 μM ($CI_{95\%}$ = 310.6 to 399.6 μM) for silymarin.

Then, dual combinations of all five flavonoids were tested. The results obtained are presented in Figure III.3.2B-K together with single flavonoid effects for an easier comparison. Several

flavonoid combinations increased the intracellular accumulation of Rh123 above the maximal intracellular accumulation achieved by individual flavonoid compounds, suggesting a synergic effect of those flavonoids when used in combination. Indeed, it is also noteworthy to emphasize that these effects were achieved with much lower concentrations of combined flavonoids. This was the case, for example, of the combination of baicalein and (-)-EPG in the three tested fixed-concentration ratios (Figure III.3.2D). Specifically, an individual concentration of baicalein and (-)-EPG of 500 μM increased 12-fold and 9-fold, respectively, the intracellular accumulation of Rh123, while the additive total concentration value of 254 μM tested experimentally for a mixture of the same two flavonoids, combined in the concentration ratio of 1:1 regarding their EC_{50} values, resulted in an augmentation of the intracellular accumulation of Rh123 of approximately 21-fold. The two flavonoid combinations that permitted to obtain the highest increase in the intracellular accumulation of Rh123 into the MDCK-MDR1 cells were considered the most promising. One of them was the combination of kaempferol and baicalein in the proportion of 1:3, regarding their EC_{50} values, with an additive total concentration of 350 μM (167 μM of kaempferol and 183 μM of baicalein; Figure III.3.2G), which increased the intracellular accumulation of Rh123 on average by 33-fold relatively to the control; and the other is the combination of (-)-EPG and silymarin in the proportion of 1:1, with an additive total concentration of 698 μM [198 μM of (-)-EPG and 500 μM of silymarin, Figure III.3.2F], increasing the intracellular accumulation of Rh123 on average by 34-fold comparatively to the control.
The best-fit values (maximum effect or Top fit, Hill slope and EC_{50}) and respective standard errors of the concentration-response curves are showed as supplementary data (Table B.1, Appendix B). Since the maximum effect varied a lot between treatments (from about 9-fold to about 64-fold increase in the intracellular accumulation of Rh123), the EC_{50} (varying between 120 and 829 μM) is not the best way to compare the drug concentration required to achieve a certain significant level of effect. Therefore, it was also calculated the theoretical concentration of flavonoid or flavonoid combination that induces an 8-fold increase of the intracellular accumulation of Rh123, an effect just below the lowest maximum effect of 8.899-fold increase, which was obtained with (-)-EPG (Table B.2, Appendix B). The 8-fold effective concentration was in the same order of magnitude for all treatments, varying between 108 and 380 μM. This means that although there is some potency difference, the most important difference is the maximum effect obtainable with different flavonoid and flavonoid combinations.

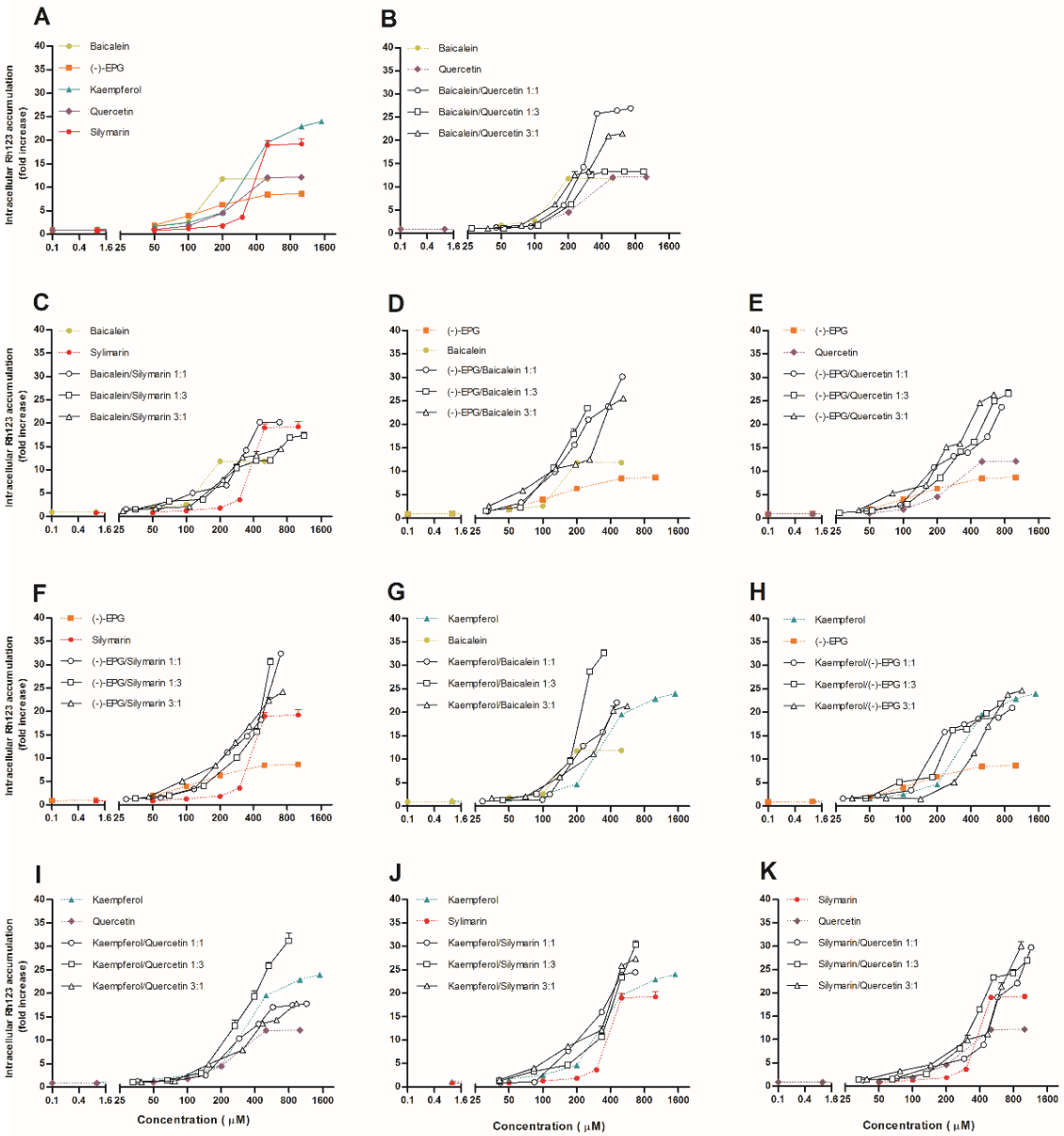

Figure III.3.2. Concentration-response curves of the effects of individual (A) or combined flavonoids (B to K) on the intracellular accumulation of rhodamine 123 (Rh123) in MDCK-MDR1 cells. The results were obtained by comparing the results obtained with flavonoid-pretreated MDCK-MDR1 cells vs. non-pretreated cells (control). (-)-EPG, (-)-epigallocatechin gallate. Data are expressed as the mean values ± standard error of the mean (n = 6).

Taking into consideration the evidence that describes flavonoids as poorly soluble in water (HENDRICH 2006; TARAHOVSKY ET AL. 2014; SELVARAJ ET AL. 2015), we could hypothesize that this was a relevant factor in explaining the differences in the maximum effect obtained with the individual flavonoids with respect to the increase of Rh123 accumulation. However, this is contradicted by (-)-EPG, the flavonoid with the highest water solubility (10 mM), having the lowest capacity in increasing the intracellular Rh123 accumulation. Moreover, some particularly combinations potentiated Rh123 accumulation in a great extension when comparing to the individual flavonoids, and it can be hypothesized that some of these flavonoids have different molecular mechanisms of P-gp interaction. Previous evidence found in literature supports this hypothesis, since opposite effects on P-gp ATPase activity have been observed for different flavonoids (ZHANG AND MORRIS 2003a). Although these mechanisms are not clear, several hypotheses have been suggested. Among the proposed mechanisms are the following: (a) flavonoids can directly bind to the C-terminal nucleotide-binding domain from P-gp (NBD2) and modulate P-gp by interacting bifunctional with the vicinal ATP-binding site and the steroid binding site within a cytosolic domain of P-gp (chrysin, flavone, quercetin, rutin, apigenin, 3-hydroxyflavone, genistein, kaempferide, and kaempferol) (CONSEIL ET AL. 1998); (b) flavonoids can act as substrate and may interact with P-gp directly either by competitive binding to the substrate-binding site or by binding to other drug-binding sites and changing the P-gp conformation [genistein, epicatechin gallate, catechin gallate, (-)-EPG and silymarin] (CASTRO AND ALTENBERG 1997; SHAPIRO AND LING 1997; JODOIN ET AL. 2002; ZHANG AND MORRIS 2003b); and (c) flavonoids may bind to an allosteric site (WANG ET AL. 2002). The latter is the case, for example, of epicatechin which may bind to and activate an allosteric site that enhances P-gp overall function or efficiency, because besides it inhibit the Rh123 transport, it can significantly enhance the active net transport of another P-gp marker substrate, LDS-751 (WANG ET AL. 2002). The combined use of flavonoid compounds has been previously successfully studied for many therapeutic approaches. For instance, baicalein and daidzein demonstrated to exert a synergic action in estrogenic and neuroprotective effects (CHOI ET AL. 2013); combination of quercetin and kaempferol enhanced the *in vitro* cytotoxicity on human colon cancer (HCT-116) cells (JARAMILLO-CARMONA ET AL. 2014); chrysin, kaempferol, morin, and silybinin combinations demonstrated to produce a synergic inhibition of proinflammatory mediator secretion from lipopolysaccharide-induced RAW 264.7 cells (HARASSTANI ET AL. 2010); and optimized combination of the flavonoids formononetin, ononin, calycosin, and calycosin-7-O-β-D-glucoside produced a strong effect in activating the regulatory element of erythropoietin at very low dosage (YU ET AL. 2013). These approaches could overcome some toxicity issues. Besides the fact that flavonoids are largely found in our daily consuming products like in plant foods and drinks, if these plant derived products will be used in a combined therapy, it would be necessary to conduct a series of clinical trials in order to evaluate either its effectiveness and toxicity (GALATI AND O'BRIEN 2004). In fact, although the side effects of their intake have not been widely studied, similarly to any chemical, flavonoids can be harmful at high doses and this should be a subject of concern (TARAHOVSKY ET AL. 2014). Particularly when we are considering their current

excessive intake in supplements, the potentially toxic effects of excessive flavonoid intake cannot be ignored (SKIBOLA AND SMITH 2000). Their possible mutagenic and genotoxic effects may overlap their therapeutic potential (POPP AND SCHIMMER 1991; JURADO ET AL. 1991; SUZUKI ET AL. 1991; SKIBOLA AND SMITH 2000), being these compounds largely recognized as inhibitors of key enzymes involved in hormone metabolism (SKIBOLA AND SMITH 2000; GALATI AND O'BRIEN 2004). Several studies have highlighted the fact that flavonoids may play a dual role in mutagenesis and carcinogenesis, emphasizing that their antimutagens/promutagens and antioxidants/pro-oxidants activities depend on the levels consumed, as well as the physiological conditions of the individual (SKIBOLA AND SMITH 2000; GALATI AND O'BRIEN 2004; KYSELOVA 2012). Nevertheless, it is also noteworthy to refer that some flavonoids are currently being used as therapeutic agents, as is the case of diosmin and hesperidin, which are included as active substances of the medicinal product with the trade name of Daflon™ (90% diosmin and 10% hesperidin), which is used in the chronic venous insufficiency (RAMELET 2001). Concerning this, and although the toxicity of these kind of compounds appears not to be pronounced, the dual combination of flavonoids in order to potentiate their effects and also permit the use of lower concentrations to achieve the intended results is a matter of strong interest regarding the P-gp inhibition. As demonstrated by our results, some dual flavonoid combinations produced a significant synergic effect, increasing the intracellular accumulation of Rh123 into the MDCK-MDR1 cells in a far greater magnitude and using concentrations well below those effective individually.

III.3.3.2. Flavonoid combinations increase the intracellular accumulation of antiepileptic drugs

Although a wide spectrum of drugs have been found to be substrates of the P-gp efflux pump (STOUCH AND GUDMUNDSSON 2002; WEISS ET AL. 2003; LUNA-TORTÓS ET AL. 2008; ZHANG ET AL. 2012a; BREIER ET AL. 2013) there is still no consensus on whether (or which) AEDs are substrates of P-gp (ZHANG ET AL. 2012a). Furthermore, the classification of these drugs as P-gp substrates is largely dependent of the *in vitro* or *in vivo* model used (ZHANG ET AL. 2012a). Therefore, the effects of the two more promising flavonoid combinations were evaluated in the intracellular accumulation of AEDs/metabolites previously identified as P-gp substrates in the same cell model.

The most promising dual flavonoid combinations previously identified in the Rh123 intracellular accumulation assay [198 μM of (-)-EPG with 500 μM of silymarin, and 167 μM of kaempferol with 183 μM of baicalein] were selected to assess their impact on the intracellular accumulation of AEDs (CBZ, OXC and PHT) and their active metabolites (CBZ-E and LIC). The results showed that these flavonoid combinations increased the intracellular accumulation of all three AEDs and their metabolites in comparison to the control (Figure III.3.3A-E; $*p < 0.05$, one-way ANOVA with Dunnett's Multiple Comparison Test). Moreover, both flavonoid combinations demonstrated a great potential in increasing the accumulation of AEDs/metabolites when compared to the standard P-gp inhibitor verapamil. Actually, with exception of the CBZ-E and

PHT for (-)-EPG/silymarin combination and CBZ-E in the case of kaempferol/baicalein, both dual combinations were more effective than verapamil in increasing the AED/metabolite intracellular accumulation in MDCK-MDR1 cells ($^{\#}p < 0.05$, one-way ANOVA with Bonferroni's Multiple Comparison Test). In these circumstances the most promising combination was (-)-EPG and silymarin in the fixed-concentration ratio of 1:1 relatively to their EC_{50} (additive total concentration of 698 μM), having increased in a greater magnitude the intracellular accumulation of the AEDs or their metabolites in MDCK-MDR1 cells, with the exception of PHT. Consequently, this combination was chosen to be used in the LIC transport experiments through MDCK-MDR1 cell monolayers, as described below. It is also noteworthy of mention that PHT is the unique case where the kaempferol/baicalein combination was shown to be superior to the (-)-EPG/silymarin combination (Figure III.3.3E; $^{\#}p < 0.05$, one-way ANOVA with Bonferroni's Multiple Comparison Test). For these in vitro studies the concentration used for each AED and metabolite corresponded to a concentration level of the upper part of the therapeutic range (PATSALOS ET AL. 2008; HOYLAND ET AL. 2013).

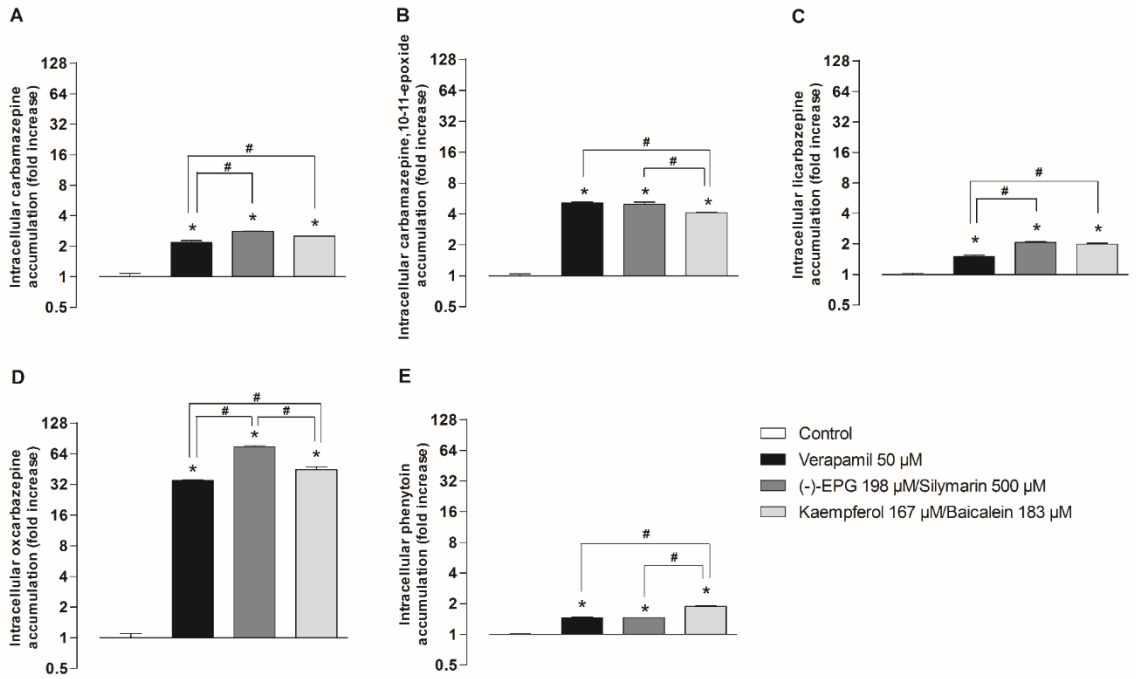

Figure III.3.3. Effect of selected flavonoid combinations in the accumulation of antiepileptic drugs or metabolites in MDCK-MDR1 cells. The combination of kaempferol and baicalein was tested in the proportion of 1:3 regarding their EC_{50} value with a final concentration of 350 μM (167 μM of kaempferol and 183 μM of baicalein), whereas the combination of (-)-epigallocatechin gallate [(-)-EPG] and silymarin was tested in the proportion of 1:1 with a final concentration of 698 μM [198 μM of (-)-EPG and 500 μM of silymarin]. Data are expressed as the mean values ± standard error of the mean ($n = 3$). Comparisons between flavonoid combinations/verapamil group *vs.* control group were performed by one-way ANOVA with the *post hoc* Dunnett's test ($^{*}p < 0.05$). Comparisons between flavonoid combinations/verapamil groups were performed by one-way ANOVA with the *post hoc* Bonferroni's test ($^{\#}p < 0.05$).

The huge differences verified with both the flavonoid combinations and verapamil in the OXC intracellular accumulation were not completely unexpected. Actually, some studies have demonstrated that OXC is strongly transported by P-gp (P-gp substrate) using the MDCK and

MDCK-MDR1 cells (ZHANG ET AL. 2011a). The important role of P-gp in refractory epilepsy has been recognized, being documented a seizure-associated P-gp upregulation mechanism (ZHANG ET AL. 2012a). Additionally, the exposure to certain AEDs appears to be also a potential mechanism for P-gp upregulation since many of them have been acknowledged as inducers of P-gp (ZHANG ET AL. 2012a; GIDAL 2014). Thus, considering the P-gp–mediated multidrug resistance, the research for therapeutically useful P-gp inhibitors that could strategically be used in combination with P-gp substrate drugs in order to overcome that functional barrier and allow drug penetration into the target tissue has been gaining increasing attention (FERREIRA ET AL. 2015).

III.3.3.3. Licarbazepine drug transport experiments in MDCK-MDR1 cells

LIC drug movement through MDCK-MDR1 cell monolayers was evaluated using Snapwell™ inserts mounted on Ussing chambers. The P_{app} of LIC at 140 μM were calculated in the logarithmic form for both drug efflux (basolateral-to-apical) and drug absorption (apical-to-basolateral) directions. Drug transport in absorption direction was determined in the presence and absence of the flavonoid combination of (-)-EPG (198 μM) with silymarin (500 μM). As expected, once that LIC was previously been recognized as a substrate of the P-gp efflux pump, the LnP_{app} of LIC was higher in the basolateral-to-apical direction than in the apical-to-basolateral direction at almost all time points (Figure III.3.4A). However, these differences were small and particularly visible at shorter times, namely at 30 min ($p < 0.05$, two-way ANOVA with the *post hoc* Bonferroni's test). Nevertheless, due to the small differences found between absorption and efflux LnP_{app}, this drug appears to be a weak substrate of P-gp in this experimental model. Indeed, the low differences obtained in the LnP_{app} for LIC transport in both directions, suggests that a small effect of the efflux carriers is determining the transepithelial transport of LIC. These data are in agreement with previous reports of LIC P_{app} across mouse small intestine for at least one of the LIC enantiomers (*S*-LIC) (FORTUNA ET AL. 2012). Nevertheless, the presence of flavonoids induced a pronounced increase of the LnP_{app} of LIC in the absorptive direction through MDCK-MDR1 cell monolayers ($p < 0.05$, one-way ANOVA with Dunnett's Multiple Comparison Test), and at all the time points, when compared to the basal apical-to-basolateral transport (control group; $p < 0.05$, two-way ANOVA with the *post hoc* Bonferroni's test). Hence, a potential mechanism of inhibition of the P-gp multidrug efflux transporter mediated by these flavonoid compounds can only partially explain the strong increase in the absorption direction. It can be hypothesized that the TEER might have partially contributed to the increased LnP_{app} of LIC as well, since a more pronounced decrease of TEER was measured over time when adding flavonoids, and average TEER during LIC incubation was significantly lower in the presence of flavonoids (mean difference of 14 $\Omega.cm^2$, Figure 4B, one-way ANOVA with Dunnett's Multiple Comparison Test, $p < 0.05$). Nonetheless, the decrease of TEER is likely not be enough to explain the overall LnP_{app} increase, since average TEER values over the period of LIC incubation also varied between independent experiments (difference of 14 $\Omega.cm^2$, $p < 0.001$, one-way ANOVA

with Dunnett's Multiple Comparison Test) without causing a significant increase in permeability (Figure III.3.4B). Previous evidence supports the existence of other mechanisms that could further contribute to the increase of the LIC permeation observed in the presence of flavonoid compounds. Flavonoids are known to be lipophilic compounds that tend to accumulate in biological membranes, where they can interact with both lipid and protein components. In fact, flavonoids appear to change significantly the membrane fluidity or rigidity. Accordingly, the lipophilicity of flavonoids as well as their planar structure and ability to interact with biological membranes can be key factors for their pharmacological activities (HENDRICH 2006; TARAHOVSKY ET AL. 2014; SELVARAJ ET AL. 2015).

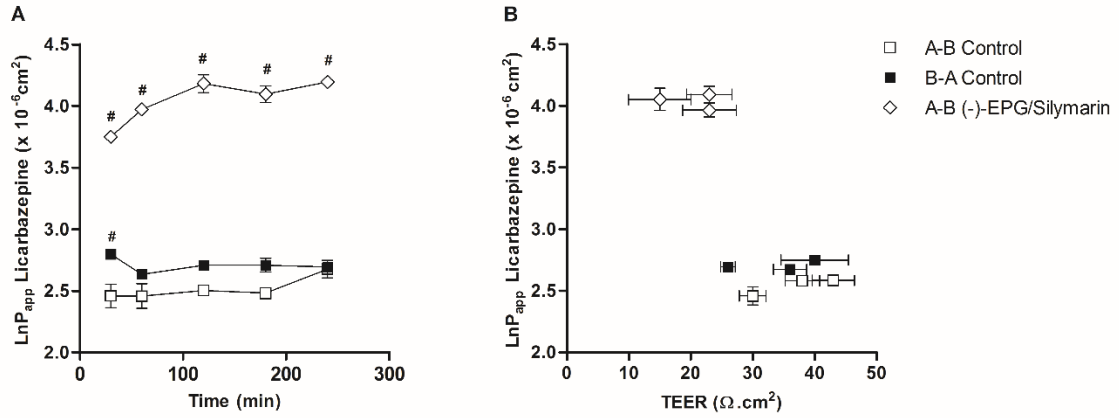

Figure III.3.4. A: Time course of the apparent permeability (LnP_{app}) coefficients considering absorption direction [apical (A)-to-basolateral (B)] of licarbazepine 140 µM in the presence and absence of the flavonoid combination [198 µM of (-)-EPG and 500 µM of silymarin] and Ln P_{app} considering efflux direction (B-A) of licarbazepine 140 µM. Each value represents mean ± standard error of the mean (*n = 3*), and **B:** Representation of transepithelial electrical resistance (TEER) values plotted against the LnP_{app} coefficients of licarbazepine 140 µM resulting from the study presented in A. Comparisons between the groups were performed by two-way ANOVA with the *post hoc* Bonferroni's test. $^{\#}p < 0.05$, compared to A-B control group.

To avoid unexpected changes in drugs kinetics, as well as undesirable clinical outcomes, it has been emphasized that drug-drug interactions at the membrane transport level, in particular involving the interaction with P-gp should be considered (YAMAZAKI ET AL. 2001). In fact, the prediction and understanding of the relevance of P-gp–mediated efflux transport have become pivotal issues in the discovery and development of CNS-active drugs (FENG ET AL. 2008). Nevertheless, although *mdr1* knockout mice have been used, studies in these strains cannot provide definitive data on human P-gp and are non-practical for a rapid and large-scale screening of compounds. Regarding this, *in vitro* assays with human P-gp–overexpressing cell lines and human P-gp transfected cell lines are necessary to evaluate the potential of compounds to act as P-gp substrates/inhibitors (YAMAZAKI ET AL. 2001). Indeed, like the first set of studies herein reported, the majority of accumulation assays are performed in multi-well plates, enabling the rapid and simultaneous identification of compounds interacting with efflux transporters and, therefore, they are readily adapted to high-throughput screening assays. Undeniably, the characteristics of Rh123, a fluorescent P-gp probe, permits the analysis of data through spectrofluorometry, thus accelerating these investigations and providing their

application in early phases of drug discovery in the identification of those compounds interfering with Rh123 cellular uptake. Moreover, Rh123 has the advantage of low interference with underlying metabolic processes (FORSTER ET AL. 2012). On the other hand, transport studies like those developed using Snapwell™ inserts and Ussing Chambers, are frequently more labor intensive and require more complex bioanalytical methods like HPLC (FORTUNA ET AL. 2011a). Nevertheless, the transwell assays have been reported as the most reliable for predicting the P-gp efflux in *in vivo* conditions, being considered the method of choice in the evaluation of drug candidates (YAMAZAKI ET AL. 2001; U.S. FOOD AND DRUG ADMINISTRATION 2006; FENG ET AL. 2008). Bearing this in mind, to explore the interest of flavonoid combinations in the inhibition of P-gp activity and, consequently, to overpass the drug resistance associated with AEDs/metabolites that are P-gp substrates, complementary experiments were performed in this work taking advantage of intracellular accumulation assays and transcellular transport assays with MDR1-transfected cells.

III.3.4. Conclusions

Our results demonstrate not only that the flavonoids baicalein, (-)-EPG, kaempferol, quercetin and silymarin have an interesting potential in the inhibition of P-gp, but also that this potential could be greatly improved by their combined use. Actually, the combination of (-)-EPG and silymarin appears to be very promising for the inhibition of P-gp and also to increase the intracellular accumulation of AEDs/metabolites that are P-gp substrates and the transepithelial permeation (in this last case LIC was used as a model compound). Hence, this approach may be a potential useful strategy to increase the levels of AEDs and of their active metabolites in the brain tissues, which could, at least partially, circumvent pharmacoresistance in epilepsy.

CHAPTER IV

In Vivo Studies

The content of this chapter is included in the following manuscripts:

FERREIRA A *ET AL*. Impact of silymarin, a flavonoid-type P-glycoprotein inhibitor, on the pharmacokinetics of carbamazepine, oxcarbazepine and phenytoin in rats (*Submitted for publication*)

FERREIRA A *ET AL*. (2017) Influence of the dual combination of silymarin and (-)-epigallocatechin gallate, natural dietary flavonoids, on the pharmacokinetics of oxcarbazepine in rats. *Food Chem Toxicol. 106: 446-454.* doi: 10.1016/j.fct.2017.06.015

IV.1. General Considerations

IV.1.1. *In vivo* assays

Despite the great advances in computer model systems, *in vitro* models and *ex vivo* models, it is indisputable that the *in vivo* animal testing continues to play an essential role in the modern drug development (ANDERS AND VIELHAUER 2007). Actually, besides several *in vitro* assays have been developed and validated for early stage screening aimed at filtering out molecules with a higher potential for toxicity, or in order to replace or reduce the use of certain *in vivo* studies, *in vivo* testing still represents a key part of safety and efficacy assessment. Indeed, despite the efforts for standardization and validation of alternative methods, the *in vitro* assays have major limitations for the evaluation of non-clinical efficacy, making essential the use of whole-animal models in the process of drug development in order to meet the requirements of the main drug regulatory agencies (GOH ET AL. 2015; ANDRADE ET AL. 2016).

Based on the results of the *in vitro* studies reported in the previous chapter, two independent *in vivo* studies were conducted using Wistar rats. In fact, the rat is one of the most widely used species in biomedical research, including in the pharmacokinetic studies (JACOB AND KWITEK 2002; IANNACCONE AND JACOB 2009). Additionally, some characteristics of this species, namely the calm temperament, easy handling and economically favourable maintenance make it suitable to be maintained and handled in the laboratory. Hence, a first study was planned to evaluate the effect of silymarin on the pharmacokinetics of the commonly used antiepileptic drugs (AEDs) carbamazepine (CBZ), oxcarbazepine (OXC) and phenytoin (PHT). Actually, silymarin demonstrated to be one of the most promising flavonoid compounds in inhibiting the P-glycoprotein (P-gp) in *in vitro* conditions, and this flavonoid also potentiated the intracellular accumulation of the target AEDs and their active metabolites. The second pharmacokinetic study was designed aiming at studying in *in vivo* conditions the synergic potential demonstrated *in vitro* by some dual flavonoid combinations. In this case, the individual and combined effect of the two flavonoids that form the most promising dual combination [(-)-epigallocatechin gallate [(-)-EPG)] and silymarin] was evaluated on the pharmacokinetics of OXC. The choice of OXC as model drug in this second study took into account not only its wide clinical use in the pharmacotherapy of epilepsy but also the interesting results obtained in the first *in vivo* pharmacokinetic study.

IV.2. Experimental

Impact of silymarin, a flavonoid-type P-glycoprotein inhibitor, on the pharmacokinetics of carbamazepine, oxcarbazepine and phenytoin in rats

IV.2.1. Introduction

In spite of the availability of a wide variety of anticonvulsants and AEDs, the pharmacoresistant epilepsy remains as a major unmet medical need (Sharma et al. 2015; Franco et al. 2016). In fact, approximately 30-40% of patients with epilepsy develop resistance to the pharmacotherapy (Sørensen and Kokaia 2013; Alexopoulos 2013; Ventola 2014; Baulac et al. 2015). Several hypotheses have been proposed to explain the therapeutic failure of the treatment with AEDs, among which the multidrug transporter hypothesis has gained increasing emphasis (Löscher et al. 2013). Accordingly, the overexpression of drug efflux transporters by cerebral endothelial cells of the blood-brain barrier of epileptic patients, such as the P-gp, seems to hamper the AEDs penetration into the biophase, leading to insufficient drug levels in the epileptogenic brain tissue. The recognition that P-gp–mediated multidrug resistance is clinically important in several diseases has promoted concerted efforts to search for therapeutically useful P-gp inhibitors, aiming at circumventing the influence of this functional barrier and increase the drug availability into the brain (Xiong et al. 2015; Ferreira et al. 2015; Feldmann and Koepp 2016). Actually, the administration of P-gp inhibitors concomitantly with central nervous system (CNS)-active drugs that are P-gp substrates is expected to overcome the extrusion of such P-gp substrate drugs, increasing their concentrations at the biophase and, consequently, the intended therapeutic effects (Ramakrishnan 2003; Ferreira et al. 2015; Chen et al. 2016).

Several AEDs have been recognised not only as P-gp substrates (Stouch and Gudmundsson 2002; Weiss et al. 2003; Luna-Tortós et al. 2008), but also as potential inducers of this drug efflux transporter (Zhang et al. 2012a; Gidal 2014). Nevertheless, in spite of the availability of P-gp inhibitors belonging to three different generations, their risk-benefit relationship is not yet clinically favourable for several reasons. While the clinical use of P-gp inhibitors of first-generation (e.g., cyclosporine and verapamil) was limited due to their unacceptable toxicity at the doses required to inhibit P-gp, the second-generation P-gp inhibitors (e.g., valspodar and dexverapamil) have been associated with unpredictable drug–drug interactions (Bansal et al. 2009; Palmeira et al. 2012; Ferreira et al. 2015). For example, the coadministration of valspodar with paclitaxel (an anticancer agent) demonstrated to reduce the paclitaxel clearance by 50% (Chico et al. 2001). In fact, the second-generation agents do not seem to be specific inhibitors of P-gp, also inhibiting other adenosine triphosphate (ATP)-binding cassette (ABC) transporters as well as isoenzymes of the cytochrome P450 (CYP) system (Varma 2003; Hennessy and Spiers 2007). Thus, the affinity of second-generation inhibitors towards P-gp appeared to be too weak to produce a significant inhibition in *in vivo* conditions at tolerable doses (Bansal et al. 2009; Palmeira et al. 2012; Ferreira et al. 2015). On the other hand, the synthetic P-gp inhibitors of third-generation (e.g., biricodar, elacridar, laniquidar, tariquidar and zosuquidar) were promising in some clinical trials (Stewart et al. 2000; Callies et al. 2003; Abraham et al. 2009), but they ended up showing undesirable side effects in non-target organs (Thomas and Coley 2003; Mohana et al. 2016). Facing this reality, the discovery of compounds capable of modulating the

functional activity and/or expression of P-gp with acceptable tolerability is still highly demanded in order to be used, in certain circumstances, in a combined therapy with some P-gp substrate drugs.

Over the last years, phytochemicals, including flavonoid-type compounds, have gained an increasing attention as P-gp modulators particularly due to their potential as non-toxic compounds. As several flavonoids share some of the optimal properties of an ideal P-gp inhibitor, the interest on testing whether these compounds inhibit P-gp has significantly increased during the search for selective and non-cytotoxic P-gp inhibitors (BANSAL ET AL. 2008; BANSAL ET AL. 2009; ABDALLAH ET AL. 2015; FERREIRA ET AL. 2015; MOHANA ET AL. 2016). Among hundreds of flavonoids already identified, silymarin is a unique flavonoid complex, containing silybinin, silydianin, and silychrisin (Figure IV.2.1) (PubChem Coumpound Database).

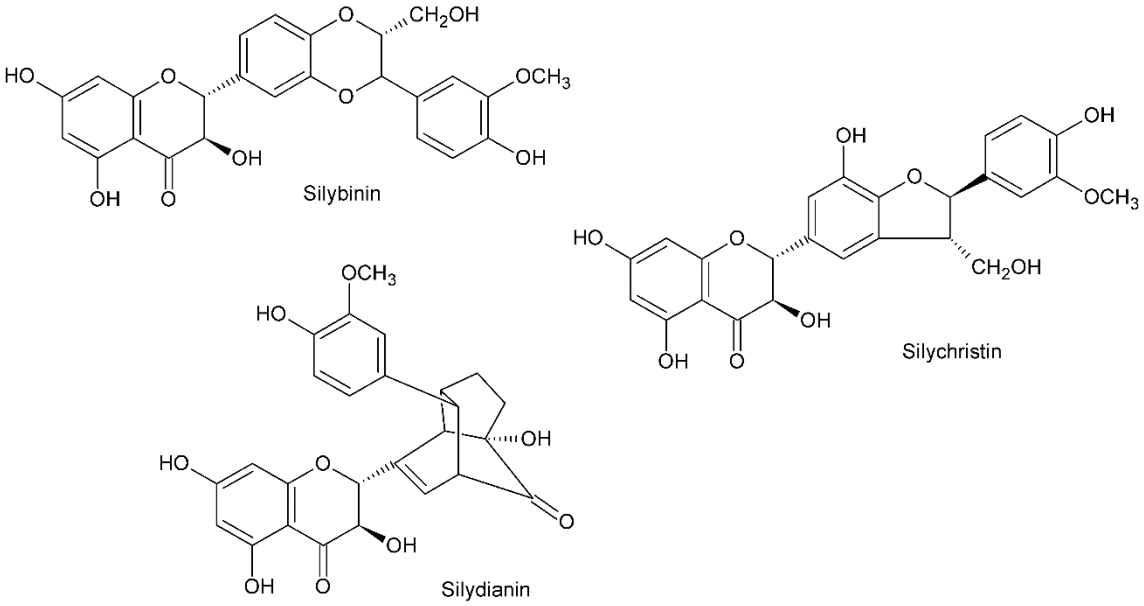

Figure IV.2.1. Chemical structures of some constituents of the flavonoid silymarin (silybinin, silychristin and silydianin).

More specifically, silymarin is a mixture of flavonolignans extracted from blessed milk thistle (*Silybum marianum*), pursuing the history as a medicinal plant for almost two millennia to the treatment of a large variety of illnesses affecting different organs (e.g., prostate, lungs, kidneys, pancreas or CNS). More recently, silymarin has received attention due to its potential benefits as anticancer, hypocholesterolemic, cardioprotective, neuroactive and neuroprotective agent (FRASCHINI ET AL. 2002; KREN AND WALTEROVÁ 2005; GAZÁK ET AL. 2007; FÉHER AND LENGYEL 2012; KABEL 2014). Additionally, numerous studies have shown that silymarin is a potential P-gp inhibitor, interacting with the P-gp substrate and ATP binding sites (ZHANG AND MORRIS 2003a; ZHANG AND MORRIS 2003b; CHUNG ET AL. 2005; PARK ET AL. 2012; FERREIRA ET AL. 2015; RAVIKUMAR REDDY ET AL. 2016).

In line with these findings, as a possible strategy to overcome the pharmacoresistance phenomenon in epilepsy, it is fully justified the *in vivo* evaluation of the effect of silymarin on

the pharmacokinetics of commonly prescribed AEDs widely recognized as P-gp substrates. Therefore, the present work was designed to investigate whether the pre-administration of silymarin to rats is able to change the rate and extent of drug exposure to CBZ, OXC and PHT, as well as to their main metabolites carbamazepine-10,11-epoxide (CBZ-E), licarbazepine (LIC) and 5-(4-hydroxyphenyl)-5-phenylhydantoin (HPPH) (Figure IV.2.2).

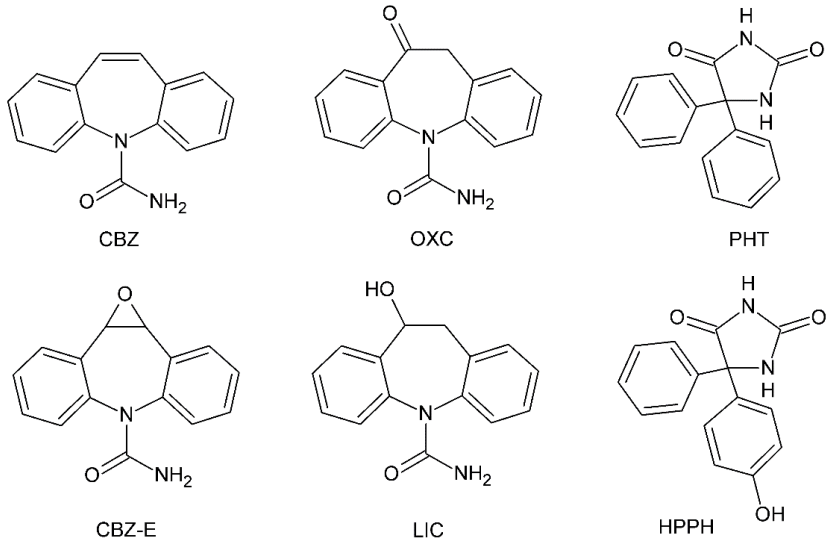

Figure IV.2.2. Chemical structures of the antiepileptic drugs (AEDs) carbamazepine (CBZ), oxcarbazepine (OXC) and phenytoin (PHT), and of their metabolites carbamazepine-10,11-epoxide (CBZ-E), licarbazepine (LIC) and 5-(4-hydroxyphenyl)-5-phenylhydantoin (HPPH).

IV.2.2. Material and methods

IV.2.2.1. Materials and methods

Standards of CBZ, CBZ-E, HPPH, OXC, PHT, silymarin, verapamil (a reference P-gp inhibitor used as positive control), and primidone [PRM; used as internal standard (IS)] were purchased from Sigma–Aldrich (St Louis, MO, USA) while LIC was supplied by Tocris Bioscience (Bristol, United Kingdom). Carboxymethylcellulose sodium salt and dimethyl sulfoxide (DMSO) were obtained from Sigma–Aldrich (St. Louis, MO, USA). Oral suspensions of CBZ (Tegretol® 20 mg/mL) and OXC (Trileptal® 60 mg/mL), sodium chloride 0.9% solution for injection (Labesfal, Portugal), heparin sodium 5000 U.I./mL for injection (B. Braun Medical, Portugal), and pentobarbital (Eutasil® 200 mg/ml, Ceva Saúde Animal; used as anaesthetic drug) were commercially acquired. Introcan® Certo IV indwelling cannulas (22G; 0.9 x 2.5 mm) made of polyurethane were supplied from B. Braun Melsungen AG (Melsungen, Germany).

Methanol and acetonitrile, both of high-performance liquid chromatography (HPLC) gradient grade, and ethyl acetate were purchased from Fisher Scientific (Leicestershire, United Kingdom). The ultra-pure water (HPLC grade, > 18 MΩ.cm) was prepared by means of a Milli-Q water apparatus from Millipore (Milford, MA, USA). Triethylamine was acquired from Merck

KGaA (Darmstadt, Germany) and the 85% *ortho*-phosphoric acid from Fisher Scientific (Leicestershire, United Kingdom).

IV.2.2.2. Animals

Healthy adult male Wistar rats (12-14 weeks old), weighing 346 ± 13 g, were obtained from local certified animal facilities (Faculty of Health Sciences of the University of Beira Interior, Covilhã, Portugal). The animals were housed under controlled environmental conditions (temperature 20 ± 2 ºC; relative humidity 55 ± 5%; 12 h light/dark cycle) with free access to tap water and standard rodent diet (4RF21, Mucedola, Italy) during all the experimental procedures. The animals were used for the pharmacokinetic experiments as well as source of blank matrices (plasma and brain tissue) required for the bioanalytical method validation assays. For the latter assays, rats not subjected to any other treatment were anesthetized with pentobarbital [60 mg/kg; intraperitoneal (ip) injection] and then decapitated. All experimental and care procedures were conducted in accordance with the European Directive (2010/63/EU) regarding the protection of laboratory animals used for scientific purposes, and the experimental procedures were reviewed and approved by the Portuguese National Authority for Animal Health, Phytosanitation and Food Safety (DGAV – Direção Geral de Alimentação e Veterinária).

IV.2.2.3. Systemic pharmacokinetic studies

At the night of the day before the pharmacokinetic studies, animals were anaesthetised [pentobarbital (60 mg/kg); ip] and then a lateral tail vein was cannulated by inserting an Introcan® Certo IV indwelling cannula (22G; 0.9 x 2.5 mm) used for serial blood sampling. After full overnight recovery, animals were pretreated with silymarin, verapamil or vehicle (ip) followed by treatment with each of the AEDs (CBZ, OXC and PHT; ip). Blood sampling was performed in conscious and freely moving rats, which were appropriately restrained only at the moment of blood collection, except for the brain experiments where the blood sampling was taken by a terminal procedure (decapitation and exsanguination under anaesthesia).

A total of fifty-four rats were used to investigate the effect of silymarin on the systemic pharmacokinetics of CBZ, OXC and PHT. For each of the AEDs, eighteen rats were randomly assigned into the following three groups: silymarin group (25 mg/kg, n = 6), verapamil (positive control) group (25 mg/kg, n = 6), and vehicle (negative control) group (n = 6). The compounds (silymarin and verapamil) were dissolved in DMSO and then suspended in carboxymethylcellulose sodium salt aqueous solution 0.5% (m/v), containing the final suspension a concentration of 5% DMSO (v/v). Silymarin and verapamil suspensions were intraperitoneally administered (5 mL/kg of rat weight) to the respective groups and the corresponding volume of vehicle was also injected to the rats of vehicle group. After 1 h, all the groups were treated with suspensions of CBZ (25 mg/kg), OXC (50 mg/kg) or PHT (100 mg/kg) by ip route (10 mL/kg of rat weight). CBZ and OXC suspensions were appropriately

prepared by dilution of the corresponding commercial formulations (Tegretol® 20 mg/mL and Trileptal® 60 mg/mL), whereas PHT suspension was prepared by suspending the powder in carboxymethylcellulose sodium salt aqueous solution 0.5% (m/v). Multiple serial blood samples of approximately 0.3 mL were collected through the cannula into heparinized tubes before (0 h) and at 0.333, 0.667, 1, 1.5, 2, 2.5, 3, 4, 5 and 6 h after AED administration. The blood samples were centrifuged at 4000 rpm for 10 min (4 ºC) to separate the plasma, which was collected and stored at −20 ºC until HPLC analysis.

IV.2.2.4. Plasma-to-brain distribution study

To further investigate the effects of silymarin on the plasma-to-brain distribution of AEDs, an independent study was designed considering OXC as the AED selected. In brief, nine rats were again randomly allocated to one of three groups: silymarin group (25 mg/kg, ip; *n* = 3), verapamil (positive control) group (25 mg/kg, ip; *n* = 3), and vehicle (negative control) group (ip; *n* = 3). Following a pretreatment period of 1 h, all the groups received OXC suspension (50 mg/kg) by ip route (10 mL/kg). All the suspensions were prepared as mentioned in the previous section. Then, at 1.5 h after treatment with OXC the rats were sacrificed by decapitation and the tissues of interest were obtained (blood and brain). Blood was immediately collected into heparinised tubes while brain tissue was quickly excised and weighed. The blood samples were centrifuged at 4000 rpm for 10 min (4 ºC) to separate and collect the plasma. The rat brain tissue was homogenized in 0.1 M sodium phosphate buffer at pH 5 (4 mL per gram of tissue) using an Ultra-Turrax® tissue homogenizer and centrifuged at 13500 rpm for 10 min (4 ºC). The plasma and brain homogenate supernatant samples were collected and stored at −20 ºC until HPLC analysis.

IV.2.2.5. Bioanalytical method validation

The HPLC analysis and quantification of AEDs and their main metabolites were performed based on the methods previous reported by Ferreira et al. (2016b, 2016c). Plasma concentrations of CBZ, OXC, PHT and their main metabolites (CBZ-E, LIC and HPPH), as well as the brain concentrations of OXC and LIC were determined using a liquid-liquid extraction (LLE) procedure followed by an HPLC analysis coupled to a diode array detector (HPLC-DAD). The bioanalytical assays were properly validated in the rat plasma and brain matrices in agreement with the international guidelines on bioanalytical method validation (U.S. Food and Drug Administration 2001; European Medicines Agency 2011).

For the assessment of the linearity, three calibration curves were prepared using six spiked plasma or brain calibration standards, which were assayed on three different days (*n = 3*). These calibration curves were constructed by plotting the ratio between the analyte and IS peak areas as function of the corresponding nominal concentrations. The data were fitted to a weighted linear regression analysis employing the weighting factor that yielded the best fit of peak-area ratios *versus* concentration (Almeida et al. 2002). The lowest calibration standard of the

calibration curves corresponded to the lower limit of quantification (LLOQ), which was established as the lowest concentration of the target analytes in plasma or brain samples that can be quantified reliably, with an acceptable accuracy and precision. The interday precision and accuracy of the assay were evaluated on three consecutive days (n = 3) and through four quality control (QC) samples analysed representing the LLOQ (QC_{LLOQ}), low (QC_1), medium (QC_2) and high (QC_3) ranges of the calibration curves. Similarly, the intraday precision and accuracy were also assessed by analysing five sets of QC samples in a single day (n = 5). Taking into account the acceptance criteria defined by the bioanalytical method validation guidelines, the intra and interday precision [expressed as percentage of coefficient of variation (CV)] must be lower than or equal to 15% (or 20% in the LLOQ) and the accuracy (expressed as percentage of *bias*) must be within ±15% (or ±20% in the LLOQ). Finally, the absolute recovery of the analytes from the samples was determined using three QC samples (QC_1, QC_2 and QC_3). The recovery was calculated comparing the analytes peak areas from extracted rat plasma or brain QC samples with those obtained after direct injection of non-extracted solutions at the same nominal concentrations (n = 5). Likewise, the calculation of the ratio of IS peak areas in extracted samples and non-extracted solutions, evaluated at the concentration used in sample analysis, was used to define its absolute recovery.

IV.2.2.6. Drug analysis

The sample preparation procedure was the same for both rat plasma or brain homogenate samples. Briefly, 20 µL of the IS working solution, 300 µL of acetonitrile and 1 mL of ethyl acetate (LLE solvent) were added to each aliquot of rat plasma or brain homogenate supernatant (100 µL). The mixture was vortex-mixed for 30 s and centrifuged at 13500 rpm for 3 min. The upper organic layer was transferred to a clean glass tube and the sample was re-extracted twice with ethyl acetate (1 mL each time), under the same conditions. The whole organic extract was evaporated to dryness under a nitrogen stream at 45 °C and the solid residue reconstituted with 100 µL of mobile phase. An aliquot (20 µL) of this final sample was injected into the HPLC system.

The chromatographic analysis was carried out using an HPLC system (Shimadzu LC-2010A HT Liquid Chromatography) coupled with DAD (Shimadzu SPD-M20A). All instrumental parts were automatically controlled by LabSolutions software (Shimadzu, Kyoto, Japan). The chromatographic separation was carried out at 35 °C on a reversed-phase LiChroCART® Purospher Star column (C_{18}, 55 mm × 4 mm; 3 µm particle size) purchased from Merck KGaA (Darmstadt, Germany). For the quantification of CBZ, CBZ-E, OXC, LIC in rat plasma, as well as OXC and LIC in rat brain tissue (method A), an isocratic elution with a mobile phase composed of water/methanol/acetonitrile (69:25:6 v/v/v) was applied at a flow rate of 1 mL/min. In this method, PRM was used as IS and the wavelength of 215 nm was selected for the detection of all compounds. On the other hand, for the quantification of PHT, HPPH in rat plasma (method B), CBZ was used as IS and an isocratic elution with acetonitrile (6%), methanol (25%) and a

mixture (69%) of water–triethylamine (99.7:0.3, v/v; pH 6.0), at 1 mL/min was employed. In this method, the wavelengths of 215 nm (CBZ and HPPH) and 235 nm (PHT) were selected for the detection of the compounds. Before use, all mobile phases were filtered through a 0.2 μm filter and degassed ultrasonically for 15 min.

IV.2.2.7. Pharmacokinetic analysis

The maximum concentration (C_{max}) of AEDs and their main metabolites in plasma and the corresponding time to reach C_{max} (t_{max}) were directly obtained from the experimental data. The remaining pharmacokinetic parameters were estimated from the individual plasma concentration-time profiles by non-compartmental pharmacokinetic analysis using the WinNonlin® version 5.2 (Pharsight Co, Mountain View, CA, USA). For each rat, the estimated pharmacokinetic parameters included the area under the concentration-time curve (AUC) from time zero to the last sampling time (AUC_{0-t}) which was calculated by the linear trapezoidal rule; the AUC from time zero to infinity ($AUC_{0-\infty}$) that was determined from $AUC_{0-t} + (C_{last}/k_{el})$, where C_{last} is the last quantifiable concentration and k_{el} is the apparent terminal rate constant calculated by log-linear regression of the terminal segment of the concentration-time profile. The apparent terminal elimination half-life ($t_{1/2el}$) and the mean residence time (MRT) were also estimated. The concentrations below the LLOQ of the assay were taken as zero for all calculations.

IV.2.2.8. Statistical analysis

Data were reported as the mean ± standard error of the mean (SEM), unless otherwise noted. Comparisons between the two groups (negative control group *vs* experimental or positive control group) were performed using unpaired two-tailed Student's *t*-test, except for the t_{max} parameter where the nonparametric Mann-Whitney test was applied. A difference was considered to be statistically significant for a *p*-value lower than 0.05 ($p < 0.05$).

IV.2.3. Results

IV.2.3.1. Bioanalytical method validation

The results obtained in the validation assays carried out to demonstrate the reliability of the HPLC-DAD methods employed to support the pharmacokinetics and biodistribution studies herein reported are summarized in Table IV.2.1. The calibration curves obtained in rat plasma and brain were linear ($r^2 \geq 0.9920$) for all the analytes within the defined concentration ranges, showing a consistent correlation between analyte-IS peak area ratios and the corresponding nominal concentrations. Due to the wide concentration ranges, and in order to compensate the heteroscedasticity detected, the calibration curves for all the analytes were subjected to weighted linear regression analysis using $1/x^2$ as the weighting factor. The LLOQs values, as

well the data for intra and interday precision and accuracy fulfilled the acceptance criteria established by the international guidelines (U.S. FOOD AND DRUG ADMINISTRATION 2001; EUROPEAN MEDICINES AGENCY 2011). The overall absolute recoveries were equal or higher than 79.8% demonstrating a good recovery of all analytes over the evaluated concentration ranges.

Table IV.2.1. Results obtained for the main validation parameters of the HPLC-DAD methods employed to quantify carbamazepine (CBZ), carbamazepine-10,11-epoxide (CBZ-E), oxcarbazepine (OXC), licarbazepine (LIC), phenytoin (PHT) and 5-(4-hydroxyphenyl)-5-phenylhydantoin (HPPH) in plasma and brain homogenate supernatant.

	Analytes	Concentration range QC_1, QC_2, QC_3 (μg/mL)	[a]Equation (*n* = 3)	r^2	[b]Interday (*n* = 3)		[b]Intraday (*n* = 5)		[c]Recovery (%, *n* = 5)
					Precision (% CV)	*Accuracy (% bias)*	*Precision (% CV)*	*Accuracy (% bias)*	
Method A: Plasma	**CBZ**	0.1–15 0.3, 7.5, 13.5	y = 0.0948x - 0.0009	0.9944	≤ 6.6	3.8 – 7.0	≤ 6.6	−4.3 – 0.73	89.3 – 92.0
	CBZ-E	0.1–5 0.3, 2.5, 4.5	y = 0.0662x - 0.0002	0.9933	≤ 6.3	1.1 – 4.2	≤ 8.9	−8.4 – −6.05	92.0 – 93.4
	OXC	0.1–25 0.3, 12.5, 22.5	y = 0.0640x - 0.0003	0.9938	≤ 11.6	−0.5 – 6.4	≤ 9.6	−4.9 – −1.05	80.0 – 85.8
	LIC	0.05–40 0.15, 20, 36	y = 0.1119x + 0.0015	0.9920	≤ 11.6	−0.5 – 5.8	≤ 6.3	−5.1 – −0.37	91.1 – 99.6
Method B: Plasma	**PHT**	0.15–30 0.45, 15, 27	y = 0.0153x + 0.0001	0.9927	≤ 6.7	−4.8 – 9.0	≤ 9.7	−7.2 – 8.69	87.7 – 92.4
	HPPH	0.1–15 0.3, 7.5, 13.5	y = 0.0146x - 0.0001	0.9971	≤ 5.2	−4.3 – −1.4	≤ 7.9	−13.4 – −5.7	79.8 – 91.6
Method A: Brain	**OXC**	0.1–25 0.3, 12.5, 22.5	y = 0.0666x + 0.0001	0.9965	≤ 3.2	−5.3 – 0.1	≤ 8.8	5.3 – 11.2	82.1 – 89.5
	LIC	0.05–40 0.15, 20, 36	y = 0.1146x + 0.0021	0.9966	≤ 4.2	−12.4 – 2.5	≤ 8.3	−0.5 – 7.3	87.4 – 91.6

bias, deviation from nominal concentration value; CBZ, carbamazepine; CBZ-E, carbamazepine-10,11-epoxide, CV, coefficient of variation; HPPH, 5-(4-hydroxyphenyl)-5-phenylhydantoin; LIC, licarbazepine; OXC, oxcarbazepine; PHT, phenytoin; r^2, coefficient of determination.

[a] y, represents analyte-IS peak area ratio, x, represents analyte concentration (μg/mL); [b] At the concentration of the lower limit of quantification (QC_{LLOQ}) the precision (% CV) did not exceed 20% and accuracy (% bias) was within ±20%; [c] The coefficient variation (%) varied between 0.49 and 11.93%.

IV.2.3.2. Effects of silymarin on the systemic pharmacokinetics of antiepileptic drugs

The mean plasma concentration-time profiles (n = 6) of CBZ, OXC, PHT and their corresponding metabolites (CBZ-E, LIC and HPPH) obtained in rats after pretreatment with a single ip dose of silymarin (25 mg/kg), verapamil (25 mg/kg) or vehicle followed by ip administration of the tested AEDs, CBZ (25 mg/kg), OXC (50 mg/kg) or PHT (100 mg/kg) are plotted in Figure IV.2.3. The corresponding main pharmacokinetic parameters are summarized in Table IV.2.2.

IV.2.3.2.1. Effects of silymarin on the pharmacokinetics of carbamazepine

As represented in Figure IV.2.3A, plasma CBZ concentrations were very comparable in silymarin and vehicle groups at the initial absorption phase (up to 0.667 h) and at the elimination phase (2.5-6 h). Notwithstanding, the pretreatment with silymarin significantly increased the CBZ concentrations over the 1-2 h post-dosing period in comparison to the concentrations achieved in the vehicle (negative control) group ($p < 0.05$). Nevertheless, it is clear that the impact of verapamil (a classic P-gp inhibitor) in increasing the plasma concentrations of CBZ was superior to that observed with silymarin. In fact, the mean plasma CBZ concentrations obtained in the verapamil (positive control) group were significantly higher than those in the vehicle group during almost all the post-dose time period (1-6 h), showing statistically significant differences ($p < 0.001$). Considering the mean concentration-time profiles obtained for CBZ-E (Figure IV.2.3B), it is evident that overall the pretreatment with silymarin had a practically negligible effect on systemic exposure to the major CBZ metabolite. However, contrary to silymarin, the pretreatment with verapamil significantly decreased the plasma CBZ-E concentrations over the 0.333-2.5 h post-dose time period ($p < 0.05$).

Looking now for the pharmacokinetic parameters shown in Table IV.2.2, it can be observed that the average C_{max} values achieved for CBZ were very close in silymarin and verapamil groups, and no statistically significant differences were detected when compared with the corresponding mean C_{max} value reached in vehicle group. Despite the similarity found for the C_{max} values of CBZ between groups, the median time to reach the C_{max} (t_{max}) was significantly prolonged by the pretreatment with silymarin and verapamil ($p < 0.05$). In addition, after verapamil pre-administration, in comparison with the vehicle group, a statistically significant higher value was estimated for the extent of systemic exposure to CBZ (AUC_{0-t}; $p < 0.001$). Actually, whereas the pretreatment with silymarin determined only minor increases in the extent of systemic exposure to CBZ (as assessed by AUC_{0-t}), such effects were considerably marked in the verapamil group; the pre-administration of verapamil increased the CBZ AUC_{0-t} value by approximately 74%, in comparison with the vehicle group.

On the other hand, considering the pharmacokinetic parameters obtained for CBZ-E, only deserves to be highlighted the verapamil-induced statistically significant decrease in the value of the AUC_{0-t} parameter ($p < 0.05$). In this case, the AUC_{0-t} for CBZ-E is the truncated AUC at 6 h post-dose and the aforementioned differences appear to be determined by a lower

metabolic rate in the pathway of conversion of CBZ to CBZ-E in the presence of verapamil. The effects of silymarin in the metabolism of CBZ were less pronounced than those observed for verapamil.

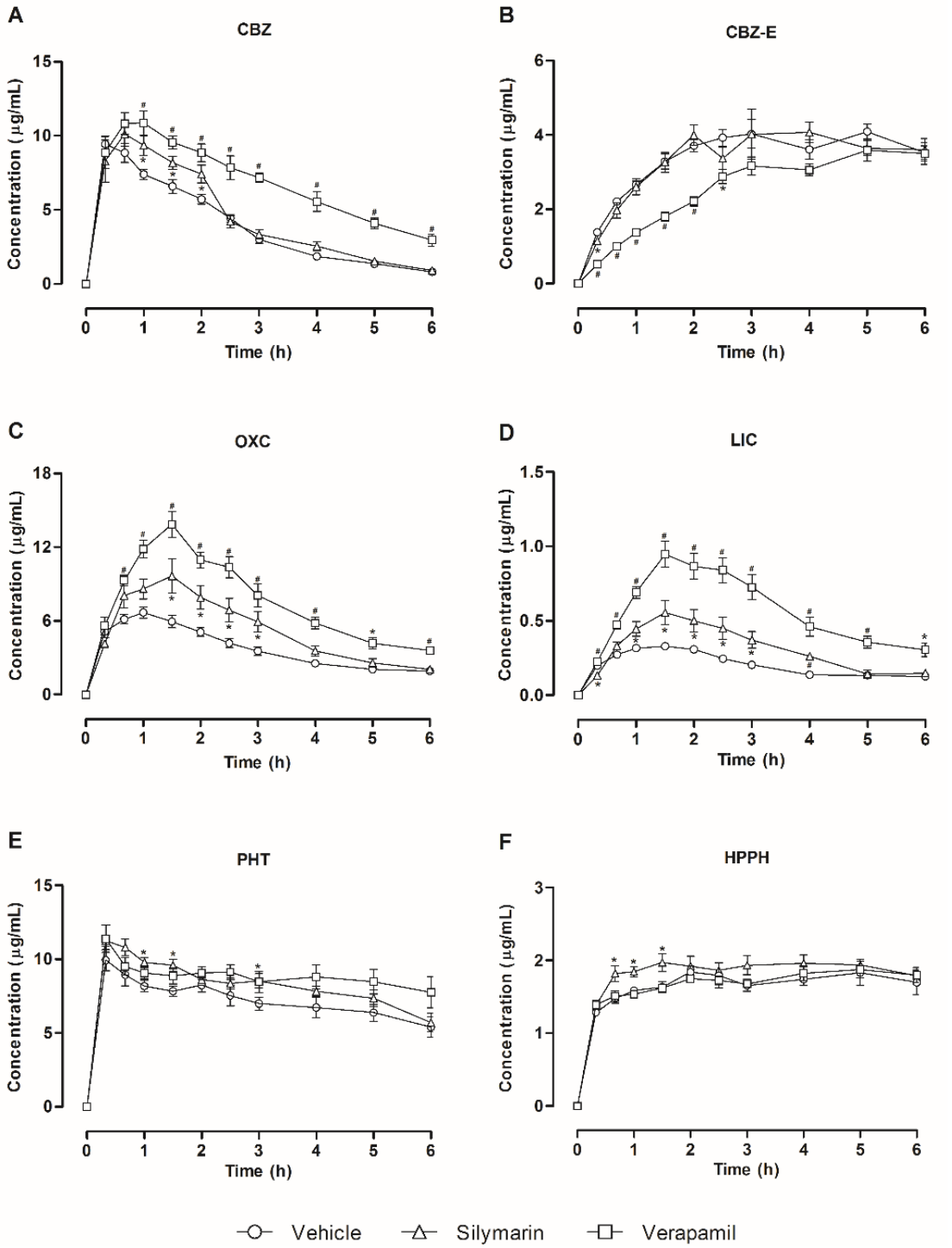

Figure IV.2.3. Mean plasma concentration-time profiles of antiepileptic drugs and their respective main metabolites: A, carbamazepine (CBZ); B, carbamazepine-10,11-epoxide (CBZ-E); C, oxcarbazepine (OXC); D, licarbazepine (LIC); E, phenytoin (PHT); and F, 5-(4-hydroxyphenyl)-5-phenylhydantoin (HPPH), over a 6-h period in rats pretreated with silymarin (25 mg/kg), verapamil (25 mg/kg) or vehicle 1 h before the intraperitoneal administration of CBZ (25 mg/kg), OXC (50 mg/kg) or PHT (100 mg/kg). Symbols represent the mean values ± standard error of the mean (SEM) of six determinations per time point (n = 6). Comparisons between vehicle (negative control) group *vs* silymarin and verapamil (positive control) groups were performed by Student's t-test. $^{*}p < 0.05$ and $^{\#}p < 0.001$, compared to vehicle group.

IV.2.3.2.2. Effects of silymarin on the pharmacokinetics of oxcarbazepine

The plasma concentrations of OXC in the silymarin group were similar to those observed in the vehicle group at the initial absorption phase (up to 1 h) and at the elimination phase (4-6 h) (Figure IV.2.3C). Nevertheless, silymarin demonstrated to significantly increase the OXC concentrations over the 1.5-3 h post-dose time period ($p < 0.05$). Regarding the plasma concentrations of LIC, the main and pharmacologically active metabolite of OXC (Figure IV.2.3D), silymarin originated a statistically significant increase not only at the initial absorption phase (0.333 h), but also over the 1-4 h post-dose time period, in comparison to the vehicle group ($p < 0.05$). Likewise, verapamil-induced statistically significant increases were found for both OXC and LIC concentrations at almost all sampling time points ($p < 0.05$).

Concerning the pharmacokinetic parameters summarized in Table IV.2.2, silymarin and verapamil significantly increased the values of C_{max} and AUC_{0-t} parameters of OXC comparatively to vehicle (negative control group) ($p < 0.05$). In addition, as expected, when compared with the vehicle group, it was observed a delay in the time to achieve the median t_{max} values of OXC in both silymarin and verapamil groups, being such differences only statistically significant for verapamil group ($p < 0.05$). As it can be inferred by the silymarin-to-vehicle and verapamil-to-vehicle ratios presented in Table IV.2.2, whereas silymarin increased the C_{max} and AUC_{0-t} values of OXC in 50 and 41%, respectively, the classic P-gp inhibitor verapamil potentiated an increase of both pharmacokinetic parameters by approximately 100%. Relatively to the pharmacokinetic parameters estimated for the metabolite LIC, only a statistically significant increase was found for the AUC_{0-t} comparing the silymarin with the vehicle group ($p < 0.05$). Notwithstanding, when compared to the vehicle group, verapamil promoted a considerable increase in the C_{max} and AUC_{0-t} values of LIC ($p < 0.001$). In this case, the effects of silymarin and verapamil on the rate and extent of systemic exposure to LIC follow the same trend but with substantially different magnitudes, in particular on the extent of systemic exposure; indeed, in the presence of verapamil the extent of systemic exposure to LIC increased by about 177%, while the corresponding increase in the silymarin group was approximately 52%, as assessed by AUC_{0-t}.

Table IV.2.2. Pharmacokinetic parameters estimated by non-compartmental analysis of the plasma concentration-time profiles of carbamazepine (CBZ), oxcarbazepine (OXC), phenytoin (PHT), and their main metabolites carbamazepine-10,11-epoxide (CBZ-E), licarbazepine (LIC) and 5-(4-hydroxyphenyl)-5-phenylhydantoin (HPPH), respectively, obtained in rats after pretreatment with silymarin (25 mg/kg), verapamil (25 mg/kg) or the corresponding volume of vehicle 1 h before intraperitoneal administration of CBZ (25 mg/kg), OXC (50 mg/kg) or PHT (100 mg/kg) (n = 6, unless otherwise noted). Data are expressed as the mean ± standard error of the mean (SEM), except for t_{max} that is expressed as the median value (range).

		Parameters						
		t_{max} (h)	C_{max} (µg/mL)	AUC_{0-t} (µg.h/mL)	$AUC_{0-\infty}$ (µg.h/mL)	k_{el} (h^{-1})	$t_{1/2el}$ (h)	MRT (h)
CBZ	Vehicle	0.333 (0.333-0.667)	9.541 ± 0.568	23.437 ± 1.504	25.294 ± 1.756	0.457 ± 0.025	1.54 ± 0.08	2.39 ± 0.08
	Silymarin	0.667 (0.333-1.000) *	10.749 ± 1.124	26.978 ± 1.302	28.943 ± 1.325	0.465 ± 0.021	1.51 ± 0.07	2.43 ± 0.10
	Verapamil	0.834 (0.667-1.500) *	11.130 ± 0.711	40.719 ± 2.590 #	43.304 ± 1.192[a]	0.443 ± 0.050[a]	1.64 ± 0.16[a]	3.20 ± 0.03[a]
	Silymarin/Vehicle	---	1.13	1.15	---	---	---	---
	Verapamil/Vehicle	---	1.17	1.74	---	---	---	---
CBZ-E	Vehicle	4.000 (2.500-5.000)	4.350 ± 0.293	20.235 ± 1.044	ND	ND	ND	ND
	Silymarin	4.000 (2.000-4.000)	4.866 ± 0.485	19.963 ± 1.413	ND	ND	ND	ND
	Verapamil	5.000 (3.000-6.000)	3.800 ± 0.323	15.292 ± 0.886 *	ND	ND	ND	ND
	Silymarin/Vehicle	---	1.12	0.99	---	---	---	---
	Verapamil/Vehicle	---	0.87	0.76	---	---	---	---
OXC	Vehicle	1.000 (0.333-1.000)	6.892 ± 0.432	22.352 ± 1.268	31.972[b]	0.346[b]	2.00[b]	3.45[b]
	Silymarin	1.500 (0.667-2.000)	10.328 ± 1.110 *	31.486 ± 3.066 *	37.618 ± 3.546[c]	0.391 ± 0.038[c]	1.85 ± 0.17[c]	3.22 ± 0.14[c]
	Verapamil	1.500 (1.000-2.500) *	14.102 ± 0.949 #	45.330 ± 2.730 #	59.040 ± 4.513[a]	0.366 ± 0.027[a]	1.93 ± 0.13[a]	3.59 ± 0.16[a]
	Silymarin/Vehicle	---	1.50	1.41	---	---	---	---
	Verapamil/Vehicle	---	2.05	2.03	---	---	---	---
LIC	Vehicle	1.500 (1.000-2.000)	0.334 ± 0.021	1.214 ± 0.069	1.610[b]	0.330[b]	2.10[b]	3.66[b]
	Silymarin	1.500 (1.000-2.500)	0.701 ± 0.175	1.846 ± 0.198 *	2.467 ± 0.155[d]	0.424 ± 0.039[d]	1.71 ± 0.18[d]	3.35 ± 0.14[d]
	Verapamil	1.750 (1.500-2.500)	0.991 ± 0.092 #	3.360 ± 0.292 #	3.696 ± 0.202[a]	0.370 ± 0.024[a]	1.90 ± 0.11[a]	3.75 ± 0.08[a]
	Silymarin/ Vehicle	---	1.11	1.52	---	---	---	---
	Verapamil/Vehicle	---	1.22	2.77		---	---	---

		Parameters						
		t_{max} (h)	C_{max} (µg/mL)	AUC_{0-t} (µg.h/mL)	$AUC_{0-\infty}$ (µg.h/mL)	k_{el} (h^{-1})	$t_{1/2el}$ (h)	MRT (h)
PHT	Vehicle	0.333 (0.333-0.667)	10.298 ± 0.752	42.549 ± 2.778	ND	ND	ND	ND
	Silymarin	0.333 (0.333-0.667)	11.478 ± 0.406	49.143 ± 1.748	ND	ND	ND	ND
	Verapamil	0.333 (0.333-0.667)	11.384 ± 0.928	51.757 ± 3.815	ND	ND	ND	ND
	Silymarin/Vehicle	---	1.12	1.15	---	---	---	---
	Verapamil/Vehicle	---	1.11	1.22	---	---	---	---
HPPH	Vehicle	2.250 (1.500-5.000)	2.043 ± 0.133	9.882 ± 0.463	ND	ND	ND	ND
	Silymarin	4.000 (0.667-6.000)	2.176 ± 0.107	10.956 ± 0.464	ND	ND	ND	ND
	Verapamil	4.000 (2.000-6.000)	2.014 ± 0.069	10.016 ± 0.279	ND	ND	ND	ND
	Silymarin/Vehicle	---	1.06	1.11	---	---	---	---
	Verapamil/Vehicle	---	0.99	1.01	---	---	---	---

*AUC, area under the concentration-time curve; AUC_{0-t}, AUC from time zero to the last sampling time; $AUC_{0-\infty}$, AUC from time zero to infinity; C_{max}, peak concentration; k_{el}, apparent terminal rate constant; MRT, mean residence time; ND, not determined; $t_{1/2el}$, apparent terminal elimination half-life; t_{max}, time to reach C_{max}; [a]n = 3; [b]n = 1; [c]n = 5; [d]n = 4; *p < 0.05, significantly different from the vehicle control group; [#] p < 0.001, significantly different from the vehicle control group. Comparisons between the negative control group (vehicle) vs experimental groups were performed by Student's t-test, the exception was the t_{max} parameter in which the nonparametric Mann-Whitney test was applied.*

IV.2.3.2.3. Effects of silymarin on the pharmacokinetics of phenytoin

The pretreatment of the rats with silymarin has not changed substantially the pharmacokinetic profile of PHT. Actually, only occasionally, at 1-1.5 h and 3 h post-dose, were identified statistically significant differences for plasma PHT concentrations determined in both silymarin and vehicle groups (Figure IV.2.3E, $p < 0.05$). Similarly, after verapamil pretreatment, although slight increases were observed in the mean plasma concentrations of PHT at almost all the sampling time points, no statistically significant differences were found at any time ($p > 0.05$). Considering the mean pharmacokinetic profiles obtained for HPPH (the main metabolite of PHT), a considerable overlap among the three groups of rats (vehicle, silymarin and verapamil) was observed (Figure IV.2.3F). Only in the silymarin group were observed statistically significant increases in plasma HPPH levels during the 0.667-1.5 h post-dose time period ($p < 0.05$), while verapamil did not induce any statistically significant difference in comparison to the vehicle group. Analysing the plasma pharmacokinetic parameters estimated for PHT and HPPH (Table IV.2.2), as expected taking the corresponding mean plasma concentration-time profiles into account, none of the pharmacokinetic parameters was significantly changed by the pretreatment with silymarin or verapamil.

IV.2.3.3. Effects of silymarin on plasma-to-brain distribution of oxcarbazepine and its main metabolite

As the pretreatment with silymarin and with verapamil (a classic P-gp inhibitor) induced a greater impact on the systemic pharmacokinetics of OXC and its main pharmacologically active metabolite LIC, the influence of such effects in the brain drug levels was subsequently investigated. For that, rats pretreated with silymarin, verapamil or vehicle were sacrificed at 1.5 h after OXC dosing and the concentration levels of parent drug (OXC) and its metabolite (LIC) were measured in plasma and brain tissue homogenate samples. The results are depicted in Figure IV.2.4. As expected, the brain concentrations of OXC and LIC in the groups pretread with silymarin and verapamil were significantly higher than those measured in the vehicle group, reflecting the differences observed in the systemic drug exposure ($p < 0.05$).

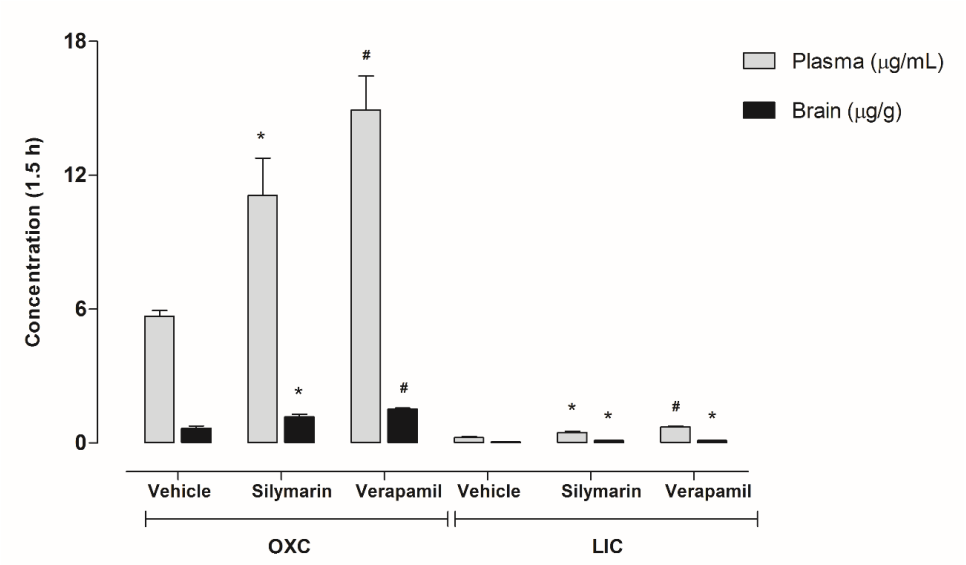

Figure IV.2.4. Mean plasma and brain concentrations of oxcarbazepine (OXC) and its active metabolite licarbazepine (LIC) obtained at 1.5 h post intraperitoneal OXC administration (50 mg/kg) in rats pretreated with silymarin (25 mg/kg), verapamil (25 mg/kg) or the vehicle of these compounds. Data are expressed as the mean values ± standard error of the mean (SEM) of three determinations (n = 3). Comparisons between vehicle (negative control) group *vs* silymarin and verapamil (positive control) groups were performed by Student's t-test, $^{*}p < 0.05$ and $^{\#}p < 0.005$ compared to vehicle group.

IV.2.4. Discussion

The pharmacoresistance verified in epilepsy makes extremely relevant the search for new AEDs and/or novel therapeutic strategies. Acknowledging that P-gp–mediated drug efflux is a major mechanism responsible for the reduction of systemic and tissue exposure to a wide variety of drugs, minimizing the extent of drug absorption and distribution and enhancing the elimination processes, the availability of safe compounds able to interact with P-gp and block its functional activity may be of interest to reverse the drug resistance in epilepsy (STĘPIEŃ ET AL. 2012; FRENCH ET AL. 2013; FELDMANN AND KOEPP 2016). Actually, P-gp transporter is largely expressed in the luminal membrane of small intestinal epithelial cells, luminal side of blood-brain barrier endothelial cells, and in the apical membranes of excretory cells such as hepatocytes and kidney proximal tubule epithelia, which can significantly determine the bioavailability, pharmacokinetics and drug biodisposition (WESSLER ET AL. 2013; PRACHAYASITTIKUL AND PRACHAYASITTIKUL 2016). Regarding this matter, the P-gp modulation arises as an attractive therapeutic approach to reverse the drug-resistant phenotype, including in cancer (VAN VLIET ET AL. 2006; AMIN 2013).

Nowadays, it is widely accepted the hypothesis that there is an association between P-gp overactivity in some regions of the brain and pharmacoresistance in epilepsy. In fact, P-gp has been shown to be up-regulated not only in animal models of refractory epilepsy (SEEGERS ET AL. 2002b; RIZZI ET AL. 2002; SEEGERS ET AL. 2002a; VAN VLIET ET AL. 2004; POTSCHKA ET AL. 2004; VOLK AND LÖSCHER 2005; MARCHI ET AL. 2006; LIU ET AL. 2007; BAUER ET AL. 2008; NISHIMURA ET AL. 2008; BARTMANN ET AL. 2010), but also in patients with drug-resistant epilepsy (TISHLER ET AL. 1995;

Lazarowski et al. 1999; Sisodiya et al. 1999; Dombrowski et al. 2001; Potschka and Löscher 2002; Aronica et al. 2003; Sisodiya 2003; Marroni et al. 2003; Aronica et al. 2004; Marchi et al. 2004; Jóźwiak 2007; Kwan et al. 2010b). For instance, Summers et al. (2004) demonstrated the presence of P-gp in the capillary endothelial cells of the blood-brain barrier at the site of the epileptic focus using brain tissue from the temporal lobe of patients with refractory epilepsy. Additionally, several animal models of drug-resistant epilepsy seem to firmly establish a role for P-gp as a target for increasing clinical response to current epilepsy treatments. Rizzi et al. (2002) showed that the overexpression of P-gp in the hippocampus of a kainate model of epilepsy was associated with a reduction of PHT concentrations in the brain. In this context, there are several reports evidencing the efficiency of the P-gp inhibitors tariquidar, nimodipine and verapamil in restoring the AEDs anticonvulsant activity in animal models of refractory epilepsy (Clinckers et al. 2005; van Vliet et al. 2006; Brandt et al. 2006; Höcht et al. 2007). To date, there are two clinical studies that addressed the functional involvement of P-gp in pharmacoresistant epilepsy, where the seizure control was improved in two patients with intractable epilepsy when verapamil was added (Summers et al. 2004; Iannetti et al. 2005). In fact, verapamil is the most extensively characterized P-gp inhibitor that entered in clinical trials (Summers et al. 2004; Iannetti et al. 2005; Pérez-Tomás 2006).

In this scope, flavonoid-type compounds, which are phytochemicals constituents present in the human diet (Deferme and Augustijns 2003), have been recently a target of interest due to their potential as safer P-gp inhibitors (Ferreira et al. 2015). The inhibitory potential of several flavonoids against P-gp efflux pump, including silymarin, was previously demonstrated in *in vitro* conditions (Zhang and Morris 2003a; Zhang and Morris 2003b; Chung et al. 2005; Lee and Choi 2010). Actually, some of them produced comparable inhibitory effects to those of classic P-gp inhibitors like verapamil or cyclosporine A (Brandt et al. 2006; Bansal et al. 2009; Schinkel and Jonker 2012; Ferreira et al. 2015; Mohana et al. 2016). Moreover, *in vivo* studies demonstrated the benefits of flavonoids in increasing bioavailability of several P-gp substrates (Piao and Choi 2008b; de Castro et al. 2008; Li and Choi 2008; Go et al. 2009; Pathak and Udupa 2010; Cho et al. 2011; Choi et al. 2011b; Choi et al. 2011a; Yang et al. 2011). Silymarin was reported to increase the paclitaxel and quinidine bioavailability, recognised P-gp substrates, in male Sprague-Dawley rats (Park et al. 2012) and male C57 mice (Ravikumar Reddy et al. 2016). Moreover, it is important to note that this flavonoid was reported to have very low toxicity in rats [median lethal dose (LD_{50}) value of 10 g/kg] (Fraschini et al. 2002). Indeed, although a 400-fold lower dose of silymarin was tested (25 mg/kg) in our studies, no evidence of toxicity was observed.

Even though the exact mechanisms underlying flavonoid–P-gp interactions are not clear, several hypotheses have been proposed (Castro and Altenberg 1997; Shapiro and Ling 1997; Conseil et al. 1998; Jodoin et al. 2002; Wang et al. 2002; Zhang and Morris 2003b). Specifically, silymarin is known to inhibit P-gp functions by a direct interaction with the substrate binding site and, possibly, by preventing ATP hydrolysis (Kwon et al. 2006).

Taken together the available evidence on the potential of silymarin as a safe P-gp inhibitor, theoretically useful as an add-on therapy to several AEDs that are substrates for P-gp, the

present study was designed to evaluate the impact of silymarin on the pharmacokinetics and disposition of CBZ, OXC and PHT, using the Wistar rat as whole-animal model. Overall, our results support that silymarin increases the systemic drug exposure of almost all the AEDs and/or their main metabolites, but such effects were particularly pronounced for OXC and its main and pharmacologically active metabolite (LIC). These findings do suggest that the effects induced by silymarin on the pharmacokinetics of OXC are certainly due to the inhibition of P-gp; indeed, the effects promoted by verapamil (a reference P-gp-inhibitor used as positive control) on the plasma concentrations of OXC and LIC were qualitatively similar, but evidencing quantitatively a greater magnitude. As expected, the differences observed in the extent of systemic exposure to OXC and LIC after the pretreatment of the rats with silymarin or verapamil had a direct impact in the concentration levels of OXC and LIC reached in the brain, increasing significantly when compared with those attained in the control (vehicle) group. Considering together the results obtained in these *in vivo* experiments, and assuming as negligible the impact of other mechanisms that may contribute to the drug biodisposition of CBZ, OXC and PHT, it can be inferred that among these three AEDs OXC is the one with the highest affinity for P-gp.

Although there is some controversy regarding the classification of CBZ, OXC and PHT, as well as their metabolites, as P-gp substrates, a review of ZHANG ET AL. (2012) discusses in detail the available literature that supports whether the major AEDs are or are not P-gp substrates. However, so far, few *in vivo* non-clinical and clinical studies were conducted with this goal, being the current data primarily reported from *in vitro* assays. Despite the results of our previous *in vitro* studies (*Chapter III, section III.2*), as well as the available evidence supporting CBZ, OXC and PHT as P-gp substrates, this classification appears to be highly dependent of the experimental model employed (ZHANG ET AL. 2012a). Nevertheless, the existing studies involving OXC support our findings. Actually, either the *in vitro* (ZHANG ET AL. 2011a; FORTUNA ET AL. 2012) or clinical studies (ZADROZNIAK ET AL. 2009; ANTUNES ET AL. 2016), evidence that OXC and LIC are P-gp substrates. However, some *in vitro* data appears to denote an enantioselective interaction of *S*-LIC and *R*-LIC with P-gp, the latter evidencing a stronger P-gp interaction (FORTUNA ET AL. 2012). Moreover, whereas the studies conducted by ANTUNES ET AL. (2016) reported an increase of 10% in the AUC values of LIC by verapamil, ZADROZNIAK ET AL. (2009) demonstrated an enhancing of the anticonvulsant effect of OXC in the maximal electroshock-induced seizure model in mice in the presence of this P-gp inhibitor. In the case of CBZ, most the of available *in vitro* reports deny the involvement of P-gp on the disposition of this drug (OWEN ET AL. 2001; MAHAR DOAN ET AL. 2002; WEISS ET AL. 2003; BALTES ET AL. 2007; ZHANG ET AL. 2011a). Notwithstanding, CBZ was reported as P-gp substrate in a clinical study (RAMBECK ET AL. 2006), while evidence from studies in animal models is dubious (OWEN ET AL. 2001; POTSCHKA ET AL. 2001). In the case of PHT, even though its broad recognition as substrate of the P-gp (WEISS ET AL. 2003; LUNA-TORTÓS ET AL. 2008; ZHANG ET AL. 2010a), some reports appear to evidence a weak interaction with this drug efflux transporter (SCHINKEL ET AL. 1996). In addition, the *in vitro* transportation of PHT by P-gp was reported to be concentration-dependent, with higher doses

evidencing to saturate P-gp and reduce the proportion of drug pumped per unit time, which may also occur in *in vivo* conditions (ZHANG ET AL. 2010a).

On the other hand, it cannot be ruled out that the changes identified in the pharmacokinetics of CBZ, OXC and PHT are due at least in part to the interference of silymarin and verapamil on the activity of CYP isoenzymes. Actually, in humans, the co-localization of P-gp and CYP3A4 in the polarized epithelial cells of excretory organs such as the liver, kidney and intestine, to eliminate foreign compounds, is responsible by a substantial overlap in substrate specificity, acting synergically as a functional barrier to the systemic exposure of xenobiotics, including therapeutic drugs (LI ET AL. 2011). Indeed, flavonoids are recognized as inducers and/or inhibitors of drug-metabolizing CYP isoenzymes (GALATI AND O'BRIEN 2004), being these effects directly dependent of their structure, concentration and experimental conditions (TASSANEEYAKUL ET AL. 1993; GUENGERICH ET AL. 1994). Nevertheless, the results of a clinical study involving the exposure to milk thistle extract (a natural source of silymarin) showed no significant influence on CYP1A2, CYP2C9, CYP2D6 and CYP3A4/5 activities (KAWAGUCHI-SUZUKI ET AL. 2014), whereas another report suggested some inhibition of the CYP2C9 isoenzyme activity by this herbal extract (BRANTLEY ET AL. 2010). Considering verapamil, it is a well-known inhibitor of the human CYP3A4 isoenzyme, which is primary involved in the oxidative metabolism of CBZ to its active metabolite CBZ-E (SUMMERS ET AL. 2004; PATSALOS ET AL. 2008). This information helps to explain the changes observed in the metabolism of CBZ after the pretreatment of rats with verapamil; indeed, a marked decreased in the CBZ-E formation was found in the first 2.5-h period after CBZ dosing (Figure IV.2.3B). However, the pretreatment with silymarin did not induce major alterations in the CBZ-E formation, suggesting that silymarin does not interfere with metabolic pathway of conversion of CBZ to CBZ-E in rat. Regarding the metabolism of PHT, it is known that this drug is extensively *para*-hydroxylated in man primarily by CYP2C9 and CYP2C19 to an inactive metabolite (HPPH) (PATSALOS ET AL. 2008). However, taking into account the pharmacokinetic profiles obtained for PHT and HPPH in rats in the presence of silymarin and verapamil, it can be inferred the absence of interference of both compounds with the corresponding CYP isoenzymes in rat (mainly CYP2C11 and CYP2D1/2) (MAGALHÃES ET AL. 2016). On the other hand, with regard to OXC metabolism, it is widely recognised that CYP isoenzymes are not involved in the reductive metabolism of OXC to LIC, which occurs enantioselectively in man in approximately a 4:1 enantiomeric ratio (MAY ET AL. 2003; FLESCH 2004; KIM ET AL. 2015). Thus, globally, confronting the results obtained in our work with the available data on the metabolism of the AEDs herein considered and the potential interference of verapamil and silymarin with CYP isoenzymes and P-gp, it is likely that the silymarin-induced effect on the pharmacokinetics of OXC is in fact due to the inhibition of the P-gp activity.

Besides the promising *in vivo* activity of silymarin as P-gp inhibitor, representing a drug candidate of interest for further pharmacological development as a reversing agent of the pharmacoresistance phenomenon in epilepsy, it is also important to highlight in this context other potentially useful neuropharmacological properties ascribed to silymarin and other flavonoid-type compounds (COLETA ET AL. 2008; HU ET AL. 2011; ABBASI ET AL. 2012; ROMANO ET AL.

2013). Indeed, several flavonoids also appear to be promising candidates as antiepileptic/anticonvulsant drugs (BALUCHNEJADMOJARAD ET AL. 2010; YOON ET AL. 2011; NASSIRI-ASL ET AL. 2013; NASSIRI-ASL ET AL. 2014), which further increases their potential for the treatment of refractory epilepsy. Specifically, the *Silybum marianum* seeds extract, in which silymarin is the an important bioactive constituent, demonstrated anticonvulsant activity against seizure in pentylenetetrazole-kindled mice (WAQAR ET AL. 2016). Hence, the silymarin and other flavonoid-type compounds are natural compounds of interest not only to optimize the AED treatment in drug-resistant epilepsy, as an add-on therapy, but also to directly potentiate the anticonvulsant activity.

IV.2.5. Conclusions

The disappointment in terms of safety and selectivity brought by the early generations P-gp inhibitors led to an incessant search for new and safer therapeutic options. Although the interest of flavonoids as P-gp inhibitors has been recognised through *in vitro* and *in vivo* models, to the best of our knowledge, the results of this work constitute the first direct evidence of the effect of the flavonoid silymarin on the pharmacokinetics of CBZ and PHT, but particularly of OXC. The pretreatment with silymarin showed a pronounced increase in the extent of systemic and brain exposure to OXC and its pharmacologically active metabolite LIC, which most likely occurred through the inhibition of P-gp. Hence, the strategy of coadministration of AEDs with safe and potent flavonoid-type P-gp inhibitors should be pursed in order to find effective agents to reverse the pharmacoresistance in epilepsy. Moreover, flavonoid compounds, such as silymarin, can also be promising drug candidates as adjuvant therapy for refractory epilepsy due to their intrinsic anticonvulsant properties.

IV.3. Experimental

Influence of the dual combination of silymarin and (-)-epigallocatechin gallate, natural dietary flavonoids, on the pharmacokinetics of oxcarbazepine in rats

IV.3.1. Introduction

In the recent years, several indigenous medicinal plants have been identified as possessing endogenous bioactive compounds that can be used to treat different human ailments (Visweswari et al. 2010; Ekor 2014; Newman and Cragg 2016). Actually, medicinal herbs are being increasingly used by the general population in the Western world and are also a subject of study interest by the scientific community (Lee 2000; Pathak and Udupa 2010). Particularly, the therapeutic potential of flavonoid compounds has been gaining relevance over the last years. These phytochemical constituents are a group of structurally related compounds present in the human diet, being widespread in vegetables, fruits, flowers, seeds and grains (Bansal et al. 2009; Mohana et al. 2016). The chemical diversity of flavonoid structures is responsible for a wide range of bioactivities including, among others, anti-inflammatory, anti-proliferative, pro-apoptotic, free-radical scavenging, antioxidant, antitumor, antimicrobial, antiviral, hormonal and anticonvulsant properties (Buer et al. 2010; Wasowski and Marder 2012; Ferreira et al. 2015; Hoensch and Oertel 2015).

Accordingly, the exploitation of potentially beneficial interactions between flavonoid-type compounds with multiple bioactivities and clinically available drugs could be a valuable strategy in certain circumstances, namely in overcoming some mechanisms underlying multidrug resistance (Boumendjel et al. 2002; Thomas and Coley 2003; Peng et al. 2006; Bansal et al. 2008; Pathak and Udupa 2010). Actually, in spite of the current availability of numerous AEDs in the clinical practice, the drug-resistant epilepsy is an unmet medical need, affecting about one third of epilepsy patients (Sørensen and Kokaia 2013; Alexopoulos 2013; Ventola 2014; Sharma et al. 2015; Baulac et al. 2015; Franco et al. 2016). The multidrug transporter hypothesis remains as one of the main accepted theories to explain the pharmacoresistance to AEDs (Löscher et al. 2013). This hypothesis emphasizes the role of the overexpression and/or overactivity of multidrug efflux transporters, such as the P-gp, in capillary endothelial cells of the blood-brain barrier, restricting the AEDs uptake into the brain of non-responsive patients (Löscher and Potschka 2005a; Pardridge 2007; Löscher and Sills 2007; Zhang et al. 2012a; Löscher et al. 2013). Moreover, P-gp is also largely expressed in the luminal membrane of small intestinal epithelial cells and in the apical membranes of excretory cells such as hepatocytes and kidney proximal tubule epithelia, determining the pharmacokinetics and drug biodisposition of P-gp substrate drugs (Wessler et al. 2013; Prachayasittikul and Prachayasittikul 2016). Regarding this matter, the P-gp inhibition arises as an attractive therapeutic approach to reverse the drug-resistant phenotype in epilepsy, particularly because several AEDs including OXC and its pharmacologically active metabolite LIC have been identified as substrates of this drug efflux pump (Figure IV.3.1) (Zhang et al. 2012a).

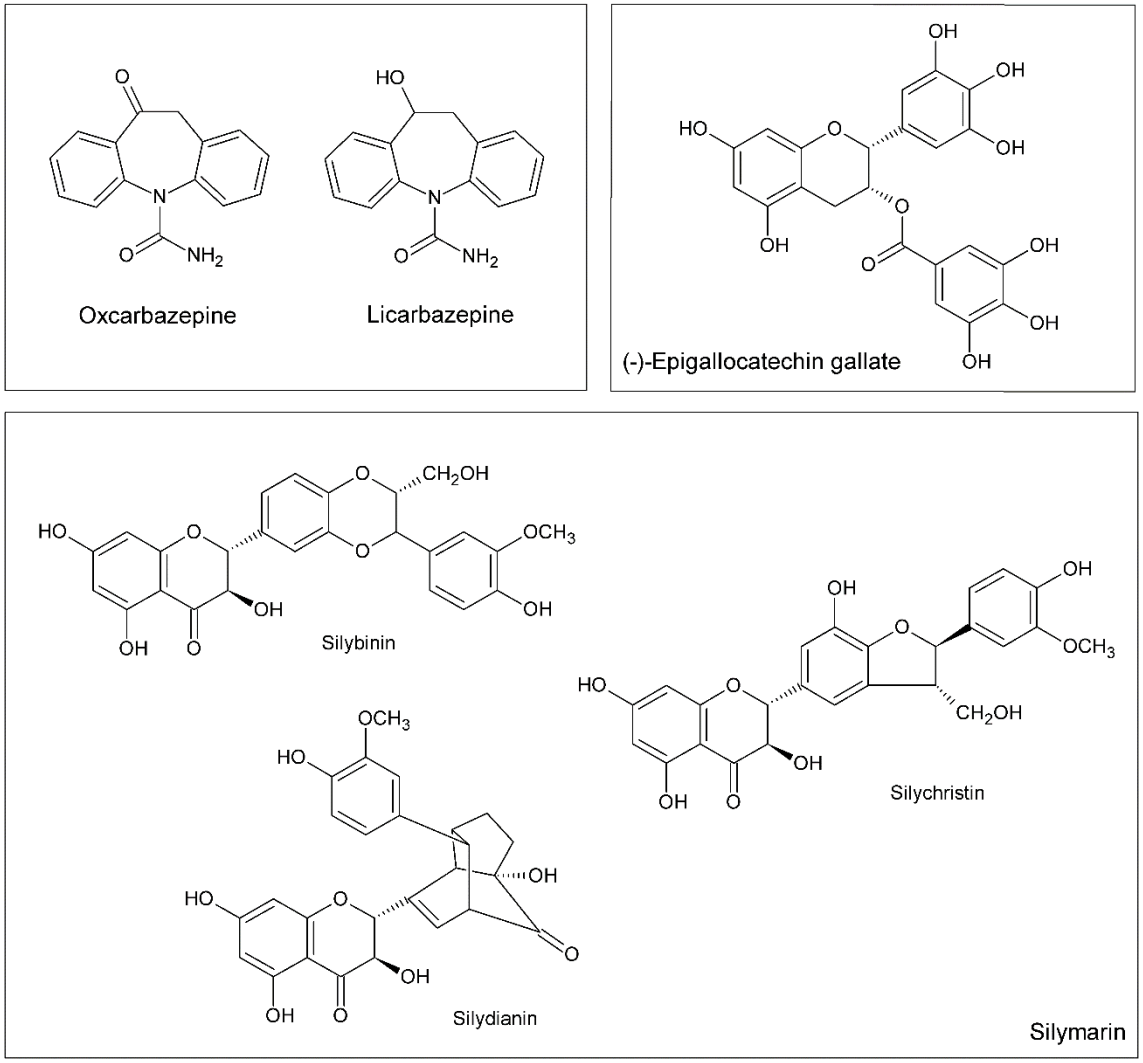

Figure IV.3.1. Chemical structures of oxcarbazepine and its active metabolite licarbazepine, the flavonoid (-)-epigallocatechin gallate and some constituents of silymarin (silybinin, silychristin and silydianin).

The recognition of the implication of the P-gp–mediated multidrug resistance not only in epilepsy but also in many other clinically important diseases has led to concerted efforts to search for therapeutically useful P-gp inhibitors (STĘPIEŃ ET AL. 2012; FRENCH ET AL. 2013; FELDMANN AND KOEPP 2016). In this context, over the last years, aiming at developing more selective and safer P-gp inhibitors than those of the early generations, a great attention has been given to naturally occurring flavonoids as selective and non-cytotoxic P-gp inhibitors (BANSAL ET AL. 2008; BANSAL ET AL. 2009; FERREIRA ET AL. 2015; MOHANA ET AL. 2016). Indeed, there are several *in vitro* and *in vivo* studies describing the potential of flavonoid compounds as P-gp inhibitors, including silymarin and (-)-EPG (Figure IV.3.1) (JODOIN ET AL. 2002; ZHANG AND MORRIS 2003a; CHUNG ET AL. 2005; KITAGAWA 2006; PARK ET AL. 2012).

Taking into account the daily consumption of complex mixtures of flavonoid compounds, exhibiting a panoply of biological activities, it is of great interest the evaluation of the synergic pharmacological effect of these compounds (HARASSTANI ET AL. 2010; CHOI ET AL. 2013; YU ET AL. 2013; JARAMILLO-CARMONA ET AL. 2014). Thus, the study of the synergic activities of dual flavonoid

combinations as P-gp inhibitors emerges as a valuable approach, which may be useful to circumvent the multidrug resistance mediated by P-gp. In fact, the combination of different flavonoids as P-gp inhibitors is supported by the recognition that there are multiple binding sites for substrates and inhibitors on P-gp (YANG AND LIU 2004). Hence, in the path to develop a strategy to reverse the P-gp–mediated AED resistance, the influence of the combined use of silymarin and (-)-EPG on the pharmacokinetics of OXC, a well-known P-gp substrate widely used in the treatment of epilepsy seizures, was evaluated herein.

IV.3.2. Materials and methods

IV.3.2.1. Drugs and materials

Standards of silymarin, verapamil (a reference P-gp inhibitor used as positive control) and PRM (used as IS) were purchased from Sigma-Aldrich (St. Louis, MO, USA), while (-)-EPG was obtained from TCI (Tokyo, Japan). Carboxymethylcellulose sodium salt and DMSO were obtained from Sigma-Aldrich (St. Louis, MO, USA). Oral suspension of OXC (Trileptal® 60 mg/mL), sodium chloride 0.9% solution for injection (Labesfal, Portugal), heparin sodium 5000 U.I./mL for injection (B. Braun Medical, Portugal), and pentobarbital (Eutasil® 200 mg/ml, Ceva Saúde Animal; used as anaesthetic drug) were commercially acquired. Introcan® Certo IV indwelling cannula (22G; 0.9 x 2.5 mm) made of polyurethane were supplied from B. Braun Melsungen AG (Melsungen, Germany).

Methanol and acetonitrile, both of HPLC gradient grade, and ethyl acetate were purchased from Fisher Scientific (Leicestershire, United Kingdom). The ultra-pure water (HPLC grade, >18 MΩ.cm) was prepared by means of a Milli-Q water apparatus from Millipore (Milford, MA, USA).

IV.3.2.2. Animals

Healthy adult male Wistar rats (381 ± 16 g) of approximately 15 weeks old were obtained from local animal facilities (Faculty of Health Sciences of the University of Beira Interior, Covilhã, Portugal). The rats were maintained under controlled environmental conditions in particular the temperature (20 ± 2 ºC), relative humidity (55 ± 5%), and light/dark cycle (12 h). During all the experimental procedures, tap water and the standard rodent diet (4RF21, Mucedola, Italy) were available *ad libitum*. All experimental and care procedures were conducted in accordance with the European Directive (2010/63/EU) regarding the protection of laboratory animals used for scientific purposes. In addition, the experimental procedures were reviewed and approved by the Portuguese National Authority for Animal Health, Phytosanitation and Food Safety (DGAV – Direção Geral de Alimentação e Veterinária).

IV.3.2.3. Systemic pharmacokinetic study

At the night on the day before the pharmacokinetic studies, a lateral tail vein of each rat was cannulated under anaesthesia [pentobarbital 60 mg/kg; ip injection] by insertion of an Introcan® Certo IV indwelling cannula (22G; 0.9 x 2.5 mm) that was used for serial blood sampling. The rats fully recovered from anaesthesia overnight, and then in the morning were subjected to pharmacological treatments all administered by ip route as mentioned below. The conscious and freely moving rats were appropriately restrained only at the moment of administration of the treatments and blood collections.

In this pharmacokinetic study a total of thirty-six rats were used. The flavonoids silymarin and (-)-EPG were tested individually and in dual combinations at three fixed-ratios (1:1; 1:3 and 3:1) taking into account the final dose of 25 mg/kg. The animals were randomly assigned to one of six groups [experimental and control (verapamil) groups, *n* = 6] receiving the ip pretreatment with silymarin (25 mg/kg), (-)-EPG (25 mg/kg), silymarin/(-)-EPG 1:1 (12.5/12.5 mg/kg; fixed-ratio combination of 1:1), silymarin/(-)-EPG 1:3 (6.25/18.75 mg/kg; fixed-ratio combination of 1:3), silymarin/(-)-EPG 3:1 (18.75/6.25 mg/kg; fixed-ratio combination of 3:1), or verapamil (25 mg/kg, positive control group). The compounds [(-)-EPG, silymarin and verapamil] were dissolved in DMSO and then suspended in carboxymethylcellulose sodium salt aqueous solution 0.5% (m/v), containing the final suspension a concentration of 5% DMSO (v/v). Appropriate volumes of these suspensions (5 mL/kg of rat weight) were administered by ip route to the respective groups. After 1-h period, all the groups of rats were treated with OXC (50 mg/kg, ip). The OXC dose was chosen taking into account the work of HAINZL ET AL. (2001), in which a OXC dose of 20 mg/kg was used. However, knowing that reduced LIC concentrations were found in rat plasma and brain (HAINZL ET AL. 2001), in the current work we considered a dose of OXC 2.5-fold higher (50 mg/kg) in order to characterize the LIC pharmacokinetic profile as much as possible. The commercial suspension of OXC (Trileptal® 60 mg/mL) was appropriately diluted with carboxymethylcellulose sodium salt aqueous solution 0.5% (m/v) and an appropriate volume was administered considering a total volume of administration of 10 mL/kg of rat weight. Multiple serial blood samples of approximately 0.3 mL were collected through the cannula inserted in a lateral tail vein into heparinized tubes before and at 0.5, 1, 1.5, 2, 3, 4, 6, 8 and 12 h after OXC administration. The blood samples were centrifuged at 4000 rpm for 10 min (4 ºC) to separate the plasma that was collected and stored at −20 ºC until analysis.

IV.3.2.4. Plasma-to-brain biodistribution study

To further investigate the potential effects of dual silymarin/(-)-EPG combinations on the plasma-to-brain distribution of OXC, a separate study was performed. In this study, twelve rats were randomly assigned to one of four groups (*n* = 3), which received the pretreatment with silymarin/(-)-EPG 1:1, silymarin/(-)-EPG 1:3, silymarin/(-)-EPG 3:1 or verapamil (25 mg/kg; positive control group). One hour after pretreatment administration, a single dose of OXC

(50 mg/kg) was given by ip route to rats of all groups. The flavonoids and OXC suspensions were prepared as previously mentioned in s*ection IV.3.2.3* Then, at 1.5 h post OXC dosing the rats were sacrificed by decapitation and the tissues of interest were obtained (blood and brain). Blood (approximately 0.3 mL) was immediately collected into heparinised tubes, and then the brain was quickly removed and weighed. The blood samples were centrifuged at 4000 rpm for 10 min (4 ºC) to separate the plasma. The brain tissue was homogenized in 0.1 M sodium phosphate buffer at pH 5.0 (4 mL per gram of tissue) using an Ultra-Turrax® tissue homogenizer and centrifuged at 13500 rpm for 10 min (4 ºC). The plasma and brain homogenate supernatant samples were collected and stored at −20 ºC until analysis.

IV.3.2.5. Bioanalytical method validation

Plasma and brain concentrations of OXC and its active metabolite (LIC) were determined using a LLE procedure followed by HPLC analysis coupled to a DAD, which is based on a previously published assay with minor modifications (FERREIRA ET AL. 2016b). This technique was posteriorly validated in rat plasma and brain matrices in agreement with the international guidelines on bioanalytical method validation (U.S. FOOD AND DRUG ADMINISTRATION 2001; EUROPEAN MEDICINES AGENCY 2011) for specific validation parameters such as linearity, LLOQ, accuracy, precision and recovery.

The linearity was assessed using three calibration curves prepared with six spiked rat plasma or brain calibration standards, assayed on three different days (*n = 3*). The calibration standards set at the concentration ranges of 0.1-25 µg/mL for OXC and 0.05-40 µg/mL for LIC were daily prepared by spiking aliquots of blank plasma or brain homogenate with each one of these combined solutions. The stock solution of the IS was also prepared in methanol (2 mg/mL) and the working solution (500 µg/mL) was obtained after diluting an appropriate volume of the stock solution with water-methanol (50:50, v/v). A plot of the ratio between the analyte and IS peak areas, as function of the corresponding nominal concentrations, were used to construct the calibration curves. The data were fitted to a weighted linear regression analysis employing the weighting factor that yielded the best fit of peak-area ratios *versus* concentration (ALMEIDA ET AL. 2002). The lowest concentration of the target analytes in plasma or brain samples that can be quantified reliably, with an acceptable accuracy and precision, was used to establish the lowest calibration standard of the calibration curves and corresponded to the LLOQ. The interday precision and accuracy of the assay were evaluated on three consecutive days (*n* = 3), using four QC samples representing the LLOQ (QC_{LLOQ}), low (QC_1), medium (QC_2) and high (QC_3) ranges of the calibration curves. These concentrations were 0.1, 0.3, 12.5 and 22.5 µg/mL for OXC; and 0.05, 0.15, 20 and 36 µg/mL for LIC. Similarly, five sets of QC samples analysed in a single day (*n* = 5) were used to assess the intraday precision and accuracy. The acceptance criteria were those referred in the bioanalytical method validation guidelines, this is, the intra and interday precision (expressed as percentage of CV) must be lower than or equal to 15% (or 20% in the LLOQ) and the accuracy (expressed as percentage of *bias*) must be within ±15%

(or ±20% in the LLOQ). Lastly, three QC samples (QC_1, QC_2 and QC_3) were used to determine the absolute recovery of the analytes from the samples. This parameter was calculated through the comparison between the analytes peak areas from extracted rat plasma or brain QC samples with those obtained after direct injection of non-extracted solutions at the same nominal concentrations (*n* = *5*).

IV.3.2.6. Drug analysis

Each aliquot (100 µL) of rat plasma or brain homogenate supernatant, spiked with 20 µL of the IS working solution (PRM, 500 µg/mL), was added of 300 µL of ice-cold acetonitrile and 1 mL of ethyl acetate (LLE solvent). Then, the mixture was vortex-mixed for 30 s and centrifuged at 13500 rpm for 3 min. The upper organic layer was transferred to a clean glass tube and, afterwards, the sample was re-extracted twice more with ethyl acetate (1 mL each time) using the conditions previously described. The whole organic extract was evaporated to dryness under a nitrogen stream at 45 °C and then reconstituted with 100 µL of the mobile phase. Finally, an aliquot (20 µL) of this final sample was injected into the chromatographic system. The LLOQ was established at 0.1 µg/mL for OXC and 0.05 µg/mL for LIC in both matrices (plasma and in brain tissue homogenate).

The chromatographic analysis was carried out using an HPLC-DAD system (Shimadzu LC-2010A HT Liquid Chromatography and Shimadzu SPD-M20A). All instrumental parts were automatically controlled by LabSolutions software (Shimadzu, Kyoto, Japan). The chromatographic separation of OXC, LIC and PRM (IS) was carried out at 35 °C on a reversed-phase LiChroCART® Purospher Star column (C_{18}, 55 mm × 4 mm, 3 µm particle size; Merck KGaA, Darmstadt, Germany) by isocratic elution with a mobile phase composed of water/methanol/acetonitrile (69:25:6, v/v/v) pumped at a flow rate of 1.0 mL/min. The wavelength of 215 nm was selected for the detection of LIC, and 230 nm for OXC and PRM (IS).

IV.3.2.6.1. Pharmacokinetic analysis

The C_{max} and t_{max} of OXC and LIC in plasma were obtained directly from the experimental data. The remaining pharmacokinetic parameters were estimated from the individual plasma concentration-time profiles determined at each time point by non-compartmental pharmacokinetic analysis using the WinNonlin® version 5.2 (Pharsight Co, Mountain View, CA, USA). For each rat, the estimated pharmacokinetic parameters included the $AUC_{0\text{-}t}$ that was calculated by the linear trapezoidal rule; the $AUC_{0\text{-}\infty}$, determined from $AUC_{0\text{-}t} + (C_{last}/k_{el})$, where C_{last} is the last quantifiable concentration and k_{el} the apparent terminal rate constant calculated by log-linear regression of the terminal segment of the concentration-time profile. Additionally, the $t_{1/2el}$ and MRT were also estimated. The concentrations lower than the limit of quantification of the assay were taken as zero for all calculations.

IV.3.2.7. Pharmacokinetic analysis

Data were reported as the mean ± SEM, unless otherwise noted. Comparisons between the positive control (verapamil) group *vs* experimental groups were performed using one-way ANOVA with the *post hoc* Dunnett's test, except for the t_{max} parameter where the nonparametric Kruskal-Wallis with the *post hoc* Dunn's test was applied. The differences were considered statistically significant for *p*-values lower than 0.05 ($p < 0.05$).

IV.3.3. Results

IV.3.3.1. Bioanalytical method validation

Through the results obtained in the validation assays, it can be concluded that the HPLC-DAD methodology was reliable in supporting the pharmacokinetics and biodistribution studies herein performed. Actually, the calibration curves obtained in rat plasma and brain demonstrated a consistent correlation between analyte-IS peak area ratios and the corresponding nominal concentrations, being linear ($r^2 \geq 0.9920$) for OXC and LIC within the defined concentration ranges. Those calibration curves were subjected to weighted linear regression analysis using $1/x^2$ as the weighting factor, considering the wide concentration ranges, and in order to compensate the heteroscedasticity detected. Additionally, the LLOQ values, as well the data for inter and intraday precision and accuracy fulfilled the acceptance criteria established by the international guidelines (U.S. FOOD AND DRUG ADMINISTRATION 2001; EUROPEAN MEDICINES AGENCY 2011). Indeed, the overall intra and interday imprecision (% CV) in rat plasma and brain was lower than 11.57% for OXC and lower than 11.56% for LIC; whereas the overall intra and interday inaccuracy (% *bias*) in rat plasma and brain ranged between –0.53–11.15% for OXC and between –12.35–7.26% for LIC. The absolute recovery values demonstrated a good recovery of all analytes over the evaluated concentration ranges, being its values equal to or higher than 80.0%. Actually, the absolute recoveries for OXC ranged between 80.0–85.8% in rat plasma and 82.1–89.5% in rat brain, and for LIC ranged between 91.1–99.6% and 87.4–91.6%, respectively.

IV.3.3.2. Effects of silymarin, (-)-EPG and their combinations on the systemic pharmacokinetics of OXC

The mean plasma concentration-time profiles ($n = 6$) of OXC and its active metabolite LIC obtained in rats after pretreatment with a single ip dose of silymarin (25 mg/kg), (-)-EPG (25 mg/kg), silymarin/(-)-EPG 1:1 (12.5/12.5 mg/kg), silymarin/(-)-EPG 1:3 (6.25/18.75 mg/kg), silymarin/(-)-EPG 3:1 (18.75/6.25 mg/kg) or verapamil (25 mg/kg, positive control), followed by an ip administration of OXC (50 mg/kg), are shown in Figure IV.3.2.

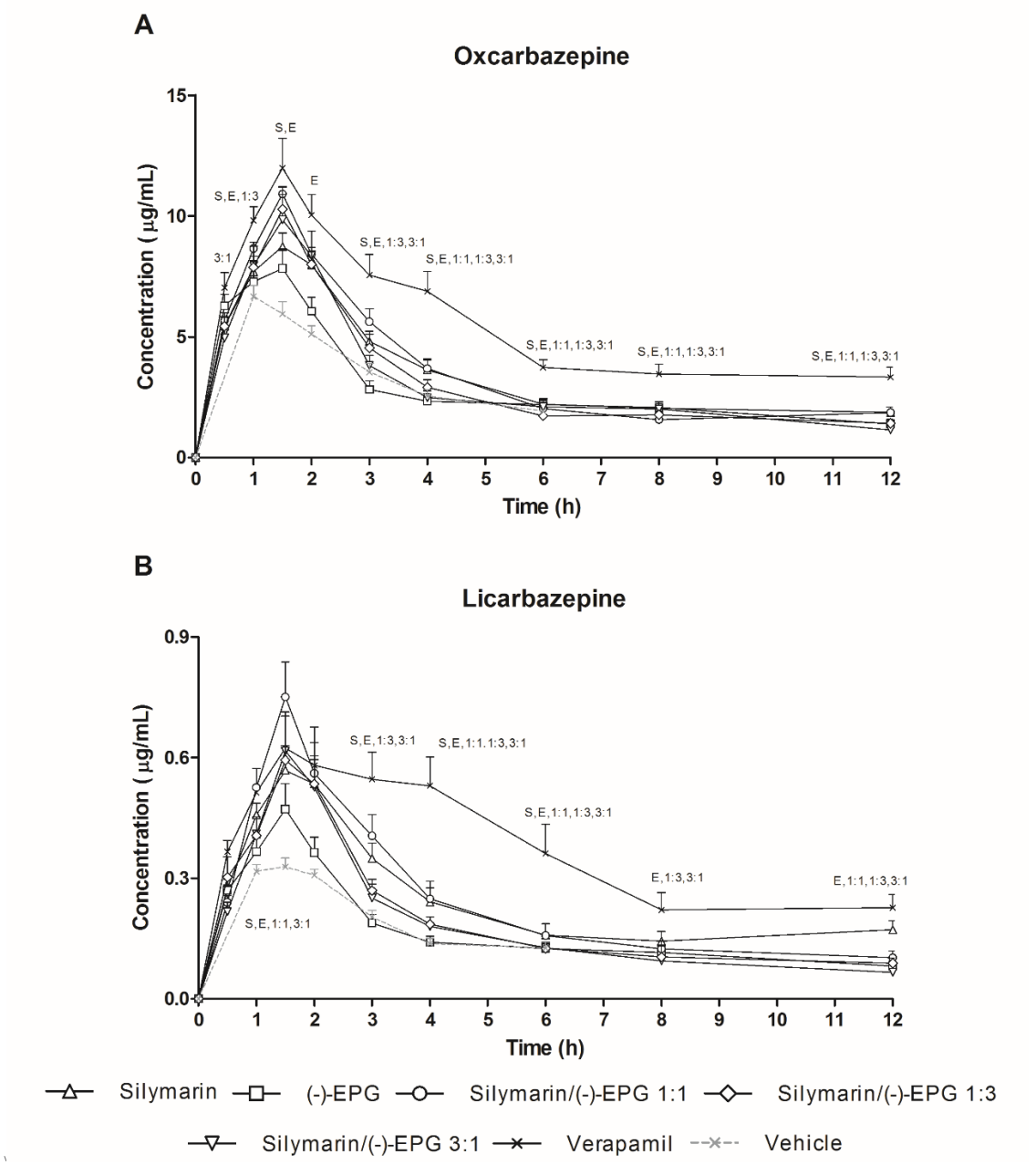

Figure IV.3.2. Mean plasma concentration-time profiles of oxcarbazepine (A) and its active metabolite licarbazepine (B) obtained, over a 12-h period, in rats pretreated with silymarin (25 mg/kg; S), (-)-EPG (25 mg/kg; E), silymarin/(-)-EPG 1:1 (12.5/12.5 mg/kg; fixed-ratio combination of 1:1), silymarin/(-)-EPG 1:3 (6.25/18.75 mg/kg; fixed-ratio combination of 1:3), silymarin/(-)-EPG 3:1 (18.75/6.25 mg/kg; fixed-ratio combination of 3:1), or verapamil (25 mg/kg) 1 h before the intraperitoneal administration of oxcarbazepine (50 mg/kg). The dashed line represents the data of a vehicle control group from previous experiments (rats pretreated with the corresponding volume of the compound's vehicle instead of flavonoids or verapamil formulations). Data are expressed as the mean values ± standard error of the mean (SEM) of six determinations (n = 6). Comparisons between the verapamil (positive control) group *vs* experimental groups were performed using one-way ANOVA with the *post hoc* Dunnett's test. Above each time point is mentioned which groups have statistically significant differences in relation to the verapamil group ($p < 0.05$).

As represented in Figure IV.3.2A, plasma OXC concentrations determined in the rats pretreated with flavonoid compounds were more comparable to those achieved in the positive control (verapamil) group during the first 2 h after OXC administration. However, this similarity in the OXC pharmacokinetic profiles was more marked for the three flavonoid combinations groups (*p*-values were usually higher than 0.05 in relation to verapamil group). Although none of the individual flavonoids [silymarin and (-)-EPG] or dual flavonoid combinations enable to achieve higher plasma OXC concentrations than those reached by the administration of the classic P-gp inhibitor (verapamil), these results are still interesting as these dual flavonoid combinations [silymarin and (-)-EPG] are potentially safer than verapamil. As in this study our primary objective was to demonstrate the non-inferiority of flavonoid combinations in relation to verapamil, a negative control (vehicle) group was not included in the experimental design. However, in previous experiments a vehicle group (a group of rats pretreated with the corresponding volume of the compound's vehicle instead of flavonoids or verapamil formulations) was considered and such data were also included in Figure IV.3.2 only for supportive purposes (dashed line). Indeed, visually we can observe that the individual flavonoids silymarin and (-)-EPG expressively increased the plasma concentration levels of OXC around the t_{max} period (1.500 h) in comparison with the drug levels found in the rats of the vehicle group. Nevertheless, the pretreatment with silymarin/(-)-EPG combinations, in the three tested fixed-ratios, permitted to achieve even greater concentrations of OXC at this post-dose time period. In point of fact, as previously mentioned, these concentrations were closer to those obtained in the verapamil (positive control) group. Analysing the mean pharmacokinetic profiles obtained for LIC (Figure IV.3.2B) and comparing these profiles with those obtained for the parent drug (OXC), it is evident a close similarity in the pattern of the concentration–time curves. However, the magnitude of the mean LIC concentrations in plasma were 15- to 18-fold lower than those of OXC.

The main plasma pharmacokinetic parameters obtained for OXC and LIC after non-compartmental analysis of their mean concentration-time profiles are presented in Table IV.3.1. As expected, the quantitative values found for the pharmacokinetic parameters confirm the observational analysis previously performed to the mean plasma pharmacokinetic profiles. The pretreatment with the individual flavonoids or their dual combinations did not significantly change the median time (1.500-1.750 h) to reach the peak plasma concentrations (C_{max}) of OXC and LIC when comparing to the verapamil group. Relatively to the degree of systemic exposure (as assessed by C_{max}), statistically significant differences were detected for OXC when comparing the silymarin or (-)-EPG individual groups with the verapamil group ($p < 0.05$). Nevertheless, statistically significant differences were not found for the comparison between the three experimental groups in which the flavonoid combinations were tested and the verapamil group. Actually, whereas silymarin and (-)-EPG individually originated OXC C_{max} values inferior to verapamil in approximately 31-36%, the flavonoid combinations allowed to obtain C_{max} values that only differed from the positive control group in about 14-18%. Indeed, the positive impact that pretreatment with flavonoids, particularly with flavonoid

combinations, had on increasing the plasma concentrations of OXC and LIC during the first 2-h period after OXC administration was translated in the absence of statistically significant differences in the rate of systemic drug exposure when compared to verapamil (as assessed by t_{max} and C_{max}). However, the effect induced by flavonoids on the biodisposition of OXC and LIC seems to be lost earlier than the effect promoted by verapamil, which was reflected in the statistically significant differences ($p < 0.05$) usually found between experimental and positive control groups for the pharmacokinetic parameters predictive of the extent of systemic drug exposure (AUC_{0-t}).

Table IV.3.1. Pharmacokinetic parameters estimated by non-compartmental analysis of the plasma concentration-time profiles of oxcarbazepine (OXC) and its active metabolite licarbazepine (LIC) obtained in rats after intraperitoneal pretreatment with silymarin (25 mg/kg), (-)-epigallocatechin gallate [(-)-EPG; 25 mg/kg], silymarin/(-)-EPG (12.5/12.5 mg/kg, fixed-ratio combination of 1:1) silymarin/(-)-EPG (6.25/18.75 mg/kg, fixed-ratio combination of 1:3), silymarin/(-)-EPG (18.75/ 6.25 mg/kg, fixed-ratio combination of 3:1) or verapamil (25 mg/kg) 1 h before a single intraperitoneal administration of OXC (50 mg/kg) (n = 6, unless otherwise noted). Data are expressed as the mean values ± standard error of the mean (SEM), exception for t_{max} that is expressed as the median value (range).

		Parameters						
		t_{max} (h)	C_{max} (µg/mL)	AUC_{0-t} (µg.h/mL)	$AUC_{0-\infty}$ (µg.h/mL)	k_{el} (h^{-1})	$t_{1/2el}$ (h)	MRT (h)
OXC	Verapamil	1.500 (1.000-2.000)	13.069 ± 0.829	64.303 ± 4.347	ND	ND	ND	ND
	Silymarin	1.500 (1.000-2.000)	8.954 ± 0.622 *	41.407 ± 1.836 *	ND	ND	ND	ND
	(-)-EPG	1.500 (0.500-1.500)	8.349 ± 0.771 *	34.902 ± 2.266 *	46.419[a]	0.135[a]	5.13[a]	6.47[a]
	Silymarin/ (-)-EPG 1:1	1.500 (1.500-2.000)	11.243 ± 0.375	42.533 ± 2.086 *	51.514 ± 1.588[b]	0.190 ± 0.007[b]	3.67 ± 0.13[b]	6.35 ± 0.21[b]
	Silymarin/ (-)-EPG 1:3	1.500 (1.000-2.000)	10.711 ± 0.714	38.255 ± 1.471 *	48.450 ± 0.199[c]	0.174 ± 0.021[c]	4.27 ± 0.58[c]	6.14 ± 0.32[c]
	Silymarin/ (-)-EPG 3:1	1.500 (1.000-2.000)	11.014 ± 0.684	37.672 ± 2.628 *	41.287 ± 1.325[b]	0.179 ± 0.013[b]	4.03 ± 0.32[b]	5.33 ± 0.17[b]
LIC	Verapamil	1.750 (1.500-4.000)	0.682 ± 0.082	4.369 ± 0.507	ND	ND	ND	ND
	Silymarin	1.500 (1.500-2.000)	0.579 ± 0.056	2.855 ± 0.172 *	ND	ND	ND	ND
	(-)-EPG	1.500 (1.500-1.500)	0.472 ± 0.064	1.937 ± 0.149 *	ND	ND	ND	ND
	Silymarin/ (-)-EPG 1:1	1.500 (1.000-2.000)	0.828 ± 0.070	2.849 ± 0.243 *	3.256 ± 0.388[c]	0.194 ± 0.006[c]	3.59 ± 0.12[c]	6.07 ± 0.12[c]
	Silymarin/ (-)-EPG 1:3	1.500 (1.500-2.000)	0.608 ± 0.043	2.338 ± 0.113 *	2.549[a]	0.204[a]	3.40[a]	5.51[a]
	Silymarin/ (-)-EPG 3:1	1.500 (1.000-2.000)	0.667 ± 0.080	2.166 ± 0.271 *	2.334 ± 0.167[d]	0.316 ± 0.087[d]	2.85 ± 0.79[d]	4.47 ± 0.85[d]

*AUC, area under the concentration-time curve; AUC_{0-t}, AUC from time zero to the last sampling time; $AUC_{0-\infty}$, AUC from time zero to infinity; C_{max}, peak concentration; k_{el}, apparent terminal rate constant; MRT, mean residence time; ND, not determined; $t_{1/2el}$, apparent terminal elimination half-life; t_{max}, time to reach C_{max}. [a]n = 1; [b]n = 4; [c]n = 3; [d]n = 2; * p < 0.05, significantly different from the verapamil group. Comparisons between the verapamil (positive control group) vs experimental groups were performed by one-way ANOVA with the post hoc Dunnett's test, the exception was the t_{max} parameter in which the nonparametric Kruskal-Wallis with the post hoc Dunn's test was applied.*

IV.3.3.3. Effects of silymarin and (-)-EPG combinations on the OXC and LIC plasma-to-brain biodistribution

As the brain is the target organ (biophase) for the therapeutic activity of OXC and LIC, an additional study was designed to assess and compare the impact of the pretreatment of the three flavonoid fixed-ratio combinations [silymarin/(-)-EPG 1:1, silymarin/(-)-EPG 1:3, silymarin/(-)-EPG 3:1] on the OXC and LIC plasma-to-brain biodistribution, also using verapamil (a classic P-gp inhibitor) as positive control. In this case, the animals were sacrificed at 1.5 h after dosing with OXC and the mean concentration levels of OXC and LIC determined in plasma samples and brain tissues are shown in Figure IV.3.3. Analysing and comparing the obtained results, it is evident that no statistically significant differences were found in the plasma and brain concentrations of OXC and LIC between the group of rats pretreated with verapamil and the groups that received flavonoid combinations. These findings support the similar efficacy between the dual flavonoid combinations tested and verapamil in the increasing of the brain exposure to OXC and LIC, reflecting the absence of differences in the systemic drug exposure observed at the time of C_{max} (1.500-1.750 h post OXC dose; Table IV.3.1).

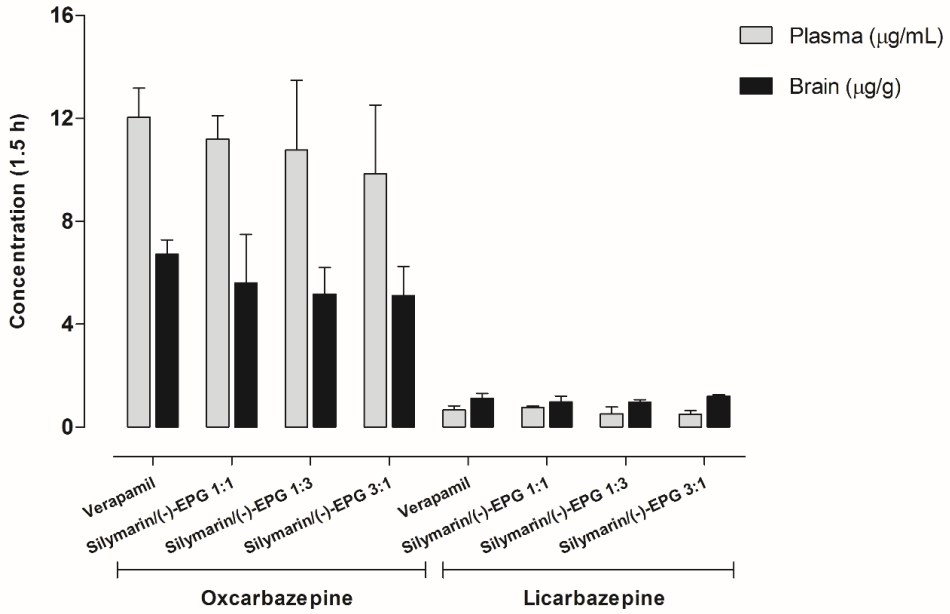

Figure IV.3.3. Mean plasma and brain tissue concentrations of oxcarbazepine and its active metabolite licarbazepine obtained at 1.5 h post-dose of oxcarbazepine (50 mg/kg, ip) in rats pretreated intraperitoneally with silymarin/(-)-EPG 1:1 (12.5/12.5 mg/kg; fixed-ratio combination of 1:1), silymarin/(-)-EPG 1:3 (6.25/18.75 mg/kg; fixed-ratio combination of 1:3), silymarin/(-)-EPG 3:1 (18.75/6.25 mg/kg; fixed-ratio combination of 3:1), or verapamil (25 mg/kg). Data are expressed as the mean values ± standard error of the mean (SEM) of three determinations (n = 3). Comparisons between the verapamil (positive control group) *vs* experimental groups were performed using one-way ANOVA with the *post hoc* Dunnett's test.

IV.3.4. Discussion

The disappointment of the standard P-gp inhibitors in overcoming the drug efflux driven by P-gp led to an incessant search for new therapeutic options. Actually, whereas the clinical use of the first generation P-gp inhibitors (e.g., verapamil or cyclosporine) was limited due to unacceptable toxicity, the second-generation P-gp inhibitors (e.g., dexverapamil or valspodar) are involved in unpredictable pharmacokinetic reactions with other membrane transporter proteins (BANSAL ET AL. 2009; PALMEIRA ET AL. 2012; FERREIRA ET AL. 2015). In turn, third-generation agents like biricodar, elacridar, laniquidar, tariquidar or zosuquidar have shown to be promising in clinical trials, but they ended up demonstrating undesirable side effects in non-target organs (STEWART ET AL. 2000; THOMAS AND COLEY 2003; CALLIES ET AL. 2003; ABRAHAM ET AL. 2009; MOHANA ET AL. 2016). The poor safety profiles exhibited by the early generations of P-gp inhibitors highly demanded the discovery of compounds that can modulate the P-gp, without unacceptable toxicity.

The classification of AEDs, as well as their metabolites, as substrates of the P-gp has been a subject of controversy, but some previous studies give support in this direction. For example, Rizzi et al. (2002) have shown that the overexpression of P-gp in the hippocampus of a kainate model of epilepsy was associated with a reduction in the brain concentrations of PHT. Additionally, several reports evocated the efficacy of the P-gp inhibitors tariquidar, nimodipine and verapamil in overcoming the AEDs pharmacoresistance in animal models of epilepsy, improving their anticonvulsant activity (VOLK AND LÖSCHER 2005; VAN VLIET ET AL. 2006; BRANDT ET AL. 2006; HÖCHT ET AL. 2007; ZADROZNIAK ET AL. 2009). There are also clinical studies which support this hypothesis, demonstrating that the seizure control was improved in two patients with intractable epilepsy when verapamil was added (SUMMERS ET AL. 2004; IANNETTI ET AL. 2005). Indeed, verapamil is reported as the most extensively characterized P-gp inhibitor and multidrug resistance reversal agent that has entered clinical trials (SUMMERS ET AL. 2004; IANNETTI ET AL. 2005; PÉREZ-TOMÁS 2006), enhancing the plasma levels of several AEDs, including OXC, in rats and patients (MACPHEE ET AL. 1986; BEATTIE ET AL. 1988; BAHLS ET AL. 1991; AL-HUMAYYD 1996; NEERATI ET AL. 2011; ALVARIZA ET AL. 2013). However, these works also emphasise the toxicity frequently reported for the first generation P-gp inhibitors. The existing studies involving OXC in particular are few, but they evidence that OXC and its active metabolite LIC as well, are P-gp substrates either in *in vitro* assays (ZHANG ET AL. 2011a; FORTUNA ET AL. 2012) or in humans (ZADROZNIAK ET AL. 2009; ANTUNES ET AL. 2016).

One of the approaches that has been explored is the combined use of traditional P-gp inhibitors. In this context, the combination of verapamil and quinine was tested, and it increased the anthracycline accumulation and retention in multidrug resistant cells to a greater extent than did either drug individually (LEHNERT ET AL. 1991). Taking this into consideration, the investigation of the potential of flavonoid combinations as P-gp inhibitors for reversing the resistance to the treatment with OXC emerged as a pertinent topic of research. The interest of flavonoids as P-gp inhibitors has been increasingly evoked, with some of them producing effects

comparable to those of the classic P-gp inhibitors, like verapamil or cyclosporine A (BRANDT ET AL. 2006; BANSAL ET AL. 2009; SCHINKEL AND JONKER 2012; FERREIRA ET AL. 2015; MOHANA ET AL. 2016). The combined use of flavonoid compounds for therapeutic approaches is not a new idea. Actually, the synergic effects of flavonoid combinations were previously demonstrated for several other activities. For instance, the combination of baicalein and daidzein demonstrated to exert synergic effects in estrogenic and neuroprotective activities (CHOI ET AL. 2013); the combination of quercetin and kaempferol enhanced the *in vitro* cytotoxicity on human colon cancer (HCT-116) cells (JARAMILLO-CARMONA ET AL. 2014); chrysin, kaempferol, morin, and silybin combinations produced a synergic inhibition of proinflammatory mediator secretion from lipopolysaccharide-induced RAW 264.7 cells (HARASSTANI ET AL. 2010); whereas the combination of the formononetin, ononin, calycosin and calycosin-7-O-β-D-glucoside may have a strong effect in activating the regulatory element of erythropoietin at very low dosage (YU ET AL. 2013). Regarding this therapeutic approach, the current study was planned to evaluate the potential of the combined use of the flavonoids silymarin and (-)-EPG, recognised as P-gp inhibitors, in improving the pharmacokinetics of OXC, and of its pharmacologically active metabolite LIC, when comparing to the standard P-gp inhibitor verapamil. The ability of silymarin and (-)-EPG in inhibiting the P-gp *in vitro* has been previously demonstrated (JODOIN ET AL. 2002; ZHANG AND MORRIS 2003b; KITAGAWA ET AL. 2004; CHUNG ET AL. 2005). To the best of our knowledge, only silymarin has been investigated *in vivo* for this purpose and it has shown to significantly enhance the bioavailability of the P-gp substrate paclitaxel in Sprague-Dawley rats (PARK ET AL. 2012). Epigallocatechin (not gallate) also demonstrated to significantly increase the bioavailability of the P-gp substrate diltiazem in Sprague-Dawley rats (LI AND CHOI 2008).

The results of the present work, support that silymarin and (-)-EPG combinations have a higher impact than their individual use in improving the magnitude of systemic exposure to OXC (as assessed by C_{max}). Nevertheless, such effects were not observed in the extent of systemic drug exposure (AUC_{0-t}) when comparing with the group pretreated with verapamil. Thus, these results suggest that the pharmacological activity induced by silymarin/(-)-EPG combinations is similar to that of verapamil in terms of potency, but the effect of verapamil appears to be more prolonged in time. This difference may be related with the different drug-like properties of verapamil and silymarin/(-)-EPG, as they were all administered at a fixed dose of 25 mg/kg. Therefore, these findings suggest the need of further studies using higher doses of flavonoid combinations until acceptable levels in terms of safety concerns or even chemically modify some of the functional groups of these flavonoid-type compounds in order to improve their druggability. Other options that deserve to be explored in the future to extend the duration of action of flavonoid compounds will be the use of new delivery strategies and improved formulations in order to achieve greater advantages of the flavonoids pharmacological potential, including as P-gp inhibitors. In addition, it can be highlighted that for LIC no statistically significant differences were observed between all the flavonoids experimental groups and the positive control group (verapamil) for the pharmacokinetic parameters t_{max} and C_{max}. Moreover, as expected, the close similarity observed in the systemic effects induced by

dual flavonoid combinations and verapamil at the time the maximum plasma concentrations were reached for OXC and LIC was also found in brain (biophase). Indeed, no statistically significant differences were found in the brain exposure to OXC and LIC after the pretreatment of the rats with the flavonoid combinations or verapamil. This potential exhibited by the flavonoids silymarin and (-)-EPG, when compared to the standard P-gp inhibitor verapamil, is of great significance mainly taking into account the toxicity profile reported for the latter.

Although the exact mechanisms underlying flavonoid-P-gp interactions are not clear, several hypotheses have been proposed (CASTRO AND ALTENBERG 1997; SHAPIRO AND LING 1997; CONSEIL ET AL. 1998; JODOIN ET AL. 2002; WANG ET AL. 2002; ZHANG AND MORRIS 2003b). Nevertheless, the combined use of flavonoids could benefit from the existence of multiple binding sites for substrates and inhibitors on the P-gp (YANG AND LIU 2004). Particularly, silymarin and (-)-EPG are known to inhibit P-gp functions acting as substrate, and they may interact with P-gp directly either by competitive binding to the substrate-binding site or by binding to other drug-binding sites and changing the P-gp conformation (CASTRO AND ALTENBERG 1997; SHAPIRO AND LING 1997; JODOIN ET AL. 2002; ZHANG AND MORRIS 2003b; KWON ET AL. 2006). Considering that dual combinations of silymarin and (-)-EPG improved the pharmacokinetics of OXC and LIC (P-gp substrates), when comparing to their individual effects, we could hypothesise that these two flavonoids have different and complementary molecular mechanisms underlying flavonoid–P-gp *in vivo* interactions. Actually, this hypothesis is supported by the observation of opposite and complementary effects on P-gp ATPase activity for different flavonoids (ZHANG AND MORRIS 2003a).

The combined used of silymarin and (-)-EPG could be relevant in overpassing the P-gp–mediated pharmacoresistance in epilepsy, but it should also be highlighted other neuropharmacological properties ascribed to flavonoids with therapeutic interest in this scope, particularly as antiepileptic/anticonvulsant drugs (COLETA ET AL. 2008; BALUCHNEJADMOJARAD ET AL. 2010; YOON ET AL. 2011; HU ET AL. 2011; ABBASI ET AL. 2012; NASSIRI-ASL ET AL. 2013; ROMANO ET AL. 2013; NASSIRI-ASL ET AL. 2014). Specifically, the *Silybum marianum* seeds extract, in which silymarin is the bioactive constituent, and (-)-EPG demonstrated to have anticonvulsant effects on pentylenetetrazole-kindled seizure in mice and rats, respectively (XIE ET AL. 2012; WAQAR ET AL. 2016). Hence, these flavonoid-type compounds emerge as natural compounds of interest not only as an add-on therapy to optimize the AED treatment in drug-resistant epilepsy, but also to directly potentiate their anticonvulsant activity.

IV.3.5. Conclusions

The disappointment brought by the classical P-gp inhibitors agents in overcoming the P-gp-mediated drug efflux has led to an incessant search for new non-cytotoxic inhibitors and novel approaches for their use as well. To the best of our knowledge, this is the first work evidencing the synergic effects of dual flavonoid combinations of silymarin and (-)-EPG in enhancing the magnitude of systemic exposure to OXC and LIC in rats in a similar potency to that exhibited by

verapamil (a reference P-gp inhibitor). Hence, our findings support that the strategy of combining flavonoid-type P-gp inhibitors should continue to be exploited for the management of the pharmacoresistant epilepsy.

CHAPTER V

General Discussion

V.1. General discussion

Nowadays, millions of people worldwide suffer from serious and debilitating brain disorders, making of great significance the continuous efforts to discover and develop novel central nervous system (CNS)-acting drugs. Besides the improvements in the treatment of epilepsy and the emergence of several new antiepileptic drugs (AEDs), a large number of epileptic patients remain pharmacoresistant. Indeed, this major concern has provided the impetus for the development of innovative and more efficient therapeutic approaches.

The acknowledgement of the P-glycoprotein (P-gp) as one of the primary mechanisms involved in pharmacoresistance verified in the epilepsy led to the recognition of the combined use of AEDs and P-gp inhibitors as a possible therapeutic strategy to be considered in the future. Nevertheless, the multiple cons presented by the first generations of P-gp inhibitors put the search for safer compounds at a high level of importance. In this context, flavonoid compounds have emerged in recent years as P-gp inhibitors of great interest. Actually, bearing in mind that about one-third of the patients with epilepsy are medically refractory to a wide range of AEDs targeting different mechanisms of action, it is fully justifiable the consideration of other avenues beyond the drug pharmacodynamics in the improvement of seizures control and tolerability. Regarding this, the work underlying this doctoral thesis intended to assess, at a nonclinical level, the potential of flavonoid compounds as P-gp inhibitors and their value in overcoming the pharmacoresistance to AEDs conferred by this drug efflux transporter.

In this section is discussed in a more integrated and broader manner the various topics dealt within the previous chapters. Thus, it will be herein provided a critical overview of the key subjects covering the overall research work carried out to achieve the main goals proposed at the beginning of this thesis.

This work started with the development and validation of appropriate and reliable high-performance liquid chromatography (HPLC) bioanalytical methods to support the accomplishment of the planned *in vitro* and *in vivo* studies, ensuring an accurate, precise and selective quantification of carbamazepine (CBZ), oxcarbazepine (OXC), phenytoin (PHT), lamotrigine (LTG) and their respective metabolites carbamazepine-10,11-epoxide (CBZ-E), licarbazepine (LIC) and 5-(4-hydroxyphenyl)-5-phenylhydantoin (HPPH) in the different biological matrices. Actually, HPLC remains the methodology of choice in this kind of studies, since it enables the separation and quantification of quite complex mixtures of several compounds within the same sample, also enabling the quantitative determination of the analytes of interest over wide concentration ranges, which are frequently attained in *in vitro* and *in vivo* pharmacokinetic studies. In fact, by the quality of the data provided, the analytical methods for quantification of drugs and metabolites in biological samples play a critic and decisive role in the evaluation and interpretation of results arising from preclinical, clinical and biopharmaceutical studies (Shah et al. 2000; U.S. Food and Drug Administration 2001; European Medicines Agency 2011). Regarding this, the iterative process of method development and validation is preponderant in obtaining reliable data (Chandran and Singh 2007). Nowadays, the

validation of bioanalytical methods to quantify small molecules in biological samples is based on the conference report published by SHAH ET AL. (2000) entitled "Bioanalytical Method Validation – A Revisit with a Decade of Progress", on the Guidance for Industry – Bioanalytical Method Validation of the U.S. Food and Drug Administration (FDA) (U.S. FOOD AND DRUG ADMINISTRATION 2001) and on the Guideline on bioanalytical method validation issued by the European Medicines Agency (EMA) (EUROPEAN MEDICINES AGENCY 2011). Accordingly, there are some validation parameters that are crucial to be evaluated, namely, selectivity, linearity, lower limit of quantification (LLOQ), precision, accuracy, recovery and stability of target compounds. Specifically, the beginning of this work took place with the development and fully validation of an HPLC coupled to a diode array detector (DAD) methodology for the simultaneous quantitative determination of a set of AEDs CBZ, LTG, OXC, phenobarbital (PB) and PHT, and their pharmacologically active metabolites CBZ-E and LIC, in human plasma, using a novel sample preparation procedure, the microextraction by packed sorbent (MEPS) (*Chapter II, section II.2*). In this way, it was possible to make available, for the first time, a novel and innovative bioanalytical tool to simultaneously quantify this set of AEDs and their active metabolites using MEPS. This bioanalytical tool proved to be selective, sensitive, precise, accurate and linear in a wide concentration range, including the corresponding therapeutic drug concentration range. This technique arises as an important analytical tool for supporting the therapeutic drug monitoring (TDM) in routine clinical practice, and also to support other pharmacokinetic-based clinical studies, such as bioequivalence and bioavailability studies. The TDM is an approach of great value for the treatment optimisation of patients with epilepsy receiving AEDs of narrow therapeutic range (NEELS ET AL. 2004; JOHANNESSEN AND LANDMARK 2008; PATSALOS ET AL. 2008; KRASOWSKI 2010). Actually, AEDs are among the most common medications for which TDM is implemented in the routine clinical practice (KRASOWSKI 2010). In this context, assuming the better correlation of the drug's concentration with their therapeutic and/or toxic effects than the administered dose, makes that the patients' clinical outcome can be significantly improved by managing their medication regimen with the assistance of measured drug concentrations in plasma/serum (JOHANNESSEN ET AL. 2003; PATSALOS ET AL. 2008). In effect, this HPLC method was successfully applied to real plasma samples of highly polymedicated patients receiving treatment with these AEDs. Although the usefulness of this bioanalytical assay for TDM could not be denied, having in mind the specific aims of this thesis, the primary objective of developing this methodology to quantify the referred AEDs in human plasma was to test and optimise the analytical conditions that could also be subsequently transposed to cellular and animal matrices. The use of human plasma as biological matrix in this first analytical technique enabled to expedite the process of method development because it is easily accessible, is available in large quantities and ethically more acceptable, reducing for instance the costs and the number of rats to be sacrificed in further steps to obtain drug-free (blank) biological matrix. Although it is fair to recognise that the HPLC methodologies developed to support the *in vitro* and *in vivo* studies have important differences in comparison

with this first HPLC technique, primarily in the sample preparation procedure, it also permitted the apprenticeship in the scope of development and validation of bioanalytical methods.

The importance of synergic activity of P-gp and cytochrome P450 (CYP) isoenzymes, primarily CYP3A4, in determining the bioavailability of several drugs is highly suggested by their shared location in small intestinal enterocytes as well as by a significant overlap in drugs that are substrates for both proteins (YASUDA ET AL. 2002; LIN AND YAMAZAKI 2003; ZHOU 2008; GAVHANE AND YADAV 2012). Regarding this, initially we intended to use a unique *in vitro* screening model, the HepaRG cell line, to foresee the interference of flavonoid compounds not only with the P-gp, but also with CYP isoenzymes involved in the metabolism of some AEDs aiming at overcoming the pharmacoresistance to these agents. Indeed, HepaRG is a new human cell line derived from a hepatocellular carcinoma recognised to express high levels of the main drug-metabolizing CYP isoenzymes (CYP1A2, 2C9, 2D6, 2E1 and 3A4) in certain culture conditions (ANINAT ET AL. 2006; FERREIRA ET AL. 2014). In addition, LE VEE ET AL. (2006) also reported the intrinsic expression of P-gp in HepaRG cells. Nevertheless, according to our preliminary studies, the activity of P-gp is highly variable in this cell line, making it a poor model for this type of evaluation. Consequently, considering the primary target of this dissertation, for the intended *in vitro* studies, we decided to use the Madin-Darby canine kidney (MDCK) cell line transfected with the human multidrug resistance-1 gene (*MDR1;* MDCK-MDR1), a well-established model for the identification of interactions with the human P-gp (GARTZKE AND FRICKER 2014a).

Although studies initially planned to be conducted with HepaRG cells have not been performed, the two HPLC methodologies validated to support the *in vitro* assays in HepaRG cell cultures (*Chapter II, section II.3 and II.4*) were able to be applied to the studies conducted with MDCK cells. Actually, for the quantitative determination of AEDs and their metabolites in MDCK II and MDCK-MDR1 culture samples, as well as in rat plasma and brain matrices, the analytical conditions employed were similar to those validated for the HepaRG cells. These new methodologies involved some modifications regarding the first HPLC-DAD method developed, namely in the sample preparation procedure. Due to the good results obtained with the liquid-liquid extraction (LLE), this sample preparation procedure was chosen to be applied to support the *in vitro* and *in vitro* studies. After the development and validation of the analytical techniques for the quantification of the intended analytes in the matrices of interest, the following steps consisted in the evaluation of the potential of flavonoid compounds in inhibiting the P-gp activity, both *in vitro and in vivo*, as well as their potential to reverse the P-gp-mediated AED resistance.

The process of drug discovery is challenging, time-consuming, expensive, and requires consideration of numerous aspects. Thus, to fulfil all these challenges, several multidisciplinary approaches are required for a rational drug development process (MANDAL ET AL. 2009). Broadly, apart from the efficacy issues, the preclinical studies aim to establish safe starting doses and dosing regimens for clinical trials; determining whether a drug candidate is deemed to be suitable for administration to humans on the basis of an acceptable risk assessment; and providing confidence that the predicted drug effects are achievable via the selected route of

administration (BHOGAL AND BALLS 2008). The current work was planned to follow a more or less rational experimental design. Hence, the evaluation of the P-gp inhibitory properties of the flavonoid compounds was initiated using simple *in vitro* methodologies. Actually, this type of assays is largely applied for the preliminary screening of drug candidates, aiming to predict their toxicity, pharmacokinetic properties and efficacy (DOKE AND DHAWALE 2015). The *in vitro* models can potentially provide more rapid, precise and relevant data than do some whole-animal models, improving the success rates and also permitting a strong commitment to the 3Rs principles (GOH ET AL. 2015). Indeed, the identification of the most promising flavonoid compounds through the initial *in vitro* studies permitted to accomplish the replacement criteria of the 3Rs principles, also allowing a reduction of the animals required during the course of this work.

Nowadays, the i*n vitro* evaluation of the P-gp inhibition is a regulatory issue that needs to be considered during the process of drug development in order to predict not only the clinical inhibition of P-gp, but also possible drug–drug interactions. On the other hand, the need for early identification of compounds that exert inhibitory effects on the P-gp drug efflux transporter made indispensable the availability of suitable screening assays. Thus, taking into account the objectives of our work, MDCK-MDR1 cells were considered to be an appropriate cell-based model. Actually, this cell line has been recognised as a useful predictor of blood-brain barrier permeability and a valuable tool in the identification and characterisation of P-gp substrates and inhibitors. One of its particular advantages is the avoidance of the interference of multiple efflux transporters, focusing specifically on P-gp (GARTZKE AND FRICKER 2014b; JOUAN ET AL. 2016). Thus, in the screening studies of the P-gp inhibition mediated by flavonoids fluorescent dye-based intracellular accumulation assays (*Chapter III, section III.2*) were considered (FARDEL ET AL. 2015). Among fluorescence dyes transported by P-gp, rhodamine 123 (Rh123) is likely to be a major one. Indeed, Rh123 (a classic P-gp probe substrate) has been successfully applied to assess the P-gp activity in a wide range of studies (LUDESCHER ET AL. 1991; DRENOU ET AL. 1993; FORTUNA ET AL. 2011; FARDEL ET AL. 2015), exhibiting a rather high sensitivity compared to the use of other dyes (e.g., Hoechst 33342 and rhodamine 6G) (SARVER ET AL. 2002).

The use of complementary and alternative therapies such as herbal or natural products has increased worldwide over the last decade, giving a new focus of opportunities in search of bioactive compounds of interest, including flavonoids. Through *in vitro* screening assays performed, it was possible to identify five flavonoids with great potential in inhibiting the P-gp activity. Actually, of the eleven flavonoids tested, five of them demonstrated to pursue potential in inhibiting the P-gp activity in *in vitro* conditions. Overall, the obtained results showed that baicalein, (-)-epigallocatechin gallate [(-)-EPG], kaempferol, quercetin and silymarin, at 200 µM, produced a marked increase in the intracellular accumulation of Rh123 in MDCK-MDR1 cells, potentially through inhibiting the P-gp–mediated activity. In addition, with the exception of LTG, all the AEDs tested (PHT, CBZ and OXC) and their active metabolites (CBZ-E and LIC) demonstrated to be P-gp substrates in this cellular model. These latter findings are particularly important in the scope of the proposed strategy. Actually, according to the

literature, the identification of AEDs as P-gp substrates appears to be highly dependent of the *in vitro* cell model used (ZHANG ET AL. 2012a). Furthermore, in this *in vitro* assays, the most promising flavonoids as P-gp inhibitors [baicalein, (-)-EPG, kaempferol, quercetin and silymarin] also promoted a significant increase of the intracellular accumulation of the AEDs (excluding the LTG) and their active metabolites in MDCK-MRD1 cells, evidencing to be important drug candidates to reverse the AED-resistance. Moreover, it is noteworthy to mention that CBZ, LIC, LTG, OXC and PHT promoted a statistically significant decrease of the intracellular concentration of Rh123 at almost all the concentrations studied, suggesting an inducer effect on the P-gp activity.

Even before their recognition as potential useful agents in inhibiting the P-gp-mediated pharmacoresistance, several other biological properties have been attributed to flavonoid compounds. Bearing in mind that complex mixtures of flavonoid are daily consumed in our diet, their synergic pharmacological potential cannot be ignored. This was the reason that led us to evaluate the dual combined effects of flavonoids as P-gp inhibitors. The combination of compounds like flavonoids could be extremely relevant to the achievement of a synergic inhibition of the P-gp activity, permitting the reduction of their individual effective concentration and minimising side effects. The combination of flavonoids was previously explored regarding other bioactivities pursued by these natural compounds. Several of these studies confirmed the synergic potential of some flavonoid combinations in neuroprotection (CHOI ET AL. 2013), as anti-cancer (JARAMILLO-CARMONA ET AL. 2014) and as anti-inflammatory agents (HARASSTANI ET AL. 2010). Thus, the second set of *in vitro* assays (*Chapter III, section III.3*) aimed to explore the combined use of the flavonoid-type P-gp inhibitors baicalein, (-)-EPG, kaempferol, quercetin and silymarin as a possible reversing strategy of the efflux of AEDs mediated by P-gp (using as surrogate the AEDs intracellular accumulation). The synthetic P-gp inhibitors verapamil and quinine, for example, previously demonstrated a synergic potential in increasing the accumulation and retention of the P-gp substrate anthracycline in MDR1-resistant cells (LEHNERT ET AL. 1991). According to our results, certain flavonoid combinations increased the intracellular accumulation of Rh123 in a far greater magnitude than their additive individual effects at similar concentrations. Given that these synergic effects were only found for some flavonoid combinations it could be hypothesized that such flavonoids have different molecular mechanisms underlying the flavonoid–P-gp interactions. In the literature are also reported opposite and complementary effects on P-gp adenosine triphosphate (ATP)ase activity for different flavonoids (ZHANG AND MORRIS 2003). The most effective flavonoid combinations in enhancing the intracellular accumulation of Rh123 [(-)-EPG/silymarin (198 μM/500 μM) and kaempferol/baicalein (167 μM/183 μM)] also demonstrated to significantly increase the intracellular accumulation of CBZ, OXC and PHT, and their active metabolites CBZ-E and LIC, in the MDCK-MDR1 cell line. It is important to highlight that some of these combinations demonstrated a similar or higher potential than verapamil (a classic P-gp inhibitor) in increasing the AED or metabolite intracellular accumulation in this cell line. Actually, while the individual flavonoids baicalein, (-)-EPG, kaempferol, quercetin and silymarin increased 1.2 to 31 times

the intracellular concentration of the AEDs and their active metabolites in MDCK-MDR1 cells, these two flavonoid combinations further enhanced the intracellular accumulation of all the AEDs and metabolites in about 1.5 to 76 times.

Considering these promising results obtained through the *in vitro* accumulation studies, and in an attempt to take a step forward in assessing the potential of this strategy of flavonoids combination, we further conducted transport studies through MDCK-MDR1 cells cultured in Snapwell™ inserts and then mounted on vertical Ussing Chambers. Actually, the transwell transport assays are considering one of the most reliable techniques for predicting the P-gp efflux liability *in vivo*, being considered the method of choice in the evaluation of drug candidates (YAMAZAKI ET AL. 2001; U.S. FOOD AND DRUG ADMINISTRATION 2006; FENG ET AL. 2008). Regarding this, and using LIC as a probe drug, we evaluated the effect of the (-)-EPG/silymarin combination on the transport of LIC through MDCK-MDR1 cell monolayer in Snapwell™ inserts. This study permitted to investigate the LIC permeability in this cell-based model, in which passive diffusion (paracellular and transcellular) and carrier-mediated mechanisms may be involved, namely the multidrug efflux transporter P-gp. Overall, it was verified a pronounced increase of apparent permeability coefficient of LIC in the presence of (-)-EPG/silymarin combination, reinforcing once again the value of this strategy in reversing the P-gp–mediated drug efflux.

Following the planned schedule of the present work, the *in vitro* assays were proceeded by *in vivo* studies in rodents aiming to confirm the obtained *in vitro* results. In this context, the *in vivo* studies could provide an assessment of changes on the pharmacokinetics of AEDs promoted by the flavonoid compounds. Nevertheless, although the rat could provide a whole-animal model for the evaluation of flavonoids as potential reversing agents of the P-gp–mediated resistance, we cannot forget the questions that may arise related to differences between species. Actually, the *in vitro* studies were conducted in a canine cell line (MCDK), but it overexpresses the human gene codifying the P-gp (*MDR1*; MDCK-MDR1). Thus, the application of human-based *in vitro* assays, combined with *in vivo* assays in relevant laboratory animal species stands up as a valuable approach to predict the drug properties in human, being a guidance in the design and selection of drug candidates with higher probability of clinical success.

For the *in vivo* experiments, adult male Wistar rat was chosen as the most appropriate whole-animal model. Actually, besides rodent's physiology and genetics could be easily compared to human, the Wistar rat is one of the species broadly used in pharmacokinetic studies (JACOB AND KWITEK 2002; IANNACCONE AND JACOB 2009), even in the generality of studies involving AEDs (SYREK ET AL. 1996; MATAR ET AL. 1999; CLINCKERS ET AL. 2008; BONARY ET AL. 2009; PRASHANTH ET AL. 2011; REETA ET AL. 2011; WU ET AL. 2014; JOSHI ET AL. 2015). Therefore, the use of adult male Wistar rats ensured that all the animals' biological systems were completely matured, also avoiding any potential interference of the female hormonal cycle on the pharmacokinetics of target compounds. The intrinsic behavioural characteristics of Wistar rats like their calm

temperament, easy handling and economically maintenance were also favourable for this choice.

The first *in vivo* study (*Chapter IV, section IV.2*) was designed to evaluate the *in vivo* effects of the flavonoid silymarin on the pharmacokinetics of CBZ, OXC and PHT. Actually, this flavonoid was chosen taken into account our previous *in vitro* studies in which it demonstrated not only to increase the intracellular accumulation of Rh123 in the MDCK-MDR1 cells, but also the intracellular concentrations of CBZ, OXC, PHT, CBZ-E and LIC. Accordingly to the results obtained in this *in vivo* study, the pretreatment of rats with silymarin appears to have some potential in increasing the plasma concentrations as well as the systemic exposure to the AEDs considered. Nevertheless, the positive effects of silymarin in the plasma peak concentration (C_{max}) and area under the concentration-time curve from time zero to the last sampling time (AUC_{0-t}) parameters were primarily observed for OXC and its main metabolite (LIC). Nonetheless, these results are not strange because the pretreatment with verapamil (a standard P-gp inhibitor) also increased the rate and extent of systemic exposure to OXC and LIC. These *in vivo* data are also supported by several reports that have demonstrated the efficacy of verapamil, but also of other P-gp inhibitors tariquidar and nimodipine in improving significantly the levels of AEDs in animal models of epilepsy and, consequently, enhancing their anticonvulsant activity (VOLK AND LÖSCHER 2005; VAN VLIET ET AL. 2006; BRANDT ET AL. 2006; HÖCHT ET AL. 2007). Moreover, flavonoid compounds, including silymarin, have also previously demonstrated a high potential for increasing the bioavailability of a panoply of P-gp substrates, other than AEDs (LI AND CHOI 2009; PATHAK AND UDUPA 2010; LEE AND CHOI 2010; CHOI ET AL. 2011; YANG ET AL. 2011; PARK ET AL. 2012). The changes observed in the plasma concentrations of OXC and LIC in the rats pretreated with silymarin or verapamil were also confirmed in the brain tissue. These *in vivo* studies clearly suggest the beneficial effects of the pretreatment with silymarin on the pharmacokinetics of AEDs that are P-gp substrates, enabling to infer that silymarin has potential to inhibit the P-gp *in vivo* conditions; these findings reinforce the potential of the combination of flavonoid and AEDs as a possible therapeutic strategy in overcoming the pharmacoresistance in epilepsy.

More or less in parallel, a second *in vivo* pharmacokinetic study was performed to investigate in *in vivo* conditions the promising results obtained *in vitro* regarding the potential of dual flavonoid combinations to inhibit the P-gp and overpass the P-gp–mediated pharmacoresistance. Considering the *in vitro* results, the (-)-EPG/silymarin combination was chosen and its effects on the pharmacokinetics of OXC were evaluated in Wistar rats, comparing with the individual flavonoids and verapamil (the standard P-gp inhibitor). For this purpose, rats were pretreated with silymarin, (-)-EPG, dual combinations of silymarin/(-)-EPG at three fixed-ratios (1:1, 1:3 and 3:1), or verapamil. Overall, the obtained pharmacokinetic data revealed that the pretreatment with dual silymarin/(-)-EPG combinations originated peak plasma concentrations of OXC and LIC (a pharmacologically active metabolite of OXC) similar to those achieved in the presence of verapamil (positive control). Moreover, the effects promoted by silymarin/(-)-EPG combinations on the magnitude of systemic drug exposure to

OXC and LIC were also reflected in the corresponding drug levels attained in the brain (biophase). These *in vivo* results support those previously obtained *in vitro* and reinforce the usefulness of flavonoid combinations in this context. Actually, to the best of our knowledge, this is the first work evidencing the synergic effects of dual flavonoid combinations of silymarin and (-)-EPG in enhancing the magnitude of systemic exposure to OXC and LIC in rats, in a similar potency to that exhibited by verapamil (a reference P-gp inhibitor), showing up as an approach that should continue to be exploited for reversing the pharmacoresistance in epilepsy.

Finally, in addition to the objectives initially proposed to this thesis, aiming to afford new data that support the strategy herein explored, a supplementary work was planned and conducted in collaboration with the group of the Professors Stanislaw Czuczwar and Jarogniew Luszczki from the Medical University of Lublin, Poland (see Supplement). This additional study aimed to evaluate the neurotoxicity and hepatotoxicity of the combination of CBZ, OXC or PHT with silymarin, one of the most promising flavonoid P-gp inhibitor, in two different cell lines [rat mesencephalic dopaminergic (N27) cells and HepaRG cells], using an approach called as isobolographic analysis.

CHAPTER VI

Conclusions & Future Perspectives

VI.1. Conclusions & future perspectives

In the last years, the value of flavonoid compounds in the treatment of several human ailments has increased. In this context, their role as inhibitors of the drug efflux transporter P-glycoprotein (P-gp) has been focused. This thesis was designed with the aim of evaluating not only the potential of flavonoids as P-gp inhibitors, but also their potential interest in reversing the P-gp–mediated multidrug resistance documented in the pharmacotherapy of epilepsy, and involving antiepileptic drugs (AEDs) soundly established in the current clinical practice. Therefore, *in vitro* and *in vivo* nonclinical studies were conducted herein in order to deepen the knowledge and evidence on all these aspects.

In summary, the most relevant key findings brought from all the experimental work carried out in the scope of the present thesis will be succinctly provided below:

- To the best of our knowledge, the first high-performance liquid chromatography method with diode array detection (HPLC-DAD) using microextraction by packed sorbent (MEPS) during the sample preparation step was herein developed and validated to simultaneously quantify carbamazepine (CBZ), lamotrigine (LTG), oxcarbazepine (OXC), phenobarbital (PB), phenytoin (PHT) and their active metabolites carbamazepine-10,11-epoxide (CBZ-E) and licarbazepine (LIC) in human plasma. This sample preparation procedure has several advantages, namely, a minimal cost per analysis compared to conventional solid-phase extraction (SPE), because each MEPS device can be reused dozens of times before being discarded while SPE cartridges are indicated for single use only; and the consumption of organic solvents is reduced. Being simple, rapid, sensitive, reliable, accurate and precise within a wide range of concentrations, including the AEDs therapeutic range, this MESP/HPLC-DAD method demonstrated to be suitable to support the routine therapeutic drug monitoring (TDM) of these AEDs and other pharmacokinetic-based studies.

- New HPLC-DAD methodologies using liquid–liquid extraction (LLE) were developed and validated to quantity CBZ, LTG, OXC, PHT and the metabolites CBZ-E, LIC and 5-(4-hydroxyphenyl)-5-phenylhydantoin (HPPH) in cellular and rat matrices (plasma and brain tissue homogenates). Their major advantages include the simple instrumentation and uncomplicated chromatographic conditions, like isocratic elution and DAD detection. All these aspects suggest that these techniques are appropriate for implementation in almost all laboratories, being fast bioanalytical assays particularly useful when a large number of samples have to be analysed, as is the case of the *in vitro* and *in vivo* studies performed in this thesis.

- With the exception of LTG, all the AEDs tested (CBZ, OXC and PHT) as well as their active metabolites (CBZ-E and LIC) demonstrated to be P-gp substrates in the Madin-

Darby canine kidney cell line overexpressing the human multidrug resistance-1 (*MDR1*, MDCK-MDR1). Additionally, CBZ, LIC, LTG, OXC and PHT promoted a statistically significant decrease of the intracellular concentration of rhodamine 123 (Rh123) in MDCK-MDR1 cells, at almost all the concentrations studied, suggesting an inducer effect on the P-gp activity.

- The flavonoids baicalein, (-)-epigallocatechin gallate [(-)-EPG], kaempferol, quercetin and silymarin demonstrated to increase the intracellular accumulation of Rh123 in the MDCK-MDR1, potentially through inhibiting the functional activity of P-gp. These most promising flavonoids as P-gp inhibitors also promoted a significant increase in the intracellular accumulation of the AEDs CBZ, OXC and PHT, and their active metabolites CBZ-E and LIC, in MDCK-MDR1 cells, evidencing to be important candidates to reverse the AED-resistance. All these findings highlight the potential of the coadministration of flavonoid compounds with AEDs as an adjuvant therapy for refractory epilepsy.

- Two-paired flavonoid combinations of baicalein, (-)-EPG, kaempferol, quercetin and silymarin demonstrated to enhance the maximal intracellular accumulation of Rh123 when compared to their individual use, suggesting a synergic effect of these flavonoids in inhibiting the P-gp activity. Indeed, these effects were achieved with much lower final concentrations. The most effective flavonoid combinations, this is (-)-EPG/silymarin and kaempferol/baicalein, also demonstrated to increase the intracellular accumulation of the AEDs (CBZ, OXC and PHT) and their metabolites (CBZ-E and LIC) in the MDCK-MDR1 cell line, and in a similar extent to the standard P-gp inhibitor verapamil. In addition, the (-)-EPG/silymarin combination originated a pronounced increase of the apparent permeability coefficient (P_{app}) of LIC through a monolayer of MDCK-MDR1 cells cultured in Snapwell™ inserts and mounted in Ussing Chambers. These results evidence the potential of flavonoid combinations in overcoming the P-gp–mediated efflux of AEDs, and their active metabolites, taking advantage of their synergic pharmacological profile.

- The flavonoid silymarin demonstrated potential in increasing the *in vivo* plasma concentrations of CBZ, PHT and OXC, in accordance with the results found for the classic P-gp inhibitor verapamil. The main effects were observed for OXC, increasing significantly its plasma peak concentration (C_{max}; 50%), as well as its extent of systemic exposure (41%). Additionally, the systemic exposure of the main pharmacologically active metabolite of OXC (LIC) also increased by the pre-administration of silymarin. These results were reflected in the concentrations of OXC and LIC determined in the rat brain. These *in vivo* results reinforce the value of flavonoids as promising agents in reversing the resistance to the treatment with AEDs, and their relevance for further drug development.

- The dual silymarin and (-)-EPG combination at three fixed-ratios (1:1; 1:3 and 3:1) demonstrated a synergic effect of these flavonoids in enhancing the degree of systemic exposure to OXC and LIC in rats (as assessed by C_{max}), which occurred in a comparable extent to that observed for the standard P-gp inhibitor verapamil. The effects promoted by the silymarin/(-)-EPG combinations were also reflected in the corresponding drug levels attained in the brain (biophase). These *in vivo* findings attest those previously found through an *in vitro* evaluation, and reinforce the potential value of this therapeutic strategy in the management of the pharmacoresistant epilepsy.

Taking into account all the results obtained during this work, it seems that the strategy of flavonoid/AED combined therapy is a promising approach, which deserves to be further investigated in order to overcome the P-gp–mediated pharmacoresistance. The availability of this *in vitro* and *in vivo* information also add supporting to the transporter hypothesis in explaining the drug-resistant epilepsy. Therefore, this strategy could be evaluated in clinical trials for the development of novel and more effective P-gp inhibitor molecules in a near future.

APPENDICES

Appendix A

Table A.1. An overview of the effects of flavonoids on P-glycoprotein (P-gp) evaluated by cell-based *in vitro* studies.

Flavonoids	Cell models	Flavonoid concentration (μM)	P-gp expression assays	P-gp functional assays				References
				Type of assays	Probe substrates	Methods	Effects	
Chalcones								
Phloretin	MCF-7/ADR MDA435/LCC6WT	50	Western blot (no significant effect)	A	[^{3}H]Daunomycin	Liquid scintillation counting	Inhibition	Zhang and Morris (2003a)
Flavanolols								
Silibinin	MCF-7/ADR	10-100	-	A	Rhodamine 123	Spectrofluorometry	Inhibition	Lee and Choi (2010)
Silymarin	Caco-2	50-150 7-300 150	Western blot	A T A	[^{3}H]Digoxin [^{3}H]Vinblastine	Liquid scintillation counting	Inhibition Inhibition Inhibition	Zhang and Morris (2003b)
	MCF-7/ADR	100	-	A/E	[^{3}H]Daunomycin	Liquid scintillation counting	Inhibition	Chung et al. (2005)
	MCF-7/ADR, MDA435/LCC6WT, MDA435/LCCM	50	Western blot (no significant effect)	A	[^{3}H]Daunomycin	Liquid scintillation counting	Inhibition	Zhang and Morris (2003a)
Flavanols								
Catechin	Caco-2	10	Western blot, flow cytometry, RT-PCR (induction-↑mRNA/↑protein)	-	-	-	-	Lohner et al. (2007)
	CH^{R}C5	100	Western blot	A/E	Rhodamine 123	Spectrofluorometry	No effect	Jodoin et al. (2002)
Catechin gallate	CH^{R}C5	100	Western blot	A/E	Rhodamine 123	Spectrofluorometry	Inhibition	Jodoin et al. (2002)

Flavonoids	Cell models	Flavonoid concentration (μM)	P-gp expression assays	P-gp functional assays				References
				Type of assays	Probe substrates	Methods	Effects	
Epicatechin	CH^RC5	100	Western blot	A/E	Rhodamine 123	Spectrofluorometry	No effect	JODOIN ET AL. (2002)
	KB-C2	100 300	Western blot	A/E	Daunorubicin Rhodamine 123	Spectrofluorometry	No effect	KITAGAWA ET AL. (2004)
Epicatechin gallate	CH^RC5	100	Western blot	A/E	Rhodamine 123	Spectrofluorometry	Inhibition	JODOIN ET AL. (2002)
	KB-C2	100	-	A/E	Daunorubicin Rhodamine 123	Spectrofluorometry	Inhibition Inhibition	KITAGAWA ET AL. (2004)
Epigallocatechin	CH^RC5	100	Western blot	A/E	Rhodamine 123	Spectrofluorometry	No effect	JODOIN ET AL. 2002)
	KB-C2	200 100	-	A/E	Daunorubicin Rhodamine 123	Spectrofluorometry	Inhibition No significant effect	KITAGAWA ET AL. (2004)
Epigallocatechin gallate	Caco-2	10	Western blot, flow cytometry, RT-PCR (induction-↑mRNA/↑protein)	-	-	-	-	LOHNER ET AL. (2007)
	Caco-2	100	Western blot	A/E	[^{3}H]Vinblastine	Liquid scintillation counting	Inhibition	JODOIN ET AL. (2002)
	CH^RC5	100	Western blot	A/E	Rhodamine 123	Spectrofluorometry	Inhibition	JODOIN ET AL. (2002)
	KB-C2	25 0-100	Western blot	A/E	Daunorubicin Rhodamine 123	Spectrofluorometry Spectrofluorometry FACS flow cytometry	Inhibition Inhibition	KITAGAWA ET AL. (2004)

Flavonoids	Cell models	Flavonoid concentration (μM)	P-gp expression assays	P-gp functional assays				References
				Type of assays	Probe substrates	Methods	Effects	
Taxifolin	Caco-2	10	Western blot, flow cytometry, RT-PCR (induction-↑mRNA/↑protein)	-	-	-	-	Lohner et al. (2007)
Flavanones								
Eriodictyol	Caco-2	10	Western blot, flow cytometry, RT-PCR (induction-↑protein)	-	-	-	-	Lohner et al. (2007)
Hesperetin	Caco-2	250	-	T	[^{3}H]Talinolol	Liquid scintillation counting	Inhibition?	Ofer et al. (2005)
Naringenin	Caco-2	10	Western blot, flow cytometry, RT-PCR (induction-↑protein)	-	-	-	-	Lohner et al. (2007)
	Caco-2	10-500	-	T	Talinolol	HPLC-FLD	Inhibition	Castro et al. (2007)
	Caco-2	855	-	T	[^{3}H]Vinblastine	Liquid scintillation counting	Inhibition	Takanaga et al. (1998)
	CR1R12, G185	-	-	T	Daunorubicin	FACS flow cytometry	No effect	Wang et al. (2001)

Flavonoids	Cell models	Flavonoid concentration (μM)	P-gp expression assays	P-gp functional assays				References
				Type of assays	Probe substrates	Methods	Effects	
Naringin	Caco-2	250	-	T	[^{3}H]Talinolol	Liquid scintillation counting	Inhibition?	Ofer et al. (2005)
	Caco-2	100-2500	-	T	Talinolol	HPLC-FLD	Inhibition	Castro et al. (2007)
	Caco-2	643	-	T	[^{3}H]Vinblastine	Liquid scintillation counting	Slightly inhibition	Takanaga et al. (1998)
	CR1R12, G185	-	-	T	Daunorubicin	FACS flow cytometry	No effect	Wang et al. (2001)
	HK-2	10-100	Western blot, RT-PCR (inhibition-↓mRNA)	A	Calcein-AM	Spectrofluorometry	Inhibition	Romiti et al. (2004)
Flavones								
Apigenin	Caco-2	10	Western blot, flow cytometry, RT-PCR (no effect)	-	-	-	-	Lohner et al. (2007)
Baicalein	KB-C2	0-200	-	A/E	Daunorubicin	Spectrofluorometry	Inhibition	Kitagawa et al. (2004)
	MCF-7/ADR	1-10	-	A	Rhodamine 123	Spectrofluorometry	Inhibition	Shin et al. (2009); Cho et al. (2011); Li et al. (2011)

Flavonoids	Cell models	Flavonoid concentration (μM)	P-gp expression assays	P-gp functional assays				References
				Type of assays	Probe substrates	Methods	Effects	
Chrysin	Caco-2	10	Western blot, flow cytometry, RT-PCR (induction-↑mRNA/↑protein)	-	-	-	-	LOHNER ET AL. (2007)
5,7-dimethoxy-flavone	LLC-GA5-COL150	1-300	Western blot	A	Rhodamine 123	Spectrofluorometry	Inhibition	PATANASETHANONT ET AL. (2007)
Diosmin	Caco-2	10-100 0-50	-	A T	Rhodamine 123 Digoxin	Spectrofluorometry LC-MS/MS	Inhibition Inhibition	YOO ET AL. (2007)
Flavone	Caco-2	10	Western blot, flow cytometry, RT-PCR (induction-↑mRNA/↑protein)	-	-	-	-	LOHNER ET AL. (2007)
3,5,6,7,8,3´,4'-Hepta-methoxy-flavone	Caco-2	0.5-50	-	T	Talinolol	HPLC-FLD	Inhibition	MERTENS-TALCOTT ET AL. (2007)
	Caco-2	1-100	-	A	[^{3}H]Vinblastine	Liquid scintillation counting	Inhibition	TAKANAGA ET AL. (2000)
	LLC-GA5-COL300	20					Inhibition	
	K562/ADR	1-1000	Western blot		[^{3}H]Vincristine	Liquid scintillation counting	Inhibition	IKEGAWA ET AL. (2000)

Flavonoids	Cell models	Flavonoid concentration (μM)	P-gp expression assays	P-gp functional assays				References
				Type of assays	Probe substrates	Methods	Effects	
Nobiletin	Caco-2	0.5-50	-	T	Talinolol	HPLC-FLD	Inhibition	MERTENS-TALCOTT ET AL. (2007)
	Caco-2	1-100	-	A	[^{3}H]Vinblastine	Liquid scintillation counting	Inhibition	TAKANAGA ET AL. (2000)
	LLC-GA5-COL300	20					Inhibition	
	K562/ADR	1-1000	Western blot	A	[^{3}H]Vincristine	Liquid scintillation counting	Inhibition	IKEGAWA ET AL. (2000)
3,5,7,3´,4´-pentame-thoxyfla-vone	LLC-GA5-COL150	1-300	Western blot	A	Daunorubicin Rhodamine 123	Spectrofluorometry Spectrofluorometry	Inhibition Inhibition	PATANASETHANONT ET AL. (2007)
Oroxylin A	NCI/ADR-RES	0.01-40 10-20	Western blot	A	Calcein-AM Paclitaxel	Spectrofluorometry HPLC-UV	Inhibition Inhibition	GO ET AL. (2009)
	MCF-7/ADR	30-90	Western blot, RT-PCR (inhibition-↓mRNA/↓protein)	A	Rhodamine 123	FACS flow cytometry	Inhibition	ZHU ET AL. (2013)
Sinensetin	Caco-2	0.5-50	-	T	Talinolol	HPLC-FLD	Inhibition	MERTENS-TALCOTT ET AL. (2007)
Tangeritin	Caco-2	0.5-50	-	T	Talinolol	HPLC-FLD	Inhibition	MERTENS-TALCOTT ET AL. (2007)
	Caco-2	1-100	-	A	[^{3}H]Vinblastine	Liquid scintillation counting	Inhibition	TAKANAGA ET AL. (2000)
	LLC-GA5-COL300	20					Inhibition	
	K562/ADR	1-1000	Western blot	A	[^{3}H]Vincristine	Liquid scintillation counting	Inhibition	IKEGAWA ET AL. (2000)

Flavonoids	Cell models	Flavonoid concentration (μM)	P-gp expression assays	P-gp functional assays				References
				Type of assays	Probe substrates	Methods	Effects	
7,3',4'-Trimethoxy-flavone	Caco-2	50-400	-	T	Paclitaxel	HPLC-UV	Inhibition	Jeong and Choi (2007)
Flavonols								
Fisetin	KB-C2	0-200	-	A/E	Daunorubicin	Spectrofluorometry	Inhibition	Kitagawa et al. (2004)
Isoquercitin	Caco-2	100	-	T	[^{3}H]Talinolol	Liquid scintillation counting	Inhibition?	Ofer et al. (2005)
	KB-C2	0-200 100	-	A/E	Daunorubicin Rhodamine 123	Spectrofluorometry Spectrofluorometry FACS flow cytometry	No effect No effect	Kitagawa et al. (2004)
Morin	KB-C2	0-200	-	A/E	Daunorubicin	Spectrofluorometry	Inhibition	Kitagawa et al. (2004)
	MCF-7/ADR, MDA435/LCC6WT, MDA435/LCCM	50	Western blot (no significant effect)	A	[^{3}H]Daunomycin	Liquid scintillation counting	Inhibition	Zhang and Morris (2003a)
Myricetin	Caco-2	10	Western blot, flow cytometry, RT-PCR (induction-↑mRNA/↑protein)	-	-	-	-	Lohner et al. (2007)
	KB-C2	0-200	-	A/E	Daunorubicin	Spectrofluorometry	Inhibition	Kitagawa et al. (2004)
	MCF-7/ADR	3-30	-	A	Rhodamine 123	Spectrofluorometry	Inhibition	Choi et al. (2010)

Flavonoids	Cell models	Flavonoid concentration (μM)	P-gp expression assays	P-gp functional assays				References
				Type of assays	Probe substrates	Methods	Effects	
Kaempferol	Caco-2	30	-	T	[^{3}H]Talinolol	Liquid scintillation counting	Inhibition?	Ofer et al. (2005)
	CR1R12, G185	-	-	T	Daunorubicin	FACS flow cytometry	No effect	Wang et al. (2001)
	HK-2	10-100	Western blot, RT-PCR (inhibition-↓mRNA)	A/E	Calcein-AM	Spectrofluorometry	Inhibition	Romiti et al. (2004)
	KB-C2	0-200 100	-	A/E	Daunorubicin Rhodamine 123	Spectrofluorometry Spectrofluorometry FACS flow cytometry	Inhibition Inhibition	Kitagawa et al. (2004)
	KB-V1	10-200	Western blot (no effect)	A/E	Rhodamine 123	Flow cytometry	Inhibition	Khantamat et al. (2004)
	MFC-7/ADR	100	Western blot	A/E	[^{3}H]Daunomycin	Liquid scintillation counting	Inhibition	Chung et al. (2007)
Kaempferol-3,4-*O*-dimethyl ether	MFC-7/ADR	100	Western blot	A/E	[^{3}H]Daunomycin	Liquid scintillation counting	Inhibition	Chung et al. (2007)
Kaempferol-3-*O*-methyl ether	MFC-7/ADR	100	Western blot	A/E	[^{3}H]Daunomycin	Liquid scintillation counting	Inhibition	Chung et al. (2007)

Flavonoids	Cell models	Flavonoid concentration (μM)	P-gp expression assays	P-gp functional assays				References
				Type of assays	Probe substrates	Methods	Effects	
Quercetin	Caco-2	10	Western blot, flow cytometry, RT-PCR (induction-↑mRNA/↑protein)	-	-	-	-	LOHNER ET AL. (2007)
	Caco-2	20	-	T	[^{3}H]Talinolol	Liquid scintillation counting	Inhibition?	OFER ET AL. (2005)
	HK-2	0.5-200	Western blot	A	Calcein-AM Rhodamine 123	Spectrofluorometry	Inhibition Inhibition	CHIELI ET AL. (2009)
	CR1R12	0-250	-	T	Daunorubicin	FACS flow cytometry	Slightly inhibition	WANG ET AL. (2001)
	EPP85-181RDB	3-12	Western blot, Immunocytochemical analysis (inhibition)	A	Calcein-AM	Spectrofluorometry	Inhibition	BORSKA ET AL. (2010)
	KB-C2	0-200 100	-	A/E	Daunorubicin Rhodamine 123	Spectrofluorometry Spectrofluorometry FACS flow cytometry	Inhibition Inhibition	KITAGAWA ET AL. (2004)
	MBEC4	5-50	ELISA (biphasic effect)	A/E	[^{3}H]Vincristine	Liquid scintillation counting	Biphasic effect	MITSUNAGA ET AL. (2000)
	MCF-7/ADR	1-10	Immunocytofluorimetric assay (inhibition-10μM)	E	Rhodamine 123	FACS flow cytometry	Inhibition	SCAMBIA ET AL. (1994)
	MCF-7/ADR	1-10	-	A	Rhodamine 123	Spectrofluorometry	Inhibition	CHOI ET AL. (2011a)

Flavonoids	Cell models	Flavonoid concentration (μM)	P-gp expression assays	P-gp functional assays				References
				Type of assays	Probe substrates	Methods	Effects	
Spiraeoside	Caco-2	100	-	T	[^{3}H]Talinolol	Liquid scintillation counting	Inhibition?	Ofer et al. (2005)
3´,4',7-trimethoxy-quercetin	MCF-7/ADR	1-10	Immunocytofluo-rimetric assay	E	Rhodamine 123	FACS flow cytometry	Inhibition	Scambia et al. (1994)
Rutin	MCF-7/ADR	1-10	Immunocytofluo-rimetric assay	E	Rhodamine 123	FACS flow cytometry	No effect	Scambia et al. (1994)
	KB-C2	100 100	-	A/E A/E	Daunorubicin Rhodamine 123	Spectrofluorometry Spectrofluorometry FACS flow cytometry	No effect No effect	Kitagawa et al. (2004)
Isoflavones								
Biochanin A	Caco-2	50, 100, 150 20, 50, 100, 150 150	Western blot	A T A	[^{3}H]Digoxin [^{3}H]Digoxin [^{3}H]Vinblastine	Liquid scintillation counting	Inhibition Inhibition Inhibition	Zhang and Morris (2003b)
	MCF-7/ADR	100	-	A/E	[^{3}H]Daunomycin	Liquid scintillation counting	Inhibition	Chung et al. (2005)
	MCF-7/ADR	10, 50	-	A	Mitoxantrone	FACS flow cytometry	Biphasic effect	An and Morris (2010)
	MCF-7/ADR, MDA435/LCC6WT, MDA435/LCC6MDR1	50	Western blot (no significant effect)	A	[^{3}H]Daunomycin	Liquid scintillation counting	Inhibition	Zhang and Morris (2003a)
Daidzein	Caco-2	10	Western blot, flow cytometry, RT-PCR (induction-↑mRNA/↑protein)	-	-	-	-	Lohner et al. (2007)

Flavonoids	Cell models	Flavonoid concentration (μM)	P-gp expression assays	P-gp functional assays				References
				Type of assays	Probe substrates	Methods	Effects	
Genistein	Caco-2	10	Western blot, flow cytometry, RT-PCR (induction-↑mRNA/↑protein)	-	-	-	-	LOHNER ET AL. (2007)
	BC19/3, MCF-7/VP, BALB/c-3T3-1000	200	Western blot, RT-PCR	A/E	Daunorubicin Rhodamine 123	Spectrofluorometry	Inhibition Inhibition	CASTRO AND ALTENBERG (1997)

*Accumulation studies; E, Efflux studies; **ELISA, Enzyme-Linked Immunosorbent Assay**; FACS, Fluorescence-activated cell sorting; FLD, **Fluorescent detection**; HPLC, High-performance liquid chromatography; LC-MS/MS, Liquid chromatography-tandem mass spectrometry; **mRNA, Messenger ribonucleic acid**; RT-PCR, Real-time polymerase chain reaction; T, Transport studies; UV, Ultraviolet detection; ?, Probably; ↓Decrease; ↑Increase*

Table A.2. An overview of the effects of flavonoids on the pharmacokinetic parameters of some drugs (P-glycoprotein substrates) evaluated by non-clinical *in vivo* studies.

Flavonoids	Animal model	Drug dose (mg/kg), route	Flavonoid dose (mg/kg), route	Effects on pharmacokinetic parameters	References
Flavanolols					
Silibinin	Male Sprague-Dawley rats	Paclitaxel, 40, *po*	0.5, *po*#	$\rightarrow t_{max}$, $\downarrow V_d$, $\uparrow AUC_{0-\infty}$, $\uparrow C_{max}$, $\uparrow t_{1/2}$, ↑F, ↑RB	Lee and Choi (2010)
			2.5-10, *po*#	$\downarrow t_{max}$, $\downarrow V_d$, $\uparrow AUC_{0-\infty}$, $\uparrow C_{max}$, $\uparrow t_{1/2}$, ↑F, ↑RB	
		Paclitaxel, 4, iv	0.5-10, *po*#	$\downarrow CL_t$, $\uparrow AUC_{0-\infty}$, $\uparrow t_{1/2}$, ↑RB	
Silymarin	Male Sprague-Dawley rats	Paclitaxel (Taxol®) *po*, 25	10-20, *po*†	$\uparrow t_{1/2}$, $\downarrow V_{ss}$, $\uparrow C_{max}$, ↑F, $\uparrow AUC_{0-t}$, $\downarrow CL_t$/F, $\uparrow t_{max}$, ↑RB	Park et al. (2012)
		Paclitaxel (micro-emulsion), 25, *po*	10, *po*†	$\downarrow t_{1/2}$, $\downarrow V_{ss}$, $\downarrow C_{max}$, ↓F, $\uparrow AUC_{0-t}$, $\uparrow CL_t$/F, $\uparrow t_{max}$, ↓RB	
			15-20, *po*†	$\downarrow t_{1/2}$, $\downarrow V_{ss}$, $\uparrow C_{max}$, ↑F, $\uparrow AUC_{0-t}$, $\downarrow CL_t$/F, $\uparrow t_{max}$, ↑RB	
	Male C57 mice	Quinidine, 5, iv	10, iv#	$\uparrow t_{1/2}$, $\rightarrow t_{max}$, $\uparrow C_{max}$, $\uparrow AUC_{0-t}$, $\uparrow AUC_{0-\infty}$	Ravikumar Reddy et al. (2016)
Flavanols					
Epigallocatechin	Male Sprague-Dawley rats	Diltiazem, 15, *po*	1-12, *po*#	$\downarrow CL_t$, $\uparrow AUC_{0-\infty}$, $\uparrow C_{max}$, $\uparrow t_{1/2}$, $\rightarrow t_{max}$, ↑F, ↑RB	Li and Choi (2008)
Hesperidin	Male Sprague-Dawley rats	Verapamil, 9, *po*	3-10, *po*†	$\downarrow CL_t$, $\downarrow K_{el}$, $\uparrow AUC_{0-\infty}$, $\uparrow C_{max}$, $\uparrow t_{max}$, $\uparrow t_{1/2}$, ↑F, ↑RB	Piao and Choi (2008)
	Male Sprague-Dawley rats	Diltiazem, 15, *po*	1, *po*#	$\rightarrow t_{max}$, $\uparrow AUC_{0-\infty}$, $\uparrow C_{max}$, $\uparrow t_{1/2}$, ↑F, ↑RB	Cho et al. (2009)
			5-15, *po*#	$\downarrow t_{max}$, $\uparrow AUC_{0-\infty}$, $\uparrow C_{max}$, $\uparrow t_{1/2}$, ↑F, ↑RB	
Morin	Female Sprague-Dawley rats	Docetaxel, 20, *po*	15, *po*#	$\downarrow t_{max}$, $\uparrow AUC_{0-\infty}$, $\uparrow t_{1/2}$, $\uparrow C_{max}$, ↑F	Yang et al. (2011)
		Docetaxel, 4, iv	15, *po*#	$\downarrow AUC_{0-\infty}$, $\downarrow t_{1/2}$, ↓MRT, $\downarrow V_{ss}$, $\uparrow CL_t$, $\uparrow CL_R$, $\uparrow CL_{NR}$	
	Male Sprague-Dawley rats	Tamoxifen, *po*, 10	3-10, *po*#	$\downarrow CL_t$, $\uparrow AUC_{0-\infty}$, $\uparrow C_{max}$, $\rightarrow t_{max}$, $\uparrow t_{1/2}$, ↑F, ↑RB	Shin et al. (2008)
	Male Sprague-Dawley rats	Diltiazem, 15, *po*	1.5-7.5, *po*†	$\uparrow C_{max}$, $\rightarrow t_{max}$, $\downarrow t_{1/2}$, $\downarrow CL_t$, $\uparrow AUC_{0-\infty}$, $\uparrow K_a$, ↑F, ↑RB	Choi and Han (2005)
			15, *po*†	$\downarrow C_{max}$, $\rightarrow t_{max}$, $\downarrow t_{1/2}$, $\downarrow CL_t$, $\uparrow AUC_{0-\infty}$, $\uparrow K_a$, ↑F, ↑RB	

Flavonoids	Animal model	Drug dose (mg/kg), route	Flavonoid dose (mg/kg), route	Effects on pharmacokinetic parameters	References
	Male Sprague-Dawley rats	Paclitaxel, 6, *po* Paclitaxel, 2, iv	5-15, *po*# 5, *po*# 15, *po*#	→t_{max}, ↑$AUC_{0-\infty}$, ↑$t_{1/2}$, ↑C_{max}, ↑F ↓CL_t, ↑$AUC_{0-\infty}$, ↑$t_{1/2}$, ↑V_{ss} ↓CL_t, ↑$AUC_{0-\infty}$, ↑$t_{1/2}$, →V_{ss}	Li et al. (2007)
	Male Sprague-Dawley rats	Nicardipine, 12, *po* Nicardipine, 4, iv	1.5, *po*# 7.5, *po*# 15, *po*# 7.5-15, *po*#	↓CL_t, ↓$t_{1/2}$, ↑$AUC_{0-\infty}$, ↑C_{max}, ↑K_{el}, ↑RB ↓CL_t, →$t_{1/2}$, ↑$AUC_{0-\infty}$, ↑C_{max}, →K_{el}, ↑RB ↓CL_t, ↑$t_{1/2}$, ↑$AUC_{0-\infty}$, ↑C_{max}, ↓K_{el}, ↑RB ↓CL_t, ↑$t_{1/2}$, ↑$AUC_{0-\infty}$, ↓K_{el}	Piao et al. (2008)
	Male Sprague-Dawley rats	Paclitaxel, 30, *po* Paclitaxel, 3, iv	3.3, *po*# 10, *po*# 3.3-10, *po*#	↓t_{max}, ↓CL_t, ↓V_d, ↑$AUC_{0-\infty}$, ↑C_{max}, →$t_{1/2}$,↑F, ↑RB ↓t_{max}, ↓CL_t, ↓V_d, ↑$AUC_{0-\infty}$, ↑C_{max}, ↑$t_{1/2}$, ↑F, ↑RB ↓CL_t, ↓V_d, ↓$t_{1/2}$, ↑$AUC_{0-\infty}$, ↑MRT	Choi et al. (2006)
	Male New Zealand white rabbits	Nimodipine, 15, *po* Nimodipine, 15, *po*	2, *po*# 10-20, *po*# 2-20, *po*†	↓K_{el}, ↑AUC_{0-24}, ↑C_{max}, →t_{max}, ↑$t_{1/2}$, ↑F, ↑RB ↓K_{el}, ↑AUC_{0-24}, ↑C_{max}, ↑t_{max}, ↑$t_{1/2}$, ↑F, ↑RB ↓K_{el}, ↑AUC_{0-24}, ↑C_{max}, →t_{max}, ↑$t_{1/2}$, ↑F, ↑RB	Choi and Burm (2006)
	Male Wistar rats	Talinolol, 10, *po* Talinolol, 1, iv	0.1, *po*# 2.5, *po*# 5, *po*# 2.5, *po*# 5, *po*#	↓CL_t, ↑$AUC_{0-\infty}$, ↑C_{max}, ↓t_{max}, ↓$t_{1/2}$, ↑F ↓CL_t, ↑$AUC_{0-\infty}$, ↑C_{max}, ↑t_{max}, ↑$t_{1/2}$, ↑F ↓CL_t, ↑$AUC_{0-\infty}$, ↑C_{max}, ↓t_{max}, ↑$t_{1/2}$, ↑F ↓$AUC_{0-\infty}$, ↑$t_{1/2}$, ↑CL_t ↑$AUC_{0-\infty}$, ↑$t_{1/2}$, ↓CL_t	Pathak and Udupa (2010)
	Yorkshire pigs	Digoxin, 0.02, *po*	40, *po*†	↓t_{max}, ↓MRT, ↑AUC_{0-t}, ↑$AUMC_{0-t}$, ↑C_{max}	Wang et al. (2004)
Naringenin	Male Sprague-Dawley rats	Talinolol, 10, *po*	0.7, *po*†	↑AUC_{0-6}, ↑$AUC_{0-\infty}$, ↑C_{max}, ↓t_{max}, →$t_{1/2}$	de Castro et al. (2008)
Naringin	Female Sprague-Dawley rats	Tamoxifen, 10, *po*	1.5-10, *po*#	↑$AUC_{0-\infty}$, ↑C_{max}, →t_{max}, ↑$t_{1/2}$, ↑F, ↑RB	Choi and Kang (2008)
	Male New Zealand rabbit	Verapamil, 9, *po*	1.5-15, *po*#	↑$AUC_{0-\infty}$, ↑C_{max}, →t_{max}, ↑K_a, ↑$t_{1/2}$, ↑F, ↑RB	Yeum and Choi (2006)

Flavonoids	Animal model	Drug dose (mg/kg), route	Flavonoid dose (mg/kg), route	Effects on pharmacokinetic parameters	References
	Male Sprague-Dawley rats	Talinolol, 10, *po*	2.4, *po*† 9.4, *po*†	↑$AUC_{0\text{-}6}$, ↑$AUC_{0\text{-}\infty}$, ↑C_{max}, ↑t_{max}, ↑$t_{1/2}$ ↑$AUC_{0\text{-}6}$, ↑$AUC_{0\text{-}\infty}$, ↑C_{max}, →t_{max}, ↑$t_{1/2}$	De Castro et al. (2008)
Flavones					
Baicalein	Male Sprague-Dawley rats	Doxorubicin, 50, *po* Doxorubicin, 10, iv	0.3-6, *po*#	↓CL_t, ↑$AUC_{0\text{-}\infty}$, ↑C_{max}, →t_{max}, ↑$t_{1/2}$, ↑F, ↑RB ↓CL_t, ↑$AUC_{0\text{-}\infty}$,↑$t_{1/2}$	Shin et al. (2009)
	Male Sprague-Dawley rats	Tamoxifen, 10, *po*	0.5-10, *po*#	↓CL_t, ↑$AUC_{0\text{-}\infty}$, ↑C_{max}, ↑t_{max}, ↑$t_{1/2}$, ↑F, ↑RB	Li et al. (2011)
	Male Sprague-Dawley rats	Irinotecan, 12, *po* Irinotecan, 3, iv	0.4-8, *po*#	↑$AUC_{0\text{-}\infty}$, ↑C_{max}, →t_{max}, ↑$t_{1/2}$, ↑F, ↑RB ↓CL_t, ↑$AUC_{0\text{-}\infty}$, ↑$t_{1/2}$, ↑RB	Cho et al. (2011)
Flavone	Male Sprague-Dawley rats	Paclitaxel, 40, *po*	2-20, *po*#	↓t_{max}, ↓K_{el}, ↑K_a, ↑$AUC_{0\text{-}24}$, ↑C_{max}, ↑$t_{1/2}$, ↑F, ↑RB	Choi et al. (2004a)
Oroxylin A	Male Sprague-Dawley rats	Paclitaxel, 15, *po*	30, *po*†	↑$AUC_{0\text{-}\infty}$, →t_{max}, ↑C_{max}, ↑RB	Go et al. (2009)
Flavonols					
Kaempferol	Male Sprague-Dawley rats	Etoposide, 6, *po* Etoposide, 2, iv	1-12, *po*#	↓CL_t, ↓K_{el}, ↑$AUC_{0\text{-}\infty}$, →t_{max}, ↑C_{max}, ↑$t_{1/2}$, ↑F, ↑RB ↓CL_t, ↓K_{el}, ↑$AUC_{0\text{-}\infty}$, ↑$t_{1/2}$, ↑RB	Li et al. (2009)
	Male Sprague-Dawley rats	Tamoxifen, 10, *po*	2.5, *po*# 10, *po*#	↓$t_{1/2}$, ↓t_{max}, ↑$AUC_{0\text{-}\infty}$, ↑C_{max}, ↑F ↓$t_{1/2}$, ↑t_{max}, ↑$AUC_{0\text{-}\infty}$, ↑C_{max}, ↑F	Piao et al. (2008)
Myricetin	Male Sprague-Dawley rats	Doxorubicin, 40, *po*	0.4-10, *po*#	↑$AUC_{0\text{-}\infty}$, ↑C_{max}, →t_{max}, ↑$t_{1/2}$, ↑F, ↑RB	Choi et al. (2011b)
	Male Sprague-Dawley rats	Losartan, 9, *po*	0.4, *po*# 2-8, *po*#	↓V_d, ↑$AUC_{0\text{-}\infty}$, ↑C_{max}, →t_{max}, ↑$t_{1/2}$, ↑F, ↑RB ↓V_d, ↑$AUC_{0\text{-}\infty}$, ↑C_{max}, ↑t_{max}, ↑$t_{1/2}$, ↑F, ↑RB	Choi et al. (2010)

Flavonoids	Animal model	Drug dose (mg/kg), route	Flavonoid dose (mg/kg), route	Effects on pharmacokinetic parameters	References
Quercetin	Female Sprague-Dawley rats	Tamoxifen, 10, *po*	2-15, *po*†	↑$AUC_{0-\infty}$, ↑C_{max}, →t_{max}, ↑K_a, ↑$t_{1/2}$, ↑F, ↑RB	Shin et al. (2006)
	Female Wistar rats	Irinotecan, 80, *po*	20, *po*#	↓t_{max}, ↓CL_t, ↓K_{el}, ↓V_d, ↑$AUC_{0-\infty}$, ↑C_{max}, ↑MRT, ↑MAT, ↑$t_{1/2}$, ↑AUC_{0-2}, ↑F, ↑RB	Bansal et al. (2008)
		Irinotecan, 20, iv		↓CL_t, ↓V_d, ↓C_0, ↑$AUC_{0-\infty}$, ↑MRT, ↑K_{el}, ↑RB	
	Male Sprague-Dawley rats	Cyclosporine, 10, *po*	50, *po*†	↓AUC_{0-t}, ↓C_{max}	Hsiu et al. (2002)
	Male Sprague-Dawley rats	Etoposide, 9, *po*	1, *po*†	↓CL_t, ↓K_{el}, ↑$AUC_{0-\infty}$, ↓C_{max}, ↑t_{max}, ↑$t_{1/2}$, ↑F, ↑RB	Li and Choi (2009)
			5-15, *po*†	↓CL_t, ↓K_{el}, ↑$AUC_{0-\infty}$, ↑C_{max}, ↑t_{max}, ↑$t_{1/2}$, ↑F, ↑RB	
		Etoposide, 3, iv	1-15, *po*†	↓CL_t, ↓K_{el}, ↑$AUC_{0-\infty}$, ↑$t_{1/2}$	
	Male Sprague-Dawley rats	Paclitaxel, 40, *po*	2-20, *po*#	↓t_{max}, ↑AUC_{0-24}, ↑C_{max}, ↑$t_{1/2}$, ↑MRT, ↑F, ↑RB	Choi et al. (2004b)
	Male Sprague-Dawley rats	Doxorubicin, 50, *po*	0.6-15, *po*†	↓V_{ss}, ↑$AUC_{0-\infty}$, ↑C_{max}, ↑$t_{1/2}$, ↑F, ↑RB	Choi et al. (2011a)
	Male C57 mice	Quinidine, 5, iv	10, iv#	→$t_{1/2}$, →t_{max}, →C_{max}, →AUC_{0-t}, →$AUC_{0-\infty}$	Ravikumar Reddy et al. (2016)
	Male New Zealand white rabbits	Diltiazem, 15, *po*	2-20, *po*#	↓K_{el}, ↑AUC_{0-24}, ↑C_{max}, →t_{max}, ↑$t_{1/2}$, ↑F, ↑RB	Choi and Li (2005)
			2-10, *po*†	↓K_{el}, ↑AUC_{0-24}, ↑C_{max}, ↑$t_{1/2}$, ↑F, ↑RB	
			20, *po*†	↓K_{el}, ↓AUC_{0-24}, ↓C_{max}, ↑$t_{1/2}$, ↓F, ↓RB	
	Male Yorkshire pigs	Cyclosporine, 10, *po*	50, *po*†	↓C_{max}, ↓AUC_{0-t}, ↓AUC_{0-3}, ↓AUC_{3-24}	Hsiu et al. (2002)
Isoflavones					
Biochanin A	Female Sprague-Dawley rats	Tamoxifen, 10, *po*	100, *po*#	↓$AUC_{0-\infty}$, ↓C_{max}, ↓t_{max}, ↓$t_{1/2}$, ↓F	Singh et al. (2012)

Flavonoids	Animal model	Drug dose (mg/kg), route	Flavonoid dose (mg/kg), route	Effects on pharmacokinetic parameters	References
	Male Sprague-Dawley rats	Digoxin, 20, *po* Fexofenadine, 20, *po* Paclitaxel, 20, *po*	100, *po*[#]	$\downarrow t_{1/2}$, $\uparrow AUC_{0-\infty}$, $\uparrow C_{max}$, $\downarrow t_{max}$, $\downarrow$MRT, $\uparrow$F $\downarrow t_{1/2}$, $\downarrow AUC_{0-\infty}$, $\downarrow C_{max}$, $\uparrow t_{max}$, $\uparrow$MRT, $\downarrow$F, $\downarrow K_a$, $\downarrow t_{1/2}$, $\uparrow AUC_{0-\infty}$, $\uparrow C_{max}$, $\uparrow t_{max}$, $\uparrow$MRT, $\uparrow$F	Peng et al. (2006)
	Male Sprague-Dawley	Doxorubicin, 7.5, iv Cyclosporine, 3, iv Cyclosporine, 10, *po*	100, ip[#] 250, *po*[#] 250, *po*[#]	$\rightarrow$ AUC, $\rightarrow t_{1/2}$, $\rightarrow CL_t$, $\rightarrow V_{ss}$ $\rightarrow$ AUC, $\rightarrow t_{1/2}$, $\rightarrow CL_t$, $\rightarrow CL$/F, $\rightarrow V_{ss}$ $\rightarrow$ AUC, $\rightarrow t_{1/2}$, $\rightarrow CL_t$, $\rightarrow CL$/F, $\rightarrow V_{ss}$, $\rightarrow C_{max}$, $\rightarrow t_{max}$, $\rightarrow F$	Zhang et al. (2010)
Genistein	Male Sprague-Dawley rats	Paclitaxel, 30, *po* Paclitaxel, 3, iv	3.3-10, *po*[#]	$\downarrow CL_t$, $\downarrow t_{max}$, $\downarrow K_{el}$, $\uparrow AUC_{0-\infty}$, $\uparrow C_{max}$, $\uparrow t_{1/2}$, $\uparrow$F, $\uparrow$RB $\downarrow CL_t$, $\downarrow K_{el}$, $\uparrow AUC_{0-\infty}$, $\uparrow t_{1/2}$, $\uparrow$RB	Li and Choi (2007)

AUC, Area under the concentration-time curve; AUC_{0-t}, AUC from 0 to t; $AUC_{0-\infty}$, AUC from 0 h to infinity; $AUMC_{0-t}$, Area under the moment curve from time zero to the last point; C_{max}, Peak concentration; CL_{NR}, Non-renal clearance; CL_R, Renal clearance; CL_t, Total body clearance; CL_t/F, Oral clearance; C_0, Initial plasma concentration of drugs obtained by back-extrapolation to y-axis; F, Absolute bioavailability; iv, Intravenous; k_a, Absorption rate constant; K_{el}, Elimination rate constant; MAT, Mean absorption time; MRT, Mean residence time; po, Per os; RB, Relative bioavailability; t_{max}, Time to reach C_{max}; $t_{1/2}$, Terminal elimination half-life; V_{ss}, Apparent volume of distribution at steady-state; V_d, Apparent volume of distribution; [#], Pretreatment with the flavonoid compound; [†], Coadministration of the drug and flavonoid; ↓Decrease; ↑Increase; →Maintain.

Appendix B

Table B.1. Best-fit values and respective standard errors of the concentration-response curves for baicalein, (-)-epigallocatechin gallate [(-)-EPG], kaempferol, quercetin and silymarin as well as for their dual combinations.

		Best-fit values					Standard Error		
	r^2	Bottom	Top	$LogEC_{50}$ (μM)	HillSlope	EC_{50} (μM)	Top	$LogEC_{50}$ (μM)	HillSlope
Baicalein	0.9912	1	11.88	2.08	9.64	120.0	0.19	0.04	4.90
(-)-EPG	0.9881	1	8.899	2.13	1.96	132.3	0.15	0.02	0.13
Kaempferol	0.9898	1	23.82	2.52	3.44	332.5	0.35	0.01	0.24
Quercetin	0.9913	1	12.44	2.38	4.04	241.2	0.19	0.01	0.47
Sylimarin	0.9765	1	19.33	2.55	11.10	352.3	0.50	0.03	3.82
Baicalein/ Quercetin 1:1	0.9784	1	27.59	2.41	5.21	259.5	0.56	0.01	0.49
Baicalein/ Quercetin 1:3	0.9756	1	13.46	2.35	6.65	221.9	0.24	0.01	1.13
Baicalein/ Quercetin 3:1	0.9912	1	24.59	2.41	2.37	255.7	1.32	0.03	0.25
Baicalein/ Sylimarin 1:1	0.9469	1	23.51	2.47	2.69	294.9	1.63	0.03	0.41
Baicalein/ Sylimarin 1:3	0.9364	1	21.16	2.58	1.39	383.2	2.11	0.08	0.19
Baicalein/ Sylimarin 3:1	0.9497	1	14.58	2.32	3.61	206.5	0.39	0.01	0.42
(-)-EPG/ Baicalein 1:1	0.9853	1	34.67	2.34	1.91	220.4	1.79	0.03	0.15
(-)-EPG/ Baicalein 1:3	0.9796	1	30.01	2.21	2.84	162.3	3.06	0.04	0.37
(-)-EPG/ Baicalein 3:1	0.9607	1	Ambiguous						
(-)-EPG/ Quercetin 1:1	0.9505	1	32.06	2.63	1.37	426.6	5.40	0.12	0.20
(-)-EPG/ Quercetin 1:3	0.9819	1	33.72	2.62	1.89	415.0	2.28	0.04	0.17
(-)-EPG/ Quercetin 3:1	0.9776	1	36.89	2.55	1.63	352.5	3.64	0.06	0.16
(-)-EPG/ Silymarin 1:1	0.9834	1	Ambiguous						
(-)-EPG/ Silymarin 1:3	0.9784	1	Ambiguous						
(-)-EPG/ Silymarin 3:1	0.9897	1	31.95	2.55	1.61	351.2	1.76	0.04	0.10
Kaempferol/ Baicalein 1:1	0.9430	1	23.99	2.39	3.06	244.2	2.34	0.04	0.54
Kaempferol/ Baicalein 1:3	0.9910	1	33.53	2.31	6.76	203.2	0.77	0.01	0.55
Kaempferol/ Baicalein 3:1	0.9703	1	30.65	2.54	1.93	348.9	4.18	0.07	0.26
Kaempferol/ (-)-EPG 1:1	0.9815	1	19.42	2.24	4.20	174.5	0.27	0.01	0.33

		Best-fit values					Standard Error		
	r^2	Bottom	Top	LogEC$_{50}$ (µM)	HillSlope	EC$_{50}$ (µM)	Top	LogEC$_{50}$ (µM)	HillSlope
Kaempferol/ (-)-EPG 1:3	0.9595	1	23.37	2.38	2.21	240.0	1.18	0.03	0.26
Kaempferol/ (-)-EPG 3:1	0.9931	1	26.48	2.68	3.28	475.5	0.50	0.01	0.17
Kaempferol/ Quercetin 1:1	0.9883	1	18.12	2.45	3.07	282.4	0.28	0.01	0.20
Kaempferol/ Quercetin 1:3	0.9620	1	35.84	2.56	2.38	362.9	2.72	0.04	0.32
Kaempferol/ Quercetin 3:1	0.9762	1	21.51	2.61	1.79	403.7	1.50	0.04	0.18
Kaempferol/ Silymarin 1:1	0.9832	1	28.06	2.46	2.49	286.3	1.32	0.03	0.23
Kaempferol/ Silymarin 1:3	0.9760	1	63.73	2.85	2.04	699.7	20.64	0.13	0.30
Kaempferol/ Silymarin 3:1	0.9574	1	60.88	2.87	1.43	744.4	25.29	0.24	0.25
Silymarin/ Quercetin 1:1	0.9615	1	44.84	2.92	1.83	829.1	8.52	0.10	0.27
Silymarin/ Quercetin 1:3	0.9854	1	26.87	2.54	3.52	346.3	0.53	0.01	0.26
Silymarin/ Quercetin 3:1	0.9574	1	Ambiguous						

EC$_{50}$, half maximal effective concentration

Table B.2. Theoretical concentration of baicalein, (-)-epigallocatechin gallate [(-)-EPG], kaempferol, quercetin and silymarin as well as of their dual combinations that induces an 8-fold increase in the intracellular accumulation of rhodamine 123.

	Fold increase	Log Concentration (μM)	Concentration (μM)
Baicalein	8	2.11	127.52
(-)-EPG	8	2.58	380.59
Kaempferol	8	2.42	261.25
Quercetin	8	2.43	269.71
Sylimarin	8	2.53	336.64
Baicalein/Quercetin 1:1	8	2.33	212.90
Baicalein/Quercetin 1:3	8	2.36	230.27
Baicalein/Quercetin 3:1	8	2.25	177.83
Baicalein/Sylimarin 1:1	8	2.34	219.46
Baicalein/Sylimarin 1:3	8	2.39	243.09
Baicalein/Sylimarin 3:1	8	2.32	210.11
(-)-EPG/Baicalein 1:1	8	2.04	109.44
(-)-EPG/Baicalein 1:3	8	2.03	108.32
(-)-EPG/Baicalein 3:1	8	Ambiguous	
(-)-EPG/Quercetin 1:1	8	2.24	173.34
(-)-EPG/Quercetin 1:3	8	2.32	208.28
(-)-EPG/Quercetin 3:1	8	2.17	147.52
(-)-EPG/Silymarin 1:1	8	Ambiguous	
(-)-EPG/Silymarin 1:3	8	Ambiguous	
(-)-EPG/Silymarin 3:1	8	2.21	163.83
Kaempferol/Baicalein 1:1	8	2.27	186.50
Kaempferol/Baicalein 1:3	8	2.22	167.82
Kaempferol/Baicalein 3:1	8	2.28	189.95
Kaempferol/(-)-EPG 1:1	8	2.19	155.38
Kaempferol/(-)-EPG 1:3	8	2.23	168.13
Kaempferol/(-)-EPG 3:1	8	2.54	353.49
Kaempferol/Quercetin 1:1	8	2.40	250.54
Kaempferol/Quercetin 1:3	8	2.31	203.32
Kaempferol/Quercetin 3:1	8	2.45	279.44
Kaempferol/Silymarin 1:1	8	2.27	187.79
Kaempferol/Silymarin 1:3	8	2.40	253.13
Kaempferol/Silymarin 3:1	8	2.26	180.73
Silymarin/Quercetin 1:1	8	2.52	334.88
Silymarin/Quercetin 1:3	8	2.42	261.07
Silymarin/Quercetin 3:1	8	Ambiguous	

EC_{50}, half maximal effective concentration

REFERENCES

List of references

ABBASI E *ET AL*. (**2012**) Neuroprotective effects of vitexin, a flavonoid, on pentylenetetrazole-induced seizure in rats. *Chem Biol Drug Des*. 80(2): 274–278.

ABDALLAH HM *ET AL*. (**2015**) P-glycoprotein inhibitors of natural origin as potential tumor chemo-sensitizers: A review. *J Adv Res*. 6(1): 45–62.

ABDEL-REHIM M (**2010**) Recent advances in microextraction by packed sorbent for bioanalysis. *J Chromatogr A*. 1217(16): 2569–2580.

ABDEL-REHIM M (**2011**) Microextraction by packed sorbent (MEPS): a tutorial. *Anal Chim Acta*. 701(2): 119–128.

ABRAHAM J *ET AL*. (**2009**) A phase I study of the P-glycoprotein antagonist tariquidar in combination with vinorelbine. *Clin Cancer Res*. 15(10): 3574–3582.

ABRAHAM S, **SHAJU M** (**2013**) Innovations in epilepsy management - an overview. *J Pharm Pharm Sci*. 16(4): 564–576.

AKAMINE Y *ET AL*. (**2012**) Carbamazepine differentially affects the pharmacokinetics of fexofenadine enantiomers. *Br J Clin Pharmacol*. 73(3): 478–481.

AL-HUMAYYD MS (**1996**) Diltiazem and verapamil elevate plasma phenytoin concentrations in the rat. *Int J Pharm*. 131(2): 153–158.

ALBANI F, **BARUZZI A** (**2006**) Oxcarbazepine long-term treatment retention in patients switched over from carbamazepine. *Neurol Sci*. 27(3): 173–175.

ALEXOPOULOS A (**2013**) Pharmacoresistant epilepsy: Definition and explanation. *Epileptology*. 1(1): 38–42.

ALEXOPOULOS A *ET AL*. (**2007**) Electrical stimulation and gene-based neuromodulation for control of medically-refractory epilepsy. *Acta Neurochir Suppl*. 97(Pt 2): 293–309.

ALI H-A *ET AL*. (**2008**) Pachypodol, a flavonol from the leaves of Calycopteris floribunda, inhibits the growth of CaCo-2 colon cancer cell line in vitro. *Phytother Res*. 22(12): 1684–1687.

ALMEIDA AM *ET AL*. (**2002**) Linear regression for calibration lines revisited: weighting schemes for bioanalytical methods. *J Chromatogr B Anal Technol Biomed Life Sci*. 774(2): 215–222.

ALONSO-CASTRO AJ *ET AL*. (**2013**) Kaempferitrin induces apoptosis via intrinsic pathway in HeLa cells and exerts antitumor effects. *J Ethnopharmacol*. 145(2): 476–489.

ALVAREZ AI *ET AL*. (**2010**) Modulation of the activity of ABC transporters (P-glycoprotein, MRP2, BCRP) by flavonoids and drug response. *J Pharm Sci*. 99(2): 598–617.

ALVARIZA S *ET AL*. (**2013**) Verapamil effect on phenytoin pharmacokinetics in rats. *Epilepsy Res*. 107(1–2): 51–55.

ALVES G *ET AL*. (**2010**) Enantioselective assay for therapeutic drug monitoring of eslicarbazepine acetate: no interference with carbamazepine and its metabolites. *Ther Drug Monit*. 32(4): 512–516.

ALVES G *ET AL*. (**2013**) A critical review of microextraction by packed sorbent as a sample preparation approach in drug bioanalysis. *Bioanalysis*. 5: 1–34.

AMIN ML (**2013**) P-glycoprotein inhibition for optimal drug delivery. *Drug Target Insights*. 7: 27–34.

AN G, MORRIS ME (**2010**) Effects of the isoflavonoid biochanin A on the transport of mitoxantrone in vitro and in vivo. *Biopharm Drug Dispos*. 31(5–6): 340–350.

ANDERS H-J, VIELHAUER V (**2007**) Identifying and validating novel targets with in vivo disease models: guidelines for study design. *Drug Discov Today*. 12(11–12): 446–451.

ANDERSSON TB (**2010**) The application of HepaRG cells in evaluation of cytochrome P450 induction properties of drug compounds. *Methods Mol Biol*. 640: 375–387.

ANDRADE EL *ET AL*. (**2016**) Non-clinical studies required for new drug development – Part I: early in silico and in vitro studies, new target discovery and validation, proof of principles and robustness of animal studies. *Braz J Med Biol Res*. 49: 1–9.

ANINAT C *ET AL*. (**2006a**) Expression of Cytochrome P450 Enzymes and Nuclear Receptors in Human Hepatoma HepaRG Cells. *Drug Metab Dispos*. 34(1): 75–83.

ANINAT C *ET AL*. (**2006b**) Expression of cytochromes P450, conjugating enzymes and nuclear receptors in human hepatoma HepaRG cells. *Drug Metab Dispos*. 34(1): 75–83.

ANNESLEY TM, CLAYTON L (**2004**) Simple extraction protocol for analysis of immunosuppressant drugs in whole blood. *Clin Chem*. 50(10): 1845–1848.

ANTHÉRIEU S *ET AL*. (**2010**) Stable expression, activity, and inducibility of cytochromes P450 in differentiated HepaRG cells. *Drug Metab Dispos*. 38(3): 516–525.

ANTHÉRIEU S *ET AL*. (**2012**) Optimization of the HepaRG cell model for drug metabolism and toxicity studies. *Toxicol Vitr*. 26(8): 1278–1285.

ANTUNES NJ *ET AL*. (**2016**) Influence of verapamil on the pharmacokinetics of oxcarbazepine and of the enantiomers of its 10-hydroxy metabolite in healthy volunteers. *Eur J Clin Pharmacol*. 72(2): 195–201.

ARONICA E *ET AL*. (**2003**) Expression and cellular distribution of multidrug transporter proteins in two major causes of medically intractable epilepsy: focal cortical dysplasia and glioneuronal tumors. *Neuroscience*. 118(2): 417–429.

ARONICA E *ET AL*. (**2004**) Expression and cellular distribution of multidrug resistance-related proteins in the hippocampus of patients with mesial temporal lobe epilepsy. *Epilepsia*. 45(5): 441–451.

ASADI M *ET AL*. (**2015**) Simultaneous extraction and quantification of lamotrigine, phenobarbital, and phenytoin in human plasma and urine samples using solidified floating organic drop microextraction and high-performance liquid chromatography. *J Sep Sci*. 38(14): 2510–2516.

ASZALOS A (**2008**) Role of ATP-binding cassette (ABC) transporters in interactions between natural products and drugs. *Curr Drug Metab*. 9(10): 1010–1018.

BADHAN R, **PENNY J** (**2006**) In silico modelling of the interaction of flavonoids with human P-glycoprotein nucleotide-binding domain. *Eur J Med Chem*. 41(3): 285–295.

BAHLS FH *ET AL*. (**1991**) Interactions between calcium channel blockers and the anticonvulsants carbamazepine and phenytoin. *Neurology*. 41(5): 740–742.

BAJPAI M, **ESMAY JD** (**2002**) In vitro studies in drug discovery and development: an analysis of study objectives and application of good laboratory practices (GLP). *Drug Metab Rev*. 34(4): 679–689.

BALAYSSAC D *ET AL*. (**2005**) Does inhibition of P-glycoprotein lead to drug-drug interactions? *Toxicol Lett*. 156(3): 319–329.

BALTES S *ET AL*. (**2007**) Differences in the transport of the antiepileptic drugs phenytoin, levetiracetam and carbamazepine by human and mouse P-glycoprotein. *Neuropharmacology*. 52(2): 333–346.

BALUCHNEJADMOJARAD T *ET AL*. (**2010**) Inhibitory effect of high dose of the flavonoid quercetin on amygdala electrical kindling in rats. *Basic Clin Neurosci*. 1(3): 57–61.

BANERJEE PN *ET AL*. (**2009**) The descriptive epidemiology of epilepsy-a review. *Epilepsy Res*. 85(1): 31–45.

BANSAL T *ET AL*. (**2008**) Pre-clinical evidence for altered absorption and biliary excretion of irinotecan (CPT-11) in combination with quercetin: possible contribution of P-glycoprotein. *Life Sci*. 83(7–8): 250–259.

BANSAL T *ET AL*. (**2009**) Emerging significance of flavonoids as P-glycoprotein inhibitors in cancer chemotherapy. *J Pharm Pharm Sci*. 12(1): 46–78.

BARTHOMEUF C *ET AL*. (**2005**) Inhibition of P-glycoprotein transport function and reversion of MDR1 multidrug resistance by cnidiadin. *Cancer Chemother Pharmacol*. 56(2): 173–181.

BARTMANN H *ET AL*. (**2010**) Imaging of P-glycoprotein–mediated pharmacoresistance in the hippocampus: proof-of-concept in a chronic rat model of temporal lobe epilepsy. *Epilepsia*. 51(9): 1780–1790.

BAUER B *ET AL*. (**2008**) Seizure-induced up-regulation of P-glycoprotein at the blood-brain barrier through glutamate and cyclooxygenase-2 signaling. *Mol Pharmacol*. 73(5): 1444–1453.

BAULAC M *ET AL*. (**2015**) Epilepsy priorities in Europe: A report of the ILAE-IBE epilepsy advocacy Europe task force. *Epilepsia*. 56(11): 1687–1695.

BEATTIE B *ET AL*. (**1988**) Verapamil-induced carbamazepine neurotoxicity. A report of two cases. *Eur Neurol*. 28(2): 104–105.

BEGHI M *ET AL*. (**2009**) Utilization and costs of antiepileptic drugs in the elderly: still an unsolved issue. *Drugs Aging*. 26(2): 157–168.

BELL GS, SANDER JW (**2002**) The epidemiology of epilepsy: the size of the problem. *Seizure*. 11 Suppl A: 306-14–6.

BELLAMY WT (**1996**) P-glycoproteins and multidrug resistance. *Annu Rev Pharmacol Toxicol*. 36: 161–183.

BENES J *ET AL*. (**1999**) Anticonvulsant and sodium channel-blocking properties of novel 10,11-dihydro-5H-dibenz[b,f]azepine-5-carboxamide derivatives. *J Med Chem*. 42(14): 2582–2587.

BENTZ J *ET AL*. (**2013**) Variability in P-glycoprotein inhibitory potency (IC50) using various in vitro experimental systems: implications for universal digoxin drug-drug interaction risk assessment decision criteria. *Drug Metab Dispos*. 41(7): 1347–1366.

BERG AT (**2009**) Identification of pharmacoresistant epilepsy. *Neurol Clin*. 27(4): 1003–1013.

BHOGAL N, BALLS M (**2008**) Translation of new technologies: from basic research to drug discovery and development. *Curr Drug Discov Technol*. 5(3): 250–262.

BIALER M (**2012a**) Why are antiepileptic drugs used for nonepileptic conditions? *Epilepsia*. 53 Suppl 7: 26–33.

BIALER M (**2012b**) Chemical properties of antiepileptic drugs (AEDs). *Adv Drug Deliv Rev*. 64(10): 887–895.

BIALER M *ET AL*. (**2017**) Progress report on new antiepileptic drugs: A summary of the Thirteenth Eilat Conference on New Antiepileptic Drugs and Devices (EILAT XIII). *Epilepsia*. 58(2): 181–221.

BIALER M, WHITE HS (**2010**) Key factors in the discovery and development of new antiepileptic drugs. *Nat Rev Drug Discov*. 9(1): 68–82.

BJORNSSON TD *ET AL*. (**2003**) The conduct of in vitro and in vivo drug-drug interaction studies: a PhRMA perspective. *Drug Metab Dispos*. 43(5): 443–469.

BLAUWBLOMME T *ET AL*. (**2014**) Mechanisms of ictogenesis. *Int Rev Neurobiol*. 114: 155–185.

BOIS F *ET AL*. (**1998**) Halogenated chalcones with high-affinity binding to P-glycoprotein: potential modulators of multidrug resistance. *J Med Chem*. 41(21): 4161–4164.

BOIS F *ET AL*. (**1999**) Synthesis and biological activity of 4-alkoxy chalcones: potential hydrophobic modulators of P-glycoprotein–mediated multidrug resistance. *Bioorg Med Chem*. 7(12): 2691–2695.

BOISON D (**2016**) The biochemistry and epigenetics of epilepsy: focus on adenosine and glycine. *Front Mol Neurosci*. 9: 26.

BONARY ARK *ET AL*. (**2009**) Effect of memantine on plasma concentrations of carbamazepine and phenytoin in rats: A controlled experimental study. *Curr Ther Res Clin Exp*. 70(5): 359–365.

BORSKA S *ET AL*. (**2010**) Quercetin as a potential modulator of P-glycoprotein expression and function in cells of human pancreatic carcinoma line resistant to daunorubicin. *Molecules*. 15(2): 857–870.

BOUMENDJEL A *ET AL*. (**2002**) Recent advances in the discovery of flavonoids and analogs with high-affinity binding to P-glycoprotein responsible for cancer cell multidrug resistance. *Med Res Rev*. 22(5): 512–529.

BRAND W *ET AL*. (**2006**) Flavonoid-mediated inhibition of intestinal ABC transporters may affect the oral bioavailability of drugs, food-borne toxic compounds and bioactive ingredients. *Biomed Pharmacother*. 60(9): 508–519.

BRANDT C *ET AL*. (**2004**) Striking differences in individual anticonvulsant response to phenobarbital in rats with spontaneous seizures after status epilepticus. *Epilepsia*. 45(12): 1488–1497.

BRANDT C *ET AL*. (**2006**) The multidrug transporter hypothesis of drug resistance in epilepsy: Proof-of-principle in a rat model of temporal lobe epilepsy. *Neurobiol Dis*. 24(1): 202–211.

BRANTLEY SJ *ET AL*. (**2010**) Two flavonolignans from milk thistle (Silybum marianum) inhibit CYP2C9-mediated warfarin metabolism at clinically achievable concentrations. *J Pharmacol Exp Ther*. 332(3): 1081–1087.

BREIER A *ET AL*. (**2013**) New insight into P-glycoprotein as a drug target. *Anticancer Agents Med Chem*. 13(1): 159–170.

BRODIE MJ (**2010**) Antiepileptic drug therapy the story so far. *Seizure*. 19(10): 650–655.

BRODIE MJ *ET AL*. (**2013**) Enzyme induction with antiepileptic drugs: cause for concern? *Epilepsia*. 54(1): 11–27.

BRODIE MJ, DICHTER MA (**1996**) Antiepileptic drugs. *N Engl J Med*. 334(3): 168–175.

BROWN C (**2016**) Pharmacological management of epilepsy. *Prog Neurol Psychiatry*. 20(2): 27–34c.

BUCHWALD A *ET AL.* (**2012**) Validation of an LC-MS/MS method to determine five immunosuppressants with deuterated internal standards including MPA. *BMC Clin Pharmacol*. 12: 2.

BUDAKOVA L *ET AL.* (**2008**) Simultaneous determination of antiepileptic drugs and their two active metabolites by HPLC. *J Sep Sci*. 31(1): 1–8.

BUER CS *ET AL.* (**2010**) Flavonoids: new roles for old molecules. *J Integr Plant Biol*. 52(1): 98–111.

BUGAMELLI F *ET AL.* (**2002**) Simultaneous analysis of six antiepileptic drugs and two selected metabolites in human plasma by liquid chromatography after solid-phase extraction. *Anal Chim Acta*. 472(1): 1–10.

CALLEGARI C *ET AL.* (**2016**) Antiepileptic drug use in a nursing home setting: a retrospective study in older adults. *Funct Neurol*. 31(2): 87–93.

CALLIES S *ET AL.* (**2003**) A population pharmacokinetic model for paclitaxel in the presence of a novel P-gp modulator, Zosuquidar Trihydrochloride (LY335979). *Br J Clin Pharmacol*. 56(1): 46–56.

CASSIDY A, MINIHANE A-M (**2016**) The role of metabolism (and the microbiome) in defining the clinical efficacy of dietary flavonoids. *Am J Clin Nutr*. 105(1): 10–22.

CASSIDY CE, SETZER WN (**2010**) Cancer-relevant biochemical targets of cytotoxic Lonchocarpus flavonoids: a molecular docking analysis. *J Mol Model*. 16(2): 311–326.

CASTRO AF, ALTENBERG GA (**1997**) Inhibition of drug transport by genistein in multidrug-resistant cells expressing P-glycoprotein. *Biochem Pharmacol*. 53(1): 89–93.

CASTRO WV *ET AL.* (**2007**) Grapefruit juice-drug interactions: grapefruit juice and its components inhibit P-glycoprotein (ABCB1) mediated transport of talinolol in Caco-2 cells. *J Pharm Sci*. 96(10): 2808–2817.

CHAN K-F *ET AL.* (**2009**) Flavonoid dimers as bivalent modulators for P-glycoprotein-based multidrug resistance: structure-activity relationships. *ChemMedChem*. 4(4): 594–614.

CHAN LMS *ET AL.* (**2004**) The ABCs of drug transport in intestine and liver: efflux proteins limiting drug absorption and bioavailability. *Eur J Pharm Sci*. 21(1): 25–51.

CHANDRAN S, SINGH R (**2007**) Comparison of various international guidelines for analytical method validation. *Pharmazie*. 62(1): 4–14.

CHANG C *ET AL.* (**2006**) Rapid identification of P-glycoprotein substrates and inhibitors. *Drug Metab Dispos*. 34(12): 1976–1984.

CHANG X (**2007**) A molecular understanding of ATP-dependent solute transport by multidrug resistance-associated protein MRP1. *Cancer Metastasis Rev*. 26(1): 15–37.

CHEN C *ET AL*. (**2010**) Quercetin: a potential drug to reverse multidrug resistance. *Life Sci*. 87(11–12): 333–338.

CHEN X *ET AL*. (**2005**) Determination of methacycline in human plasma by liquid chromatography coupled to tandem mass spectrometry. *Anal Chim Acta*. 553(1): 15–20.

CHEN Z *ET AL*. (**2016**) Mammalian drug efflux transporters of the ATP binding cassette (ABC) family in multidrug resistance: A review of the past decade. *Cancer Lett*. 370(1): 153–164.

CHHUN S *ET AL*. (**2009**) Gefitinib-phenytoin interaction is not correlated with the C-erythromycin breath test in healthy male volunteers. *Br J Clin Pharmacol*. 68(2): 226–237.

CHICO I *ET AL*. (**2001**) Phase I study of infusional paclitaxel in combination with the P-glycoprotein antagonist PSC 833. *J Clin Oncol*. 19(3): 832–842.

CHIELI E *ET AL*. (**2009**) In vitro effects of Mangifera indica and polyphenols derived on ABCB1/P-glycoprotein activity. *Food Chem Toxicol*. 47(11): 2703–2710.

CHO CW *ET AL*. (**2000**) Carrier-mediated uptake of rhodamine 123: implications on its use for MDR research. *Biochem Biophys Res Commun*. 279(1): 124–130.

CHO Y-A *ET AL*. (**2009**) Effect of hesperidin on the oral pharmacokinetics of diltiazem and its main metabolite, desacetyldiltiazem, in rats. *J Pharm Pharmacol*. 61(6): 825–829.

CHO Y-A *ET AL*. (**2011**) Effects of the antioxidant baicalein on the pharmacokinetics of nimodipine in rats: a possible role of P-glycoprotein and CYP3A4 inhibition by baicalein. *Pharmacol Rep*. 63(4): 1066–1073.

CHOI B-C *ET AL*. (**2006**) Altered pharmacokinetics of paclitaxel by the concomitant use of morin in rats. *Int J Pharm*. 323(1–2): 81–85.

CHOI D-H *ET AL*. (**2010**) Effects of myricetin, an antioxidant, on the pharmacokinetics of losartan and its active metabolite, EXP-3174, in rats: possible role of cytochrome P450 3A4, cytochrome P450 2C9 and P-glycoprotein inhibition by myricetin. *J Pharm Pharmacol*. 62(7): 908–914.

CHOI J-S *ET AL*. (**2004a**) Enhanced bioavailability of paclitaxel after oral coadministration with flavone in rats. *Int J Pharm*. 275(1–2): 165–170.

CHOI J-S *ET AL*. (**2004b**) Enhanced paclitaxel bioavailability after oral administration of paclitaxel or prodrug to rats pretreated with quercetin. *Eur J Pharm Biopharm*. 57(2): 313–318.

CHOI J-S *ET AL*. (**2011a**) Effects of quercetin on the bioavailability of doxorubicin in rats: role of CYP3A4 and P-gp inhibition by quercetin. *Arch Pharm Res*. 34(4): 607–613.

CHOI J-S, **BURM JP** (**2006**) Enhanced nimodipine bioavailability after oral administration of nimodipine with morin, a flavonoid, in rabbits. *Arch Pharm Res*. 29(4): 333–338.

CHOI J-S, **HAN H-K** (**2005**) Pharmacokinetic interaction between diltiazem and morin, a flavonoid, in rats. *Pharmacol Res*. 52(5): 386–391.

CHOI J-S, **KANG KW** (**2008**) Enhanced tamoxifen bioavailability after oral administration of tamoxifen in rats pretreated with naringin. *Arch Pharm Res*. 31(12): 1631–1636.

CHOI J-S, **LI X** (**2005**) Enhanced diltiazem bioavailability after oral administration of diltiazem with quercetin to rabbits. *Int J Pharm*. 297(1–2): 1–8.

CHOI RCY ***ET AL***. (**2013**) Synergic action of flavonoids, baicalein, and daidzein in estrogenic and neuroprotective effects: A development of potential health products and therapeutic drugs against alzheimer's disease.

CHOI S-J ***ET AL***. (**2011b**) Effects of myricetin on the bioavailability of doxorubicin for oral drug delivery in rats: possible role of CYP3A4 and P-glycoprotein inhibition by myricetin. *Arch Pharm Res*. 34(2): 309–315.

CHOKCHAISIRI R ***ET AL***. (**2009**) Bioactive flavonoids of the flowers of Butea monosperma. *Chem Pharm Bull (Tokyo)*. 57(4): 428–432.

CHUNG SY ***ET AL***. (**2005**) Inhibition of P-glycoprotein by natural products in human breast cancer cells. *Arch Pharm Res*. 28(7): 823–828.

CHUNG SY ***ET AL***. (**2007**) Modulation of P-glycoprotein–mediated resistance by kaempferol derivatives isolated from Zingiber zerumbet. *Phytother Res*. 21(6): 565–569.

CLINCKERS R ***ET AL***. (**2005**) Quantitative in vivo microdialysis study on the influence of multidrug transporters on the blood-brain barrier passage of oxcarbazepine: concomitant use of hippocampal monoamines as pharmacodynamic markers for the anticonvulsant activity. *J Pharmacol Exp Ther*. 314(2): 725–731.

CLINCKERS R ***ET AL***. (**2008**) Impact of efflux transporters and of seizures on the pharmacokinetics of oxcarbazepine metabolite in the rat brain. *Br J Pharmacol*. 155(7): 1127–1138.

CLOUSTON TS (**1868**) Experiments to determine the precise effect of Bromide of Potassium in Epilepsy. *Br J Psychiatry*. 14(67): 305–321.

COLETA M ***ET AL***. (**2008**) Assessment of luteolin (3',4',5,7-tetrahydroxyflavone) neuropharmacological activity. *Behav Brain Res*. 189(1): 75–82.

COLEY HM (**2010**) Overcoming multidrug resistance in cancer: clinical studies of p-glycoprotein inhibitors. *Methods Mol Biol*. 596: 341–358.

CONSEIL G ***ET AL***. (**1998**) Flavonoids: a class of modulators with bifunctional interactions at vicinal ATP- and steroid-binding sites on mouse P-glycoprotein. *Proc Natl Acad Sci U S A*. 95(17): 9831–9836.

COOK N, **SAMMAN S** (**1996**) Flavonoids - Chemistry, metabolism, cardioprotective effects, and dietary sources. *J Nutr Biochem*. 7(2): 66–76.

COREA G *ET AL*. (**2009**) Jatrophane diterpenes from Euphorbia spp. as modulators of multidrug resistance in cancer therapy. *Phytochem Rev*. 8(2): 431–447.

COSTA A *ET AL*. (**2014**) An evaluation of the latest in vitro tools for drug metabolism studies. *Expert Opin Drug Metab Toxicol*. 10(1): 103–119.

CRIVELLATO E *ET AL*. (**2002**) The fluorescent probe Bodipy-FL-verapamil is a substrate for both P-glycoprotein and multidrug resistance-related protein (MRP)-1. *J Histochem Cytochem*. 50(5): 731–734.

CROZIER A *ET AL*. (**2009**) Dietary phenolics: chemistry, bioavailability and effects on health. *Nat Prod Rep*. 26(8): 1001–1043.

DALIC L, COOK MJ (**2016**) Managing drug-resistant epilepsy: challenges and solutions. *Neuropsychiatr Dis Treat*. 12: 2605–2616.

DANIEL W, NETTER KJ (**1988**) Metabolic interaction between imipramine and carbamazepine in vivo and in vitro in rats. *Naunyn Schmiedebergs Arch Pharmacol*. 337(1): 105–110.

DANTZIG AH *ET AL*. (**2003**) Considerations in the design and development of transport inhibitors as adjuncts to drug therapy. *Adv Drug Deliv Rev*. 55(1): 133–150.

DARNELL M *ET AL*. (**2011**) Cytochrome P450-dependent metabolism in HepaRG cells cultured in a dynamic three-dimensional bioreactor. *Drug Metab Dispos*. 39(7): 1131–1138.

DE CASTRO WV *ET AL*. (**2008**) Effect of grapefruit juice, naringin, naringenin, and bergamottin on the intestinal carrier-mediated transport of talinolol in rats. *J Agric Food Chem*. 56(12): 4840–4845.

DE KINDEREN RJA *ET AL*. (**2014**) Side-effects of antiepileptic drugs: the economic burden. *Seizure*. 23(3): 184–190.

DE WET H *ET AL*. (**2001**) Sequence requirements of the ATP-binding site within the C-terminal nucleotide-binding domain of mouse P-glycoprotein: structure-activity relationships for flavonoid binding. *Biochemistry*. 40(34): 10382–10391.

DECKERS CL *ET AL*. (**2000**) Selection of antiepileptic drug polytherapy based on mechanisms of action: the evidence reviewed. *Epilepsia*. 41(11): 1364–1374.

DEELEY RG *ET AL*. (**2006**) Transmembrane transport of endo- and xenobiotics by mammalian ATP-binding cassette multidrug resistance proteins. *Physiol Rev*. 86(3): 849–899.

DEFERME S, AUGUSTIJNS P (**2003**) The effect of food components on the absorption of P-gp substrates: a review. *J Pharm Pharmacol*. 55(2): 153–162.

DEL AMO EM *ET AL*. (**2009**) In vitro-in vivo correlation in P-glycoprotein mediated transport in intestinal absorption. *Eur J Pharm Sci*. 36(2–3): 200–211.

DINIS-OLIVEIRA RJ *ET AL*. (**2006**) P-glycoprotein induction: an antidotal pathway for paraquat-induced lung toxicity. *Free Radic Biol Med*. 41(8): 1213–1224.

DOKE SK, **DHAWALE SC** (**2015**) Alternatives to animal testing: A review. *Saudi Pharm J*. 23(3): 223–229.

DOMBROWSKI SM ***ET AL***. (**2001**) Overexpression of multiple drug resistance genes in endothelial cells from patients with refractory epilepsy. *Epilepsia*. 42(12): 1501–1506.

DONATO MT, **CASTELL J V** (**2003**) Strategies and molecular probes to investigate the role of cytochrome P450 in drug metabolism: focus on in vitro studies. *Clin Pharmacokinet*. 42(2): 153–178.

DORAN A ***ET AL***. (**2005**) The impact of P-glycoprotein on the disposition of drugs targeted for indications of the central nervous system: evaluation using the MDR1A/1B knockout mouse model. *Drug Metab Dispos*. 33(1): 165–174.

DRENOU B ***ET AL***. (**1993**) Detection of P glycoprotein activity on normal and leukemic CD34+ cells. *Leuk Res*. 17(12): 1031–1035.

DU G-J ***ET AL***. (**2012**) Epigallocatechin Gallate (EGCG) is the most effective cancer chemopreventive polyphenol in green tea. *Nutrients*. 4(11): 1679–1691.

DUNCAN JS ***ET AL***. (**2006**) Adult epilepsy. *Lancet*. 367(9516): 1087–1100.

DUPUY J ***ET AL***. (**2010**) Interaction of anthelmintic drugs with P-glycoprotein in recombinant LLC-PK1-mdr1a cells. *Chem Biol Interact*. 186(3): 280–286.

DZODIC P ***ET AL***. (**2012**) Development and validation of SPE-HPLC method for the determination of carbamazepine and its metabolites carbamazepine epoxide and carbamazepine trans-diol in plasma. *J Serb Chem Soc*. 77(10): 1423–1436.

EGNELL A-C ***ET AL***. (**2003**) In vivo CYP3A4 heteroactivation is a possible mechanism for the drug interaction between felbamate and carbamazepine. *J Pharmacol Exp Ther*. 305(3): 1251–1262.

EKINS S ***ET AL***. (**2002**) Application of three-dimensional quantitative structure-activity relationships of P-glycoprotein inhibitors and substrates. *Mol Pharmacol*. 61(5): 974–981.

EKOR M (**2014**) The growing use of herbal medicines: issues relating to adverse reactions and challenges in monitoring safety. *Front Pharmacol*. 4: 177.

ENGEL J (**2006**) Report of the ILAE classification core group. *Epilepsia*. 47(9): 1558–1568.

EURACHEM (**2014**) The fitness for purpose of analytical methods - a laboratory guide to method validation and related topics. *In*: https://www.eurachem.org/images/stories/Guides/pdf/MV_guide_2nd_ed_EN.pdf.

EUROPEAN MEDICINES AGENCY (**2011**) Guideline on bioanalytical method validation. *In*: http://www.ema.europa.eu/docs/en_GB/document_library/Scientific_guideline/2011/08/WC500109686.pdf.

FABRE G *ET AL*. (**1990**) Human hepatocytes as a key in vitro model to improve preclinical drug development. *Eur J Drug Metab Pharmacokinet*. 15(2): 165–171.

FANG S-H *ET AL*. (**2005**) Pharmacokinetic and pharmacodynamic interactions of morin and cyclosporin. *Toxicol Appl Pharmacol*. 205(1): 65–70.

FARDEL O *ET AL*. (**2015**) Nature and uses of fluorescent dyes for drug transporter studies. *Expert Opin Drug Metab Toxicol*. 11(8): 1233–1251.

FARHADI K *ET AL*. (**2012**) Microextraction techniques in therapeutic drug monitoring. *Biomed Chromatogr*. 26(8): 972–989.

FAUGHT E (**2004**) Treatment of refractory primary generalized epilepsy. *Rev Neurol Dis*. 1 Suppl 1: S34-43.

FÉHER J, **LENGYEL G** (**2012**) Silymarin in the prevention and treatment of liver diseases and primary liver cancer. *Curr Pharm Biotechnol*. 13(1): 210–217.

FELDMANN M, **KOEPP M** (**2016**) ABC transporters and drug resistance in patients with epilepsy. *Curr Pharm Des*. 22(38): 5793–5807.

FENG B *ET AL*. (**2008**) In vitro P-glycoprotein assays to predict the in vivo interactions of P-glycoprotein with drugs in the central nervous system. *Drug Metab Dispos*. 36(2): 268–275.

FERNÁNDEZ SP *ET AL*. (**2005**) Synergic interaction between hesperidin, a natural flavonoid, and diazepam. *Eur J Pharmacol*. 512(2–3): 189–198.

FERREIRA A *ET AL*. (**2014a**) Liquid chromatographic assay based on microextraction by packed sorbent for therapeutic drug monitoring of carbamazepine, lamotrigine, oxcarbazepine, phenobarbital, phenytoin and the active metabolites carbamazepine-10,11-epoxide and licarbazepine. *J Chromatogr B Anal Technol Biomed Life Sci*. 971: 20–29.

FERREIRA A *ET AL*. (**2014b**) HepaRG cell line as an in vitro model for screening drug-drug interactions mediated by metabolic induction: amiodarone used as a model substance. *Toxicol Vitr*. 28(8): 1531–1535.

FERREIRA A *ET AL*. (**2015**) Flavonoid compounds as reversal agents of the P-glycoprotein-mediated multidrug resistance: biology, chemistry and pharmacology. *Phytochem Rev*. 14(2): 233–272.

FERREIRA A *ET AL*. (**2016a**) Huperzine A from Huperzia serrata: a review of its sources, chemistry, pharmacology and toxicology. *Phytochem Rev*. 15(1): 51–85.

FERREIRA A *ET AL*. (**2016b**) HPLC–DAD method for the quantification of carbamazepine, oxcarbazepine and their active metabolites in HepaRG Cell culture samples. *Chromatographia*. 79(9): 581–590.

FERREIRA A *ET AL*. (**2016c**) A rapid and sensitive HPLC–DAD assay to quantify lamotrigine, phenytoin and its main metabolite in samples of cultured HepaRG cells. *J Chromatogr Sci*. 54(8): 1352–1358.

FISHER RS *ET AL*. (**2005**) Epileptic seizures and epilepsy: definitions proposed by the International League Against Epilepsy (ILAE) and the International Bureau for Epilepsy (IBE). *Epilepsia*. 46(4): 470–472.

FISHER RS *ET AL*. (**2017a**) Instruction manual for the ILAE 2017 operational classification of seizure types. *Epilepsia*. 58(4): 531–542.

FISHER RS *ET AL*. (**2017b**) Operational classification of seizure types by the International League Against Epilepsy: Position Paper of the ILAE Commission for Classification and Terminology. *Epilepsia*. 58(4): 522–530.

FLESCH G (**2004**) Overview of the clinical pharmacokinetics of oxcarbazepine. *Clin Drug Investig*. 24(4): 185–203.

FOGER F *ET AL*. (**2006**) In vivo evaluation of an oral delivery system for P-gp substrates based on thiolated chitosan. *Biomaterials*. 27(23): 4250–4255.

FOLDVARY N *ET AL*. (**2001**) Surgical treatment of epilepsy. *Neurol Clin*. 19(2): 491–515.

FORSTER S *ET AL*. (**2012**) Characterization of rhodamine-123 as a tracer dye for use in in vitro drug transport assays. *PLoS One*. 7(3): e33253.

FORTUNA A *ET AL*. (**2010**) Development and validation of an HPLC-UV method for the simultaneous quantification of carbamazepine, oxcarbazepine, eslicarbazepine acetate and their main metabolites in human plasma. *Anal Bioanal Chem*. 397(4): 1605–1615.

FORTUNA A *ET AL*. (**2011a**) In vitro and in vivo relevance of the P-glycoprotein probe substrates in drug discovery and development: Focus on rhodamine 123, digoxin and talinolol. *J Bioequiv Availab*. 1(2): 1–23.

FORTUNA A *ET AL*. (**2011b**) A chiral HPLC-UV method for the quantification of dibenz[b,f]azepine-5-carboxamide derivatives in mouse plasma and brain tissue: eslicarbazepine acetate, carbamazepine and main metabolites. *J Sep Sci*. 34(12): 1391–1401.

FORTUNA A *ET AL*. (**2012**) Evaluation of the permeability and P-glycoprotein efflux of carbamazepine and several derivatives across mouse small intestine by the Ussing chamber technique. *Epilepsia*. 53(3): 529–538.

FORTUNA A *ET AL*. (**2014**) Chiral chromatographic resolution of antiepileptic drugs and their metabolites: a challenge from the optimization to the application. *Biomed Chromatogr*. 28(1): 27–58.

FRANCESCHI L, FURLANUT M (**2005**) A simple method to monitor plasma concentrations of oxcarbazepine, carbamazepine, their main metabolites and lamotrigine in epileptic patients. *Pharmacol Res*. 51(4): 297–302.

FRANCO V *ET AL.* (**2016**) Challenges in the clinical development of new antiepileptic drugs. *Pharmacol Res*. 103: 95–104.

FRASCHINI F *ET AL.* (**2002**) Pharmacology of silymarin. *Clin Drug Inves*. 22(1): 51–65.

FRENCH JA *ET AL.* (**2013**) P-glycoprotein expression and antiepileptic drug resistance. *Lancet Neurol*. 12(8): 732–733.

FRENCH JA, **FAUGHT E** (**2009**) Rational polytherapy. *Epilepsia*. 50 Suppl 8: 63–68.

FRENCH JA, **GAZZOLA DM** (**2011**) New generation antiepileptic drugs: what do they offer in terms of improved tolerability and safety? *Ther Adv Drug Saf*. 2(4): 141–158.

FRESHNEY RI (**2010**) Culture of Animal Cells - A manual of Basic Technique and Specialized Applications, 6th edn. Hoboken, New Jersey

FROMM MF (**2004**) Importance of P-glycoprotein at blood-tissue barriers. *Trends Pharmacol Sci*. 25(8): 423–429.

GALANOPOULOU AS *ET AL.* (**2012**) Identification of new epilepsy treatments: issues in preclinical methodology. *Epilepsia*. 53(3): 571–582.

GALATI G, **O'BRIEN PJ** (**2004**) Potential toxicity of flavonoids and other dietary phenolics: Significance for their chemopreventive and anticancer properties. *Free Radic Biol Med*. 37(3): 287–303.

GAMEIRO M *ET AL.* (**2017**) Cellular models and in vitro assays for the screening of modulators of P-gp, MRP1 and BCRP. *Molecules*. 22(4): 600.

GARNETT WR *ET AL.* (**2009**) Transitional polytherapy: tricks of the trade for monotherapy to monotherapy AED conversions. *Curr Neuropharmacol*. 7(2): 83–95.

GARTZKE D, **FRICKER G** (**2014**) Establishment of optimized MDCK cell lines for reliable efflux transport studies. *J Pharm Sci*. 103(4): 1298–1304.

GAVHANE YN, **YADAV AV** (**2012**) Loss of orally administered drugs in GI tract. *Saudi Pharm J*. 20(4): 331–344.

GAZÁK R *ET AL.* (**2007**) Silybin and silymarin-new and emerging applications in medicine. *Curr Med Chem*. 14(3): 315–338.

GEICK A *ET AL.* (**2001**) Nuclear receptor response elements mediate induction of intestinal MDR1 by rifampin. *J Biol Chem*. 276(18): 14581–14587.

GHAFFARPOUR M *ET AL.* (**2013**) Pharmacokinetic and pharmacodynamic properties of the new AEDs: A review article. *Iran J Neurol*. 12(4): 157–165.

GIACOMINI KM *ET AL.* (**2010**) Membrane transporters in drug development. *Nat Rev Drug Discov*. 9(3): 215–236.

GIDAL BE (**2014**) P-glycoprotein expression and pharmacoresistant epilepsy: Cause or consequence? *Epilepsy Curr*. 14(3): 136–138.

GIESSMANN T ***ET AL***. (**2004**) Carbamazepine regulates intestinal P-glycoprotein and multidrug resistance protein MRP2 and influences disposition of talinolol in humans. *Clin Pharmacol Ther*. 76(3): 192–200.

GIRARDIN F (**2006**) Membrane transporter proteins: a challenge for CNS drug development. *Dialogues Clin Neurosci*. 8(3): 311–321.

GIUSSANI G, **BEGHI E** (**2013**) Does mechanism of drug action matter to inform rational polytherapy in epilepsy? *CNS Neurol Disord Drug Targets*. 12(3): 426–435.

GO WJ ***ET AL***. (**2009**) Evaluation of the flavonoid oroxylin A as an inhibitor of P-glycoprotein–mediated cellular efflux. *J Nat Prod*. 72(9): 1616–1619.

GOH J-Y ***ET AL***. (**2015**) Development and use of in vitro alternatives to animal testing by the pharmaceutical industry 1980–2013. *Toxicol Res*. 4(5): 1297–1307.

GOLDENBERG MM (**2010**) Overview of drugs used for epilepsy and seizures: etiology, diagnosis, and treatment. *P T*. 35(7): 392–415.

GREINER-SOSANKO E ***ET AL***. (**2007**) Drug monitoring: simultaneous analysis of lamotrigine, oxcarbazepine, 10-hydroxycarbazepine, and zonisamide by HPLC-UV and a rapid GC method using a nitrogen-phosphorus detector for levetiracetam. *Curr Neuropharmacol*. 45(9): 616–622.

GSCHWIND M, **SEECK M** (**2016**) Modern management of seizures and epilepsy. *Swiss Med Wkly*. 146: w14310.

GUBERMAN A (**1998**) Monotherapy or polytherapy for epilepsy? *Can J Neurol Sci*. 25(4): S3-8.

GUENGERICH FP ***ET AL***. (**1994**) Interactions of ingested food, beverage, and tobacco components involving human cytochrome P450 1A2, 2A6, 2E1, and 3A4 enzymes. *Env Heal Perspect*. 102 Suppl: 49–53.

GUILLOUZO A (**2008**) New perspectives in the use of human hepatocytes in the preclinical drug development process. *Ann Pharm Fr*. 66(5–6): 288–295.

GUILLOUZO A, **GUGUEN-GUILLOUZO C** (**2008**) Evolving concepts in liver tissue modeling and implications for in vitro toxicology. *Expert Opin Drug Metab Toxicol*. 4(10): 1279–1294.

HADJERI M ***ET AL***. (**2003**) Modulation of P-glycoprotein–mediated multidrug resistance by flavonoid derivatives and analogues. *J Med Chem*. 46(11): 2125–2131.

HAINZL D ***ET AL***. (**2001**) Metabolism of two new antiepileptic drugs and their principal metabolites S(+)- and R(-)-10,11-dihydro-10-hydroxy carbamazepine. *Epilepsy Res*. 44(2–3): 197–206.

HARASSTANI OA *ET AL*. (**2010**) Flavonoid combinations cause synergic inhibition of proinflammatory mediator secretion from lipopolysaccharide-induced RAW 264.7 cells. *Inflamm Res*. 59(9): 711–721.

HARBORNE JB (**1962**) Plant polyphenols. 5. Occurrence of azalein and related pigments in flowers of Plumbago and Rhododendron species. *Arch Biochem Biophys*. 96: 171–178.

HASEGAWA M, SHIRATO T (**2002**) Two new flavonoid glycosides from the leaves of Phellodendron amurense Ruprecht. *J Am Chem Soc*. 75(22): 5507–5511.

HENDRICH AB (**2006**) Flavonoid-membrane interactions: possible consequences for biological effects of some polyphenolic compounds. *Acta Pharmacol Sin*. 27(1): 27–40.

HENNESSY M, SPIERS JP (**2007**) A primer on the mechanics of P-glycoprotein the multidrug transporter. *Pharmacol Res*. 55(1): 1–15.

HILL DS *ET AL*. (**2010**) Teratogenic effects of antiepileptic drugs. *Expert Rev Neurother*. 10(6): 943–959.

HÖCHT C *ET AL*. (**2007**) Nimodipine restores the altered hippocampal phenytoin pharmacokinetics in a refractory epileptic model. *Neurosci Lett*. 413(2): 168–172.

HOENSCH HP, OERTEL R (**2015**) The value of flavonoids for the human nutrition: Short review and perspectives. *Clin Nutr Exp*. 3: 8–14.

HOOSAIN FG *ET AL*. (**2015**) Bypassing P-glycoprotein drug efflux mechanisms: Possible applications in pharmacoresistant schizophrenia therapy. *Biomed Res Int*. 2015: 484963.

HOROWITZ RM, GENTILI B (**1960**) Flavonoids of the Ponderosa lemon. *Nature*. 185(4709): 319.

HOU Y *ET AL*. (**2010**) Anti-depressant natural flavonols modulate BDNF and beta amyloid in neurons and hippocampus of double TgAD mice. *Neuropharmacology*. 58(6): 911–920.

HOYLAND K *ET AL*. (**2013**) Successful use of haemodialysis to treat phenobarbital overdose. *BMJ Case Rep*. pii: bcr20.

HSIU S-L *ET AL*. (**2002**) Quercetin significantly decreased cyclosporin oral bioavailability in pigs and rats. *Life Sci*. 72(3): 227–235.

HU K *ET AL*. (**2011**) Protective effects of quercetin against status epilepticus induced hippocampal neuronal injury in rats: involvement of X-linked inhibitor of apoptosis protein. *Acta Neurol Belg*. 111(3): 205–212.

HUISMAN MT *ET AL*. (**2003**) Assessing safety and efficacy of directed P-glycoprotein inhibition to improve the pharmacokinetic properties of saquinavir coadministered with ritonavir. *J Pharmacol Exp Ther*. 304(2): 596–602.

IANNACCONE PM, JACOB HJ (**2009**) Rats! *Dis Model Mech*. 2(5–6): 206–210.

IANNETTI P *ET AL*. (**2005**) Calcium-channel blocker verapamil administration in prolonged and refractory status epilepticus. *Epilepsia*. 46(6): 967–969.

IKEGAWA T *ET AL.* (**2000**) Inhibition of P-glycoprotein by orange juice components, polymethoxyflavones in adriamycin-resistant human myelogenous leukemia (K562/ADM) cells. *Cancer Lett*. 160(1): 21–28.

IQBAL J *ET AL.* (**2010**) Design and in vitro evaluation of a novel polymeric P-glycoprotein (P-gp) inhibitor. *J Control Release*. 147(1): 62–69.

JACOB HJ, **KWITEK AE** (**2002**) Rat genetics: attaching physiology and pharmacology to the genome. *Nat Rev Genet*. 3(1): 33–42.

JACOB S, **NAIR AB** (**2016**) An updated overview on therapeutic drug monitoring of recent antiepileptic drugs. *Drugs R D*. 16(4): 303–316.

JACOBY A *ET AL.* (**1998**) Uptake and costs of care for epilepsy: findings from a U.K. regional study. *Epilepsia*. 39(7): 776–786.

JÄGER AK, **SAABY L** (**2011**) Flavonoids and the CNS. *Molecules*. 16(2): 1471–1485.

JAMILU Y *ET AL.* (**2007**) Studies on anticonvulsant activity fractions of hydro-alcoholic root bark extract of Carissa Edulis (Vahl). *Nig Journ Pharm Sci*. 6(2): 61–66.

JARAMILLO-CARMONA S *ET AL.* (**2014**) Combination of quercetin and kaempferol enhances in vitro cytotoxicity on human colon cancer (HCT-116) cells. *Rec Nat Prod*. 8(3): 262–271.

JEONG J-M, **CHOI C-H** (**2007**) Enhancement of paclitaxel transport and cytotoxicity by 7,3',4'-trimethoxyflavone, a P-glycoprotein inhibitor. *J Pharm Pharm Sci*. 10(4): 547–553.

JIN X *ET AL.* (**2014**) Comparison of MDCK-MDR1 and Caco-2 cell based permeability assays for anti-malarial drug screening and drug investigations. *J Pharmacol Toxicol Methods*. 70(2): 188–194.

JODOIN J *ET AL.* (**2002**) Inhibition of the multidrug resistance P-glycoprotein activity by green tea polyphenols. *Biochim Biophys Acta*. 1542(1–3): 149–159.

JOHANNESSEN SI *ET AL.* (**2003**) Therapeutic drug monitoring of the newer antiepileptic drugs. *Ther Drug Monit*. 25(3): 347–363.

JOHANNESSEN SI, **LANDMARK CJ** (**2008**) Value of therapeutic drug monitoring in epilepsy. *Expert Rev Neurother*. 8(6): 929–939.

JOHANNESSEN SI, **LANDMARK CJ** (**2010**) Antiepileptic drug interactions - principles and clinical implications. *Curr Neuropharmacol*. 8(3): 254–267.

JOHANNESSEN LANDMARK C, **PATSALOS PN** (**2012**) Methodologies used to identify and characterize interactions among antiepileptic drugs. *Expert Rev Clin Pharmacol*. 5(3): 281–292.

JONKER DM *ET AL.* (**2007**) Synergic combinations of anticonvulsant agents: what is the evidence from animal experiments? *Epilepsia*. 48(3): 412–434.

JOSHI R *ET AL*. (**2015**) Pharmacodynamic and pharmacokinetic interaction of Panchagavya Ghrita with phenytoin and carbamazepine in maximal electroshock induced seizures in rats. *Ayu*. 36(2): 196–202.

JOSSÉ R *ET AL*. (**2008**) Long-term functional stability of human HepaRG hepatocytes and use for chronic toxicity and genotoxicity studies. *Drug Metab Dispos*. 36(6): 1111–1118.

JOUAN E *ET AL*. (**2016**) Evaluation of P-glycoprotein inhibitory potential using a rhodamine 123 accumulation assay. *Pharmaceutics*. 8(2): pii: E12.

JÓŹWIAK S (**2007**) Contemporary opinions on classification, pathogenesis and treatment of drug-resistant epilepsy. *Wiad Lek*. 60(5–6): 258–264.

JUENKE JM *ET AL*. (**2006**) Drug monitoring and toxicology: a procedure for the monitoring of oxcarbazepine metabolite by HPLC-UV. *J Chromatogr Sci*. 44(1): 45–48.

JULIANO RL, **LING V** (**1976**) A surface glycoprotein modulating drug permeability in Chinese hamster ovary cell mutants. *Biochim Biophys Acta*. 455(1): 152–162.

JURADO J *ET AL*. (**1991**) Study on the mutagenic activity of 13 bioflavonoids with the Salmonella Ara test. *Mutagenesis*. 6(4): 289–295.

KABEL AM (**2014**) Silymarin: insights into properties and therapeutic indications. *World J Nutr Heal*. 2(3): 33–34.

KADI AA *ET AL*. (**2013**) Simultaneous determination of phenytoin and lamotrigine in human plasma using hydrophilic interaction liquid. *Dig J Nanomater Biostruct*. 8(3): 1113–1122.

KAMINSKI RM *ET AL*. (**2009**) Benefit of combination therapy in epilepsy: a review of the preclinical evidence with levetiracetam. *Epilepsia*. 50(3): 387–397.

KATAOKA H *ET AL*. (**2016**) Recent progress in solid-phase microextraction and its pharmaceutical and biomedical applications. *Anal Methods*. 8(29): 5773–5788.

KATIYAR SK *ET AL*. (**2008**) Silymarin, a flavonoid from milk thistle (Silybum marianum L.), inhibits UV-induced oxidative stress through targeting infiltrating CD11b+ cells in mouse skin. *Photochem Photobiol*. 84(2): 266–271.

KAUR H *ET AL*. (**2016**) Antiepileptic drugs in development pipeline: A recent update. *eNeurologicalSci*. 4: 42–51.

KAWAGUCHI-SUZUKI M *ET AL*. (**2014**) The effects of milk thistle (Silybum marianum) on human cytochrome P450 activity. *Drug Metab Dispos*. 42(10): 1611–1616.

KELLENBERGER E *ET AL*. (**2011**) Flavonoids as inhibitors of human CD38. *Bioorg Med Chem Lett*. 21(13): 3939–3942.

KEMPER EM *ET AL*. (**2003**) Increased penetration of paclitaxel into the brain by inhibition of P-Glycoprotein. *Clin Cancer Res*. 9(7): 2849–2855.

KESSEL D *ET AL.* (**1968**) Uptake and retention of daunomycin by mouse leukemic cells as factors in drug response. *Cancer Res*. 28(5): 938–941.

KEUNG WM, **VALLEE BL** (**1993**) Daidzin: a potent, selective inhibitor of human mitochondrial aldehyde dehydrogenase. *Proc Natl Acad Sci U S A*. 90(4): 1247–1251.

KHAN IA *ET AL.* (**2000**) Antigiardial activity of isoflavones from Dalbergia frutescens bark. *J Nat Prod*. 63(10): 1414–1416.

KHANTAMAT O *ET AL.* (**2004**) Screening of flavonoids for their potential inhibitory effect on P-glycoprotein activity in human cervical carcinoma KB cells. *Chiang Mai Med Bull*. 43(2): 45–56.

KHODAPARAST A *ET AL.* (**2012**) Anticonvulsant activity of hydroalcoholic extract and aqueous fraction of Ebenus stellata in mice. *Iran J Basic Med Sci*. 15(3): 811–819.

KHOSCHSORUR GA *ET AL.* (**2001**) Simple and rapid HPLC method for simultaneous determination of multiple antiepileptic drugs in human serum. *Chromatographia*. 54(5–6): 345–349.

KIM D-H *ET AL.* (**2004**) Eupatilin, a pharmacologically active flavone derived from Artemisia plants, induces cell cycle arrest in ras-transformed human mammary epithelial cells. *Biochem Pharmacol*. 68(6): 1081–1087.

KIM K-A *ET AL.* (**2009**) Short-term effect of quercetin on the pharmacokinetics of fexofenadine, a substrate of P-glycoprotein, in healthy volunteers. *Eur J Clin Pharmacol*. 65(6): 609–614.

KIM TH *ET AL.* (**2015**) Oxcarbazepine and its active metabolite, (S)-licarbazepine, exacerbate seizures in a mouse model of genetic generalized epilepsy. *Epilepsia*. 56(1): e6-9.

KIM YH *ET AL.* (**2010**) Chrysoeriol isolated from Eurya cilliata leaves protects MC3T3-E1 cells against hydrogen peroxide-induced inhibition of osteoblastic differentiation. *J Appl Toxicol*. 30(7): 666–673.

KITAGAWA S (**2006**) Inhibitory effects of polyphenols on P-glycoprotein–mediated transport. *Biol Pharm Bull*. 29(1): 1–6.

KITAGAWA S *ET AL.* (**2004**) Inhibition of P-glycoprotein function by tea catechins in KB-C2 cells. *J Pharm Pharmacol*. 56(8): 1001–1005.

KITAGAWA S *ET AL.* (**2005**) Structure-activity relationships of the inhibitory effects of flavonoids on P-glycoprotein-mediated transport in KB-C2 cells. *Biol Pharm Bull*. 28(12): 2274–2278.

KNIGHT JL, **WEAVER DF** (**1998**) A computational quantitative structure-activity relationship study of carbamate anticonvulsants using quantum pharmacological methods. *Seizure*. 7(5): 347–354.

KONSOULA Z, **JUNG M** (**2009**) Involvement of P-glycoprotein and multidrug resistance associated protein 1 on the transepithelial transport of a mercaptoacetamide-based histone-deacetylase inhibitor in Caco-2 cells. *Biol Pharm Bull*. 32(1): 74–78.

KORFMACHER WA (**2011**) Bioanalytical support for both in vitro and in vivo assays across drug discovery and drug development. *Encyclopedia of Drug Metabolism and Interactions*. 1–18.

KRASOWSKI MD (**2010**) Therapeutic drug monitoring of the newer anti-epilepsy medications. *Pharm (Basel)*. 3(6): 1909–1935.

KREN V, **WALTEROVÁ D** (**2005**) Silybin and silymarin-new effects and applications. *Biomed Pap Med Fac Univ Palacky Olomouc Czech Repub*. 149(1): 29–41.

KRISHNA R, **MAYER LD** (**2000**) Multidrug resistance (MDR) in cancer. Mechanisms, reversal using modulators of MDR and the role of MDR modulators in influencing the pharmacokinetics of anticancer drugs. *Eur J Pharm Sci*. 11(4): 265–283.

KUBOTA H ***ET AL***. (**2006**) Distribution and functional activity of P-glycoprotein and multidrug resistance-associated proteins in human brain microvascular endothelial cells in hippocampal sclerosis. *Epilepsy Res*. 68(3): 213–228.

KUHN J ***ET AL***. (**2010**) Simultaneous measurement of amiodarone and desethylamiodarone in human plasma and serum by stable isotope dilution liquid chromatography-tandem mass spectrometry assay. *J Pharm Biomed Anal*. 51(1): 210–216.

KUMAR G ***ET AL***. (**2013**) Phytochemical composition and in vitro antioxidant activity of aqueous extract of Aerva lanata (L.) Juss. ex Schult. Stem (Amaranthaceae). *Asian Pac J Trop Med*. 6(3): 180–187.

KUTEYKIN-TEPLYAKOV K ***ET AL***. (**2010**) Differences in the expression of endogenous efflux transporters in MDR1-transfected versus wildtype cell lines affect P-glycoprotein mediated drug transport. *Br J Pharmacol*. 160(6): 1453–1463.

KWAN P ***ET AL***. (**2001**) The mechanisms of action of commonly used antiepileptic drugs. *Pharmacol Ther*. 90(1): 21–34.

KWAN P ***ET AL***. (**2010a**) Definition of drug resistant epilepsy: consensus proposal by the ad hoc Task Force of the ILAE Commission on Therapeutic Strategies. *Epilepsia*. 51(6): 1069–1077.

KWAN P ***ET AL***. (**2010b**) Association between temporal lobe P-glycoprotein expression and seizure recurrence after surgery for pharmacoresistant temporal lobe epilepsy. *Neurobiol Dis*. 39(2): 192–197.

KWAN P, **BRODIE MJ** (**2005**) Potential role of drug transporters in the pathogenesis of medically intractable epilepsy. *Epilepsia*. 46(2): 224–235.

KWON YJ ***ET AL***. (**2006**) Study on the mechanism of P-glycoprotein inhibitory activity of silymarin in human breast cancer cell. *J Kor Pharm Sci*. 36: 315–320.

KYSELOVA Z (**2012**) Toxicological aspects of the use of phenolic compounds in disease prevention. *Interdiscip Toxicol*. 4(4): 173–183.

LAM IK *ET AL.* (**2012**) In vitro and in vivo structure and activity relationship analysis of polymethoxylated flavonoids: identifying sinensetin as a novel antiangiogenesis agent. *Mol Nutr Food Res*. 56(6): 945–956.

LASOŃ W *ET AL.* (**2013**) Research advances in basic mechanisms of seizures and antiepileptic drug action. *Pharmacol Rep*. 65(4): 787–801.

LAXER KD *ET AL.* (**2014**) The consequences of refractory epilepsy and its treatment. *Epilepsy Behav*. 37: 59–70.

LAZAROWSKI A *ET AL.* (**1999**) Tuberous sclerosis associated with MDR1 gene expression and drug-resistant epilepsy. *Pediatr Neurol*. 21(4): 731–734.

LE VEE M *ET AL.* (**2006**) Functional expression of sinusoidal and canalicular hepatic drug transporters in the differentiated human hepatoma HepaRG cell line. *Eur J Pharm Sci*. 28(1–2): 109–117.

LEE C-K, **CHOI J-S** (**2010**) Effects of silibinin, inhibitor of CYP3A4 and P-glycoprotein in vitro, on the pharmacokinetics of paclitaxel after oral and intravenous administration in rats. *Pharmacology*. 85(6): 350–356.

LEE JW, **DWORETZKY B** (**2010**) Rational Polytherapy with Antiepileptic Drugs. *Pharm (Basel)*. 3(8): 2362–2379.

LEE KH (**2000**) Research and future trends in the pharmaceutical development of medicinal herbs from Chinese medicine. *Public Heal Nutr*. 3(4A): 515–522.

LEE S-A *ET AL.* (**2010**) Clinical feasibility of immediate overnight switching from slow-release carbamazepine to oxcarbazepine in Korean patients with refractory partial epilepsy. *Seizure*. 19(6): 356–358.

LEES G, **LEACH MJ** (**1993**) Studies on the mechanism of action of the novel anticonvulsant lamotrigine (Lamictal) using primary neurological cultures from rat cortex. *Brain Res*. 612(1–2): 190–199.

LEHNERT M *ET AL.* (**1991**) Synergic inhibition by verapamil and quinine of P-glycoprotein-mediated multidrug resistance in a human myeloma cell line model. *Blood*. 77(2): 348–354.

LEVERT H *ET AL.* (**2002**) Simultaneous determination of four antiepileptic drugs in serum by high-performance liquid chromatography. *Biomed Chromatogr*. 16(1): 19–24.

LEY JP *ET AL.* (**2005**) Evaluation of bitter masking flavanones from Herba Santa [Eriodictyon californicum (H. and A.) Torr., Hydrophyllaceae]. *J Agric Food Chem*. 53(15): 6061–6066.

LHATOO SD, **SANDER JS** (**2005**) Cause-specific mortality in epilepsy. *Epilepsia*. 46 Suppl 1: 36–39.

LI AP (**2005**) Preclinical in vitro screening assays for drug-like properties. *Drug Discov Today Technol*. 2(2): 179–185.

LI C *ET AL*. (**2009**) Enhanced bioavailability of etoposide after oral or intravenous administration of etoposide with kaempferol in rats. *Arch Pharm Res*. 32(1): 133–138.

LI C *ET AL*. (**2011**) Effects of baicalein on the pharmacokinetics of tamoxifen and its main metabolite, 4-hydroxytamoxifen, in rats: possible role of cytochrome P450 3A4 and P-glycoprotein inhibition by baicalein. *Arch Pharm Res*. 34(11): 1965–1972.

LI C, **CHOI JS** (**2008**) Effects of epigallocatechin gallate on the bioavailability and pharmacokinetics of diltiazem in rats. *Pharmazie*. 63(11): 815–818.

LI X *ET AL*. (**2007**) Effects of morin on the pharmacokinetics of etoposide in rats. *Biopharm Drug Dispos*. 28(3): 151–156.

LI X, **CHOI J-S** (**2007**) Effect of genistein on the pharmacokinetics of paclitaxel administered orally or intravenously in rats. *Int J Pharm*. 337(1–2): 188–193.

LI X, **CHOI J-S** (**2009**) Effects of quercetin on the pharmacokinetics of Etoposide after oral or intravenous administration of etoposide in rats. *Anticancer Res*. 29(4): 1411–1415.

LIM S-C, **CHOI J-S** (**2006**) Effects of naringin on the pharmacokinetics of intravenous paclitaxel in rats. *Biopharm Drug Dispos*. 27(9): 443–447.

LIN JH (**2003**) Drug-drug interaction mediated by inhibition and induction of P-glycoprotein. *Adv Drug Deliv Rev*. 55(1): 53–81.

LIN JH, **LU AY** (**1997**) Role of pharmacokinetics and metabolism in drug discovery and development. *Pharmacol Rev*. 49(4): 403–449.

LIN JH, **YAMAZAKI M** (**2003a**) Role of P-Glycoprotein in Pharmacokinetics. *Clin Pharmacokinet*. 42(1): 59–98.

LIN JH, **YAMAZAKI M** (**2003b**) Role of P-glycoprotein in pharmacokinetics: clinical implications. *Clin Pharmacokinet*. 42(1): 59–98.

LING V (**1997**) Multidrug resistance: molecular mechanisms and clinical relevance. *Cancer Chemother Pharmacol*. 40 Suppl: S3-8.

LINNET K, **EJSING TB** (**2008**) A review on the impact of P-glycoprotein on the penetration of drugs into the brain. Focus on psychotropic drugs. *Eur Neuropsychopharmacol*. 18(3): 157–169.

LIU X *ET AL*. (**2007**) Increased P-glycoprotein expression and decreased phenobarbital distribution in the brain of pentylenetetrazole-kindled rats. *Neuropharmacology*. 53(5): 657–663.

LOHNER K *ET AL*. (**2007**) Flavonoids alter P-gp expression in intestinal epithelial cells in vitro and in vivo. *Mol Nutr Food Res*. 51(3): 293–300.

LÖSCHER W (**2002**) Current status and future directions in the pharmacotherapy of epilepsy. *Trends Pharmacol Sci*. 23(3): 113–118.

LÖSCHER W (**2011**) Critical review of current animal models of seizures and epilepsy used in the discovery and development of new antiepileptic drugs. *Seizure*. 20(5): 359–368.

LÖSCHER W ***ET AL***. (**2013**) New avenues for anti-epileptic drug discovery and development. *Nat Rev Drug Discov*. 12(10): 757–776.

LÖSCHER W, **POTSCHKA H** (**2002a**) Role of multidrug transporters in pharmacoresistance to antiepileptic drugs. *J Pharmacol Exp Ther*. 301(1): 7–14.

LÖSCHER W, **POTSCHKA H** (**2002b**) Role of drug efflux transporters in the brain for drug disposition and treatment of brain diseases. *Prog Neurobiol*. 76(1): 22–76.

LÖSCHER W, **POTSCHKA H** (**2005a**) Drug resistance in brain diseases and the role of drug efflux transporters. *Nat Rev Neurosci*. 6(8): 591–602.

LÖSCHER W, **POTSCHKA H** (**2005b**) Blood-brain barrier active efflux transporters: ATP-binding cassette gene family. *NeuroRx*. 2(1): 86–98.

LÖSCHER W, **POTSCHKA H** (**2005c**) Drug resistance in brain diseases and the role of drug efflux transporters. *Nat Rev Neurosci*. 6(8): 591–602.

LÖSCHER W, **SCHMIDT D** (**2002**) New horizons in the development of antiepileptic drugs. *Epilepsy Res*. 50(1–2): 3–16.

LÖSCHER W, **SCHMIDT D** (**2006**) New Horizons in the development of antiepileptic drugs: Innovative strategies. *Epilepsy Res*. 69(3): 183–272.

LÖSCHER W, **SILLS GJ** (**2007**) Drug resistance in epilepsy: why is a simple explanation not enough? *Epilepsia*. 48(12): 2370–2372.

LÜ Y ***ET AL***. (**2004**) Antiepileptic drug-induced multidrug resistance P-glycoprotein overexpression in astrocytes cultured from rat brains. *Chin Med J*. 117(11): 1682–1626.

LÜBBERSTEDT M ***ET AL***. (**2011**) HepaRG human hepatic cell line utility as a surrogate for primary human hepatocytes in drug metabolism assessment in vitro. *J Pharmacol Toxicol Methods*. 63(1): 59–68.

LUDESCHER C ***ET AL***. (**1991**) Rapid functional assay for the detection of multidrug-resistant cells using the fluorescent dye rhodamine 123. *Blood*. 78(5): 1385–1387.

LUNA-TORTÓS C ***ET AL***. (**2008**) Several major antiepileptic drugs are substrates for human P-glycoprotein. *Neuropharmacology*. 55(8): 1364–1375.

MACPHEE GJ ***ET AL***. (**1986**) Verapamil potentiates carbamazepine neurotoxicity: a clinically important inhibitory interaction. *Lancet*. 1(8483): 700–703.

MAGALHÃES P ***ET AL***. (**2016**) Can the CEIBA cocktail designed for human cytochrome P450 enzymes be used in the rat for drug interaction studies? *J Pharm Pharm Sci*. 19(4): 520–559.

MAHAR DOAN KM *ET AL*. (**2002**) Passive permeability and P-glycoprotein–mediated efflux differentiate central nervous system (CNS) and non-CNS marketed drugs. *J Pharmacol Exp Ther*. 303(3): 1029–1037.

MAKINO T *ET AL*. (**2013**) Anti-allergic effects of enzymatically modified isoquercitrin (α-oligoglucosyl quercetin 3-O-glucoside), quercetin 3-O-glucoside, α-oligoglucosyl rutin, and quercetin, when administered orally to mice. *J Nat Med*. 67(4): 881–886.

MANDAL S *ET AL*. (**2009**) Rational drug design. *Eur J Pharmacol*. 625(1–3): 90–100.

MARCHI N *ET AL*. (**2004**) Significance of MDR1 and multiple drug resistance in refractory human epileptic brain. *BMC Med*. 2: 37.

MARCHI N *ET AL*. (**2006**) Determinants of drug brain uptake in a rat model of seizure-associated malformations of cortical development. *Neurobiol Dis*. 24(3): 429–442.

MARCHI N *ET AL*. (**2011**) The etiological role of blood-brain barrier dysfunction in seizure disorders. *Cardiovasc Psychiatry Neurol*. 2011: 482415.

MARIANA B *ET AL*. (**2011**) Gender-related differences on P-glycoprotein–mediated drug intestinal transport in rats. *J Pharm Pharmacol*. 63(5): 619–626.

MARQUEZ B, VAN BAMBEKE F (**2011**) ABC multidrug transporters: target for modulation of drug pharmacokinetics and drug-drug interactions. *Curr Drug Targets*. 12(5): 600–620.

MARRONI M *ET AL*. (**2003**) Vascular and parenchymal mechanisms in multiple drug resistance: a lesson from human epilepsy. *Curr Drug Targets*. 4(4): 297–304.

MATAR KM *ET AL*. (**1999**) Effect of valproic acid on the pharmacokinetic profile of oxcarbazepine in the rat. *Pharm Acta Helv*. 73(5): 247–50.

MATHENY CJ *ET AL*. (**2001**) Pharmacokinetic and pharmacodynamic implications of P-glycoprotein modulation. *Pharmacotherapy*. 21(7): 778–796.

MATSUI T *ET AL*. (**2009**) Effect of natsudaidain isolated from Citrus plants on TNF-alpha and cyclooxygenase-2 expression in RBL-2H3 cells. *J Pharm Pharmacol*. 61(1): 109–114.

MAY TW *ET AL*. (**2003**) Clinical pharmacokinetics of oxcarbazepine. *Clin Pharmacokinet*. 42(12): 1023–1042.

MCCORMICK JW *ET AL*. (**2015**) Multiple drug transport pathways through human P-glycoprotein. *Biochemistry*. 54(28): 4374–4390.

MCGINNITY DF, RILEY RJ (**2001**) Predicting drug pharmacokinetics in humans from in vitro metabolism studies. *Biochem Soc Trans*. 29(Pt 2): 135–139.

MEADOR KJ (**2008**) Suicide in patients with epilepsy. *Epilepsy Curr*. 8(2): 40–42.

MERCOLINI L *ET AL*. (**2014**) A fast and feasible microextraction by packed sorbent (MEPS) procedure for HPLC analysis of the atypical antipsychotic ziprasidone in human plasma. *J Pharm Biomed Anal*. 88: 467–471.

MERTENS-TALCOTT SU *ET AL*. (**2007**) Polymethoxylated flavones and other phenolic derivates from citrus in their inhibitory effects on P-glycoprotein-mediated transport of talinolol in Caco-2 cells. *J Agric Food Chem*. 55(7): 2563–2568.

MEYLER M *ET AL*. (**1993**) New method for the determination of four antiepileptic drugs in human plasma by high performance liquid chromatography. *Chromatographia*. 36(1): 27–32.

MILLER DS *ET AL*. (**2009**) Modulation of P-glycoprotein at the blood-brain barrier: Opportunities to improve CNS pharmacotherapy. *Pharmacol Rev*. 60(2): 196–209.

MINKOVA G, **GETOVA D** (**2001**) Determination of carbamazepine and its metabolite carbamazepine-10,11-epoxide in serum with gas-chromatography mass spectrometry. *Methods Find Exp Clin Pharmacol*. 23(9): 481–485.

MITSUNAGA Y *ET AL*. (**2000**) Effect of bioflavonoids on vincristine transport across blood–brain barrier. *Eur J Pharmacol*. 395(3): 193–201.

MIYAKE Y *ET AL*. (**2007**) Isolation of antioxidative phenolic glucosides from lemon juice and their suppressive effect on the expression of blood adhesion molecules. *Biosci Biotechnol Biochem*. 71(8): 1911–1919.

MIZUNO N *ET AL*. (**2003**) Impact of drug transporter studies on drug discovery and development. *Pharmacol Rev*. 55(3): 425–461.

MOHANA S *ET AL*. (**2016**) Screening dietary flavonoids for the reversal of P-glycoprotein–mediated multidrug resistance in cancer. *Mol Biosyst*. 12(8): 2458–2470.

MOON YJ *ET AL*. (**2006**) Dietary flavonoids: effects on xenobiotic and carcinogen metabolism. *Toxicol Vitr*. 20(2): 187–210.

MORENO ESCOBOSA MC *ET AL*. (**2012**) Erythema and hand edema due to flavoxate. *J Investig Allergol Clin Immunol*. 22(5): 390–391.

MORRIS ME, **ZHANG S** (**2006**) Flavonoid-drug interactions: effects of flavonoids on ABC transporters. *Life Sci*. 78(18): 2116–2630.

MULA M, **SANDER JW** (**2016**) Psychosocial aspects of epilepsy: a wider approach. *BJPsych Open*. 2(4): 270–274.

NASSIRI-ASL M *ET AL*. (**2007**) Anticonvulsant effects of aerial parts of Passiflora incarnata extract in mice: involvement of benzodiazepine and opioid receptors. *BMC Complement Altern Med*. 7: 26.

NASSIRI-ASL M *ET AL*. (**2013**) Effects of quercetin on oxidative stress and memory retrieval in kindled rats. *Epilepsy Behav*. 28(2): 151–155.

NASSIRI-ASL M *ET AL*. (**2014**) Comparison between the effects of quercetin on seizure threshold in acute and chronic seizure models. *Toxicol Ind Heal*. 32(5): 936–944.

NEELS HM *ET AL*. (**2004**) Therapeutic drug monitoring of old and newer anti-epileptic drugs. *Clin Chem Lab Med*. 42(11): 1228–1255.

NEERATI P *ET AL*. (**2011**) Study on in situ and in vivo absorption kinetics of phenytoin by modulating P-glycoprotein with verapamil in rats. *Eur J Pharm Sci*. 44(1–2): 27–31.

NEWMAN DJ, **CRAGG GM** (**2012**) Natural products as sources of new drugs over the 30 years from 1981 to 2010. *J Nat Prod*. 75(3): 311–335.

NEWMAN DJ, **CRAGG GM** (**2016**) Natural Products as Sources of New Drugs from 1981 to 2014. *J Nat Prod*. 79(3): 629–661.

NGUGI AK *ET AL*. (**2011**) Incidence of epilepsy: A systematic review and meta-analysis. *Neurology*. 77(10): 1005–1012.

NIJVELDT RJ *ET AL*. (**2001**) Flavonoids: a review of probable mechanisms of action and potential applications. *Am J Clin Nutr*. 74(4): 418–425.

NISHIMURA A *ET AL*. (**2008**) Evaluation of carbamazepine pharmacokinetic profiles in mice with kainic acid-induced acute seizures. *Biol Pharm Bull*. 31(12): 2302–2308.

NOVÁKOVÁ L, **VLCKOVÁ H** (**2009**) A review of current trends and advances in modern bio-analytical methods: chromatography and sample preparation. *Anal Chim Acta*. 656(1–2): 8–35.

OFER M *ET AL*. (**2005**) Modulation of drug transport by selected flavonoids: Involvement of P-gp and OCT? *Eur J Pharm Sci*. 25(2–3): 263–271.

OGAWA Y *ET AL*. (**2006**) Allergy-preventive phenolic glycosides from Populus sieboldii. *J Nat Prod*. 69(8): 1215–1217.

OWEN A *ET AL*. (**2001**) Carbamazepine is not a substrate for P-glycoprotein. *Br J Clin Pharmacol*. 51(4): 345–349.

OWEN A *ET AL*. (**2006**) Induction of P-glycoprotein in lymphocytes by carbamazepine and rifampicin: the role of nuclear hormone response elements. *Br J Clin Pharmacol*. 62(2): 237–242.

PALMEIRA A *ET AL*. (**2011**) New uses for old drugs: pharmacophore-based screening for the discovery of P-glycoprotein inhibitors. *Chem Biol Drug Des*. 78(1): 57–72.

PALMEIRA A *ET AL*. (**2012**) Three decades of P-gp inhibitors: skimming through several generations and scaffolds. *Curr Med Chem*. 19(13): 1946–2025.

PANDEY S *ET AL*. (**2010**) Bioanalysis in drug discovery and development. *Pharm Methods*. 1(1): 14–24.

PARDRIDGE WM (**2007**) Blood-brain barrier delivery. *Drug Discov Today*. 12(1–2): 54–61.

PARK JH *ET AL*. (**2012**) Effects of silymarin and formulation on the oral bioavailability of paclitaxel in rats. *Eur J Pharm Sci*. 45(3): 296–301.

PATANASETHANONT D *ET AL.* (**2007**) Effects of Kaempferia Parviflora extracts and their flavone constituents on P-glycoprotein function. *J Pharm Sci*. 96(1): 223–233.

PATHAK SM, **UDUPA N** (**2010**) Pre-clinical evidence of enhanced oral bioavailability of the P-glycoprotein substrate talinolol in combination with morin. *Biopharm Drug Dispos*. 31(2–3): 202–214.

PATI S, **ALEXOPOULOS A V** (**2010**) Pharmacoresistant epilepsy: from pathogenesis to current and emerging therapies. *Cleve Clin J Med*. 77(7): 457–467.

PATIL KM, **BODHANKAR SL** (**2005**) Simultaneous determination of lamotrigine, phenobarbitone, carbamazepine and phenytoin in human serum by high-performance liquid chromatography. *J Pharm Biomed Anal*. 39(1–2): 181–186.

PATSALOS PN *ET AL.* (**2002**) The importance of drug interactions in epilepsy therapy. *Epilepsia*. 43(4): 365–385.

PATSALOS PN *ET AL.* (**2008**) Antiepileptic drugs-best practice guidelines for therapeutic drug monitoring: a position paper by the subcommission on therapeutic drug monitoring, ILAE Commission on Therapeutic Strategies. *Epilepsia*. 49(7): 1239–1276.

PATSALOS PN, **PERUCCA E** (**2003**) Clinically important drug interactions in epilepsy: general features and interactions between antiepileptic drugs. *Lancet Neurol*. 2(6): 347–356.

PELKONEN O *ET AL.* (**2005**) Prediction of drug metabolism and interactions on the basis of in vitro investigations. *Basic Clin Pharmacol Toxicol*. 96(3): 167–175.

PENG SX *ET AL.* (**2006**) Altered oral bioavailability and pharmacokinetics of P-glycoprotein substrates by coadministration of biochanin A. *J Pharm Sci*. 95(9): 1984–1993.

PÉREZ-TOMÁS R (**2006**) Multidrug resistance: retrospect and prospects in anti-cancer drug treatment. *Curr Med Chem*. 13(16): 1859–1876.

PERNELLE K *ET AL.* (**2011**) Automated detection of hepatotoxic compounds in human hepatocytes using HepaRG cells and image-based analysis of mitochondrial dysfunction with JC-1 dye. *Toxicol Appl Pharmacol*. 254(3): 256–266.

PERUCCA E (**2001**) Clinical pharmacology and therapeutic use of the new antiepileptic drugs. *Fundam Clin Pharmacol*. 15(6): 405–417.

PERUCCA E (**2006**) Clinically relevant drug interactions with antiepileptic drugs. *Br J Clin Pharmacol*. 61(3): 246–255.

PIAO Y-J *ET AL.* (**2008**) Effects of oral kaempferol on the pharmacokinetics of tamoxifen and one of its metabolites, 4-hydroxytamoxifen, after oral administration of tamoxifen to rats. *Biopharm Drug Dispos*. 29(4): 245–249.

PIAO Y-J, **CHOI J-S** (**2008a**) Effects of morin on the pharmacokinetics of nicardipine after oral and intravenous administration of nicardipine in rats. *J Pharm Pharmacol*. 60(5): 625–629.

PIAO Y-J, **CHOI J-S** (**2008b**) Enhanced bioavailability of verapamil after oral administration with hesperidin in rats. *Arch Pharm Res*. 31(4): 518–522.

PIETRO A DI *ET AL*. (**2002**) Cellular and molecular life sciences modulation by flavonoids of cell multidrug resistance mediated by P-glycoprotein and related ABC transporters. *Cell Mol Life Sci*. 59(2): 307–322.

POPP R, **SCHIMMER O** (**1991**) Induction of sister-chromatid exchanges (SCE), polyploidy, and micronuclei by plant flavonoids in human lymphocyte cultures. A comparative study of 19 flavonoids. *Mutat Res*. 246(1): 205–213.

POTSCHKA H (**2012**) Role of CNS efflux drug transporters in antiepileptic drug delivery: overcoming CNS efflux drug transport. *Adv Drug Deliv Rev*. 64(10): 943–952.

POTSCHKA H *ET AL*. (**2001**) P-glycoprotein and multidrug resistance-associated protein are involved in the regulation of extracellular levels of the major antiepileptic drug carbamazepine in the brain. *Neuroreport*. 12(16): 3557–3560.

POTSCHKA H *ET AL*. (**2004**) Pharmacoresistance and expression of multidrug transporter P-glycoprotein in kindled rats. *Neuroreport*. 15(10): 1657–1661.

POTSCHKA H, **LÖSCHER W** (**2002**) A comparison of extracellular levels of phenytoin in amygdala and hippocampus of kindled and non-kindled rats. *Neuroreport*. 13(1): 167–171.

PRACHAYASITTIKUL VV, **PRACHAYASITTIKUL VV** (**2016**) P-glycoprotein transporter in drug development. *EXCLI J*. 15: 113–118.

PRASHANTH S *ET AL*. (**2011**) Pharmacokinetic and pharmacodynamic drug interactions of carbamazepine and glibenclamide in healthy albino Wistar rats. *J Pharmacol Pharmacother*. 2(1): 7–10.

PUBCHEM COUMPOUND DATABASE PubChem Coumpound Database. *In*: http://www.ncbi.nlm.nih.gov/pccompound/.

PUGLIATTI M *ET AL*. (**2007**) Estimating the cost of epilepsy in Europe: a review with economic modeling. *Epilepsia*. 48(12): 2224–2233.

QUEIROZ MEC *ET AL*. (**2002**) Determination of lamotrigine simultaneously with carbamazepine, carbamazepine epoxide, phenytoin, phenobarbital, and primidone in human plasma by SPME-GC-TSD. *J Chromatogr Sci*. 40(4): 219–223.

RAJ (**2001**) Bioflavonoids classification, pharmacological, biochemical effects and therapeutic potential. Indian J. Pharmacol. 33:2.

RAKWAL R *ET AL*. (**2000**) Naringenin 7-O-methyltransferase involved in the biosynthesis of the flavanone phytoalexin sakuranetin from rice (Oryza sativa L.). *Plant Sci*. 155(2): 213–221.

RAMAKRISHNAN P (**2003**) The role of P-glycoprotein in the blood-brain barrier. *Einstein J Biol Med*. 19: 160–165.

RAMBECK B *ET AL*. (**2006**) Comparison of brain extracellular fluid, brain tissue, cerebrospinal fluid, and serum concentrations of antiepileptic drugs measured intraoperatively in patients with intractable epilepsy. *Epilepsia*. 47(4): 681–694.

RAMELET AA (**2001**) Clinical benefits of Daflon 500 mg in the most severe stages of chronic venous insufficiency. *Angiology*. 52 Suppl 1: S49-56.

RANI S *ET AL*. (**2012**) Novel micro-extraction by packed sorbent procedure for the liquid chromatographic analysis of antiepileptic drugs in human plasma and urine. *J Sep Sci*. 35(3): 359–366.

RANI S, MALIK AK (**2012**) A novel microextraction by packed sorbent-gas chromatography procedure for the simultaneous analysis of antiepileptic drugs in human plasma and urine. *J Sep Sci*. 35(21): 2970–2977.

RAO BN *ET AL*. (**2007**) Effect of silymarin on the oral bioavailability of ranitidine in healthy human volunteers. *Drug Metab Drug Interact*. 22(2–3): 175–185.

RAO YK *ET AL*. (**2011**) Insulin-mimetic action of Rhoifolin and Cosmosiin isolated from Citrus grandis (L.) Osbeck leaves: Enhanced adiponectin secretion and insulin receptor phosphorylation in 3T3-L1 cells. *Evid Based Complement Altern Med*. 2011: 624375.

RAUB TJ (**2006**) P-glycoprotein recognition of substrates and circumvention through rational drug design. *Mol Pharm*. 3(1): 3–25.

RAVIKUMAR REDDY D *ET AL*. (**2016**) Natural flavonoids silymarin and quercetin improve the brain distribution of co-administered P-gp substrate drugs. *SpringerPlus*. 5(1): 1618.

REETA KH *ET AL*. (**2011**) Pharmacokinetic and pharmacodynamic interactions of valproate, phenytoin, phenobarbitone and carbamazepine with curcumin in experimental models of epilepsy in rats. *Pharmacol Biochem Behav*. 99(3): 399–407.

REMY S, BECK H (**2006**) Molecular and cellular mechanisms of pharmacoresistance in epilepsy. *Brain*. 129(Pt 1): 18–35.

RIVA R *ET AL*. (**1996**) Pharmacokinetic interactions between antiepileptic drugs. Clinical considerations. *Clin Pharmacokinet*. 31(6): 470–493.

RIZZI M *ET AL*. (**2002**) Limbic seizures induce P-glycoprotein in rodent brain: functional implications for pharmacoresistance. *J Neurosci*. 22(14): 5833–5839.

ROBEY R *ET AL*. (**2008**) P-Glycoprotein - a Clinical Target in Drug-Refractory Epilepsy? *Mol Pharmacol*. 73(5): 1343–1346.

RODRIGUES M *ET AL*. (**2013**) First liquid chromatographic method for the simultaneous determination of amiodarone and desethylamiodarone in human plasma using microextraction by packed sorbent (MEPS) as sample preparation procedure. *J Chromatogr B Anal Technol Biomed Life Sci*. 913-4: 90–97.

ROGAWSKI MA (**2013**) The intrinsic severity hypothesis of pharmacoresistance to antiepileptic drugs. *Epilepsia*. 54 Suppl 2: 33–40.

ROGAWSKI MA, **LÖSCHER W** (**2004**) The neurobiology of antiepileptic drugs. *Nat Rev Neurosci*. 5(7): 553–564.

ROMANO B ***ET AL***. (**2013**) Novel insights into the pharmacology of flavonoids. *Phytother Res*. 27(11): 1588–1596.

ROMITI N ***ET AL***. (**2004**) Effects of grapefruit juice on the multidrug transporter P-glycoprotein in the human proximal tubular cell line HK-2. *Life Sci*. 76(3): 293–302.

ROSS JA, **KASUM CM** (**2002**) Dietary flavonoids: bioavailability, metabolic effects, and safety. *Annu Rev Nutr*. 22: 19–34.

ROWLAND A ***ET AL***. (**2006**) In vitro characterization of lamotrigine N 2-glucuronidation and the lamotrigine-valproic acid interaction. *Drug Metab Dispos*. 34(6): 1055–1062.

SACCO S, **MAFFEI M** (**1997**) The effect of isosakuranetin (5,7-dihydroxy 4′-methoxy flavanone) on potassium uptake in wheat root segments. *Phytochemistry*. 46(2): 245–248.

SANDER JW (**2003**) The epidemiology of epilepsy revisited. *Curr Opin Neurol*. 16(2): 165–170.

SARACINO MA ***ET AL***. (**2010**) Liquid chromatographic analysis of oxcarbazepine and its metabolites in plasma and saliva after a novel microextraction by packed sorbent procedure. *Anal Chim Acta*. 661(2): 222–228.

SARMA AK ***ET AL***. (**2016**) Medical management of epileptic seizures: challenges and solutions. *Neuropsychiatr Dis Treat*. 12: 467–485.

SARVER JG ***ET AL***. (**2002**) Microplate screening of the differential effects of test agents on Hoechst 33342, rhodamine 123, and rhodamine 6G accumulation in breast cancer cells that overexpress P-glycoprotein. *J Biomol Screen*. 7(1): 29–34.

SAUNA ZE ***ET AL***. (**2001**) The mechanism of action of multidrug-resistance-linked P-glycoprotein. *J Bioenerg Biomembr*. 33(6): 481–491.

SAVAGE N (**2014**) Epidemiology: The complexities of epilepsy. *Nature*. 511(7508): S2-3.

SAYYAH M ***ET AL***. (**2011**) Screening of the anticonvulsant activity of some plants from Fabaceae family in experimental seizure models in mice. *Daru*. 19(4): 301–305.

SCAMBIA G ***ET AL***. (**1994**) Quercetin potentiates the effect of Adriamycin in a multidrug-resistant MCF-7 human breast-cancer cell line: P-glycoprotein as a possible target. *Cancer Chemother Pharmacol*. 34(6): 459–464.

SCHINKEL A (**1999**) P-Glycoprotein, a gatekeeper in the blood-brain barrier. *Adv Drug Deliv Rev*. 36(2–3): 179–194.

SCHINKEL AH ***ET AL***. (**1996**) P-glycoprotein in the blood-brain barrier of mice influences the brain penetration and pharmacological activity of many drugs. *J Clin Invest*. 97(11): 2517–2524.

SCHINKEL AH, **JONKER JW** (**2012**) Mammalian drug efflux transporters of the ATP binding cassette (ABC) family: An overview. *Adv Drug Deliv Rev*. 55(1): 3–29.

SCHMIDER J ***ET AL***. (**1997**) Inhibition of CYP2C9 by selective serotonin reuptake inhibitors in vitro: studies of phenytoin p-hydroxylation. *Br J Clin Pharmacol*. 44(5): 495–498.

SCHMIDT D (**2009**) Drug treatment of epilepsy: options and limitations. *Epilepsy Behav*. 15(1): 56–65.

SCHMIDT D, **LÖSCHER W** (**2005**) Drug resistance in epilepsy: putative neurobiologic and clinical mechanisms. *Epilepsia*. 46(6): 858–877.

SCHMIDT D, **SCHACHTER SC** (**2014**) Drug treatment of epilepsy in adults. *BMJ*. 348: g2546.

SCHWAB D ***ET AL***. (**2003**) Comparison of in vitro P-glycoprotein screening assays: recommendations for their use in drug discovery. *J Med Chem*. 46(9): 1716–1725.

SEEGERS U ***ET AL***. (**2002a**) Transient increase of P-glycoprotein expression in endothelium and parenchyma of limbic brain regions in the kainate model of temporal lobe epilepsy. *Epilepsy Res*. 51(3): 257–268.

SEEGERS U ***ET AL***. (**2002b**) Expression of the multidrug transporter P-glycoprotein in brain capillary endothelial cells and brain parenchyma of amygdala-kindled rats. *Epilepsia*. 43(7): 675–684.

SEEGERS U ***ET AL***. (**2002c**) Lack of effects of prolonged treatment with phenobarbital or phenytoin on the expression of P-glycoprotein in various rat brain regions. *Eur J Pharmacol*. 451(2): 149–155.

SELVARAJ S ***ET AL***. (**2015**) Influence of membrane lipid composition on flavonoid-membrane interactions: Implications on their biological activity. *Prog Lipid Res*. 58: 1–13.

SERRALHEIRO A ***ET AL***. (**2013**) First HPLC-UV method for rapid and simultaneous quantification of phenobarbital, primidone, phenytoin, carbamazepine, carbamazepine-10,11-epoxide, 10,11-trans-dihydroxy-10,11-dihydrocarbamazepine, lamotrigine, oxcarbazepine and licarbazepine in human plas. *J Chromatogr B Anal Technol Biomed Life Sci*. 925: 1–9.

SHAH VP ***ET AL***. (**2000**) Bioanalytical method validation-a revisit with a decade of progress. *Pharm Res*. 17(12): 1551–1557.

SHAJIB MTI ***ET AL***. (**2012**) Phytotoxic effect, uptake, and transformation of biochanin A in selected weed species. *J Agric Food Chem*. 60(43): 10715–10722.

SHAPIRO AB ***ET AL***. (**1999**) Stimulation of P-glycoprotein–mediated drug transport by prazosin and progesterone. Evidence for a third drug-binding site. *Eur J Biochem*. 259(3): 841–850.

SHAPIRO AB, **LING V** (**1997**) Positively cooperative sites for drug transport by P-glycoprotein with distinct drug specificities. *Eur J Biochem*. 250(1): 130–137.

SHARMA AK *ET AL*. (**2015**) Pharmacoresistant epilepsy: A current update on non-conventional pharmacological and non-pharmacological interventions. *J Epilepsy Res*. 5(1): 1–8.

SHETH RD *ET AL*. (**2005**) Nonpharmacological treatment options for epilepsy. *Semin Pediatr Neurol*. 12: 106–113.

SHEU M-T *ET AL*. (**2010**) A quantitative structure-activity relationship for the modulation effects of flavonoids on P-glycoprotein–mediated transport. *Chem Pharm Bull (Tokyo)*. 58(9): 1187–1194.

SHIN S-C *ET AL*. (**2009**) Effects of baicalein, an antioxidant, on the bioavailability of doxorubicin in rats: possible role of P-glycoprotein inhibition by baicalein. *Pharmazie*. 64(9): 579–583.

SHIN S-C *ET AL*. (**2006**) Enhanced bioavailability of tamoxifen after oral administration of tamoxifen with quercetin in rats. *Int J Pharm*. 313(1–2): 144–149.

SHIN S-C *ET AL*. (**2008**) Effects of morin on the bioavailability of tamoxifen and its main metabolite, 4-hydroxytamoxifen, in rats. *In vivo*. 22(3): 391–395.

SHOHAI T *ET AL*. (**2011**) Importance of flavonoides in therapeutics. *Hygeia J D Med*. 3(1): 1–18.

SHORVON S, **SCHMIDT D** (**2016**) The right and the wrong with epilepsy and her science. *Epilepsia Open*. 1(3-4): 76–85.

SIDHU HS, **SADHOTRA A** (**2016**) Current status of the new antiepileptic drugs in chronic pain. *Front Pharmacol*. 7: 276.

SINGH S, **BRASHIER DS** (**2014**) Perampanel: New drug for treatment of refractory partial onset seizures. *Muller J Med Sci Res*. 5(2): 195–199.

SINGH SP *ET AL*. (**2012**) Reduced bioavailability of tamoxifen and its metabolite 4-hydroxytamoxifen after oral administration with biochanin A (an isoflavone) in rats. *Phytother Res*. 26(2): 303–307.

SISODIYA SM (**2003**) Mechanisms of antiepileptic drug resistance. *Curr Opin Neurol*. 16(2): 197–201.

SISODIYA SM *ET AL*. (**1999**) Over-expression of P-glycoprotein in malformations of cortical development. *Neuroreport*. 10(10): 3437–3441.

SKIBOLA CF, **SMITH MT** (**2000**) Potential health impacts of excessive flavonoid intake. *Free Radic Biol Med*. 29(3–4): 375–383.

SMITH M *ET AL*. (**2007**) Discovery of antiepileptic drugs. *Neurotherapeutics*. 4(1): 12–17.

SØRENSEN AT, **KOKAIA M** (**2013**) Novel approaches to epilepsy treatment. *Epilepsia*. 54(1): 1–10.

SPENCER JPE (**2007**) The interactions of flavonoids within neuronal signalling pathways. *Genes Nutr*. 2(3): 257–273.

SRINIVAS NR (**2006**) Applicability of bioanalysis of multiple analytes in drug discovery and development: review of select case studies including assay development considerations. *Biomed Chromatogr*. 20(5): 383–414.

STAFSTROM CE (**2010**) Mechanisms of action of antiepileptic drugs: the search for synergy. *Curr Opin Neurol*. 23(2): 157–163.

ST LOUIS EK ***ET AL***. (**2009**) Antiepileptic drug monotherapy: the initial approach in epilepsy management. *Curr Neuropharmacol*. 7(2): 77–82.

ST LOUIS EK, **LOUIS EK** (**2009**) Minimizing AED adverse effects: improving quality of life in the interictal state in epilepsy care. *Curr Neuropharmacol*. 7(2): 106–114.

STĘPIEŃ KM ***ET AL***. (**2012**) The multidrug transporter P-glycoprotein in pharmacoresistance to antiepileptic drugs. *Pharmacol Rep*. 64(5): 1011–1019.

STEWART A ***ET AL***. (**2000**) Phase I trial of XR9576 in healthy volunteers demonstrates modulation of P-glycoprotein in CD56+ lymphocytes after oral and intravenous administration. *Clin Cancer Res*. 6(11): 4186–4191.

STOUCH TR, **GUDMUNDSSON O** (**2002**) Progress in understanding the structure-activity relationships of P-glycoprotein. *Adv Drug Deliv Rev*. 54(3): 315–328.

SUGIMOTO H ***ET AL***. (**2011**) Quantitative investigation of the impact of P-glycoprotein inhibition on drug transport across blood-brain barrier in rats. *Drug Metab Dispos*. 39(1): 8–14.

SUMMERS MA ***ET AL***. (**2004**) Use of verapamil as a potential P-glycoprotein inhibitor in a patient with refractory epilepsy. *Ann Pharmacother*. 38(10): 1631–1634.

SUN H ***ET AL***. (**2003**) Drug efflux transporters in the CNS. *Adv Drug Deliv Rev*. 55(1): 83–105.

SUZUKI S ***ET AL***. (**1991**) Quercetin induces recombinational mutations in cultured cells as detected by DNA fingerprinting. *Jpn J Cancer Res*. 82(10): 1061–1064.

SYREK M ***ET AL***. (**1996**) Effect of carbamazepine on the pharmacokinetics of promazine. *Pol J Pharmacol*. 48(6): 601–608.

SZABO M ***ET AL***. (**2013**) Comparison of human hepatoma HepaRG cells with human and rat hepatocytes in uptake transport assays in order to predict a risk of drug induced hepatotoxicity. *PLoS One*. 8(3): e59432.

TAKANAGA H ***ET AL***. (**1998**) Inhibition of vinblastine efflux mediated by P-glycoprotein by grapefruit juice components in caco-2 cells. *Biol Pharm Bull*. 21(10): 1062–1066.

TAKANAGA H ***ET AL***. (**2000**) Polymethoxylated flavones in orange juice are inhibitors of P-glycoprotein but not cytochrome P450 3A4. *J Pharmacol Exp Ther*. 293(1): 230–236.

TANDON VR ***ET AL***. (**2006**) P-glycoprotein: Pharmacological relevance relevance. *Indian J Pharmacol*. 38(1): 13–24.

TAPAS AR *ET AL*. (**2008**) Flavonoids as nutraceuticals: A Review. *Trop J Pharm Res*. 7(3): 1089–1099.

TARAHOVSKY YS *ET AL*. (**2014**) Flavonoid-membrane interactions: involvement of flavonoid-metal complexes in raft signaling. *Biochim Biophys Acta*. 1838(5): 1235–1246.

TASSANEEYAKUL W *ET AL*. (**1993**) Specificity of substrate and inhibitor probes for human cytochromes P450 1A1 and 1A2. *J Pharmacol Exp Ther*. 265(1): 401–407.

THILAKARATHNA SH, **RUPASINGHE HPV** (**2013**) Flavonoid bioavailability and attempts for bioavailability enhancement. *Nutrients*. 5(9): 3367–3387.

THOMAS H, **COLEY HM** (**2003**) Overcoming multidrug resistance in cancer: an update on the clinical strategy of inhibiting p-glycoprotein. *Cancer Control*. 10(2): 159–165.

THUERAUF N, **FROMM MF** (**2006**) The role of the transporter P-glycoprotein for disposition and effects of centrally acting drugs and for the pathogenesis of CNS diseases. *Eur Arch Psychiatry Clin Neurosci*. 256(5): 281–286.

TISHLER DM *ET AL*. (**1995**) MDR1 gene expression in brain of patients with medically intractable epilepsy. *Epilepsia*. 36(1): 1–6.

TIWARI G, **TIWARI R** (**2010**) Bioanalytical method validation: An updated review. *Pharm Methods*. 1(1): 25–38.

TOH JY *ET AL*. (**2013**) Flavonoids from fruit and vegetables: A focus on cardiovascular risk factors. *Curr Atheroscler Rep*. 15(12): 368.

TOKI K *ET AL*. (**2008**) 7-O-Methylated anthocyanidin glycosides from Catharanthus roseus. *Phytochemistry*. 69(5): 1215–1219.

TRAN VH *ET AL*. (**2011**) Modulation of P-glycoprotein–mediated anticancer drug accumulation, cytotoxicity, and ATPase activity by flavonoid interactions. *Nutr Cancer*. 63(3): 435–443.

TROMPIER D *ET AL*. (**2003**) Multiple flavonoid-binding sites within multidrug resistance protein MRP1. *Cell Mol Life Sci*. 60(10): 2164–2177.

TSUJI PA *ET AL*. (**2013**) Structure-activity analysis of flavonoids: Direct and indirect antioxidant, and antiinflammatory potencies and toxicities. *Nutr Cancer*. 65(7): 1014–1025.

TSUKAMOTO JS *ET AL*. (**2016**) Tonic-clonic seizure following cytoreductive surgery with intraperitoneal oxaliplatin: A case report and review of the literature. *Case Rep Oncol*. 9(1): 89–94.

TURPEINEN M *ET AL*. (**2009**) Functional expression, inhibition and induction of CYP enzymes in HepaRG cells. *Toxicol Vitr*. 23(4): 748–753.

U.S. FOOD AND DRUG ADMINISTRATION (**2001**) Guidance for Industry: Bioanalytical Method Validation. *In*: https://www.fda.gov/downloads/Drugs/Guidance/ucm070107.pdf.

U.S. FOOD AND DRUG ADMINISTRATION (**2006**) Guidance for Industry: Drug interaction studies – study design, data analysis, and implications for dosing and labelling. *In*: https://www.fda.gov/OHRMS/DOCKETS/98fr/06d-0344-gdl0001.pdf.

U.S. FOOD AND DRUG ADMINISTRATION (**2010**) Guidance for Industry: M3(R2) Nonclinical Safety Studies for the Conduct of Human Clinical Trials and Marketing Authorization for Pharmaceuticals. *In*: https://www.fda.gov/downloads/drugs/guidances/ucm073246.pdf.

U.S. FOOD AND DRUG ADMINISTRATION (**2011**) Drug Development and Drug Interactions: Table of Substrates, Inhibitors and Inducers. *In*: http://www.fda.gov/Drugs/DevelopmentApprovalProcess/DevelopmentResources/DrugInteractionsLabeling/ucm093664.htm. Acessed in May 2017.

U.S. FOOD AND DRUG ADMINISTRATION (**2012**) Guidance for Industry: Drug interaction studies – study design, data analysis, and implications for dosing and labelling. *In*: https://www.fda.gov/downloads/drugs/guidances/ucm292362.pdf.

UDAYA KUMAR N *ET AL.* (**2011**) Virtual screening of flavonoids as inhibitory agents of p-glycoprotein. *IJABPT*. 2(3): 130–140.

VAISLEIB II, NEFT RA (**2008**) Overnight transition from carbamazepine to oxcarbazepine in children and adolescents. *Pharmacotherapy*. 28(10): 1211–1214.

VAN DER KOLK DM *ET AL.* (**2000**) P-glycoprotein and multidrug resistance protein activities in relation to treatment outcome in acute myeloid leukemia. *Clin Cancer Res*. 6(8): 3205–3214.

VAN HOUT B *ET AL.* (**1997**) Relationship between seizure frequency and costs and quality of life of outpatients with partial epilepsy in France, Germany, and the United Kingdom. *Epilepsia*. 38(11): 1221–1226.

VAN VLIET EA *ET AL.* (**2004**) Selective and persistent upregulation of mdr1b mRNA and P-glycoprotein in the parahippocampal cortex of chronic epileptic rats. *Epilepsy Res*. 60(2–3): 203–213.

VAN VLIET EA *ET AL.* (**2006**) Inhibition of the multidrug transporter P-glycoprotein improves seizure control in phenytoin-treated chronic epileptic rats. *Epilepsia*. 47(4): 672–680.

VAN VLIET EA *ET AL.* (**2007**) Region-specific overexpression of P-glycoprotein at the blood-brain barrier affects brain uptake of phenytoin in epileptic rats. *J Pharmacol Exp Ther*. 322(1): 141–147.

VARMA M (**2003**) P-glycoprotein inhibitors and their screening: a perspective from bioavailability enhancement. *Pharmacol Res*. 48(4): 347–359.

VAUZOUR D *ET AL.* (**2008**) The neuroprotective potential of flavonoids: a multiplicity of effects. *Genes Nutr*. 3(3–4): 115–126.

VENTOLA CL (**2014**) Epilepsy management: newer agents, unmet needs, and future treatment strategies. *P T*. 39(11): 776–792.

VERROTTI A ***ET AL***. (**2008**) Epilepsy and suicide: pathogenesis, risk factors, and prevention. *Neuropsychiatr Dis Treat*. 4(2): 365–370.

VIJAYALAKSHMI A ***ET AL***. (**2011**) Anticonvulsant and neurotoxicity profile of the rhizome of Smilax china Linn. in mice. *Indian J Pharmacol*. 43(1): 27–30.

VISK D (**2015**) Will advances in preclinical in vitro models lower the costs of drug development? *Appl Vitr Toxicol*. 1(1): 79–82.

VISWANATHAN CT ***ET AL***. (**2007**) Quantitative bioanalytical methods validation and implementation: best practices for chromatographic and ligand binding assays. *Pharm Res*. 24(10): 1962–1973.

VISWESWARI G ***ET AL***. (**2010**) Evaluation of the anticonvulsant effect of Centella asiatica (gotu kola) in pentylenetetrazol-induced seizures with respect to cholinergic neurotransmission. *Epilepsy Behav*. 17(3): 332–335.

VOLK H ***ET AL***. (**2004a**) Neuronal expression of the drug efflux transporter P-glycoprotein in the rat hippocampus after limbic seizures. *Neuroscience*. 123(3): 751–759.

VOLK HA ***ET AL***. (**2004b**) Increased expression of the multidrug transporter P-glycoprotein in limbic brain regions after amygdala-kindled seizures in rats. *Epilepsy Res*. 58(1): 67–79.

VOLK HA, **LÖSCHER W** (**2005**) Multidrug resistance in epilepsy: rats with drug-resistant seizures exhibit enhanced brain expression of P-glycoprotein compared with rats with drug-responsive seizures. *Brain*. 128(Pt 6): 1358–1368.

WAGNER H ***ET AL***. (**1969**) Synthesis of poncirin, an isosakuranetin-7-beta-neohesperidoside from Poncirus trifoliata Raf. *Chem Ber*. 102(3): 785–791.

WAHAB A (**2010**) Difficulties in treatment and management of epilepsy and challenges in new drug development. *Pharm (Basel)*. 3(7): 2090–2110.

WALSKY RL, **BOLDT SE** (**2008**) In vitro cytochrome P450 inhibition and induction. *Curr Drug Metab*. 9(9): 928–939.

WANG E ***ET AL***. (**2002**) Elevation of P-glycoprotein function by a catechin in green tea. *Biochem Biophys Res Commun*. 297(2): 412–418.

WANG EJ ***ET AL***. (**2001**) Inhibition of P-glycoprotein transport function by grapefruit juice psoralen. *Pharm Res*. 18(4): 432–438.

WANG G-X ***ET AL***. (**2016**) Intractable epilepsy and the P-glycoprotein hypothesis. *Int J Neurosci*. 126(5): 385–392.

WANG H ***ET AL***. (**2007**) Potential toxicities of flavonoids. *Wei Sheng Yan Jiu*. 36(5): 640–642.

WANG RB *ET AL*. (**2003**) Structure-activity relationship: analyses of P-glycoprotein substrates and inhibitors. *J Clin Pharm Ther*. 28(3): 203–228.

WANG Y-H *ET AL*. (**2004**) Lethal quercetin-digoxin interaction in pigs. *Life Sci*. 74(10): 1191–1197.

WANG Y-H *ET AL*. (**2005**) An in silico approach for screening flavonoids as P-glycoprotein inhibitors based on a Bayesian-regularized neural network. *J Comput Aided Mol Des*. 19(3): 137–147.

WAQAR H *ET AL*. (**2016**) Antiepileptic potential of Silybum marianum seeds in pentylenetetrazol-induced kindled mice. *Bangladesh J Pharmacol*. 11(3): 603–609.

WASOWSKI C, **MARDER M** (**2012**) Flavonoids as GABA A receptor ligands: the whole story? *J Exp Pharmacol*. 4: 9–24.

WEAVER DF (**2013**) Design of innovative therapeutics for pharmacoresistant epilepsy: challenges and needs. *Epilepsia*. 54 Suppl 2: 56–59.

WEAVER DF, **POHLMANN-EDEN B** (**2013**) Pharmacoresistant epilepsy: unmet needs in solving the puzzle(s). *Epilepsia*. 54 Suppl 2: 80–85.

WEIERGRÄBER M *ET AL*. (**2010**) Voltage-gated calcium channels in the etiopathogenesis and treatment of absence epilepsy. *Brain Res Rev*. 62(2): 245–271.

WEISS J *ET AL*. (**2003**) Interaction of antiepileptic drugs with human P-glycoprotein in vitro. *J Pharmacol Exp Ther*. 307(1): 262–267.

WERZ MA (**2008**) Pharmacotherapeutics of epilepsy: use of lamotrigine and expectations for lamotrigine extended release. *Ther Clin Risk Manag*. 4(5): 1035–1046.

WESOŁOWSKA O (**2011**) Interaction of phenothiazines, stilbenes and flavonoids with multidrug resistance-associated transporters, P-glycoprotein and MRP1. *Acta Biochim Pol*. 58(4): 433–448.

WESOŁOWSKA O *ET AL*. (**2009**) Perturbation of the lipid phase of a membrane is not involved in the modulation of MRP1 transport activity by flavonoids. *Cell Mol Biol Lett*. 14(2): 199–221.

WESSLER JD *ET AL*. (**2013**) The P-glycoprotein transport system and cardiovascular drugs. *J Am Coll Cardiol*. 61(25): 2495–2502.

WIEBE S, **JETTE N** (**2012**) Pharmacoresistance and the role of surgery in difficult to treat epilepsy. *Nat Rev Neurol*. 8(12): 669–677.

WIENKERS LC, **HEATH TG** (**2005**) Predicting in vivo drug interactions from in vitro drug discovery data. *Nat Rev Drug Discov*. 4(10): 825–833.

WILKENS S (**2015**) Structure and mechanism of ABC transporters. *F1000Prime Rep*. 7: 14.

WORLD HEALTH ORGANIZATION (**2005**) Atlas: Epilepsy care in the world. 1–91.

WORLD HEALTH ORGANIZATION (**2013**) "WHO Model List of Essential Medicines". *In*: http://apps.who.int/iris/bitstream/10665/93142/1/EML_18_eng.pdf?ua=1.

WU T ***ET AL***. (**2014**) Pharmacodynamic and pharmacokinetic interactions of perampanel and other antiepileptic drugs in a rat amygdala kindling model. *Seizure*. 23(9): 732–739.

XIE T ***ET AL***. (**2012**) Effects of epigallocatechin-3-gallate on pentylenetetrazole-induced kindling, cognitive impairment and oxidative stress in rats. *Neurosci Lett*. 516(2): 237–241.

XIONG J ***ET AL***. (**2015**) Research progress on the role of ABC transporters in the drug resistance mechanism of intractable epilepsy. *Biomed Res Int*. 2015: 194541.

YAMAZAKI M ***ET AL***. (**2001**) In vitro substrate identification studies for P-glycoprotein–mediated transport: species difference and predictability of in vivo results. *J Pharmacol Exp Ther*. 296(3): 723–735.

YANG J ***ET AL***. (**2013**) Identification of the major metabolites of hyperoside produced by the human intestinal bacteria using ultra performance liquid chromatography/quadrupole-time-of-flight mass spectrometry. *J Ethnopharmacol*. 147(1): 174–179.

YANG K ***ET AL***. (**2008**) Recent advances in the research of P-glycoprotein inhibitors. *Biosci Trends*. 2(4): 137–146.

YANG SH ***ET AL***. (**2011**) Effects of morin on the pharmacokinetics of docetaxel in rats with 7,12-dimethylbenz[a]anthracene (DMBA)-induced mammary tumors. *Arch Pharm Res*. 34(10): 1729–1734.

YANG ZY, **LIU GQ** (**2004**) Effect of P-glycoprotein inhibitor combinations on drug efflux from rat brain microvessel endothelial cells. *Pharmazie*. 59(12): 952–956.

YASUDA K ***ET AL***. (**2002**) Interaction of Cytochrome P450 3A Inhibitors with P-Glycoprotein. *J Pharmacol Exp Ther*. 303(1): 323–332.

YAZDI A ***ET AL***. (**2011**) Evaluation of the anticonvulsant activity of the leaves of Glycyrrhiza glabra var. glandulifera grown in Iran, as a possible renewable source for anticonvulsant compounds. *Iran J Pharm Res*. 10(1): 75–82.

YEUM C-H, **CHOI J-S** (**2006**) Effect of naringin pretreatment on bioavailability of verapamil in rabbits. *Arch Pharm Res*. 29(1): 102–107.

YOO HH ***ET AL***. (**2007**) Effects of diosmin, a flavonoid glycoside in citrus fruits, on P-glycoprotein-mediated drug efflux in human intestinal Caco-2 cells. *J Agric Food Chem*. 55(18): 7620-7625.

YOON SY ***ET AL***. (**2011**) Convulsion-related activities of Scutellaria flavones are related to the 5,7-dihydroxyl structures. *Eur J Pharmacol*. 659(2–3): 155–160.

YU H *ET AL*. (**2013**) Optimizing combinations of flavonoids deriving from Astragali Radix in activating the regulatory element of erythropoietin by a feedback system control scheme.

ZADROZNIAK A *ET AL*. (**2009**) Verapamil enhances the anticonvulsant effect of oxcarbazepine in the maximal electroshock-induced seizure model in mice. *Ann Univ Mariae Curie-Skłodowska*. 22(2): 115–124.

ZHANG C *ET AL*. (**2010a**) In vitro concentration dependent transport of phenytoin and phenobarbital, but not ethosuximide, by human P-glycoprotein. *Life Sci*. 86(23–24): 899–905.

ZHANG C *ET AL*. (**2011a**) In vitro transport profile of carbamazepine, oxcarbazepine, eslicarbazepine acetate, and their active metabolites by human P-glycoprotein. *Epilepsia*. 52(10): 1894–1904.

ZHANG C *ET AL*. (**2012a**) The transport of antiepileptic drugs by P-glycoprotein. *Adv Drug Deliv Rev*. 64(10): 930–942.

ZHANG D *ET AL*. (**2012b**) Preclinical experimental models of drug metabolism and disposition in drug discovery and development. *Acta Pharm Sin B*. 2(6): 549–561.

ZHANG J *ET AL*. (**2011b**) Determination of paeoniflorin, calycosin-7-O-ß-D-glucoside, ononin, calycosin and formononetin in rat plasma after oral administration of Buyang Huanwu decoction for their pharmacokinetic study by liquid chromatography-mass spectrometry. *Biomed Chromatogr*. 25(4): 450–457.

ZHANG L *ET AL*. (**2006**) Scientific perspectives on drug transporters and their role in drug interactions. *Mol Pharm*. 3(1): 62–69.

ZHANG S *ET AL*. (**2010b**) Interactions between the flavonoid biochanin A and P-glycoprotein substrates in rats: In vitro and in vivo. *J Pharm Sci*. 99(1): 430–441.

ZHANG S, MORRIS ME (**2003a**) Effects of the flavonoids biochanin A, morin, phloretin, and silymarin on P-glycoprotein–mediated transport. *J Pharmacol Exp Ther*. 304(3): 1258–1267.

ZHANG S, MORRIS ME (**2003b**) Effect of the flavonoids biochanin A and silymarin on the P-glycoprotein-mediated transport of digoxin and vinblastine in human intestinal Caco-2 cells. *Pharm Res*. 20(8): 1184–1191.

ZHAO M *ET AL*. (**2015**) Optogenetic tools for modulating and probing the epileptic network. *Epilepsy Res*. 116: 15–26.

ZHOU G-X *ET AL*. (**2009**) An acetyl flavonol from Nervilia fordii (Hance) Schltr. *J Asian Nat Prod Res*. 11(6): 498–502.

ZHOU S-F (**2008**) Drugs behave as substrates, inhibitors and inducers of human cytochrome P450 3A4. *Curr Drug Metab*. 9(4): 310–322.

ZHU L ***ET AL***. (**2013**) Oroxylin A reverses P-glycoprotein-mediated multidrug resistance of MCF7/ADR cells by G2/M arrest. *Toxicol Lett*. 219(2): 107–115.

ZOU P ***ET AL***. (**2012**) Comparative evaluation of the teratogenicity of genistein and genistin using rat whole embryo culture and limbud micromass culture methods. *Food Chem Toxicol*. 50(8): 2831–2836.

SUPPLEMENT

Isobolographic analysis of the neuro and hepatotoxic profile resulting from the combination of carbamazepine, oxcarbazepine or phenytoin with the flavonoid silymarin

The content of this supplement is included in the following manuscript:

FERREIRA A *ET AL*. Isobolographic analysis of the neuro and hepatotoxic profile resulting from the combination of carbamazepine, oxcarbazepine or phenytoin with the flavonoid silymarin (*In preparation for publication*).

S.1. Introduction

Flavonoids are a group of structurally related polyphenolic compounds present in the human diet (Bansal et al. 2009; Mohana et al. 2016). The diversity of chemical structures is responsible for the wide range of bioactivities presented by these compounds, emphasizing their interest in the treatment of numerous pathological conditions. Among them could be mentioned central nervous system (CNS)-related disorders like depression (Guan and Liu 2016), cancer (Farzaei et al. 2016), gastrointestinal disorders (Jain 2016), and cardiovascular (El Haouari and Rosado 2016), Alzheimer's (Uriarte-Pueyo and Calvo 2011), Parkinson's (Jäger and Saaby 2011) and cognitive and neurodegenerative diseases (Bell et al. 2015), as well as epilepsy (Hanrahan et al. 2011; Sucher and Carles 2015). This aspect is primarily relevant regarding the frequent coexistence of numerous illnesses in several chronic conditions (Gaitatzis et al. 2004; Wiebe and Hesdorffer 2007). Particularly, silymarin, a mixture of flavonolignans extracted from blessed milk thistle (*Silybum marianum*), is recognised as a medicinal plant for almost two millennia for the treatment of a large variety of diseases. Moreover, this flavonoid has recently received attention due to its benefits as anticonvulsant agent (Waqar et al. 2016) and recognised potential as P-glycoprotein inhibitor, one of the major pathomechanisms underlying the resistance against a variety of chemically unrelated drugs including antiepileptic drugs (AEDs) (Park et al. 2012; Ferreira et al. 2015; Ravikumar Reddy et al. 2016), highlighting their potential intrinsic value in the treatment of epilepsy.

Nowadays, the resurgence of the use of medicinal herbs in the Western world make increasingly common the combined use of modern and traditional therapies (Pathak and Udupa 2010; Newman and Cragg 2016). Indeed, the exploitation of potentially beneficial interactions between dietary supplements and drugs could be a valuable strategy in certain circumstances (Bansal et al. 2008; Pathak and Udupa 2010). In this context, and taking into account all the pharmacological properties of flavonoids, the coadministration of these compounds with AEDs could be of great significance. However, despite the promising safety profile provided by the widespread comsumption of flavonoids in our daily diet products, as well as in several nutraceuticals existing in the market, their toxicity has not been thoroughly evaluated and it remains an issue of concern (Tapas et al. 2008). Furthermore, the few existing studies that evaluated some toxicity aspects of flavonoid compounds are sometimes controversial (Dunnick and Hailey 1992; Skibola and Smith 2000; Galati and O'Brien 2004; Kyselova 2012). In opposition to flavonoids, the adverse effects of AEDs are obviously well characterized. Since these drugs act by modulating the activity of cerebral neurons, it is not surprising that the majority of their adverse effects are related with the CNS (Kennedy and Lhatoo 2008; Zaccara et al. 2008). Additionally, the drug-induced liver injury associated with AEDs is also well recognized. Indeed, although the frequency of hepatotoxicity induced by the most common AEDs is rare, the consequences can be very serious leading to liver transplantation or death (Ahmed and Siddiqi 2006; Björnsson 2008; Perucca and Gilliam 2012; Hussein et al. 2013).

Bearing in mind the pharmacotherapeutic benefits that could outcome from the coadministration of AEDs and flavonoids, it is essential the evaluation of the toxicity resulting from this combined use (CHAPMAN ET AL. 2013). Accurate prediction of drug safety remains one of the greatest challenges facing the pharmaceutical industry today (LI 2005; MCKIM 2010), arising the early toxicity screening of drug candidates of great relevance in the drug discovery and development process (PARASURAMAN 2011). Nonetheless, despite *in vivo* testing be a vital part of safety assessment, the need to support the early identification of promising drug candidates and the legislation requiring adherence to the 3Rs policy, makes the availability of *in vitro* systems a priority (KANDÁROVÁ AND LETAŠIOVÁ 2011; EUROPEAN MEDICINES AGENCY 2012; SOLDATOW ET AL. 2013; GOH ET AL. 2015). The use of *in vitro* models in toxicity testing could not only allow the decrease of the numbers of animals used, but also to reduce the costs associated with animal maintenance and care; diminish the required quantity of chemicals; shorten the experiences time; and increase the throughput for evaluating multiple chemicals and their metabolites (LIEBSCH ET AL. 2011; KANDÁROVÁ AND LETAŠIOVÁ 2011; SOLDATOW ET AL. 2013). Cytotoxicity assays are widely used for *in vitro* toxicity studies, being the 3-(4,5-dimethylthiazol-2-yl)-2,5-diphenyltetrazolium bromide (MTT) assay, whose endpoint is the mitochondrial function, one the most common employed for the detection of cytotoxicity or cell viability following exposure to the target compounds. One of the important assumptions is that acute toxicity is related to a compound's basal cytotoxicity (LI 2005). Furthermore, the isobolographic techniques have been increasingly used in the evaluation of drug-drug interactions. The isobolography is a precise and rigorous pharmacodynamic method to determine the type of interactions between active agents in mixture exhibiting a broad range of concentrations (TALLARIDA 2006; ZHAO ET AL. 2010). Theoretically, four types of interaction can be distinguished, as follows: supraadditivity (synergism), additivity, subadditivity (relative antagonism) and infraadditivity (absolute antagonism) (GRECO ET AL. 1995; LUSZCZKI AND CZUCZWAR 2003; LUSZCZKI AND CZUCZWAR 2004a; LUSZCZKI AND CZUCZWAR 2004b; LUSZCZKI AND CZUCZWAR 2006). In the last years, this methodology has also been applied in the evaluation of the toxic effects of combined anticancer drugs in several cell lines (WAWRUSZAK ET AL. 2015; GUMBAREWICZ ET AL. 2016; JARZĄB ET AL. 2017).

Hence, the present investigation aimed to explore, through an isobolographic methodology, the neuro and hepatotoxic profile resulting from the dual combinations of the commonly used AEDs carbamazepine (CBZ), oxcarbazepine (OXC) or phenytoin (PHT) with the flavonoid silymarin in the N27 rat dopaminergic neural and HepaRG cell lines, obtained experimentally in MTT assays.

S.2. Material and methods

S.2.1. Compounds and reagents

CBZ, PHT, OXC and silymarin were purchased from Sigma–Aldrich (St Louis, MO, USA). Silymarin is composed by silybinin, silydianin and silychristin, and the molar concentration was calculated based on the molecular weight of silybinin because this is the main flavonoid component

present (ZHANG AND MORRIS 2003a; ZHANG AND MORRIS 2003b). HepaRG cells (lot no. #48588) were obtained from Life Technologies – Invitrogen™ (through Alfagene, Portugal). Rat mesencephalic dopaminergic (N27) cells were kindly donated by Dr. Ana Clara Cristovão (CICS-UBI, Covilhã, Portugal). All the cell culture reagents including Williams' E medium, Roswell Park Memorial Institute (RPMI)-1640 medium, fetal bovine serum (FBS), hydrocortisone hemisuccinate, insulin, penicillin, streptomycin, MTT, dimethyl sulfoxide (DMSO), trypsin-ethylenediaminetetraacetic acid (EDTA) (0.5 g/L porcine trypsin, 0.2 g/L EDTA) and phosphate-buffered saline (PBS) were acquired from Sigma-Aldrich (St Louis, MO, USA).

S.2.2. Cell lines and culture conditions

N27 (passages 7-19) and HepaRG (passages 14-21) cells were cultured in 75-cm^2 culture flasks in RPMI-1640 supplemented with 10% FBS, 100 IU/mL penicillin and 100 µg/mL streptomycin and Williams' E medium supplemented with 10% FBS, 100 IU/mL penicillin, 100 µg/mL streptomycin, 5 µg/mL insulin and 5 x 10^{-5} M hydrocortisone hemisuccinate, respectively. Both the cell lines were maintained at 37°C in a humidified air incubator with 5% CO_2, renewing the medium every 2-3 days.

S.2.3. Cell viability assay

The MTT assays were performed according to the procedure described by FRESHNEY (2010). N27 cells and HepaRG cells were platted on 96-well microplates at a density of 10 x 10^4 cells/cm^2 and 20 x 10^4 cells/cm^2, respectively. After 24 h, the cells were incubated for more 24 h in the presence of the AEDs CBZ, OXC and PHT or the flavonoid silymarin tested at increasing concentrations (1-1000 µM). In the untreated control cells the same percentage of drug vehicle was maintained (respective culture medium with 1% DMSO, v/v). Then, the cell medium was removed and 100 µL of FBS- and antibiotic-free medium containing MTT (1 mg/mL) was loaded to each well, followed by incubation during 4 h under the same conditions. Subsequently, the MTT-containing medium was removed and replaced with 100 µL DMSO to dissolve the formazan crystals. After 10 min under gentle stirring, the absorbance was measured at 570 nm using a microplate spectrophotometer xMark™ (Bio-Rad, Hercules, CA, USA). Cell viability was expressed as a percentage relatively to the absorbance determined in the untreated control cells.

The results of combined treatment of the AEDs with flavonoids in N27 and HepaRG cells were analysed according to the isobolographic protocol. The drug concentrations were determined based on the half maximal inhibitory concentration (IC_{50}) values calculated from this cytotoxicity test.

S.2.4. Isobolographic analysis of interactions

Isobolographic interactions between CBZ, OXC or PHT and silymarin in two cell lines (N27 and HepaRG) were analysed according to the methodology described by GRABOVSKY AND TALLARIDA (2004), TALLARIDA (2006, 2007) and LUSZCZKI (2007). The isobolographic analysis is based on a comparison of equieffective compound concentrations. In isobolography, it is accepted that half the $IC_{50\ 1}$ of one compound plus half the $IC_{50\ 2}$ of the second compound should have the same effect as a full concentration of either compound tested separately. This concept of adding fractions of the IC_{50}s of compounds is a basic principle of isobolography (LOEWE 1953; BERENBAUM 1989).

The percent inhibition of cell viability per concentrations of the AEDs CBZ, OXC and PHT, or flavonoid silymarin tested alone, and the concentration-response relationship curves (CRRCs) for each investigated compound in the two cell lines (N27 and HepaRG) measured *in vitro* by the MTT assay, were fitted using log-probit linear regression analysis according to LITCHFIELD AND WILCOXON (1949). Thereafter, the median inhibitory concentrations (IC_{50}s) of CBZ, OXC, PHT, and silymarin tested alone were calculated from the respective linear equations. The test for parallelism of CRRCs for each AEDs and flavonoid, based on the log-probit analysis, was used in order to precisely and correctly analyse the experimental data with isobolography (LUSZCZKI AND CZUCZWAR 2004a; LUSZCZKI 2007). This test was performed according to LITCHFIELD AND WILCOXON (1949) and it was previously described in detail (LUSZCZKI AND CZUCZWAR 2006). In general, the CRRC of each AEDs was parallel to that of silymarin in both the cell lines measured by the MTT assay. If the CRRCs for the two compounds to be tested are parallel, at least three fixed-ratio combinations of compounds need to be examined in order to determine the type of interaction. Actually, there is no *priori* reason to expect that all combinations of tested drugs will produce the same interaction. In the present study, proportions of each AED and flavonoid in the mixture were calculated at three fixed-ratio combinations (1:1; 1:3 and 3:1).

Based upon the IC_{50}s values denoted experimentally for each compound tested alone, median additive inhibitory concentrations of the mixture of CBZ, OXC or PHT with silymarin, this is, the concentrations of the mixture that theoretically should inhibit the cell viability in 50% ($IC_{50\ add}$), were calculated from two equations of additivity presented by TALLARIDA ET AL. (1997, 2006, 2007):

$$(IC_{50})_{add} = f_1 \times (IC_{50})_{compound\ 1} + f_2 \times (IC_{50})_{compound\ 2} \quad (1)$$

where f_1 is a fraction of compound 1 in the total amount of compound mixture and f_2 is a fraction of drug 2, when $f_1 + f_2 = 1$.

The fraction may be expressed as percentage of the IC_{50} values of the respective compound of the mixture. For instance, the combination of 1:3 consists of 0.25 of $(IC_{50})_{compound\ 1}$ + 0.75 of $(IC_{50})_{compound\ 2}$ = 1 of $(IC_{50})_{add}$, which theoretically should give the $(IC_{50})_{add}$ value, or equivalently:

$$25\%\ \text{of}\ (IC_{50})_{compound\ 1} + 75\%\ \text{of}\ (IC_{50})_{compound\ 2} = 100\%\ \text{of}\ (IC_{50})_{add} \quad (2)$$

The effects of mixtures (AED/flavonoid) in the N27 and HepaRG cell lines were also measured experimentally *in vitro* by the MTT assay. The evaluation of the experimentally-derived $IC_{50\ mix}$ at the fixed-ratios of 1:1, 1:3 and 3:1 was based upon the concentration of the mixture inhibiting 50% of cell viability in N27 and HepaRG cell lines. To determine the separate concentrations of CBZ, OXC, PHT or silymarin in the mixture, the $IC_{50\ mix}$ values were multiplied by the respective proportions of drugs (denoted for additive mixture).

To visualize the types of interactions regarding parallel CRRC, the isoboles were drawn by plotting points reflecting the respective concentrations of AEDs (on the *x*-axis) and concentrations of flavonoids on the *y*-axis. The straight line connecting IC_{50} values for the two compounds, tested alone, represents the theoretic isobole for the additive effect. Consequently, if experimentally determined data points are placed on this line, the compounds effects are additive (zero interaction). On the other hand, when the points reflecting combinations of various fixed-ratios are significantly below this line, the two components act synergically, whereas antagonistic effects could be recognised if these points are located above the additive isobole.

The unique exception obtained in the test for parallelism was in the CRRC of PHT and silymarin, which demonstrated to be non-parallel in the N27 cells. In this case, the proportions of each compound in the mixture were calculated only for the fixed-ratio combination of 1:1. For the lower line of additivity the equation at a 50% inhibitory effect for the combination of PHT with silymarin is as follows: $y = IC_{50\ PHT} - [IC_{50\ PHT}/(IC_{50\ Silymarin}/x)^{q/p}]$; where *y* is the concentration of PHT; *x* is the concentration of silymarin; *p* and *q* are curve-fitting parameters (Hill coefficients) for PHT and silymarin, respectively. Similarly, for the upper line of additivity the equation at a 50% inhibitory effect for the combination of PHT with silymarin is: $y = IC_{50\ PHT}\ [(IC_{50\ Silymarin} - x)/IC_{50\ Silymarin}]^{q/p}$. To calculate the curve-fitting parameters (*p* and *q*), probits of response for PHT and silymarin tested alone were transformed to % effect. In this case, when two compounds produce maximal effect but are "heterodynamic" (i.e. have non-parallel CRRCs), the additivity is represented as an area bounded by two defined curves (lower and upper isoboles of additivity). The experimentally-derived $IC_{50\ mix}$ values are statistically different if their points are placed outside this region. For supraadditivity (synergism), the experimentally-derived $IC_{50\ mix}$ points are placed below the area bounded by the lower and upper isoboles of additivity, and for subadditivity (antagonism) above this region (TALLARIDA 2006; TALLARIDA 2007). All these concepts are further detailed in previous publications (TALLARIDA 2006; TALLARIDA 2007; LUSZCZKI 2007).

S.2.5. Statistical analysis

The IC_{50} and $IC_{50\ mix}$ values for CBZ, OXC, PHT and silymarin tested alone or in combination at the fixed-ratio of 1:1, 1:3 and 3:1 were calculated by computer-assisted log-probit analysis according to LITCHFIELD AND WILCOXON (1949). The experimentally-derived $IC_{50\ mix}$ values for the mixture of CBZ, OXC or PHT with silymarin were statistically compared with their respective

theoretical additive $IC_{50\,add}$ values by the use of unpaired Student's *t*-test, according to TALLARIDA (2000). A *p* value lower than 0.05 was considered to indicate a statistically significant difference. Results were presented as mean ± standard error of the mean (SEM).

S.3. Results

S.3.1. Antiproliferative effects of CBZ, OXC, PHT or silymarin in N27 and HepaRG cells

The antiproliferative action of CBZ, OXC, PHT or silymarin was determined in the N27 and HepaRG cell lines using the MTT assay in order to establish IC_{50} values for each analysed compound in both cell lines. The IC_{50} values are the concentrations resulting in 50% cell growth inhibition by a 24 h exposition to the tested AEDs or flavonoid, as compared with control (untreated cells). In our study the concentration-dependent growth inhibition effect of each compound was evident for CBZ, OXC, PHT and silymarin in both cell lines (Figure S.1).

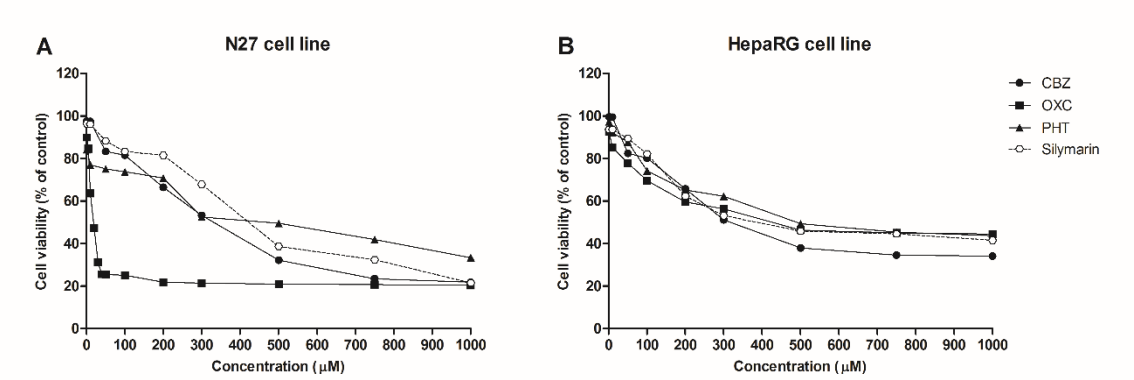

Figure S.1. The antiproliferative effects of carbamazepine (CBZ), oxcarbazepine (OXC), phenytoin (PHT), and silymarin in N27 (A) and HepaRG (B) cell lines after 24 h treatment with increasing concentrations (1–1000 μM) of active substances. The cell viability was measured by the MTT assay (*n* = 6).

S.3.1.1. Antiproliferative effects in the N27 cell line

Silymarin tested alone produced antiproliferative effects on N27 cells. The equation of CRRC for silymarin (y = 2.4077x – 1.3934; Figure S.2) allowed the calculation of its IC_{50} value that amounted to 452.35 ± 111.57 μM (Table S.1).

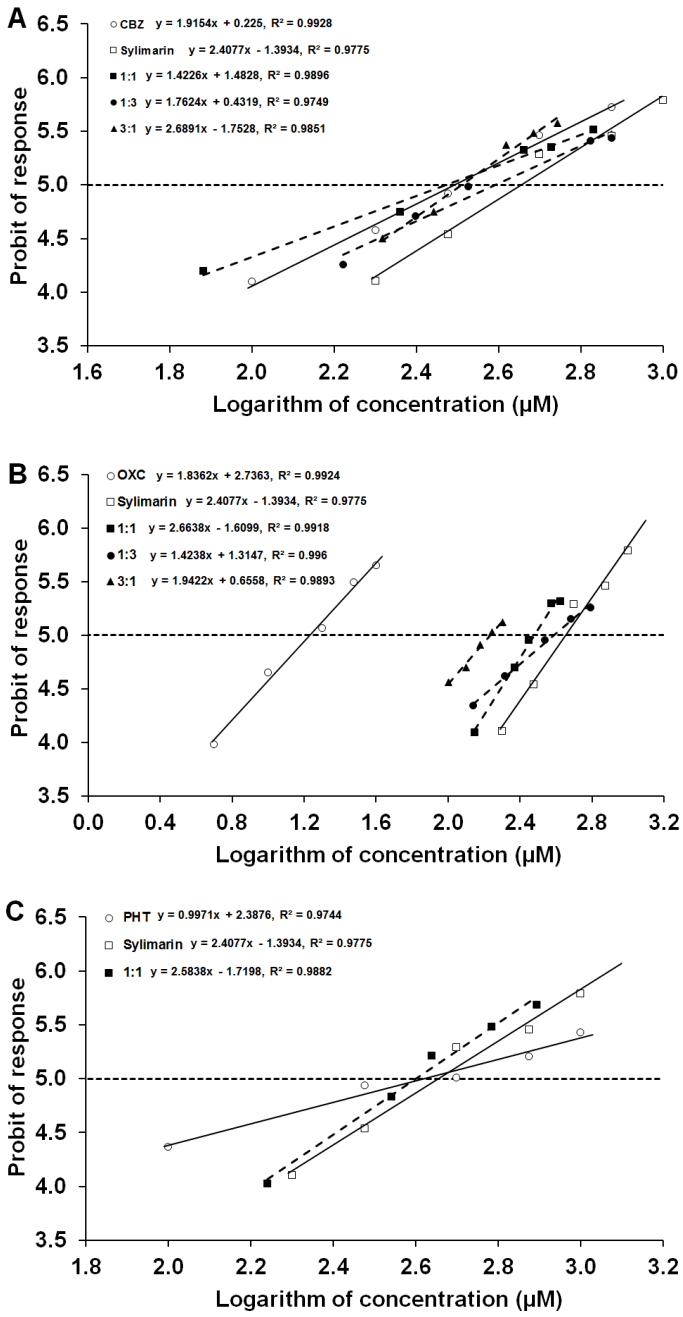

Figure S.2. Log-probit concentration-response relationship curves (CRRCs) for carbamazepine (CBZ), oxcarbazepine (OXC), phenytoin (PHT) and silymarin, and for their paired combinations at the fixed-ratios of 1:1, 1:3 and 3:1 in N27 cell line, illustrating the antiproliferative effects of the compounds measured *in vitro* by the MTT assay. Exception for the combination of PHT and silymarin tested only at the fixed-ratio of 1:1. Concentrations of CBZ, OXC, PHT and silymarin tested separately and the mixture of the compounds at the fixed-ratio combinations were transformed into logarithms, whereas the antiproliferative effects produced by the compounds were transformed into probits according to LITCHFIELD AND WILCOXON (1949). Linear regression equations of CRRCs are presented on the graph. *y* is the probit of response; *x* is the logarithm (to the base 10) of a compound concentration; and R^2 is the coefficient of determination.

Table S.1. Antiproliferative effects of carbamazepine (CBZ), oxcarbazepine (OXC), phenytoin (PHT) and silymarin tested individually in N27 and HepaRG cell lines measured *in vitro* by the MTT assay.

	Drug	IC_{50} (μM)	n	S.R.	F ratio S.R.	Parallelism
N27 cell line	Silymarin	452.35 ± 111.57	30	-	-	-
	CBZ	311.17 ± 96.48	30	1.28	1.66	P
	OXC	17.09 ± 5.53	30	1.35	1.69	P
	PHT	416.86 ± 248.27	30	3.87	3.77	NP
HepaRG cell line	Silymarin	448.83 ± 271.20	30	-	-	-
	CBZ	326.88 ± 129.43	24	6.26	37.65	P
	OXC	409.56 ± 209.11	30	1.58	54.29	P
	PHT	550.59 ± 363.04	30	1.91	53.87	P

Results are presented as median inhibitory concentrations (IC_{50} values in μM ± SEM) of CBZ, OXC, PHT and silymarin tested singly with respect to their antiproliferative effects on N27 and HepaRG cell lines measured in vitro by the MTT assay. n, total number of items used at concentrations whose expected antiproliferative effects ranged between 4 and 6 probits (16% and 84%); S.R., slope function ratio; f ratio S.R., factor for slope function ratio; P, parallel; NP, not parallel. Test for parallelism of two concentration-response relationship curves (CRRCs) was performed according to LITCHFIELD AND WILCOXON (1949). If the S.R. value is higher than the factor for f ratio S.R. value, the examined two CRRCs are not parallel to each other; the contrary is true for parallel CRRCs. For more detailed calculations see the Appendix to the paper by LUSZCZKI AND CZUCZWAR (2006).

S.3.1.1.1. Antiproliferative effects of CBZ tested individually and in combination with silymarin

CBZ tested alone produced antiproliferative effects in the N27 cells. The equation of CRRC for CBZ (y = 1.9154x + 0.2250; Figure S.2A) allowed the determination of its IC_{50} value, which was 311.17 ± 96.48 μM (Table S.1). The test for parallelism of CRRCs between CBZ and silymarin revealed that the CRRCs of the compounds were parallel to each other (Table S.1; Figure S.2A). In this case, the combination of CBZ with silymarin at the fixed-ratios of 1:1, 1:3 and 3:1 produced antiproliferative effects in the N27 cells. The $IC_{50\ mix}$ values were calculated from the CRRC for the mixture of CBZ and silymarin represented in the Figure S.2A; their respective $IC_{50\ mix}$ values are included in the Table S.2.

Table S.2. Isobolographic analysis of interactions for parallel concentration-response relationship curves between carbamazepine (CBZ), oxcarbazepine (OXC) or phenytoin (PHT) and silymarin at the fixed-ratio combination of 1:1, 1:3 and 3:1 in N27 and HepaRG cell lines, measured *in vitro* by the MTT assay.

	Combination	Proportion	$IC_{50\ mix}$ (µM)	n_{mix}	$IC_{50\ add}$ (µM)	n_{add}
N27 cell line	CBZ + Silymarin	1:1	296.71 ± 123.85	30	381.76 ± 104.03	56
		1:3	390.82 ± 131.69	30	417.05 ± 107.80	56
		3:1	324.47 ± 71.66	30	346.46 ± 100.25	56
	OXC + Sylimarin	1:1	302.94 ± 67.53	30	234.72 ± 58.55	56
		1:3	387.55 ± 161.64	30	343.53 ± 85.06	56
		3:1	172.49 ± 52.74	30	125.91 ± 32.04	56
HepaRG cell line	CBZ + Sylimarin	1:1	433.22 ± 193.80	30	387.85 ± 250.31	50
		1:3	410.18 ± 191.93	30	418.34 ± 310.76	50
		3:1	449.64 ± 219.15	30	357.37 ± 189.87	50
	OXC + Sylimarin	1:1	417.21 ± 353.23	30	429.19 ± 330.66	56
		1:3	422.4 ± 156.44	30	439.01 ± 350.93	56
		3:1	300.4 ± 257.52	30	419.38 ± 310.39	56
	PHT + Sylimarin	1:1	374.74 ± 275.16	30	499.65 ± 367.12	56
		1:3	561.3 ± 159.87	30	474.24 ± 369.16	56
		3:1	723.7 ± 165.59	30	525.07 ± 365.08	56

Results are presented as median inhibitory concentrations (IC_{50} values in µM ± SEM) for two-compound mixtures, determined either experimentally ($IC_{50\ mix}$) or theoretically calculated ($IC_{50\ add}$) from the equation of additivity TALLARIDA *(2006; 2007), blocking proliferation in 50% of tested cells in N27 and HepaRG cell lines measured in vitro by the MTT assay.* n_{mix}*, total number of items used at those concentrations whose expected antiproliferative effects ranged between 16% and 84% (i.e., 4 and 6 probits) for the experimental mixture;* n_{add}*, total number of items calculated for the additive mixture of the compounds examined. Statistical evaluation of data was performed with unpaired Student's t-test according to* TALLARIDA *(2000). There was no statistical difference between the* $IC_{50\ mix}$ *and* $IC_{50\ add}$ *values (p = 0.05), inferring that the analysed interactions were additive in both the cell lines.*

S.3.1.1.2. Antiproliferative effects of OXC tested individually and in combination with silymarin

OXC tested alone reduced the proliferation of N27 cells. The equation of CRRC for OXC (y = 1.8362x + 2.7363; Figure S.2B) allowed the calculation of its IC_{50} value that amounted to 17.09 ± 5.53 µM (Table S.1). The test for parallelism of CRRCs between OXC and silymarin revealed that the CRRCs of OXC/flavonoid were parallel to each other (Table S.1, Figure S.2B). The combinations of OXC with silymarin at the fixed-ratios of 1:1, 1:3 and 3:1 produced antiproliferative effects in the N27 cells. The $IC_{50\ mix}$ value were calculated from the CRRC for the mixture of OXC and silymarin represented in the Figure S.2B. The $IC_{50\ mix}$ values are included in the Table S.2.

S.3.1.1.3. Antiproliferative effects of PHT tested individually and in combination with silymarin

PHT tested alone produced antiproliferative effects on N27 cells. The equation of CRRC for PHT (y = 0.9971x + 2.3876; Figure S.2C) allowed the calculation of its IC_{50} value, which was 416.86 ± 248.27 µM (Table S.1). The test for parallelism of CRRCs between PHT and silymarin revealed that the CRRCs of PHT and silymarin were nonparallel to each other (Table S.1, Figure S.2C).

In this case, the combinations of PHT with silymarin at the fixed-ratio of 1:1 produced antiproliferative effects in the N27 cells. The $IC_{50\ mix}$ values were calculated from the CRRC for the mixture of PHT and silymarin represented in Figure S.2C. The $IC_{50\ mix}$ value calculated from the CRRC for the mixture of PHT and silymarin was 398.81 ± 91.66 µM. Additionally, the respective $IC_{50\ add}$ values calculated from the equation for the lower and upper line of additivity for the PHT and silymarin mixture were 214.00 ± 297.65 µM and 620.38 ± 295.04 µM, respectively.

S.3.1.2. Antiproliferative effects in the HepaRG cell line

Silymarin tested alone produced antiproliferative effects on HepaRG cells. The equation of CRRC for silymarin (y = 0.718x + 3.0957; Figure S.3) allowed the calculation of its IC_{50} value that amounted to 448.83 ± 271.20 µM (Table S.1).

S.3.1.2.1. Antiproliferative effects of CBZ tested individually and in combination with silymarin

CBZ tested alone produced antiproliferative effects in the HepaRG cells. The equation of CRRC for CBZ (y = 1.6769x + 0.7837; Figure S.3A), allowed the determination of the IC_{50} value for CBZ, which was 326.88 ± 129.43 µM (Table S.1). The test for parallelism of CRRCs between CBZ and silymarin revealed that the CRRCs of the compounds were parallel to each other (Table S.1, Figure S.3A). In this case, the combination of CBZ with silymarin at the fixed-ratios of 1:1, 1:3 and 3:1 produced antiproliferative effects in the HepaRG cells. The $IC_{50\ mix}$ values were calculated from the CRRC for the mixture of CBZ and silymarin as shown in the Figure S.3A, whereas the respective $IC_{50\ mix}$ values are represented in the Table S.2.

S.3.1.2.2. Antiproliferative effects of OXC tested individually and in combination with silymarin

OXC tested alone reduced the proliferation of HepaRG cells. The equation of CRRC for OXC (y = 0.8384x + 2.81; Figure S.3B), allowed the determination of its IC_{50} value, which was 409.56 ± 209.112 µM (Table S.1). The test for parallelism of CRRCs between OXC and silymarin revealed that the CRRCs of the compounds were parallel to each other (Table S.1, Figure S.3B). The combination of OXC with silymarin at the fixed-ratios of 1:1, 1:3 and 3:1 produced antiproliferative effects in the HepaRG cells. The $IC_{50\ mix}$ values were calculated from the CRRC for the mixture of OXC and silymarin represented in the Figure S.3B. The respective $IC_{50\ mix}$ values are included in the Table S.2.

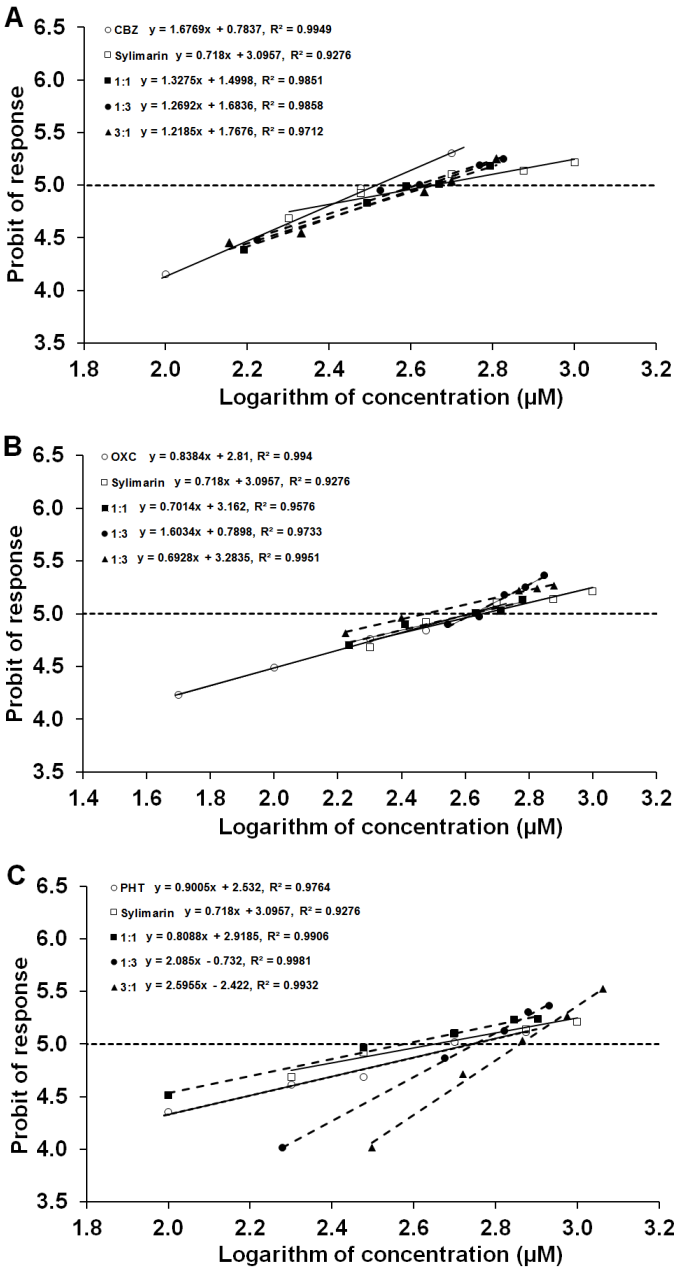

Figure S.3. Log-probit concentration-response relationship curves (CRRCs) for carbamazepine (CBZ), oxcarbazepine (OXC), phenytoin (PHT) and silymarin, and for their paired combinations at the fixed-ratios of 1:1, 1:3 and 3:1 in HepaRG cell line, illustrating the antiproliferative effects of the compounds measured *in vitro* by the MTT assay. Concentrations of CBZ, OXC, PHT and silymarin tested separately and the mixture of the compounds at the fixed-ratio combinations were transformed into logarithms, whereas the antiproliferative effects produced by the compounds were transformed into probits according to LITCHFIELD AND WILCOXON (1949). Linear regression equations of CRRCs are presented on the graph. *y* is the probit of response; *x* is the logarithm (to the base 10) of a compound concentration; and R^2 is the coefficient of determination.

S.3.1.2.3. Antiproliferative effects of PHT tested individually and in combination with silymarin

PHT tested alone produced antiproliferative effects in the HepaRG cells. The equation of CRRC for PHT (y = 0.9005x + 2.532; Figure S.3C) allowed the determination of its IC_{50} that was 550.59 ± 363.04 µM (Table S.1). The test for parallelism of CRRCs between PHT and silymarin revealed that the CRRCs of the compounds were parallel to each other (Table S.1, Figure S.3C). In this case, the combination of PHT with silymarin at the fixed-ratios of 1:1, 1:3 and 3:1 produced antiproliferative effects in the HepaRG cells. The $IC_{50\ mix}$ values were calculated from the CRRC for the mixture of PHT and silymarin represented in the Figure S.3C, whereas the respective $IC_{50\ mix}$ values are represented in the Table S.2.

S.3.2. Isobolographic analysis

S.3.2.1. Isobolographic analysis in the N27 cell line

S.3.2.1.1. Isobolographic analysis of interactions between CBZ and silymarin

The isobolographic analysis of interaction for parallel CRRCs revealed that the mixture of CBZ with silymarin at the fixed-ratio of 1:1, 1:3 and 3:1 exerted additive interactions in the N27 cells (Figure S.4A). The experimentally derived $IC_{50\ mix}$ values as well as the additively calculated $IC_{50\ add}$ values are included in the Table S.2. For these combinations, the $IC_{50\ mix}$ values did not significantly differ from the $IC_{50\ add}$ values. Nevertheless, the combination of CBZ and silymarin at the fixed ratio of 1:1 showed a tendency toward supraaditivity (synergic interactions).

S.3.2.1.2. Isobolographic analysis of interactions between OXC and silymarin

By observing the isobolographic analysis of interaction depicted in the Figure S.4B for parallel CRRCs, it could be inferred that the mixture of OXC with silymarin at the fixed-ratio of 1:1, 1:3 and 3:1 exerted additive interactions in the N27 cell line. The experimentally derived $IC_{50\ mix}$ values as well as the additively calculated $IC_{50\ add}$ values are included in the Table S.2. Indeed, the $IC_{50\ mix}$ values for these combinations did not significantly differ from the $IC_{50\ add}$ values. However, the combination of OXC and silymarin at the three tested ratios (1:1, 1:3 and 3:1) demonstrated a tendency to antagonistic interactions.

S.3.2.1.3. Isobolographic analysis of interactions between PHT and silymarin

The isobolographic analysis of interaction for nonparallel CRRCs revealed that the mixture of PHT with silymarin at the fixed-ratio of 1:1 exerted only additive interactions in the N27 cells (Figure S.4C).

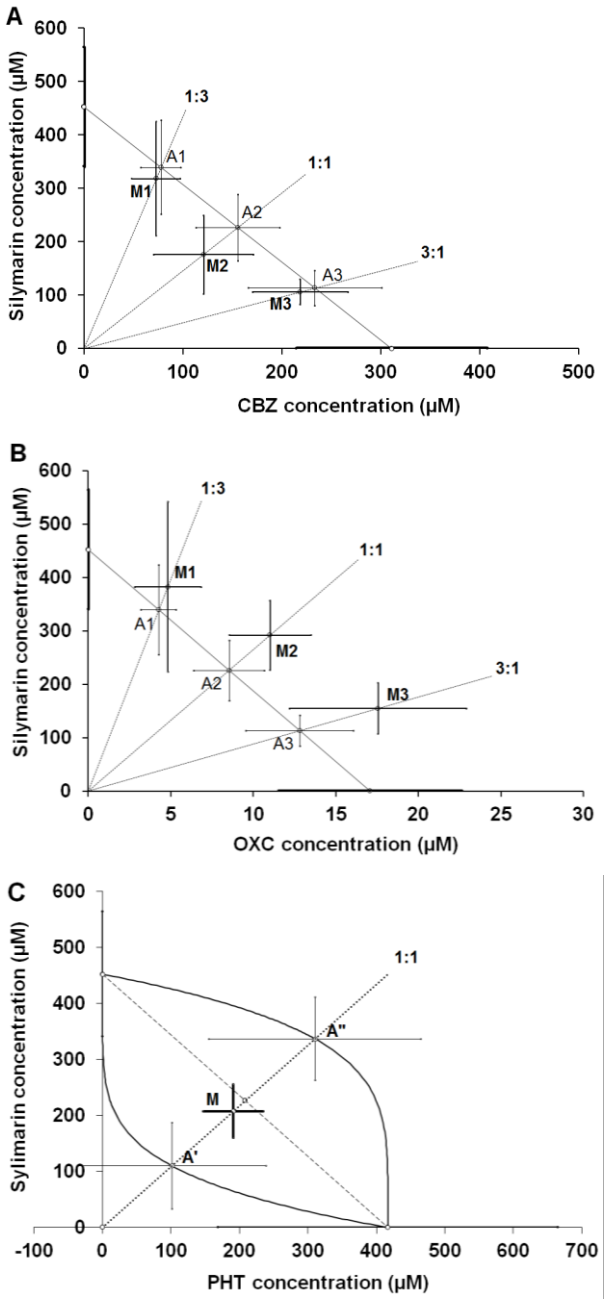

Figure S.4. Isobolographic analysis of interactions between carbamazepine (CBZ), oxcarbazepine (OXC) and phenytoin (PHT) with silymarin in the N27 cell line. The median inhibitory concentrations (IC_{50}) for antiepileptic drugs and flavonoids are plotted graphically on the X- and Y-axes, respectively. The solid horizontal and vertical error bars lines on the X and Y axes represent the standard error of the mean (SEM) for the IC_{50} values for the studied compounds tested alone. *Figures A to B*: the solid line on the axes represents the SEM for the antiepileptic drugs and flavonoids tested alone. The straight line connecting these two IC_{50} values on each isobologram represents the theoretical line of additivity for a continuum of different fixed-concentration ratios. A1-A3 represents the theoretically calculated $IC_{50\ add}$ values for the fixed-ratio combination of 1:1, 1:3 and 3:1, respectively. M1-M3 represents the experimentally-derived IC_{50} mix value for total concentration of the antiepileptic drugs-flavonoids mixture in the fixed-ratios of 1:1, 1:3 and 3:1, respectively. *Figure C*: the lower and upper isoboles of additivity represent the curves connecting the IC_{50} values for PHT and silymarin tested alone. The dotted line starting from the point (0, 0) corresponds to the fixed-ratio of 1:1 for the combination of PHT with silymarin. The diagonal dashed line connects the IC_{50} for PHT and silymarin on the X- and Y-axes. The points A' and A" depict the theoretically calculated $IC_{50\ add}$ values for both, lower and upper isoboles of additivity. The point M represents the experimentally-derived IC_{50} mix value for total concentration of the mixture expressed as proportions of PHT and silymarin that produced a 50% antiproliferative effect (50% isobole) in N27 cell line measured *in vitro* by the MTT assay.

S.3.2.2. Isobolographic analysis in the HepaRG cell line

S.3.2.2.1. Isobolographic analysis of interactions between CBZ and silymarin

The isobolographic analysis of interaction for parallel CRRCs revealed that the mixture of CBZ with silymarin at the fixed-ratio of 1:1, 1:3 and 3:1 exerted additive interactions in the HepaRG cell line (Figure S.5A). The experimentally derived $IC_{50\ mix}$ value for these fixed-ratio combinations as well as the additively calculated $IC_{50\ add}$ values are presented in the Table S.2. It can be observed that the $IC_{50\ mix}$ values did not significantly differ from the $IC_{50\ add}$ values. Nonetheless, the combination of CBZ and silymarin at the fixed ratio of 3:1 demonstrated a tendency to an antagonistic interaction.

S.3.2.2.2. Isobolographic analysis of interactions between OXC and silymarin

The isobolographic analysis of interaction for parallel CRRCs revealed that the mixture of OXC with silymarin at the fixed-ratios of 1:1, 1:3 and 3:1 exerted additive interactions in the HepaRG cell line (Figure S.5B). The Table S.2 includes the experimentally derived $IC_{50\ mix}$ values as well as the additively calculated $IC_{50\ add}$ values. Indeed, for this combination, the $IC_{50\ mix}$ values did not significantly differ from the $IC_{50\ add}$ values. Nevertheless, the interaction of OXC and silymarin at the fixed ratio of 3:1 showed a slight tendency toward supraadditivity (synergic interactions).

S.3.2.2.3. Isobolographic analysis of interactions between PHT and silymarin

By observing the isobolographic analysis of interaction depicted in the Figure S.5C for parallel CRRCs, it could be inferred that the mixture of PHT with silymarin at the fixed-ratios of 1:1, 1:3 and 3:1 exerted additive interactions in the HepaRG cell line. The experimentally derived $IC_{50\ mix}$ values as well as the additively calculated $IC_{50\ add}$ values are included in the Table S.2. In this case, the $IC_{50\ mix}$ values for these interactions did not significantly differ from the $IC_{50\ add}$ values. However, the combination of PHT and silymarin at the fixed ratio of 1:1 demonstrated a tendency to a synergic interaction, whereas the combination of PHT and silymarin, at the fixed ratio of 3:1, demonstrated a tendency to an antagonistic interaction.

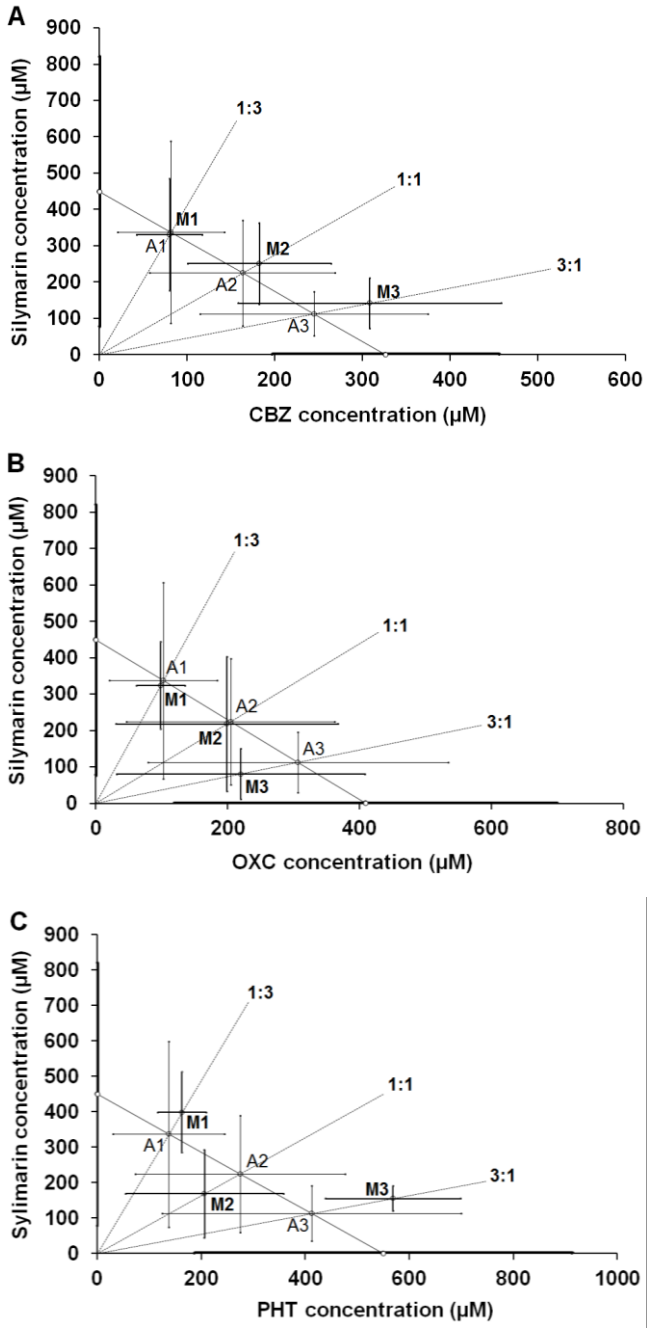

Figure S.5. Isobolographic analysis of interactions between carbamazepine (CBZ), oxcarbazepine (OXC) and phenytoin (PHT) with silymarin in the HepaRG cell line. The median inhibitory concentrations (IC_{50}) for antiepileptic drugs and silymarin are plotted graphically on the X- and Y-axes, respectively. The solid horizontal and vertical error bars lines on the X and Y axes represent the SEM for the IC_{50} values for the studied compounds tested alone. The solid line on the axes represents the standard error of the mean (SEM) for the antiepileptic drugs and silymarin tested alone. The straight line connecting these two IC_{50} values on each isobologram represents the theoretical line of additivity for a continuum of different fixed-concentration ratios. A1-A3 represents the theoretically calculated $IC_{50\ add}$ values for the fixed-ratio combination of 1:1, 1:3 and 3:1, respectively. M1-M3 represents the experimentally-derived $IC_{50\ mix}$ value for total concentration of the antiepileptic drugs-flavonoids mixture in the fixed-ratios of 1:1, 1:3 and 3:1, respectively.

S.4. Discussion

The isobolographic evaluation of the toxicity profile originated by the combination of the AEDs CBZ, OXC or PHT with the flavonoid silymarin emerge as of great interest bearing in mind the pharmacotherapeutic benefits that could outcome, particularly in the treatment of epilepsy. For this purpose, N27 rat dopaminergic neural and HepaRG were the chosen cell lines. Actually, this is a choice easily explained taking into account that the primary adverse effects of the AEDs are attributed to the CNS and the liver (Ahmed and Siddiqi 2006; Kennedy and Lhatoo 2008; Zaccara et al. 2008; Björnsson 2008; Perucca and Gilliam 2012; Hussein et al. 2013).

The immortalized rat mesencephalic dopaminergic neuronal cell line (N27) has long been used as an *in vitro* model for the evaluation of neurotoxicity of several compounds including drugs (Chen et al. 2008; Saminathan et al. 2011; Wang et al. 2013; Chen et al. 2015; Harischandra et al. 2015). Since the AEDs act to suppress the pathological neuronal hyperexcitability that characteristic of seizure disorders, it is not surprising that these kind of compounds are prone to cause adverse reactions that affect the CNS, which may be predictable, dose-dependent and reversible (Perucca and Meador 2005; Loring et al. 2007; Kennedy and Lhatoo 2008; Perucca and Gilliam 2012). Preceding studies have shown that the long-term use of AEDs can cause nervous system damage (Liu et al. 2015). CBZ and OXC have been previously recognised to exert toxic effects in hippocampal neurons (Ambrósio et al. 2000; Araújo et al. 2004). Both the drugs caused nuclear chromatin condensation in some neurons, which was characteristic for apoptosis; increased the activity of caspase-3-like enzymes, mainly in neurons (Ambrósio et al. 2000); and induced degeneration and swelling of neurites (Araújo et al. 2004). Furthermore, the exposure to AEDs during a critical period in brain development was recognised as responsible by long-term detrimental effects on cognitive and behavioural outcomes (Glauser 2004; Wolansky and Azcurra 2005; Motamedi and Meador 2006; Kim et al. 2007). In fact, PHT is primarily recognised to induce neurotoxicity during these stages (Ohmori et al. 1992; Ohmori et al. 1997; Hatta et al. 1999; Bittigau et al. 2002; Bittigau et al. 2003). In opposition, the neurotoxic profile of CBZ during pregnancy and childhood has not been reported (Meador 2004; Kim et al. 2007). In our studies, OXC exerted a marked cytotoxic effect in the N27 cells. Indeed, whereas the IC_{50} value for this second-generation AED was 17.09 ± 5.53 μM, the values for CBZ and PHT were far higher, 311.17 ± 96.48 μM and 416.86 ± 248.27 μM, respectively. These results are in accordance with the studies developed by Araújo et al. (2004) and Morte et al. (2013), where OXC demonstrated to be more toxic than CBZ in primary rat hippocampal neurons. Nevertheless, some clinical studies indicate a decreasing in neurotoxicity while shifting from CBZ to OXC monotherapy (Clemens et al. 2004). Actually, although the neurotoxic potential of OXC appear to be high in *in vitro* and *in vivo* models, the true is that in humans, contrary to what happens in rodents, the OXC is rapidly metabolized to its main but less toxic metabolite licarbazepine (LIC) (Morte et al. 2013).

In the past decades, a great number of natural medicinal plants have gained attention as potential neuroprotective agents (Magalingam et al. 2015; Pérez-Hernández et al. 2016; Cirmi et

AL. 2016). Specifically, several dietary flavonoid compounds have been reported as pursuing neuroprotective activities. Their neuroprotective actions involve a number of effects within the brain, and it includes potential to protect neurons against injury induced by neurotoxins, ability to suppress neuroinflammation, and potential to improve memory, learning and cognitive functions (VAUZOUR ET AL. 2008; SPENCER 2009). The multiplicity of neuroprotective effects exhibited by the flavonoids appears to be underpinned by two processes: interactions with important neuronal signalling cascades leading to inhibition of apoptosis triggered by neurotoxic agents and promotion of neuronal survival and differentiation; and induction of the peripheral and cerebral vascular blood flow in a manner which may lead to the stimulation of angiogenesis, and new nerve cell growth in the hippocampus (VAUZOUR ET AL. 2008; SPENCER 2009). Experimental and epidemiological evidences demonstrated the role of flavonoids in improving age-related cognitive decline, as well as neuroprotective effects in models of Parkinson's, Alzheimer's and cerebral ischemia/reperfusion injuries (MANDEL ET AL. 2004; BORAH ET AL. 2013; SINGH ET AL. 2016). Indeed, neuroprotective effects for silymarin have been documented not only in several animal models (LU ET AL. 2009; BALUCHNEJADMOJARAD ET AL. 2010; HOU ET AL. 2010; SINGHAL ET AL. 2010; MURATA ET AL. 2010; CHTOUROU ET AL. 2010; CHTOUROU ET AL. 2013), but also in neuronal and non-neuronal cellular models (WANG ET AL. 2002; MURATA ET AL. 2010; YIN ET AL. 2011; YAGHMAEI ET AL. 2014; LI ET AL. 2017) of neurodegeneration. The mechanisms underlying the neuroprotective activity of silymarin involve its capacity to inhibit oxidative stress in the brain as well as additional effects in ß-amyloid aggregation, inflammatory mechanisms, cellular apoptotic machinery, and estrogenic receptor mediation (CHTOUROU ET AL. 2010; CHTOUROU ET AL. 2013; BORAH ET AL. 2013). In our N27 cellular model, the IC_{50} value for silymarin was 452.35 ± 111.57 µM. This high IC_{50} value is in accordance with the literature describing the silymarin neuroprotective and low toxic profile. The isobolographic analysis of interactions revealed that the mixture of CBZ, OXC or PHT with (-)-silymarin at the fixed-ratios of 1:1, 1:3 and 3:1 exerted only additive toxicity interactions in the N27 cell line. These results are very important regarding the strategy of combination of P-gp substrates AEDs (CBZ, OXC and PHT) with flavonoids P-gp inhibitors (silymarin) in order to overpass the pharmacoresistance observed in epilepsy. However, even without statistical significance, in some cases, the combinations of AEDs and silymarin demonstrated a trend toward subadditivity (antagonistic interactions). This means that the toxicity of the final combination was lower than their individual effects, evidencing some potential of the flavonoids in decreasing the AEDs neurotoxicity. Although the opposite effects have also been observed with some combinations, these kinds of synergic interactions were less markedly when comparing to the antagonistic ones.

Several hepatic cell-based *in vitro* models have been used for early safety risk assessment during drug development (MCGILL ET AL. 2011; DONATO ET AL. 2013). The HepaRG cell line was the chosen model to evaluate the hepatotoxic potential of individual AEDs and flavonoids, as well as their paired-combinations. Actually, considering the several disadvantages present not only

by the human hepatocytes, the *gold standard* model for hepatotoxic studies, but also by other human hepatic cell lines like the HepG2 and HuH7, the HepaRG cell line is an unique *in vitro* tool for understanding drug metabolism and toxicity (PERNELLE ET AL. 2011; ANDERSSON ET AL. 2012; SZABO ET AL. 2013; SUSUKIDA ET AL. 2016; SAITO ET AL. 2016).

Drug-induced liver injury attributed to several AEDs is a significant leading cause of liver disease and post-market failure of approved drugs in general (AHMED AND SIDDIQI 2006; NORRIS ET AL. 2008; GÓMEZ-LECHÓN ET AL. 2014; IIDA ET AL. 2015). Since the liver is the primary organ for drug metabolism and elimination for many AEDs, this kind of drug-induced toxicity is easily understood (HUSSEIN ET AL. 2013). AEDs-induced liver diseases are recognised to be part of a generalized hypersensitivity reaction (BRYANT AND DREIFUSS 1995; AHMED AND SIDDIQI 2006), including either production of reactive toxic metabolite(s) and induction of immunoallergic reactions (LEE 2003; BJÖRNSSON 2008). There is a wide range of hepatotoxic reactions, which varying from mild and transient elevations of hepatic enzymes to fatal hepatic failure (ARROYO AND DE LA MORENA 2001). Actually, contrary to what happens with OXC, for which were only reported modest elevations of liver enzymes (BOSDURE ET AL. 2004; BJÖRNSSON 2008), CBZ and PHT are reported to induce a more severe hepatotoxicity (DREIFUSS AND LANGER 1987; AHMED AND SIDDIQI 2006; BJÖRNSSON 2008; SASAKI ET AL. 2013). The hepatic injury due to PHT is reported as an uncommon occurrence. However, once it develops, 10-38% of cases will progress to a fatal outcome (HARDEN 2000). In our studies, besides the high IC_{50} values obtained, the CBZ (IC_{50} = 326.88 ± 129.43 μM) was, in fact, the most hepatotoxic AED, followed by OXC (IC_{50} = 409.56 ± 209.112 μM) and PHT (IC_{50} = 550.59 ± 363.04 μM).

The use of medicinal plants for the treatment of liver diseases has a long history (ADEWUSI AND AFOLAYAN 2010). A number of flavonoids and flavonoids-containing plants are claimed to be effective as antihepatotoxic agents (ADEWUSI AND AFOLAYAN 2010; EL-SAWI AND SLEEM 2010; PEREZ GUTIERREZ ET AL. 2011; MADRIGAL-SANTILLÁN ET AL. 2014; GUPTA ET AL. 2015; MA ET AL. 2016). Particularly, silymarin evidenced hepatoprotective activity in several models of hepatotoxicity (HASSAN AND EL-GENDY A.M 2003; PRADEEP ET AL. 2007; YADAV ET AL. 2008; SHAARAWY ET AL. 2009; MAHLI ET AL. 2015). Nevertheless, silymarin is mainly referred to in the literature as having high protective effects in the liver against several hepatotoxic drugs. This *is the case of a*cetaminophen (KAZEMIFAR ET AL. 2012; JASHITHA ET AL. 2013; FREITAG ET AL. 2015; HAMZA AND AL-HARBI 2015; BEKTUR ET AL. 2016), anti-tuberculosis drugs (BANSAL ET AL. 2007), doxorubicin (PATEL ET AL. 2010; RAŠKOVIĆ ET AL. 2011), epirubicin (SASU ET AL. 2015) or isoniazid (JAHAN ET AL. 2015), for example. Besides its antioxidative and anti-inflammatory effects, silymarin also stimulates RNA and protein synthesis leading to a faster regeneration after liver injury (SONG ET AL. 2006; PATEL ET AL. 2010; BEKTUR ET AL. 2016). Other properties like ability to block hepatotoxic binding sites were also attributed to silymarin, evidencing its value in the treatment of liver diseases (BORAH ET AL. 2013). The lack of hepatotoxic effects attributed to silymarin is corroborated by the high IC_{50} obtained in the HepaRG cells (448.83 ± 271.20 μM). Additionally, our *in vitro* results demonstrated only an additive interaction between CBZ, OXC or PHT with the flavonoid silymarin at all the tested ratios (1:1, 1:3 and 3:1). These results are very important regarding

the strategy of combination of AEDs with flavonoids that could have a great relevance particularly in the treatment of epilepsy. In this case, although without statistical significance value, only the combinations between OXC and silymarin, at the fixed ratio of 3:1, and between PHT and silymarin, at the fixed ratio of 1:1, demonstrated a slight tendency to synergic interactions. On the other hand, the combination of CBZ and silymarin, at the fixed ratio of 3:1, as well as the combination of PHT and silymarin, at the fixed ratio of 3:1, demonstrated a tendency to antagonistic interactions, indicating a lower cytotoxic potential when the compounds are used together.

Taking into account our results, the flavonoid silymarin did not demonstrate significant neuro and hepatotoxic effects. Additionally, the neuro and hepatotoxic profiles resulting from the combinations of CBZ, OXC and PHT with silymarin were merely additive. Indeed, considering its favourable cytotoxic profile, this arises as a promising flavonoid to be use in combination with AEDs. The AEDs here studied were representative of the most commonly used in clinical practice, highlighting the valuable use of this strategy in the management of epilepsy, particularly considering the anticonvulsant and P-gp inhibitory activities ascribed to silymarin.

S.5. Acknowledgements

Part of the present work was conducted in the Department of Pathophysiology from the Medical University of Lublin, Poland, under the supervision of Professors Jarogniew J. Luszczki and Stanislaw J. Czuczwar, to whom I would like to express my sincere thanks. I would like also to acknowledge the support provided by the Fundação para a Ciência e a Tecnologia (FCT, Portugal) for the period of time spent abroad.

S.6. References

ADEWUSI EA, **AFOLAYAN AJ** (**2010**) A review of natural products with hepatoprotective activity. *J Med Plants Res*. 4(13): 1318–1334.

AHMED SN, **SIDDIQI ZA** (**2006**) Antiepileptic drugs and liver disease. *Seizure*. 15(3): 156–164.

AMBRÓSIO AF ***ET AL***. (**2000**) Neurotoxic/neuroprotective profile of carbamazepine, oxcarbazepine and two new putative antiepileptic drugs, BIA 2-093 and BIA 2-024. *Eur J Pharmacol*. 406(2): 191–201.

ANDERSSON TB ***ET AL***. (**2012**) The HepaRG cell line: a unique in vitro tool for understanding drug metabolism and toxicology in human. *Expert Opin Drug Metab Toxicol*. 8(7): 909–920.

ARAÚJO IM ***ET AL***. (**2004**) Neurotoxicity induced by antiepileptic drugs in cultured hippocampal neurons: a comparative study between carbamazepine, oxcarbazepine, and two new putative antiepileptic drugs, BIA 2-024 and BIA 2-093. *Epilepsia*. 45(12): 1498–1505.

ARROYO S, **DE LA MORENA A** (**2001**) Life-threatening adverse events of antiepileptic drugs. *Epilepsy Res*. 47(1): 155–174.

BALUCHNEJADMOJARAD T *ET AL*. (**2010**) Neuroprotective effect of silymarin in 6-hydroxydopamine hemi-parkinsonian rat: involvement of estrogen receptors and oxidative stress. *Neurosci Lett*. 480(3): 206–210.

BANSAL S *ET AL*. (**2007**) Hepatoprotective Effect of Silymarin Against Hepatotoxicity Induced by Anti-tubercular Drugs in Malnourished Rats. *FASEB J*. 21(6): A808.

BANSAL T *ET AL*. (**2008**) Pre-clinical evidence for altered absorption and biliary excretion of irinotecan (CPT-11) in combination with quercetin: possible contribution of P-glycoprotein. *Life Sci*. 83(7–8): 250–259.

BANSAL T *ET AL*. (**2009**) Emerging significance of flavonoids as P-glycoprotein inhibitors in cancer chemotherapy. *J Pharm Pharm Sci*. 12(1): 46–78.

BEKTUR NE *ET AL*. (**2016**) Protective effects of silymarin against acetaminophen-induced hepatotoxicity and nephrotoxicity in mice. *Toxicol Ind Heal*. 32(4): 589–600.

BELL L *ET AL*. (**2015**) A Review of the Cognitive Effects Observed in Humans Following Acute Supplementation with Flavonoids, and Their Associated Mechanisms of Action. *Nutrients*. 7(12): 10290–10306.

BERENBAUM MC (**1989**) What is synergy? *Pharmacol Rev*. 41(2): 93–141.

BITTIGAU P *ET AL*. (**2002**) Antiepileptic drugs and apoptotic neurodegeneration in the developing brain. *Proc Natl Acad Sci U S A*. 99(23): 15089–15094.

BITTIGAU P *ET AL*. (**2003**) Antiepileptic drugs and apoptosis in the developing brain. *Ann N Y Acad Sci*. 993: 103-114-124.

BJÖRNSSON E (**2008**) Hepatotoxicity associated with antiepileptic drugs. *Acta Neurol Scand*. 118(5): 281–290.

BORAH A *ET AL*. (**2013**) Neuroprotective potential of silymarin against CNS disorders: insight into the pathways and molecular mechanisms of action. *CNS Neurosci Ther*. 19(11): 847–853.

BOSDURE E *ET AL*. (**2004**) Oxcarbazepine and DRESS syndrome: a paediatric cause of acute liver failure. *Arch Pediatr*. 11(9): 1073–1077.

BRYANT AE, **DREIFUSS FE** (**1995**) Hepatotoxicity Associated with Antiepileptic Drug Therapy. *CNS Drugs*. 4(2): 99–113.

CHAPMAN KL *ET AL*. (**2013**) Pharmaceutical toxicology: designing studies to reduce animal use, while maximizing human translation. *Regul Toxicol Pharmacol*. 66(1): 88–103.

CHEN D *ET AL*. (**2015**) EGCG Protects against 6-OHDA-Induced Neurotoxicity in a Cell Culture Model. *Park Dis*. 2015: 1–10.

CHEN P *ET AL*. (**2008**) Protective effects of a new metalloporphyrin on paraquat-induced oxidative stress and apoptosis in N27 cells. *Acta Biochim Biophys Sin (Shanghai)*. 40(2): 125–132.

CHTOUROU Y *ET AL*. (**2010**) Silymarin, a natural antioxidant, protects cerebral cortex against manganese-induced neurotoxicity in adult rats. *Biometals*. 23(6): 985–996.

CHTOUROU Y *ET AL*. (**2013**) Therapeutic efficacy of silymarin from milk thistle in reducing manganese-induced hepatic damage and apoptosis in rats. *Hum Exp Toxicol*. 32(1): 70–81.

CIRMI S *ET AL*. (**2016**) Neurodegenerative Diseases: Might Citrus Flavonoids Play a Protective Role? *Molecules*. 21(10): 1312.

CLEMENS B *ET AL*. (**2004**) Objective assessment of neurotoxicity while shifting from carbamazepine to oxcarbazepine. *Acta Neurol Scand*. 109(5): 324–329.

DONATO MT *ET AL*. (**2013**) Hepatic cell lines for drug hepatotoxicity testing: limitations and strategies to upgrade their metabolic competence by gene engineering. *Curr Drug Metab*. 14(9): 946–968.

DREIFUSS FE, LANGER DH (**1987**) Hepatic considerations in the use of antiepileptic drugs. *Epilepsia*. 28 Suppl 2: S23-29.

DUNNICK JK, HAILEY JR (**1992**) Toxicity and carcinogenicity studies of quercetin, a natural component of foods. *Fundam Appl Toxicol*. 19(3): 423–431.

EL-SAWI SA AND, SLEEM AA (**2010**) Flavonoids and Hepatoprotective Activity of Leaves of Senna Surattensis (Burm. f.) In CCl 4 Induced Hepatotoxicity in Rats. *Aust J Basic Appl Sci*. 4(6): 1326–1334.

EL HAOUARI M, ROSADO JA (**2016**) Medicinal Plants with Antiplatelet Activity. *Phytother Res*. 30(7): 1059–1071.

EUROPEAN MEDICINES AGENCY (**2012**) Revised Concept paper on the need for revision of the position on the replacement of animal studies by in vitro models (CPMP/SWP/728/95). *In*: http://www.ema.europa.eu/docs/en_GB/document_library/Scientific_guideline/2012/07/WC500130365.pdf.

FARZAEI MH *ET AL*. (**2016**) Phytochemicals as Adjunctive with Conventional Anticancer Therapies. *Curr Pharm Des*. 22(27): 4201–4218.

FERREIRA A *ET AL*. (**2015**) Flavonoid compounds as reversal agents of the P-glycoprotein-mediated multidrug resistance: biology, chemistry and pharmacology. *Phytochem Rev*. 14(2): 233–272.

FREITAG AF *ET AL*. (**2015**) Hepatoprotective Effect of Silymarin (Silybum marianum) on Hepatotoxicity Induced by Acetaminophen in Spontaneously Hypertensive Rats. *Evid Based Complement Altern Med*. 2015: 538317.

FRESHNEY RI (**2010**) Culture of Animal Cells - A manual of Basic Technique and Specialized Applications, 6th edn. Hoboken, New Jersey

GAITATZIS A *ET AL*. (**2004**) The epidemiology of the comorbidity of epilepsy in the general population. *Epilepsia*. 45(12): 1613–1622.

GALATI G, O'BRIEN PJ (**2004**) Potential toxicity of flavonoids and other dietary phenolics: Significance for their chemopreventive and anticancer properties. *Free Radic Biol Med*. 37(3): 287–303.

GLAUSER TA (**2004**) Behavioral and psychiatric adverse events associated with antiepileptic drugs commonly used in pediatric patients. *J Child Neurol*. 19 Suppl 1: S25-38.

GOH J-Y *ET AL*. (**2015**) Development and use of in vitro alternatives to animal testing by the pharmaceutical industry 1980–2013. *Toxicol Res*. 4(5): 1297–1307.

GÓMEZ-LECHÓN M *ET AL*. (**2014**) Cell-based models to predict human hepatotoxicity of drugs. *Rev Toxicol*. 31: 149–156.

GRABOVSKY Y, **TALLARIDA RJ** (**2004**) Isobolographic analysis for combinations of a full and partial agonist: curved isoboles. *J Pharmacol Exp Ther*. 310(3): 981–986.

GRECO WR *ET AL*. (**1995**) The search for synergy: a critical review from a response surface perspective. *Pharmacol Rev*. 47(2): 331–385.

GUAN L-P, **LIU B-Y** (**2016**) Antidepressant-like effects and mechanisms of flavonoids and related analogues. *Eur J Med Chem*. 121: 47–57.

GUMBAREWICZ E *ET AL*. (**2016**) Isobolographic analysis demonstrates additive effect of cisplatin and HDIs combined treatment augmenting their anti-cancer activity in lung cancer cell lines. *Am J Cancer Res*. 6(12): 2831–2845.

GUPTA A *ET AL*. (**2015**) Screening of flavonoids rich fractions of three Indian medicinal plants used for the management of liver diseases. *Rev Bras Farm*. 25(5): 485–490.

HAMZA RZ, **AL-HARBI MS** (**2015**) Amelioration of paracetamol hepatotoxicity and oxidative stress on mice liver with silymarin and Nigella sativa extract supplements. *Asian Pac J Trop Biomed*. 5(7): 521–531.

HANRAHAN JR *ET AL*. (**2011**) Flavonoid modulation of GABA(A) receptors. *Br J Pharmacol* . 163(2): 234–245.

HARDEN CL (**2000**) Therapeutic safety monitoring: what to look for and when to look for it. *Epilepsia*. 41 Suppl 8: S37-44.

HARISCHANDRA DS *ET AL*. (**2015**) α-Synuclein protects against manganese neurotoxic insult during the early stages of exposure in a dopaminergic cell model of Parkinson's disease. *Toxicol Sci*. 143(2): 454–468.

HASSAN HA, **EL-GENDY A.M** (**2003**) Evaluation of silymarin and/or ginger effect on induced hepatotoxicity by carbon tetrachloride in male albino rats. *EJHM*. 12: 101–112.

HATTA T *ET AL*. (**1999**) Neurotoxic effects of phenytoin on postnatal mouse brain development following neonatal administration. *Neurotoxicol Teratol*. 21(1): 21–28.

HOU Y-C *ET AL*. (**2010**) Preventive effect of silymarin in cerebral ischemia–reperfusion-induced brain injury in rats possibly through impairing NF-κB and STAT-1 activation. *Phytomedicine*. 17(12): 963–973.

HUSSEIN RRS *ET AL*. (**2013**) Effect of antiepileptic drugs on liver enzymes. *Beni-Seuf Univ J Appl Sci*. 2(1): 14–19.

IIDA A *ET AL*. (**2015**) Carbamazepine-Induced Liver Injury Requires CYP3A-Mediated Metabolism and Glutathione Depletion in Rats. *Drug Metab Dispos*. 43(7): 958–968.

JÄGER AK, SAABY L (**2011**) Flavonoids and the CNS. *Molecules*. 16(2): 1471–1485.

JAHAN S *ET AL*. (**2015**) The hepatoprotective role of Silymarin in isoniazid induced liver damage of rabbits. *J Pak Med Assoc*. 65(6): 620–622.

JAIN P (**2016**) Secondary metabolites for antiulcer activity. *Nat Prod Res*. 30(6): 640–656.

JARZĄB A *ET AL*. (**2017**) Additive Interaction of Cisplatin and Histone Deacetylase Inhibitors Combined Treatment in Rhabdomyosarcoma Cells – An Isobolographic Analysis. *Anticancer Res*. 37(3): 1067–1074.

JASHITHA M *ET AL*. (**2013**) Pharmacodynamic interaction of Quercetin with Silymarin against paracetamol induced hepatotoxicity in rats. *Int J Pharm Pharm Sci*. 5(Suppl.4): 104–106.

KANDÁROVÁ H, LETAŠIOVÁ S (**2011**) Alternative methods in toxicology: pre-validated and validated methods. *Interdiscip Toxicol*. 4(3): 107–113.

KAZEMIFAR AM *ET AL*. (**2012**) Hepatoprotective Property of Oral Silymarin is Comparable to N-Acetyl Cysteine in Acetaminophen Poisoning. *Gastroenterol Res*. 5(5): 190–194.

KENNEDY GM, LHATOO SD (**2008**) CNS adverse events associated with antiepileptic drugs. *CNS Drugs*. 22(9): 739–760.

KIM J-S *ET AL*. (**2007**) Neurodevelopmental impact of antiepileptic drugs and seizures in the immature brain. *Epilepsia*. 48 Suppl 5: 19–26.

KYSELOVA Z (**2012**) Toxicological aspects of the use of phenolic compounds in disease prevention. *Interdiscip Toxicol*. 4(4): 173–183.

LEE WM (**2003**) Drug-Induced Hepatotoxicity. *N Engl J Med*. 349(5): 474–485.

LI AP (**2005**) Preclinical in vitro screening assays for drug-like properties. *Drug Discov Today Technol*. 2(2): 179–185.

LI L *ET AL*. (**2017**) Silymarin protects against acrylamide-induced neurotoxicity via Nrf2 signalling in PC12 cells. *Food Chem Toxicol*. 102: 93–101.

LIEBSCH M *ET AL*. (**2011**) Alternatives to animal testing: current status and future perspectives. *Arch Toxicol*. 85(8): 841–858.

LITCHFIELD JT, WILCOXON F (**1949**) A simplified method of evaluating dose-effect experiments. *J Pharmacol Exp Ther*. 96(2): 99–113.

LIU Y *ET AL*. (**2015**) Short-term use of antiepileptic drugs is neurotoxic to the immature brain. *Neural Regen Res*. 10(4): 599–604.

LOEWE S (**1953**) The problem of synergism and antagonism of combined drugs. *Arzneimittelforschung*. 3(6): 285–290.

LORING DW *ET AL*. (**2007**) Neuropsychological and behavioral effects of antiepilepsy drugs. *Neuropsychol Rev*. 17(4): 413–425.

LU P *ET AL.* (**2009**) Silibinin Attenuates Amyloid 25-35 Peptide-Induced Memory Impairments: Implication of Inducible Nitric-Oxide Synthase and Tumor Necrosis Factor- in Mice. *J Pharmacol Exp Ther*. 331(1): 319–326.

LUSZCZKI JJ (**2007**) Isobolographic analysis of interaction between drugs with nonparallel dose-response relationship curves: a practical application. *Naunyn Schmiedebergs Arch Pharmacol*. 375(2): 105–114.

LUSZCZKI JJ, **CZUCZWAR SJ** (**2003**) Isobolographic and subthreshold methods in the detection of interactions between oxcarbazepine and conventional antiepileptics--a comparative study. *Epilepsy Res*. 56(1): 27–42.

LUSZCZKI JJ, **CZUCZWAR SJ** (**2004a**) Isobolographic profile of interactions between tiagabine and gabapentin: a preclinical study. *Naunyn Schmiedebergs Arch Pharmacol*. 369(4): 434–446.

LUSZCZKI JJ, **CZUCZWAR SJ** (**2004b**) Preclinical profile of combinations of some second-generation antiepileptic drugs: an isobolographic analysis. *Epilepsia*. 45(8): 895–907.

LUSZCZKI JJ, **CZUCZWAR SJ** (**2006**) Biphasic characteristic of interactions between stiripentol and carbamazepine in the mouse maximal electroshock-induced seizure model: a three-dimensional isobolographic analysis. *Naunyn Schmiedebergs Arch Pharmacol*. 374(1): 51–64.

MA Q *ET AL.* (**2016**) Hepatoprotective effect of flavonoids from Cirsium japonicum DC on hepatotoxicity in comparison with silymarin. *Food Funct*. 7(5): 2179–2184.

MADRIGAL-SANTILLÁN E *ET AL.* (**2014**) Review of natural products with hepatoprotective effects. *World J Gastroenterol*. 20(40): 14787–14804.

MAGALINGAM KB *ET AL.* (**2015**) Protective Mechanisms of Flavonoids in Parkinson's Disease. *Oxid Med Cell Longev*. 2015: 1–14.

MAHLI A *ET AL.* (**2015**) Hepatoprotective effect of oral application of a silymarin extract in carbon tetrachloride-induced hepatotoxicity in rats. *Clin Phytosci*. 1(1): 5.

MANDEL S *ET AL.* (**2004**) Cell signaling pathways in the neuroprotective actions of the green tea polyphenol (-)-epigallocatechin-3-gallate: implications for neurodegenerative diseases. *J Neurochem*. 88(6): 1555–1569.

MCGILL MR *ET AL.* (**2011**) HepaRG cells: A human model to study mechanisms of acetaminophen hepatotoxicity. *Hepatology*. 53(3): 974–982.

MCKIM JM (**2010**) Building a tiered approach to in vitro predictive toxicity screening: a focus on assays with in vivo relevance. *Comb Chem High Throughput Screen*. 13(2): 188–206.

MEADOR K (**2004**) Cognitive deficits from in utero AED exposure. *Epilepsy Curr*. 4(5): 196–197.

MOHANA S *ET AL.* (**2016**) Screening dietary flavonoids for the reversal of P-glycoprotein–mediated multidrug resistance in cancer. *Mol Biosyst*. 12(8): 2458–2470.

MORTE MI *ET AL.* (**2013**) Evaluation of neurotoxic and neuroprotective pathways affected by antiepileptic drugs in cultured hippocampal neurons. *Toxicol Vitr*. 27(8): 2193–2202.

MOTAMEDI GK, **MEADOR KJ** (**2006**) Antiepileptic drugs and neurodevelopment. *Curr Neurol Neurosci Rep*. 6(4): 341–346.

MURATA N ***ET AL***. (**2010**) Silymarin attenuated the amyloid ß plaque burden and improved behavioral abnormalities in an Alzheimer's disease mouse model. *Biosci Biotechnol Biochem*. 74(11): 2299–2306.

NEWMAN DJ, **CRAGG GM** (**2016**) Natural Products as Sources of New Drugs from 1981 to 2014. *J Nat Prod*. 79(3): 629–661.

NORRIS W ***ET AL***. (**2008**) Drug-induced liver injury in 2007. *Curr Opin Gastroenterol*. 24(3): 287–297.

OHMORI H ***ET AL***. (**1992**) Neurotoxicity of phenytoin administered to newborn mice on developing cerebellum. *Neurotoxicol Teratol*. 14(3): 159–165.

OHMORI H ***ET AL***. (**1997**) Effects of low-dose phenytoin administered to newborn mice on developing cerebellum. *Neurotoxicol Teratol*. 19(3): 205–211.

PARASURAMAN S (**2011**) Toxicological screening. *J Pharmacol Pharmacother*. 2(2): 74.

PARK JH ***ET AL***. (**2012**) Effects of silymarin and formulation on the oral bioavailability of paclitaxel in rats. *Eur J Pharm Sci*. 45(3): 296–301.

PATEL N ***ET AL***. (**2010**) Silymarin modulates doxorubicin-induced oxidative stress, Bcl-xL and p53 expression while preventing apoptotic and necrotic cell death in the liver. *Toxicol Appl Pharmacol*. 245(2): 143–152.

PATHAK SM, **UDUPA N** (**2010**) Pre-clinical evidence of enhanced oral bioavailability of the P-glycoprotein substrate talinolol in combination with morin. *Biopharm Drug Dispos*. 31(2–3): 202–214.

PÉREZ-HERNÁNDEZ J ***ET AL***. (**2016**) A Potential Alternative against Neurodegenerative Diseases: Phytodrugs. *Oxid Med Cell Longev*. 2016: 1–19.

PEREZ GUTIERREZ RM ***ET AL***. (**2011**) Effect of flavonoids from Prosthechea michuacana on carbon tetrachloride induced acute hepatotoxicity in mice. *Pharm Biol*. 49(11): 1121–1127.

PERNELLE K ***ET AL***. (**2011**) Automated detection of hepatotoxic compounds in human hepatocytes using HepaRG cells and image-based analysis of mitochondrial dysfunction with JC-1 dye. *Toxicol Appl Pharmacol*. 254(3): 256–266.

PERUCCA E, **MEADOR KJ** (**2005**) Adverse effects of antiepileptic drugs. *Acta Neurol Scand Suppl*. 181: 30–35.

PERUCCA P, **GILLIAM FG** (**2012**) Adverse effects of antiepileptic drugs. *Lancet Neurol*. 11(9): 792–802.

PRADEEP K ***ET AL***. (**2007**) Silymarin: An Effective Hepatoprotective Agent Against Diethylnitrosamine-Induced Hepatotoxicity in Rats. *Pharm Biol*. 45(9): 707–714.

RAŠKOVIĆ A ***ET AL***. (**2011**) The Protective Effects of Silymarin against Doxorubicin-Induced Cardiotoxicity and Hepatotoxicity in Rats. *Molecules*. 16(12): 8601–8613.

RAVIKUMAR REDDY D *ET AL.* (**2016**) Natural flavonoids silymarin and quercetin improve the brain distribution of co-administered P-gp substrate drugs. *SpringerPlus*. 5(1): 1618.

RODRIGUES RM *ET AL.* (**2013**) Assessment of an automated in vitro basal cytotoxicity test system based on metabolically-competent cells. *Toxicol Vitr*. 27(2): 760–767.

SAITO J *ET AL.* (**2016**) High content analysis assay for prediction of human hepatotoxicity in HepaRG and HepG2 cells. *Toxicol Vitr*. 33: 63–70.

SAMINATHAN H *ET AL.* (**2011**) Environmental neurotoxic pesticide dieldrin activates a non receptor tyrosine kinase to promote PKCδ-mediated dopaminergic apoptosis in a dopaminergic neuronal cell model. *Neurotoxicology*. 32(5): 567–577.

SASAKI E *ET AL.* (**2013**) A novel mouse model for phenytoin-induced liver injury: involvement of immune-related factors and P450-mediated metabolism. *Toxicol Sci*. 136(1): 250–263.

SASU A *ET AL.* (**2015**) Protective effects of silymarin on epirubicin-induced mucosal barrier injury of the gastrointestinal tract. *Drug Chem Toxicol*. 38(4): 442–451.

SHAARAWY SM *ET AL.* (**2009**) Protective effects of garlic and silymarin on NDEA-induced rats hepatotoxicity. *Int J Biol Sci*. 5(6): 549–557.

SINGH NA *ET AL.* (**2016**) Potential neuroprotective properties of epigallocatechin-3-gallate (EGCG). *Nutr J*. 15(1): 60.

SINGHAL NK *ET AL.* (**2010**) Melatonin or silymarin reduces maneb- and paraquat-induced Parkinson's disease phenotype in the mouse. *J Pineal Res*. 50(2): 97–109.

SKIBOLA CF, SMITH MT (**2000**) Potential health impacts of excessive flavonoid intake. *Free Radic Biol Med*. 29(3–4): 375–383.

SOLDATOW VY *ET AL.* (**2013**) In vitro models for liver toxicity testing. *Toxicol Res (Camb)*. 2(1): 23–39.

SONG Z *ET AL.* (**2006**) Silymarin protects against acute ethanol-induced hepatotoxicity in mice. *Alcohol Clin Exp Res*. 30(3): 407–413.

SPENCER JPE (**2009**) Flavonoids and brain health: multiple effects underpinned by common mechanisms. *Genes Nutr*. 4(4): 243–250.

SUCHER NJ, CARLES MC (**2015**) A pharmacological basis of herbal medicines for epilepsy. *Epilepsy Behav*. 52(Pt B): 308–318.

SUSUKIDA T *ET AL.* (**2016**) Establishment of a Drug-Induced, Bile Acid-Dependent Hepatotoxicity Model Using HepaRG Cells. *J Pharm Sci*. 105(4): 1550–1560.

SZABO M *ET AL.* (**2013**) Comparison of human hepatoma HepaRG cells with human and rat hepatocytes in uptake transport assays in order to predict a risk of drug induced hepatotoxicity. *PLoS One*. 8(3): e59432.

TALLARIDA R (**2000**) Drug synergism and dose-effect data analysis. Chapman and Hall/CRC, Boca Raton, USA.

TALLARIDA RJ *ET AL.* (**1997**) Efficient designs for studying synergistic drug combinations. *Life Sci*. 61(26): PL 417-425.

TALLARIDA RJ (**2006**) An overview of drug combination analysis with isobolograms. *J Pharmacol Exp Ther*. 319(1): 1–7.

TALLARIDA RJ (**2007**) Interactions between drugs and occupied receptors. *Pharmacol Ther*. 113(1): 197–209.

TAPAS AR *ET AL.* (**2008**) Flavonoids as nutraceuticals: A Review. *Trop J Pharm Res*. 7(3): 1089-1099.

URIARTE-PUEYO I, **CALVO MI** (**2011**) Flavonoids as acetylcholinesterase inhibitors. *Curr Med Chem*. 18(34): 5289–5302.

VAUZOUR D *ET AL.* (**2008**) The neuroprotective potential of flavonoids: a multiplicity of effects. *Genes Nutr*. 3(3–4): 115–126.

WANG M-J *ET AL.* (**2002**) Silymarin protects dopaminergic neurons against lipopolysaccharide-induced neurotoxicity by inhibiting microglia activation. *Eur J Neurosci*. 16(11): 2103-2012.

WANG Y *ET AL.* (**2013**) A DNA methyltransferase inhibitor, 5-aza-2'-deoxycytidine, exacerbates neurotoxicity and upregulates Parkinson's disease-related genes in dopaminergic neurons. *CNS Neurosci Ther*. 19(3): 183–190.

WAQAR H *ET AL.* (**2016**) Antiepileptic potential of Silybum marianum seeds in pentylenetetrazol-induced kindled mice. *Bangladesh J Pharmacol*. 11(3): 603–609.

WAWRUSZAK A *ET AL.* (**2015**) Assessment of Interactions between Cisplatin and Two Histone Deacetylase Inhibitors in MCF7, T47D and MDA-MB-231 Human Breast Cancer Cell Lines - An Isobolographic Analysis. *PLoS One*. 10(11): e0143013.

WIEBE S, **HESDORFFER DC** (**2007**) Epilepsy: being ill in more ways than one. *Epilepsy Curr*. 7(6): 145–148.

WOLANSKY MJ, **AZCURRA JM** (**2005**) Permanent motor activity and learning disorders induced by exposure to phenytoin during gestation and early infancy in the rat. *Neurotoxicol Teratol*. 27(2): 299–310.

YADAV NP *ET AL.* (**2008**) Synergistic effect of silymarin and standardized extract of Phyllanthus amarus against CCl4-induced hepatotoxicity in Rattus norvegicus. *Phytomedicine*. 15(12): 1053–1061.

YAGHMAEI P *ET AL.* (**2014**) Silymarin effect on amyloid-ß plaque accumulation and gene expression of APP in an Alzheimer's disease rat model. *Daru*. 22(1): 24.

YIN F *ET AL.* (**2011**) Silibinin: A novel inhibitor of Aß aggregation. *Neurochem Int*. 58(3): 399-403.

ZACCARA G *ET AL.* (**2008**) Central nervous system adverse effects of new antiepileptic drugs. A meta-analysis of placebo-controlled studies. *Seizure*. 17(5): 405–421.

ZHANG S, **MORRIS ME** (**2003a**) Effects of the flavonoids biochanin A, morin, phloretin, and silymarin on P-glycoprotein–mediated transport. *J Pharmacol Exp Ther*. 304(3): 1258–1267.

ZHANG S, **MORRIS ME** (**2003b**) Effect of the flavonoids biochanin A and silymarin on the P-glycoprotein-mediated transport of digoxin and vinblastine in human intestinal Caco-2 cells. *Pharm Res*. 20(8): 1184–1191.

ZHAO L ***ET AL***. (**2010**) Comparison of methods for evaluating drug-drug interaction. *Front Biosci (Elite Ed)*. 2: 241–249.